Optical feedback in semiconductor lasers

Langley, Lloyd Nicholas

Award date:
1994

Awarding institution:
University of Bath

Optical Feedback in Semiconductor Lasers

Submitted by ***Lloyd Nicholas Langley***

for the degree of PhD

of the University of Bath

1994

COPYRIGHT

ProQuest LLC
789 East Eisenhower Parkway
P.O. Box 1346
Ann Arbor, MI 48106-1346

Summary.

This thesis considers how semiconductor lasers are influenced by optical feedback. Optical feedback occurs when some of the light leaving the laser is reflected back into it by an external mirror.

Accidental reflections often occur from the elements of an optical communication system. These reflections cause optical feedback into the semiconductor laser, resulting in performance degradation. The turn-on delay jitter, an important parameter in determining the system performance, is studied in the presence of optical feedback using a rate equation model.

An iterative travelling wave model is developed to investigate the behaviour of semiconductor laser subject to strong optical feedback. The dynamics and intensity noise behaviour of external cavity laser diodes are investigated. External cavity frequency modulated laser diodes are also considered, in which a phase modulator is placed in the external cavity.

Vertical Cavity Surface Emitting Lasers (VCSEL's) have a radically different structure from conventional edge emitting lasers. Most importantly, VCSEL's have a very high facet reflectivity. Numerical investigations consider whether the high facet reflectivity improves the feedback immunity of the VCSEL compared to edge emitting lasers.

A special type of feedback occurs from phase conjugate mirrors, in which a wave mixing process is used to generate the reflection. The behaviour of laser diodes subject to phase conjugate feedback is investigated and compared to the behaviour under conventional optical feedback. The effects of sluggish phase conjugate feedback in which the mirror reflectivity is time dependent is also considered.

Future communications systems may use chaotic data encryption. Optical feedback can be used to create chaotic output of the laser. The rate equation model is used to target specific output waveforms of the laser to demonstrate this possibility.

Acknowledgements

Special thanks to Alan Shore, my PhD supervisor, from Bath University for expert guidance and assistance.

Thanks also to the following people who helped with collaborative work:

-Jesper Mørk from Tele Danmark Research, Denmark for assistance with the strong optical feedback work performed in chapters 3 and 4.

-Govind Agrawal from Rochester University, USA for assistance with the sluggish phase conjugate feedback investigations performed in chapter 7.

-Peter Willis and Deb Kane from Macquarie University, Australia for assistance with the external cavity FM laser work in parts of chapters 3 and 4, and whom also provided Fig. 4.34.

-Eva Miltényi from Marburg University, Germany for assistance with the investigations into the laminar lengths of Low Frequency Fluctuations in parts of chapter 4, and whom also provided Figs. 4.25-4.27 and 4.29.

-Sergei Turovets from The Institute of Physics, Minsk, Belarus for assistance with the targetting of dynamics investigations in chapter 7.

Thanks to Northern Telecom for sponsorship and to Adrian Janssen for discussions on my work over the last three years.

Contents.

List of Symbols used in the Thesis

Symbol	Description
$A^+(t)$	Slowly varying envelope of the right moving field.
$A^-(t)$	Slowly varying envelope of the left moving field.
c	Speed of light.
C_p	Parasitic chip capacitance.
d	Diameter of Vertical Cavity Surface Emitting Laser
e	Electronic charge.
E(t)	Electric field.
$E(t_i)$	Electric field at start of Langevin noise application interval.
$E^*(t)$	Phase conjugate of electric field.
$E_c(t)$	Phase conjugate reflected field.
$E_i(t)$	Incident optical field.
E_o	Steady state value of electric field .
$E_\omega(z,t)$	Total electric field.
$E_\omega^-(z,t)$	Left moving electric field.
$E_\omega^+(z,t)$	Right moving electric field.
$F_L(\omega)$	Electric field Langevin noise term in frequency domain.
$F_L(t)$	Electric field Langevin noise term in time domain.
f	Frequency.
f_{LFF}	Frequency of Low Frequency Fluctuations.
f_m	Modulation frequency.
f_r	Laser relaxation oscillation frequency.
$F_n(t)$	Carrier density Langevin noise term.
$F_s(t)$	Photon density Langevin noise term.
$F_{shot}(t)$	Shot noise Langevin noise term.
$F_\phi(t)$	Electric field phase Langevin noise term.
$g(\omega,n)$	Modal gain per unit length.
G	Gain per unit time.
G_n	Gain slope.
G_ω	Rate of change of gain with emission frequency.
h	Planck's constant.
I(t)	Injection current.
I_{th}	Threshold injection current.
$I_{th,r}$	Modified threshold current with optical feedback.
$I_{th(sol)}$	Threshold injection current of solitary laser.
J_q	Bessel functions.
$k(\omega,n)$	Complex wave number.
k_{crit}	Critical feedback strength to cause coherence collapse.

Symbol	Description
k_{ext}	External feedback strength.
k_{pcm}	External feedback strength from phase conjugate mirror.
Δk	Dynamical change in the complex wave number.
L_p	Inductance of bond wires to laser chip.
L_{ext}	Distance to external mirror or reflection.
ℓ	Laser length.
m	Modulation depth for resonantly enhancement.
M(f)	Modulation response.
n(t)	Carrier density.
n_o	Transparency carrier density.
n_{th}	Threshold carrier density.
$n_{th,r}$	Modified threshold carrier density with feedback.
$P_{av}(t)$	Average output power evolution.
P_{dec}	Logic decision output power.
P_o	Steady State Output Power.
$P_o(t)$	Output power.
$P_{ref}(t)$	Reflected power.
P_{sol}	Solitary laser steady state output power.
r_1, r_2	Laser facet field reflectivity.
r_3	External mirror field reflectivity.
r_{pcm}	Phase conjugate mirror field reflectivity.
$r_L(\omega,n)$	Laser effective left reflectivity.
$r_R(\omega)$	Effective laser right reflectivity.
R_1, R_2	Laser facet power reflectivity
R(t)	Time dependent phase conjugate reflectivity.
R_{crit}	Critical reflectivity to cause coherence collapse.
R_{ext}	External mirror power reflectivity.
R_{pcm}	Phase conjugate mirror power reflectivity.
R_s	Series resistance of laser chip.
RIN	Relative Intensity Noise.
RIN(f)	Frequency dependency of Relative Intensity Noise.
s(t)	Photon density.
$S(t_i)$	Photon density at start of Langevin noise application interval.
$S_E(\omega)$	Laser emission spectrum.
$s_{ref}(t)$	Reflected photon density.
$s_{o,r}$	Stationary photon density with feedback.
$S_\phi(\omega)$	Spectral density of frequency fluctuations.
t	Time.
Δt	Langevin noise application interval.

Symbol	Description
T_{101},T_{1001}	Turn-on delay for 101 and 1001 bit sequences.
T_A,T_B	Turn-on delay from points A and B.
t_i	Time at start of Langevin noise application interval.
T_{mod}	Modulation bit duration.
T_{on}	Turn-on delay.
T_r	Rise time of sluggish phase conjugate mirror.
T_{LFF}	Low Frequency Fluctuation period.
$T_{LAM(AV)}$	Laminar length of Low Frequency Fluctuations.
V	Active region volume.
v_g	Group velocity.
x_n,x_s,x_ϕ	Gaussian distributed random variables for rate equations.
x_1,x_2	Gaussian distributed random variables for iterative model.
α	Linewidth enhancement factor.
α_i	Laser internal loss per unit length.
$\chi^{(3)}$	3rd order susceptibility (non linear polarisation).
Δ_m	Single pass phase modulation for FM laser.
ε	Gain saturation parameter.
ε_o	Permittivity of free space.
$\phi(t)$	Electric field phase.
Γ	Confinement factor.
Γ_ϕ	Peak phase deviation of a phase modulated signal.
γ	Spontaneous emission factor.
η	Laser to fibre coupling efficiency.
η_q	Quantum efficiency.
λ_L	Lyapunov exponent
μ	Refractive index.
μ'	Real part of refractive index.
μ''	Imaginary part of refractive index.
μ_g	Group refractive index.
$\Delta\nu$	Linewidth.
$\theta(t)$	Feedback phase parameter.
$\sigma(\omega,n)$	Conversion factor between electric field and photon density.
$\sigma_P(t)$	Standard deviation of the average output power evolution.
σ_T	Turn-on delay jitter.
τ_{ext}	External cavity round trip time.
τ_L	Laser internal cavity round trip time.
τ_{ph}	Photon lifetime.
$\tau_{ph,r}$	Modified photon lifetime with optical feedback.
τ_{sp}	Carrier lifetime.

Symbol	Description
ω	Emission frequency (angular).
ω_c	Frequency of reflection from phase conjugate mirror.
ω_d	Phase modulation detuning from longitudinal mode spacing.
ω_i	Frequency of incident wave onto phase conjugate mirror.
ω_m	Phase modulation frequency.
ω_o	Steady State emission frequency.
ω_p	Frequency of phase conjugate mirror pump beams.
ω_r	Circular relaxation oscillation frequency.
ω_s	External cavity laser steady state emission frequency.
ω_{th}	Emission frequency at threshold.
$\Delta\omega$	Phase conjugate mirror incident beam detuning from pump.

List of Tables.

Chapter 1:

Semiconductor Lasers, Modulation and Optical Feedback.

1.1 Introduction.

This thesis investigates the behaviour of semiconductor lasers (laser diodes) when they are subject to external optical feedback. Optical feedback occurs when some of the light output of the laser is returned back into the laser, and may cause dramatic effects on the behaviour of the laser. Unwanted optical feedback can occur in optical communications systems due to reflections from fibre ends [1-5]. Optical isolators are usually required to minimise the amount of light that is returned into the laser. An external mirror can also be deliberately placed in the path of the laser light to feedback a portion of the light into the laser. A laser in this configuration is called an external cavity laser diode. This thesis investigates semiconductor lasers in both optical feedback and external cavity laser configurations.

Chapter 1 describes semiconductor lasers and how they are modelled using rate equations. The chapter also discusses the modulation and noise properties of the laser with and without optical feedback. Chapter 2 extends the rate equations for a semiconductor laser to include weak optical feedback, and investigates how unwanted optical feedback in communications systems affects the system performance, with particular emphasis on the turn-on delay jitter. In chapter 3 an iterative model is developed to describe the behaviour of an external cavity semiconductor laser with strong optical feedback. In chapter 4 the behaviour of external cavity lasers is investigated using the strong optical feedback model developed in chapter 3. Particular emphasis is paid to the dynamics and intensity noise of the device. Chapter 5 uses the optical feedback models developed in earlier chapters to discuss the effect of optical feedback on the behaviour of Vertical Cavity Semiconductor Lasers (VCSEL's). In chapter 6 a special type of optical feedback known as phase conjugate feedback is examined and compared to conventional feedback. Lastly, chapter 7

extends the optical feedback rate equations to include a time dependent external reflectivity. The model is used to investigate sluggish phase conjugate feedback. Chapter 7 also considers the possibility of using optical feedback to target particular operation states for chaotic communication systems. Chapter 8 summarises the conclusions of the thesis.

1.2 Semiconductor Lasers.

A laser consists of a gain medium placed between two mirrors. The device will operate as a laser if the net round trip gain including material and mirror losses is unity [6]. A laser diode is a simple device consisting of a p-n junction made from direct bandgap semiconductor material. The n-doped side has an excess of electrons and the p-doped side has an excess of holes. A potential barrier exists between the two sides of the junction preventing recombination. When a forward bias is applied the barrier is lowered allowing the electrons and holes to be injected into the active region of the p-n junction. A population inversion necessary for lasing action is formed in the active region [6]. The electrons and holes recombine, emitting photons which experience gain by stimulated emission producing more photons. The mirrors at each end of the device reflect some of the photons back into the laser for further stimulated emission to occur. Double heterostructure lasers are most commonly used [7], in which the laser is fabricated from a combination of semiconductor materials which have different band gap energies for current confinement and different refractive indices for optical confinement within the active region. This optimises the interaction between the gain medium and the laser light, thus increasing the efficiency and keeping the operating current low. Guiding of the light in the lateral direction of the device is achieved by placing the laser in a waveguide structure (index guiding) and/or injecting the current into the laser along a metal strip on top of the device (gain guiding).

There are many different types of semiconductor laser in common use. Three in particular which this thesis is concerned with, are Fabry-Perot lasers [6], the Distributed Feedback (DFB) laser [6], and the Vertical Cavity Surface Emitting Laser (VCSEL) [8], shown in figs. 1.1 to 1.3 respectively. The Fabry-Perot laser has cleaved facets to provide the reflections at either end of the device. A DFB laser has a grating placed adjacent to the active region which provides distributed feedback all along the device. The grating ensures single frequency emission. The VCSEL is oriented on a vertical axis, with multiple layers of different refractive indices being grown above and below the active region to provide the reflections at the ends of the

cavity.

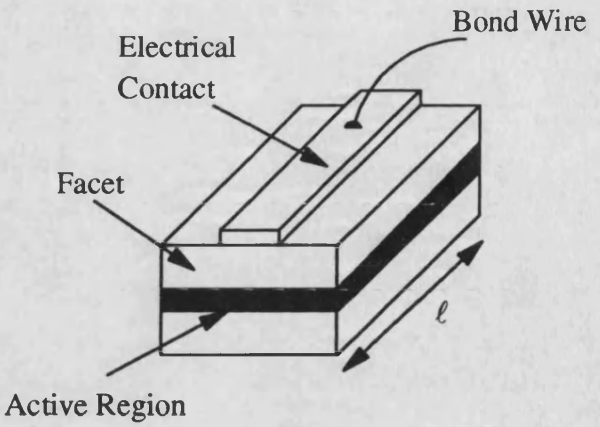

Fig. 1.1: A Fabry-Perot Laser.

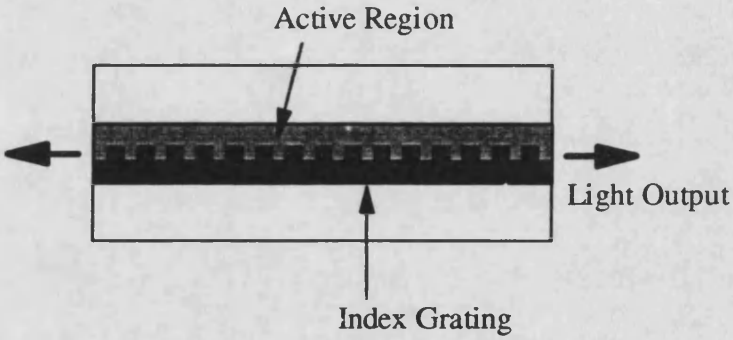

Fig. 1.2: A Distributed Feedback (DFB) Laser.

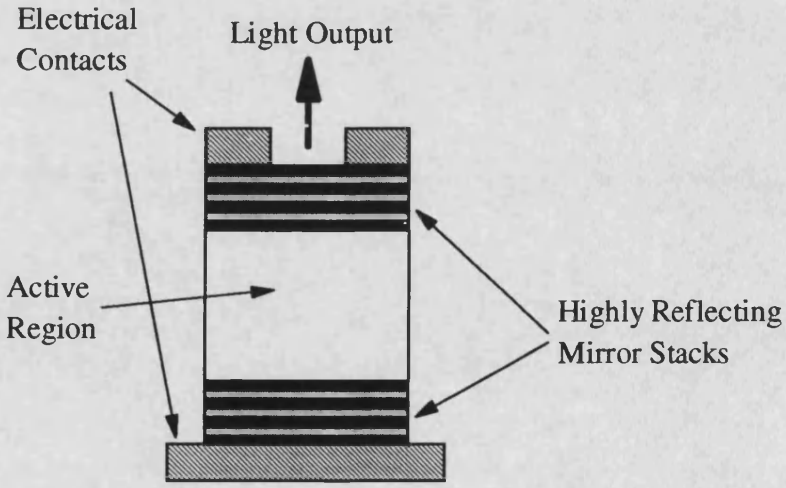

Fig. 1.3: A Vertical Cavity Surface Emitting Laser (VCSEL).

1.3 Optical Communication Systems.

Semiconductor lasers are used extensively in optical communication systems because of their small size and high efficiency [9]. Optical communications system have a much greater information handling capacity than electrical or microwave systems. A simple optical fibre communication system consists of modulated laser diode, a length of optical fibre, and an optical receiver, as shown in fig. 1.4. Repeaters may be needed for long distance communications. The light is modulated to send the desired information. The modulation is usually achieved by changing the gain of the laser by modulating the injection current, though external modulation is also sometimes implemented.

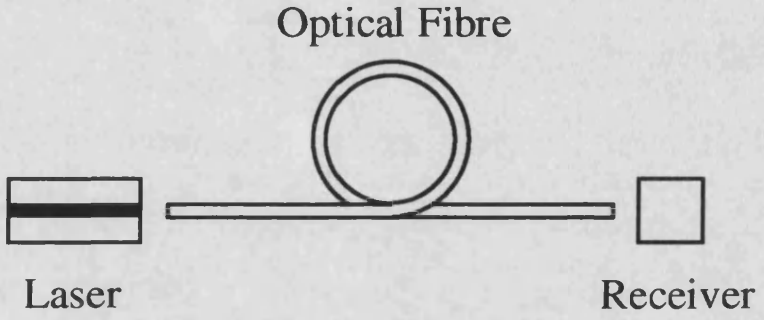

Fig. 1.4: A Simple Optical Communication System.

1.4 Rate Equation Model of a Semiconductor Laser.

The dynamical behaviour of semiconductor lasers is conventionally described using single mode rate equations [6,10]. The equations describe the time behaviour of the laser carrier density n(t), the photon density s(t), and the phase of the light $\phi(t)$. The derivation of the rate equations is detailed in appendix 1. The rate equations are:

$$\frac{dn(t)}{dt} = \frac{I(t)}{eV} - \frac{n(t)}{\tau_{sp}} - s(t)G_n\{n(t)-n_o\}\left\{\frac{1}{1+\varepsilon s(t)}\right\} + F_n(t), \tag{1.1}$$

$$\frac{ds(t)}{dt} = \frac{\gamma n(t)\Gamma}{\tau_{sp}} - \frac{s(t)}{\tau_{ph}} + s(t)G_n\{n(t)-n_o\}\Gamma\left\{\frac{1}{1+\varepsilon s(t)}\right\} + F_s(t), \tag{1.2}$$

$$\frac{d\phi(t)}{dt} = \omega - \omega_{th} = \frac{\alpha}{2}G_n\{n(t)-n_{th}\}\Gamma + F_\phi(t). \tag{1.3}$$

The carrier rate equation (1.1) considers the flow of carriers into the laser active

region and the loss of carriers as they are used to create photons. The first term in (1.1) is the rate of carriers injected into the active region volume V by the current I(t) into the device. The second term in (1.1) is the loss of carriers due to electron-hole recombination. This process is known as spontaneous emission. The decay of carriers has a characteristic time called the carrier lifetime τ_{sp}. The third term in (1.1) is the rate of loss of carriers as they recombine due to the stimulated amplification process. The gain of the laser is linearised as,

$$G = G_n\{n(t) - n_o\} \tag{1.4}$$

around the transparency carrier density n_o. The transparency carrier density is the carrier density at which the stimulated gain term in (1.2) becomes positive. An extra term including the effects of gain compression at high photon density is included [10],

$$\frac{1}{1+\varepsilon s(t)}. \tag{1.5}$$

where ε is the gain compression factor. Several mechanisms for the origin of the non-linear gain have been proposed, including spectral hole burning and carrier heating.

The photon rate equation (1.2) considers the generation and loss of photons. The first term in (1.2) is the average spontaneous emission rate. The spontaneous emission factor γ is the proportion of spontaneous emission photons (generated by the carrier decay) that fall into the lasing mode. The second term in (1.2) is the photon losses, which include the laser output through the facets and the laser internal losses. The photon losses are characterised by a photon lifetime τ_{ph} given by [6,10],

$$\tau_{ph} = \frac{\mu_g}{c\left(\alpha_i - \frac{\ln(R_2)}{\ell}\right)}, \tag{1.6}$$

where μ_g is the group refractive index, c is the speed of light, α_i is the material absorption per unit length, R_2 is the facet reflectivity, and ℓ is the cavity length. The third term in (1.2) is the stimulated emission of photons and also appears in the carrier rate equation. The term Γ is the confinement factor and represents the fraction of the optical field contained within the active region.

The laser phase rate equation (1.3) relates the instantaneous laser emission frequency $\omega(t)$ with the carrier density n(t). The term α is the linewidth enhancement factor [6]

and relates the rate of change of the real part μ' of the refractive index with carrier density, to the rate of change of the imaginary part μ" of the refractive index with carrier density,

$$\alpha = \frac{\partial \mu' / \partial n}{\partial \mu'' / \partial n}. \tag{1.7}$$

The device starts to operate as a laser when the carrier density reaches the threshold carrier density n_{th}, at which point the stimulated gain has overcome the photon losses through the facets and the material absorption. The last terms in (1.1)-(1.3) are the Langevin noise terms $F_n(t)$, $F_s(t)$, $F_\phi(t)$ which model the random noise events caused by spontaneous emission of photons.

1.5 Steady State Solutions.

Under steady state operating conditions equations (1.1) and (1.2) give dn(t)/dt=0 and ds(t)/dt=0. This can be used to calculate steady state values of the carrier and photon densities. For clarity, the gain compression is neglected in the following discussion. At threshold the photon density is zero, giving the threshold current I_{th} from (1.1) as

$$I_{th} = \frac{n_{th} e V}{\tau_{sp}}. \tag{1.8}$$

The threshold carrier density can be calculated by neglecting the spontaneous emission term in (1.2), giving

$$n_{th} = n_o + \frac{1}{G_n \tau_{ph}}. \tag{1.9}$$

At a particular current above threshold the carrier density is clamped at its stationary value n_{th}, resulting in a steady state photon density S_o from (1.1) of

$$s_o = \tau_{ph}\left(\frac{I}{eV} - \frac{n_{th}}{\tau_{sp}}\right). \tag{1.10}$$

1.6 Spontaneous Emission Noise.

In addition to the deterministic output of the laser discussed in the previous section, random noise processes also need to be modelled to properly describe the behaviour of the laser. Spontaneous emission causes both intensity noise and frequency noise in the laser output. Spontaneous emission is modelled in the laser rate equations by the Langevin noise terms $F_n(t)$, $F_s(t)$ and $F_\phi(t)$ [10-12], and are described fully in appendix 2. The Langevin noise in the photon and electric field phase rate equations is due to the random nature of the spontaneous emission process. The Langevin noise in the carrier rate equation is due to the shot noise nature of the injection current and also the spontaneous and stimulated recombination.

1.7 Optical Feedback.

Semiconductor lasers are particularly sensitive to optical feedback [10], which usually results in a detrimental performance. The important parameters when considering the effects of optical feedback are the external reflectivity R_{ext}, the external cavity round trip delay τ_{ext}, and the external reflection phase $\omega_{th}\tau_{ext}$, as shown in fig. 1.5.

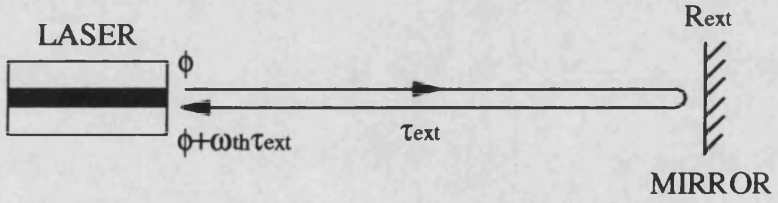

Fig. 1.5: A Semiconductor Laser with Optical Feedback Showing the Important Parameters used to Describe Optical Feedback, Where $\omega_{th}\tau_{ext}$ is the External Cavity Round Trip Phase Change, τ_{ext} is the External Cavity Round Trip Delay, and R_{ext} is the External Reflectivity.

The effects of optical feedback at different strengths can be summarised using the diagram in fig. 1.6 [13,14]. The behaviour of the laser with optical feedback is described with five operating regimes known as I-V. In regime I the linewidth of the laser is increased or decreased depending on the phase of the external reflection. Only a single external cavity mode exists in this regime. In regime II it is possible to adjust the phase of the reflection to achieve considerable linewidth narrowing. However, for most values of the reflection phase many external cavity modes exist. Mode hopping between these external cavity modes occurs, thus increasing the linewidth above that of the solitary laser. The boundary between regimes I and II is dependent on the distance to the reflection. For longer external cavities the border between regimes I

and II occurs at lower levels of feedback than for shorter external cavities. Regime III only occurs for a narrow range of external reflectivity. The laser stabilises onto the external cavity mode with the strongest linewidth reduction. The linewidth reduction is independent of the phase of the external reflection. For higher levels of external reflectivity the laser enters operating regime IV known as coherence collapse [15-21]. The coherence of the laser is drastically reduced, resulting in an extremely large linewidth. There is also a tremendous amount of intensity noise in the laser output. If the external reflectivity is increased further to give very strong optical feedback the laser again operates in a stable manner. This is known as regime V. Lasers in this regime are known as external cavity diode lasers and are introduced in section 1.8. The intensity noise of the laser output for increasing levels of optical feedback is shown in fig. 1.7, and was calculated using a rate equation model for a semiconductor laser with optical feedback (see chapter 2). The sudden increase in intensity noise is characteristic of regime IV or coherence collapse operation. In the coherence collapse regime the intensity noise spectrum contains peaks spaced at multiples of the inverse of the external cavity round trip delay $1/\tau_{ext}$, as shown in fig. 1.8. The effect of unwanted optical feedback from communication systems into a diode laser is investigated in chapters 2 and 5.

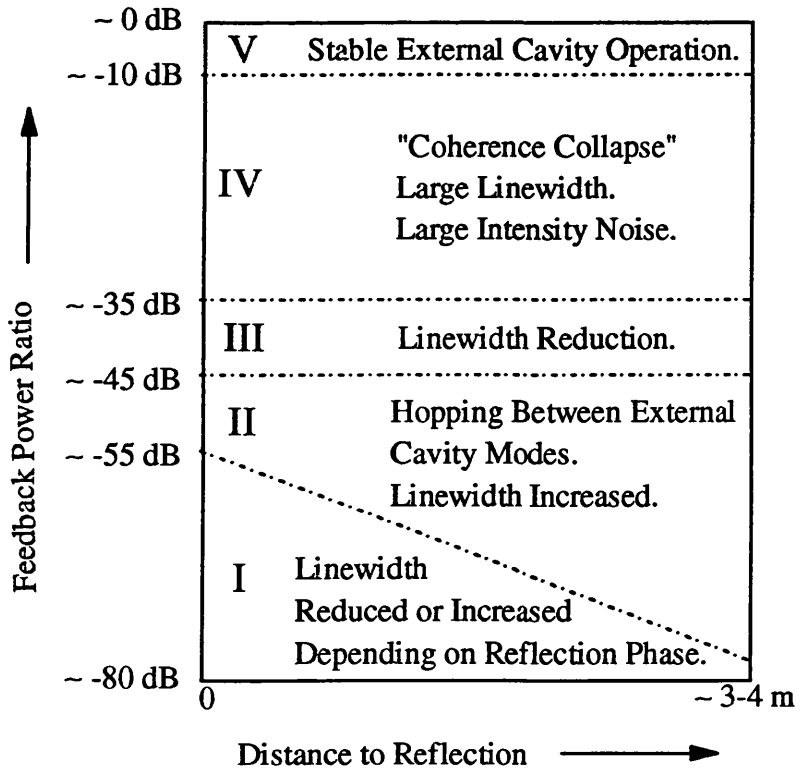

Fig. 1.6: The Operating Regimes (I-V) Used to Describe the Behaviour of a Semiconductor Laser Subject to Optical Feedback (Redrawn from Reference [14]).

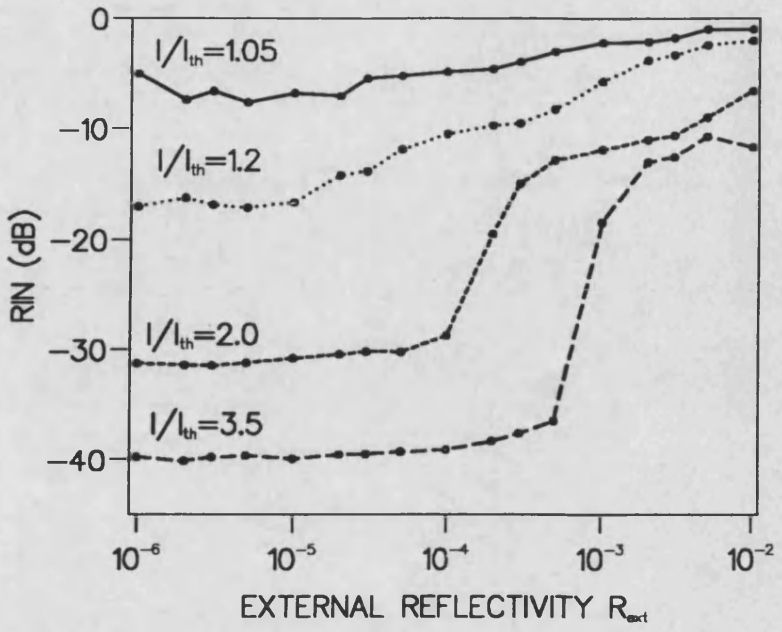

Fig. 1.7: Relative Intensity Noise (RIN) for Increasing Optical Feedback at various Bias Currents (τ_{ext}=2 ns).

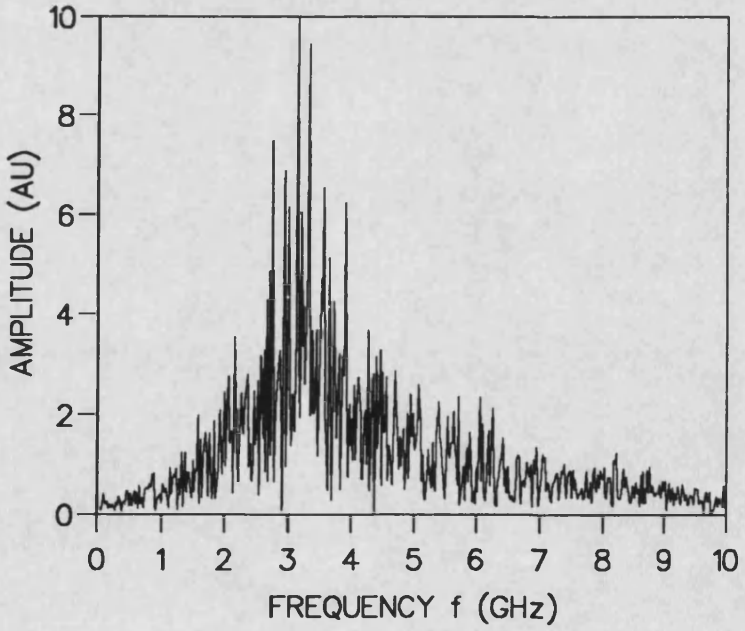

Fig. 1.8: Intensity Noise Spectrum of Output Power Fluctuations for a Laser with Optical Feedback ($I=2I_{th}$, R_{ext}=0.01, τ_{ext}=2 ns).

1.8 External Cavity Lasers.

In an external cavity laser [22] a mirror is placed in the path of the light leaving the laser, reflecting it back into the active region, as shown in fig. 1.9. The laser facet is often coated to lower its reflectivity. In this case, the laser cavity is defined by the external mirror and the remaining laser facet, and the laser operates in regime V. The benefit of using such a configuration is that the linewidth is dramatically reduced by factors of 100 or more [23,24]. The behaviour of such lasers is investigated in chapter 4 using the model for external cavity lasers developed in chapter 3.

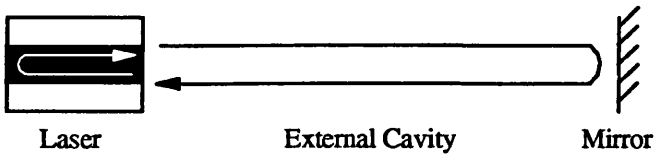

Fig. 1.9: An External Cavity Laser Diode With the Lasing Cavity Defined Between One Laser Facet and the External Mirror.

1.9 Phase Conjugate Feedback.

A special type of optical feedback is generated by a phase conjugate mirror [25]. A phase conjugate mirror can be implemented using a multi-wave mixing process. The principal property of phase conjugate mirrors is that the light has its phase reversed, as described in more detail in chapter 6. The reflected light can be considered to be a time-reversal of the incident beam. The reversal of the phase results in the phase change due to the return path length cancelling any phase change due to the outward journey [26]. This zero external cavity round trip phase change is the major difference between phase conjugate and conventional optical feedback. The behaviour of lasers subject to phase conjugate feedback is discussed in chapters 6 and 7.

1.10 Conclusion.

Semiconductor lasers (laser diodes), their structure, and their characteristics have been briefly introduced. The rate equations usually used to describe the dynamical behaviour of laser diodes have been introduced. The common problem of optical feedback into laser diodes has been discussed. In particular feedback induced coherence collapse has been introduced. Feedback induced noise and coherence collapse will play an important part in the rest of this thesis. Strong optical feedback in

which lasers operate as external cavity has also been described. The special case of phase conjugate feedback has also been introduced.

Chapter 1 References.

[1] K Petermann and G Arnold, "Noise and Distortion Characteristics of Semiconductor Lasers in Optical Fiber Communication Systems", IEEE J. Quantum Electron., Vol. 18, No. 4, pp. 543-555, 1982.

[2] B H Verbeek, D Lenstra, and A J den Boef, "Noise due to Optical Feedback in Semiconductor Lasers", Philips Tech. Rev., Vol. 43, No. 10, pp. 292-302, 1987.

[3] B R Clarke, "The Effect of Reflections on the System Performance of Intensity Modulated Laser Diodes", IEEE J. Lightwave Tech., Vol. 9, No. 6, pp. 741-749, 1991.

[4] N Schunk and K Petermann, "Measured Feedback-Induced Intensity Noise for 1.3 μm DFB Laser Diodes", Electron. Lett., Vol. 25, No. 1, pp. 63-64, 1989.

[5] D M Byrne, D MacLean, and R Plumb, "Optical Feedback-Induced Noise in Pigtailed Laser Diode Modules", IEEE Phot. Technol. Lett., Vol. 3, No. 10, pp. 891-894, 1991.

[6] G P Agrawal, "Long Wavelength Semiconductor Lasers", Van Nostrand Reinhold, 1986.

[7] H Kressel, and J K Butler, "Semiconductor Lasers and Heterojunction LED's", Academic Press, 1977.

[8] G A Evans, and J M Hammer (Eds.), "Surface Emitting Semiconductor Lasers and Arrays", Academic Press, 1993.

[9] G Keiser, "Optical Fiber Communications", McGraw-Hill, 1991.

[10] K Petermann, "Laser Diode Modulation and Noise", Kluwer, 1988.

[11] N Schunk and K Petermann, "Noise Analysis of Injection-Locked Semiconductor Injection Lasers", IEEE J. Quantum Electron., Vol. 22, No. 5, pp. 642-650, 1986.

[12] D Marcuse, "Computer Simulation of Laser Photon Fluctuations: Theory of Single-Cavity Laser", IEEE J. Quantum. Electron, Vol. 20, No. 10, pp. 1139-1148, 1984.

[13] N Schunk and K Petermann, "Numerical Analysis of the Feedback Regimes for a Single-Mode Semiconductor Laser With External Optical Feedback", IEEE J. Quantum Electron., Vol. 24, No. 7, pp. 1242-1247, 1988.

[14] R Tkach and A Chraplyvy, "Regimes of Feedback Effects in 1.5-μm Distributed Feedback Lasers", IEEE J. Lightwave Tech., Vol. 4, No. 11, pp. 1655-1661, 1986.

[15] H Li, J Ye, and J G McInerney, "Detailed Analysis of Coherence Collapse in Semiconductor Lasers", IEEE J. Quantum Electron., Vol. 29, No. 9, pp. 2421-2432, 1993.

[16] D Lenstra, B H Verbeek, and A J Den Boef, "Coherence Collapse in Single-Mode Semiconductor Lasers Due to Optical Feedback", IEEE J. Quantum Electron., Vol. 21, No. 6, pp. 674-679, 1985.

[17] J Mørk, B Tromborg, and J Mark, "Chaos in Semiconductor Lasers with Optical Feedback: Theory and Experiment", IEEE J. Quantum Electron., Vol. 28, No. 1, pp. 93-108, 1992.

[18] J S Cohen and D Lenstra, "Noise, Chaos and Coherence Collapse in Semiconductor Lasers", Philips. J. Res., Vol. 44, No. 1, pp. 43-55, 1989.

[19] J S Cohen and D Lenstra, "Spectral Properties of the Coherence Collapsed State of a Semiconductor Laser with Delayed Optical Feedback", IEEE J. Quantum Electron., Vol. 25, No. 6, pp. 1143-1151, 1989.

[20] J Wang and K Petermann, "Noise Analysis of Semiconductor Lasers within the Coherence Collapse Regime", IEEE J. Quantum Electron., Vol. 27, No. 1, pp. 3-9, 1991.

[21] S L Woodward and E J Thompson, "The Onset of Coherence Collapse in DFB Lasers", IEEE Phot. Technol. Lett., Vol. 4, No. 3, pp. 221-223, 1992.

[22] L A Coldren and T L Koch, "External-Cavity Laser Design", IEEE J. Lightwave Tech., Vol. 2, No. 6, pp. 1045-1051, 1984.

[23] A R Chraplyvy, K Y Liou, R W Tkach, G Eisenstein, Y K Jhee, T L Koch, P J Anthony, and U K Chakrabarti, "Simple Narrow-Linewidth 1.5 μm InGaAsP DFB External-Cavity Laser", Electron. Lett., Vol. 22, No. 2, pp. 88-90, 1986.

[24] T P Lee, S G Menocal, and H Matsumura, "Characteristics of Linewidth Narrowing of a 1.5 μm DFB Laser with a Short GRIN-ROD External Coupled Cavity", Electron. Lett., Vol. 21, No. 15, pp. 655-656, 1985.

[25] R A Fisher, "Optical Phase Conjugation", Academic Press, 1983.

[26] G P Agrawal, and G R Gray, "Effect of Phase-Conjugate Feedback on the Noise Characteristics of Semiconductor Lasers", Phys. Rev. A, Vol. 46, No. 9, pp. 5890-5898, 1992.

Chapter 2:

The Effect of Optical Feedback on the Turn-on Statistics of Laser Diodes.

2.1 Introduction to Turn-on Delay Jitter in Laser Diodes.

Considerable effort has been given to studying the effects of noise on the turn-on delay jitter which plays a significant role in determining the system performance of semiconductor lasers. Both experimental [1-8] and numerical simulations [7-22] have been used to investigate the turn-on delay jitter. The turn-on delay is the short delay between the application of an increase in injection current into the laser and the leading edge of the resultant optical pulse. The turn-on delay jitter is a measure of the variations in the turn-on delay and is defined as the standard deviation of the turn-on delay probability distribution function (pdf). The turn-on delay jitter is usually caused by spontaneous emission induced intensity noise in the laser optical output [1-22]. The carrier and photon fluctuations ensure that the rise in optical power at the onset of a pulse begins from a random starting value, as illustrated in fig. 2.1. Thus the time taken for the light pulse to be emitted is also random, resulting in a different turn-on delay for each pulse.

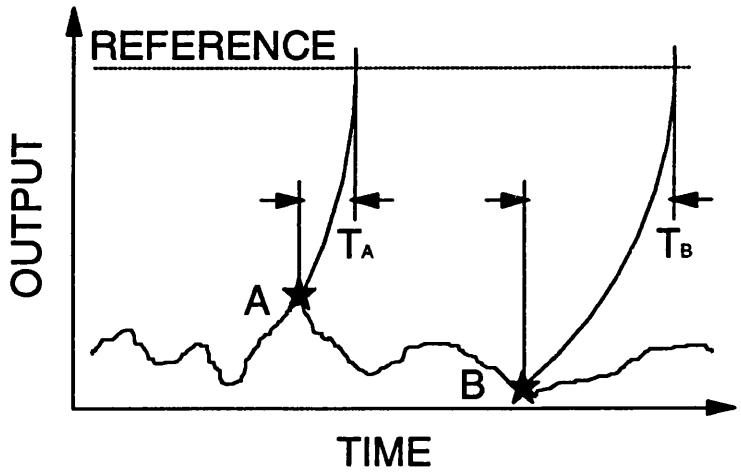

Fig. 2.1: How Turn-on Delay Jitter Arises from Intensity Noise. Different Turn-on Delays (T_A, T_B) Occur for Different Initial Output Powers.

The turn-on delay jitter is significantly larger in distributed feedback (DFB) lasers than in Fabry-Perot lasers [6-9]. It has been demonstrated that this is due to the rapidity of turn-on [9], as the rate of increase of the photon number during turn-on is lower in DFB than in Fabry-Perot lasers. Hence a noise-induced change in the starting point for the photon number rise causes a larger change in the turn-on delay in a DFB laser, resulting in a larger value of jitter.

The turn-on delay jitter degrades the laser performance by reducing the temporal resolution of the optical pulses. Analytical expressions for turn-on delay jitter have been found for various operating conditions [4,5,7,8,10,14-17] and lead to calculations of both the jitter induced system bit-error rate and power penalty [5]. The turn-on delay jitter is greater when the laser is biased below threshold [1,2,5,7,11-14,17,22] due to the lower number of photons present. The turn-on delay jitter decreases for increasing bias current above threshold [5,7,12,13,17,22] but at the expense of reduced on/off ratio. Recent work has focused on the shape of the turn-on delay pdf and the dependence of the jitter on modulation frequency. For periodic modulation the turn-on delay pdf has been found to be approximately gaussian in shape for bias currents both above and below threshold [5,14].

During pseudorandom modulation, if the modulation frequency is sufficiently high the carrier density is prevented from relaxing to its steady state value during a single logic zero bit. Hence different turn-on delays occur, depending on the number of preceding zero bits, and double peaks known as pattern effects are seen in the turn-on delay pdf with no external optical feedback present [11,14,19-21]. The different turn-on delay times T_{101} and T_{1001} for 101 and 1001 bit combinations are illustrated in fig. 2.2. At lower frequencies the carrier density reaches its steady state value during a single logic zero bit, thus preventing pattern effects and giving a gaussian turn-on delay pdf [5,14,19,20]. Such pattern effects also depend upon the device parameters and particularly the carrier lifetime. For shorter carrier lifetimes pattern effects will occur only at higher modulation frequencies. In addition the pattern effect is dependent upon the modulation format with pattern effects in the RZ (Return to Zero) format occurring at lower frequencies compared to the NRZ (Non-Return to Zero) format. This is because for the RZ format the current returns to its lower value for part of the bit period so that the carrier density has insufficient time to relax to the steady state value. Thus, for pseudorandom modulation pattern effects become important and can cause the turn-on delay pdf to become double peaked when the laser is operated above threshold, resulting in a very large jitter. A modulated laser that exhibits pattern effects is said to have memory because each turn-on delay is dependent on the

previous bits. There exists a value of bias current just below threshold at which pattern effects are negligible and the turn-on delay pdf has an approximately gaussian shape for both pseudorandom and periodic modulation. Memory diagrams have been calculated to indicate the operating conditions necessary to avoid the pattern effects [19-21].

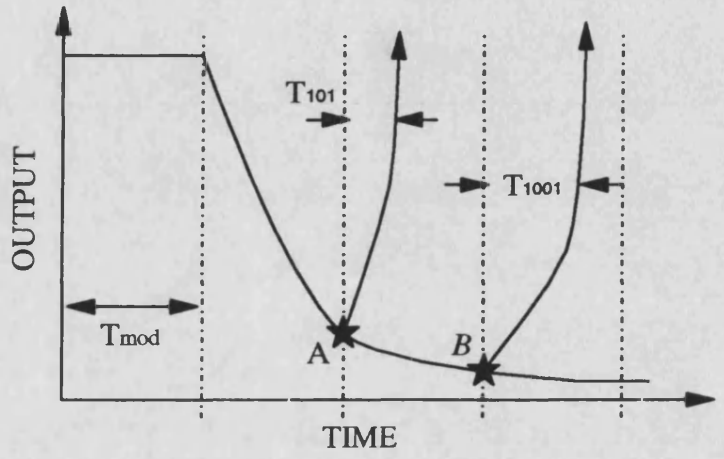

Fig. 2.2: Pattern Effect Caused by Different Turn-on Delay Times (T_{101} and T_{1001}) for 101 and 1001 Bit Combinations.

2.2 Performance Degradation due to Optical Feedback.

The system performance of semiconductor lasers subject to direct intensity modulation can be significantly degraded due to external optical feedback. Much attention has been given to the dramatic changes in noise properties of the laser which can occur for feedback levels typical of optical communications systems [22-33]. Five regimes have been identified in which the semiconductor laser can operate when subjected to external optical feedback, depending on the strength of the feedback and the distance to the reflection [24,25]. The five optical feedback regimes are described in detail in chapter 1. At low feedback levels linewidth narrowing can occur but at larger feedback levels the coherence collapse regime may occur. The dynamics of the laser in the coherence collapse regime are chaotic, with the route to chaos being quasi-periodicity or period doubling [26-30]. In the coherence collapse regime there are very large amounts of intensity noise in the laser output power, and a dramatic broadening of the laser linewidth [24,25]. The intensity noise can significantly reduce the performance of optical communications systems due to the generation of false information bits, resulting in large power penalties. External optical feedback has been investigated both by numerical simulations [22,25,31] and experimentally [23,24,32,33]. It has been found that very low external reflectivities such as may

occur from the connector on the fibre pigtail of a laser diode module can cause the laser to enter the very noisy coherence collapse regime. Reflections also occur from other components in optical communication systems as shown in fig. 2.3. Isolators are nearly always required to minimise the effect of optical feedback on the laser.

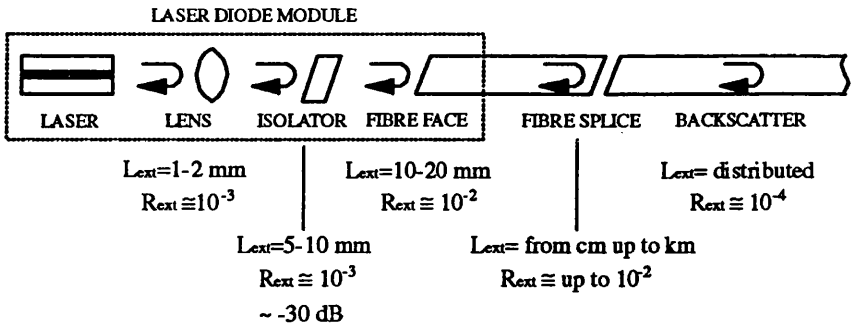

Fig. 2.3: Possible Reflections (With Distances and Strengths) in a Typical Optical Communication System.

2.3 Optical Feedback and Turn-on Delay Jitter.

In this chapter external optical feedback and turn-on delay jitter are considered in conjunction for directly modulated semiconductor lasers. Recent work has shown that moderate optical feedback enhances the turn-on delay jitter in semiconductor laser diodes [34-36]. Optical feedback from a reflection close to the laser may cause an increase or decrease in the jitter depending on whether the reflection is in or out of phase with the laser facet reflection [37]. By frequency selective feedback from a grating it is also possible to reduce the jitter by a process known as self-seeding [38]. It is the spontaneous emission induced intensity noise in the laser output that causes the turn-on delay fluctuations. Therefore it is expected that external optical feedback will also influence the turn-on delay and jitter as it also introduces intensity noise into the laser output. These two effects are investigated by numerical simulation of the single-mode rate equations for a typical distributed feedback (DFB) laser. The model takes into account both external optical feedback and Langevin noise terms for spontaneous emission noise. It is shown that external optical feedback gives rise to markedly different changes in the turn-on delay jitter for pseudorandom and periodic modulation formats.

2.4 Laser Model for Weak Optical Feedback.

The laser model used in this investigation is appropriate to a distributed feedback (DFB) laser typically used in optical communications systems [31]. The system configuration is shown in fig. 2.4. The rate equations are single-mode and include optical feedback terms. The field rate equation for a solitary laser (see appendix 1) is extended with the addition of optical feedback terms [23,25,31],

$$\frac{dE(t)}{dt} = \left\{ j(\omega - \omega_{th}) + \frac{1}{2}\left\{ G_n(n(t) - n_o) - \frac{1}{\tau_{ph}} \right\} \right\} E(t) + \frac{k_{ext}}{\tau_L} E(t - \tau_{ext}) e^{-j\omega_{th}\tau_{ext}}, \tag{2.1}$$

and must be manipulated into rate equations for photon density and phase in order for ease of numerical solution. In (2.1) E(t) is the field, ω is the angular emission frequency, ω_{th} is the angular emission frequency at threshold, τ_{ph} is the photon lifetime, G_n is the gain slope, n(t) is the carrier density, τ_L is the laser cavity round trip time, k_{ext} is the feedback strength, $E(t-\tau_{ext})$ is the reflected optical field, τ_{ext} is the external cavity round trip delay, and $\omega_{th}\tau_{ext}$ is the external cavity round trip phase change. The gain is linearised around the transparency carrier density n_o. The feedback strength is a measure of the proportion of light reflected back into the laser and is calculated from

$$k_{ext} = \frac{(1 - R_2)\sqrt{R_{ext}}\eta}{\sqrt{R_2}}, \tag{2.2}$$

where R_2 is the laser facet reflectivity, R_{ext} is the external reflectivity and η is the laser to fibre coupling efficiency. The method for finding the photon density and field rate equations follows the same steps as in appendix 1 for the solitary laser rate equations.

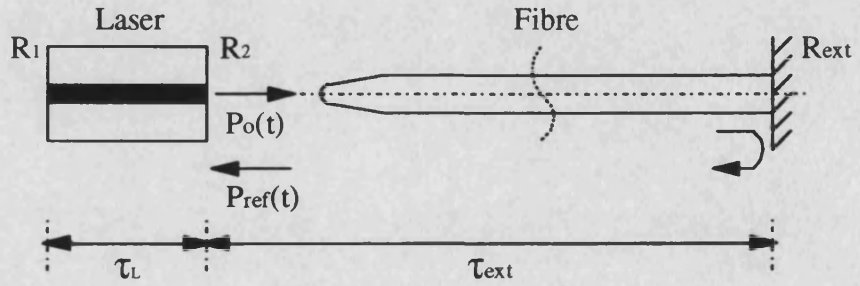

Fig. 2.4: Schematic Diagram of the Laser with Optical Feedback from the Far End of a Fibre Pigtail.

Two simple relationships between the photon density s(t), the optical field E(t) and its phase $\phi(t)$ are:

$$E(t) = \sqrt{s(t)}e^{j\phi(t)} \tag{2.3}$$

and

$$s(t) = E(t)E^*(t), \tag{2.4}$$

where $E^*(t)$ is the phase conjugate of the field. The photon rate equation is calculated using

$$\frac{ds(t)}{dt} = \frac{d}{dt}\left\{E(t)E^*(t)\right\}. \tag{2.5}$$

Inserting (2.1) into (2.5) gives

$$\begin{aligned}\frac{ds(t)}{dt} &= E(t)E^*(t)\left\{G_n\left(n(t)-n_o\right)-\frac{1}{\tau_{ph}}\right\} \\ &+\frac{k_{ext}}{\tau_L}\left\{E(t)E^*(t-\tau_{ext})e^{j\omega_{th}\tau_{ext}}+E^*(t)E(t-\tau_{ext})e^{j\omega_{th}\tau_{ext}}\right\}\end{aligned} \tag{2.6}$$

Using (2.3) and (2.4) in (2.6) gives

$$\begin{aligned}\frac{ds(t)}{dt} &= s(t)\left\{G_n\left(n(t)-n_o\right)-\frac{1}{\tau_{ph}}\right\} \\ &+\frac{k_{ext}}{\tau_L}\sqrt{s(t)}\sqrt{s(t-\tau_{ext})}\left\{\begin{array}{l} e^{j\left(\phi(t)-\phi(t-\tau_{ext})+\omega_{th}\tau_{ext}\right)} \\ +e^{-j\left(\phi(t)-\phi(t-\tau_{ext})+\omega_{th}\tau_{ext}\right)}\end{array}\right\},\end{aligned} \tag{2.7}$$

which can be further simplified using the identity

$$e^x + e^{-x} = 2\cos(x), \tag{2.8}$$

resulting in the rate equation for the photon density in the presence of optical feedback.

$$\frac{ds(t)}{dt} = -\frac{s(t)}{\tau_{ph}} + s(t)G_n(n(t)-n_o) + \frac{2k_{ext}}{\tau_L}\sqrt{s(t)}\sqrt{s(t-\tau_{ext})}\cos\left(\phi(t)-\phi(t-\tau_{ext})+\omega_{th}\tau_{ext}\right) \quad (2.9)$$

The phase rate equation is calculated using the following relationship

$$\frac{d\phi(t)}{dt} = \frac{1}{s(t)}\mathrm{Im}\left\{E^*(t)\frac{dE(t)}{dt}\right\}, \quad (2.10)$$

where Im represents taking the imaginary part of the expression in parenthesis. Inserting (2.1) into (2.10) gives

$$\frac{d\phi(t)}{dt} = \frac{1}{s(t)}\mathrm{Im}\left\{\begin{array}{l} E^*(t)E(t)\left\{j(\omega-\omega_{th})+\frac{1}{2}\left\{G_n(n(t)-n_o)-\frac{1}{\tau_{ph}}\right\}\right\} \\ +\frac{k_{ext}}{\tau_L}E^*(t)E(t-\tau_{ext})e^{-j\omega_{th}\tau_{ext}} \end{array}\right\}. \quad (2.11)$$

Using (2.3) results in

$$\frac{d\phi(t)}{dt} = \mathrm{Im}\left\{\begin{array}{l} j(\omega-\omega_{th})+\frac{1}{2}\left\{G_n(n(t)-n_o)-\frac{1}{\tau_{ph}}\right\} \\ +\frac{k_{ext}}{\tau_L}\frac{\sqrt{s(t-\tau_{ext})}}{\sqrt{s(t)}}e^{-j(\phi(t-\tau_{ext})-\phi(t)-\omega_{th}\tau_{ext})} \end{array}\right\}. \quad (2.12)$$

Substituting

$$e^{jx} = \cos(x) + j\sin(x) \quad (2.13)$$

for the exponential term in (2.12) and taking the imaginary part of the result gives

$$\frac{d\phi(t)}{dt} = (\omega-\omega_{th}) - \frac{k_{ext}}{\tau_L}\frac{\sqrt{s(t-\tau_{ext})}}{\sqrt{s(t)}}\sin\left(\phi(t-\tau_{ext})-\phi(t)-\omega_{th}\tau_{ext}\right). \quad (2.14)$$

Because

$$\sin(x) = -\sin(-x), \quad (2.15)$$

the rate equation for the electric field phase in the presence of optical feedback (2.14) can be rewritten as

$$\frac{d\phi(t)}{dt} = (\omega - \omega_{th}) - \frac{k_{ext}}{\tau_L}\frac{\sqrt{s(t-\tau_{ext})}}{\sqrt{s(t)}}\sin\left(\phi(t) - \phi(t-\tau_{ext}) + \omega_{th}\tau_{ext}\right). \quad (2.16)$$

From appendix 1 it is seen that in the absence of optical feedback

$$\omega - \omega_{th} = \frac{1}{2}\alpha G_n(n(t) - n_{th}), \quad (2.17)$$

Substituting (2.17) for ω-ω_{th} in (2.16) results in the final rate equation for the phase of the electric field in the presence of optical feedback

$$\begin{aligned}\frac{d\phi(t)}{dt} &= \frac{1}{2}\alpha G_n(n(t) - n_{th}) \\ &\quad - \frac{k_{ext}}{\tau_L}\frac{\sqrt{s(t-\tau_{ext})}}{\sqrt{s(t)}}\sin\left(\phi(t) - \phi(t-\tau_{ext}) + \omega_{th}\tau_{ext}\right)\end{aligned}. \quad (2.18)$$

To complete the model a confinement factor Γ, gain saturation ε and spontaneous emission factor γ are included, giving the final rate equations for a semiconductor laser with weak optical feedback. The confinement factor is the proportion of the optical field confined within the active region and reduces the gain term in the photon rate equation. The gain saturation takes into account non-linear gain by reducing the gain at high photon densities. The spontaneous emission factor corresponds to the rate of spontaneous recombination into the considered laser mode. To complete the formalism a carrier rate equation is added but is unchanged from that of the solitary laser described in appendix 1. The rate equations are single-mode and are written below with added Langevin noise terms $F_n(t)$, $F_s(t)$, $F_\phi(t)$ to model spontaneous emission noise:

$$\frac{dn(t)}{dt} = \frac{I(t)}{eV} - \frac{n(t)}{\tau_{sp}} - s(t)G_n\{n(t) - n_o\}\left\{\frac{1}{1+\varepsilon s(t)}\right\} + F_n(t), \quad (2.19)$$

$$\begin{aligned}\frac{ds(t)}{dt} &= \frac{\gamma n(t)\Gamma}{\tau_{sp}} - \frac{s(t)}{\tau_{ph}} + s(t)G_n\{n(t) - n_o\}\Gamma\left\{\frac{1}{1+\varepsilon s(t)}\right\} \\ &\quad + \frac{k_{ext}}{\tau_L}\sqrt{s(t)}\sqrt{s(t-\tau_{ext})}\cos(\theta(t)) + F_s(t)\end{aligned}, \quad (2.20)$$

$$\frac{d\phi(t)}{dt}=\frac{1}{2}\alpha G_n\{n(t)-n_{th}\}\Gamma-\frac{k_{ext}}{\tau_L}\frac{\sqrt{s(t-\tau_{ext})}}{\sqrt{s(t)}}\sin(\theta(t))+F_\phi(t), \tag{2.21}$$

where

$$\theta(t)=\phi(t)-\phi(t-\tau_{ext})+\omega_{th}\tau_{ext}. \tag{2.22}$$

The values of the laser diode parameters used in (2.19)-(2.22) are given in table 2.1, and those for the optical feedback terms are given in table 2.2. An external cavity round trip delay of 1.7 ns is used which corresponds to reflections from a fibre pigtail of 17 cm length (since the fibre refractive index is approximately 1.5, 1 ns of external cavity round trip delay is equivalent to 10 cm of fibre) and the phase change in the external cavity is assumed to be zero. The choice of τ_{ext}=1.7 ns introduces external cavity modes of spacing $1/\tau_{ext}\approx$0.6 GHz into the intensity spectrum. Resonance effects between the external cavity modes and the modulation frequency are avoided because the modulation frequencies of interest in this work are 2-4 GHz. The model represents the worst case situation because the assumption in the rate equations is that the reflected light has the same polarisation as the emitted light.

Symbol	Description	Value
V	Active Region Volume	1.5×10^{-16} m^3
τ_{sp}	Carrier Lifetime	2 ns
G_n	Gain Slope	2.125×10^{-12} m^{3}s^{-1}
n_{th}	Threshold Carrier Density	9.9×10^{23} m^{-3}
ε	Saturation Parameter	3×10^{-23} m^3
γ	Spontaneous Emission Factor	10^{-5}
Γ	Confinement Factor	0.4
τ_{ph}	Photon Lifetime	2 ps
α	Linewidth Broadening Factor	5.5
n_o	Transparency Carrier Density	4×10^{23} m^{-3}
ω_o	Operating Wavelength	$\equiv$1.55 μm
R_2	Laser Facet Reflectivity	0.309
η	Laser to Fibre Coupling Efficiency	0.4
τ_L	Laser Cavity Round Trip Delay	9 ps
η_q	Quantum Efficiency	0.4

Table 2.1: Laser Parameters (Taken from Reference [31]).

Symbol	Description	Value
R_{ext}	External Reflectivity	0 - 0.01
τ_{ext}	External Cavity Round Trip Delay	1.7 ns
$\omega_{th}\tau_{ext}$	External Cavity Round Trip Phase change	0 rads

Table 2.2: Optical Feedback Parameters.

The Langevin noise terms used in the rate equations (2.19)-(2.22), are described in appendix 2. They are written below for completeness:

$$F_n(t) = -\sqrt{\frac{2s(t_i)\gamma n(t)\Gamma}{\tau_{sp}\Delta t}}x_s + \sqrt{\frac{2n(t_i)}{\tau_{sp}\Delta t V}}x_n, \tag{2.23}$$

$$F_s(t) = \sqrt{\frac{2s(t_i)\gamma n(t)\Gamma}{\tau_{sp}\Delta t}}x_s, \tag{2.24}$$

$$F_\phi(t) = \frac{1}{s(t)}\sqrt{\frac{s(t_i)\gamma n(t)\Gamma}{2\tau_{sp}\Delta t}}x_\phi, \tag{2.25}$$

where $s(t_i)$ is the photon density at the start of the time interval Δt, $n(t_i)$ is the carrier density at the start of the interval Δt, V is the active region volume, and x_n, x_s, x_ϕ are gaussian distributed random variables with zero mean and unity variance. The Langevin noise in the photon and electric field phase rate equations is due to the random nature of the spontaneous emission process. The Langevin noise in the carrier rate equation is due to the shot noise nature of the injection current, and spontaneous and stimulated recombination.

2.5 Numerical Solution of Model.

The rate equations with external optical feedback and Langevin noise terms are solved numerically using a variable-step, variable-order Runge-Kutta algorithm. To evaluate the reflection terms in the rate equations, values of photon density and electric field phase calculated at an earlier solution step are required. Thus at each solution step the values of photon density and electric field phase are recorded for use at a later solution step. The number of solution steps between the recording and the use of these values is equivalent to the external cavity round trip delay. Langevin noise is modelled by applying random noise forces as calculated in (2.23)-(2.25). The gaussian

distributed random variables, x_n, x_s and x_ϕ, are calculated at the start of, and are held constant throughout, each Langevin noise application interval, Δt. The interval, Δt, is chosen to be 20 ps. This results in a power spectral density for the noise which has its first zero at a frequency $1/\Delta t$ = 50 GHz. The noise forces should describe a white noise spectrum at least up to the relaxation oscillation frequency [39]. The influence of Δt on the power spectral density of the noise is discussed in appendix A of [39]. The 3 dB cut-off frequency is found to be approximately 22 GHz, which is several times the maximum relaxation oscillation frequency encountered in the following investigations. Hence the condition that the noise spectrum is white up to a frequency greater than the relaxation oscillation frequency is satisfied. A more detailed description of the numerical solution of the rate equations for weak optical feedback is given in appendix 3.

Pseudorandom modulation and periodic modulation injection current formats in the GHz modulation frequency range are modelled, as well as independent pulses. An equivalent circuit of a semiconductor laser is shown in fig. 2.5 [22], with R_s being the series resistance within the laser chip, C_p being the parasitic chip capacitance, and L_p is the inductance of the bond wires to the laser chip. The values of the equivalent circuit parameters are dependent on the laser structure, particularly C_p. Typical values of these parameters are R_s=8 Ω, C_p=0.5 pF and L_p=0.2 nH. The semiconductor laser and drive circuit parasitics are modelled by exponential current rises and falls, with a rise time of 0.15 ns [31]. The threshold current is 12.0 mA. An injection current of 3.5 I_{th} is used for the logic one state, corresponding to an output power of 2.0 mW.

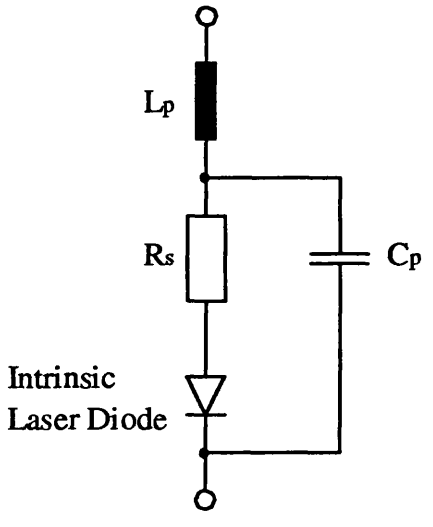

Fig. 2.5: Equivalent Circuit of a Laser Diode.

The output power per facet $P_o(t)$ passed into a fibre pigtail is calculated from the photon density using the following equation [22,31],

$$P_o(t) = \frac{\eta_q \omega_{th} h \eta s(t) V}{4\pi\Gamma\tau_{ph}}, \tag{2.26}$$

where h is Planck's constant and η_q is the quantum efficiency of the laser. The optical turn-on delay for each transition from the logic zero state up to the logic one state is recorded. The turn-on delay is defined as the time taken between the increase in injection current and the output power passing 50% of the logic one state output power when there is no optical feedback, though at the low feedback levels considered the output power is virtually unchanged.. This power level is termed the logic decision power P_{dec}. The number of data bits used to calculate the turn-on delay probability distribution functions (pdf's) is 1000 for the periodic and pseudorandom modulation formats, and 100 for the gain-switching modulation format. Using these limited numbers of samples of the turn-on delay, the randomness of the noise processes investigated will introduce errors into the calculated values of the average turn-on delay and jitter. Repeated simulations for identical bias, modulation and reflection conditions suggest that errors of up to ±0.5% in the average turn-on delay and ±2.5% in the jitter can be expected. These errors are much smaller than the changes seen in these parameters as optical feedback increases. The turn-on delay jitter σ_T is defined as the standard deviation of the turn-on delay pdf, and is calculated as below,

$$\sigma_T = \sqrt{\frac{\sum_{m=1}^{m=n} \left\{ T_{on(m)} - \overline{T_{on}} \right\}^2}{n}} \tag{2.27}$$

Where $\overline{T_{on}}$ is the average turn-on delay, $T_{on(m)}$ are the turn-on delays calculated from the numerical simulation, and n is the number of turn-on events used in the calculation.

2.6 Turn-on Jitter With External Feedback for Independent Pulses.

In the independent pulses modulation format single current pulses are used to modulate the laser, with sufficient time between them so that both carrier and photon densities have time to relax to their steady state values before the onset of the next pulse. This ensures that each optical pulse is independent of the previous pulse. Figs. 2.6 and 2.7 show a pulse evolving from the preceding intensity noise with and without

optical feedback respectively. It is seen that optical feedback of moderate strength is dominant over the spontaneous emission noise. However, at low optical feedback levels the spontaneous emission noise dominates. Figs. 2.8 and 2.9 show a series of values of turn-on delay. The spread is larger with optical feedback indicating a larger jitter value. It is seen that the turn-on delay values are random and do not follow any patterns or frequencies present in the model. Figs. 2.10 and 2.11 show how the average turn-on delay T_{on} and jitter σ_T change with increasing external optical feedback, for a bias current of 26% and 10% above threshold respectively. The average turn-on delay increases by a few percent when optical feedback is present for all bias currents above threshold. The shape of the graph of average turn-on delay shows a rise as external reflectivity increases. The turn on delay increase is largely independent of the bias current. It is possible to decrease the average turn-on delay to a value below that of no optical feedback at some combinations of external reflectivities and operating conditions. This is achieved at an external reflectivity of below 10^{-4} for the 26% threshold bias current of fig. 2.10. The turn-on delay jitter increases dramatically as the level of optical feedback increases [35]. The jitter without optical feedback is smaller at lower bias currents. The value of the jitter with no optical feedback is 3.1 ps at a bias current 10% above threshold. This value is close to an experimental value of approximately 4 ps obtained for a current pulse of $3.5I_{th}$ and similar modulation conditions [7]. The dramatic increase in jitter occurs at a higher external reflectivity when the laser is biased closer to threshold. Close to threshold there is already a large jitter due to spontaneous emission noise. Therefore small amounts of optical feedback do not increase the jitter significantly. The values of jitter obtained in the simulation at large levels of optical feedback are similar to the value of 20.7 ps obtained in simulations for an external reflectivity of R_{ext}=0.005 [34]. Both the turn-on delay changes and jitter increase are seen in the changing shape of the turn-on delay probability distribution function (pdf) as optical feedback increases, shown in fig. 2.12, for a bias current 10% above threshold. The turn-on delay pdf is approximately gaussian for all bias currents with no external optical feedback and remains so when external optical feedback is added. The turn-on delay pdf becomes considerably broadened when the external reflectivity exceeds 10^{-4}.

The mean intensity evolution $P_{av}(t)$ and the intensity standard deviation $\sigma_P(t)$ are shown in fig. 2.13 for bias currents 10% and 26% above threshold. The graph shows the evolutions with and without optical feedback. As expected the mean intensity evolution is slower at lower bias current. Optical feedback is seen to increase the intensity standard deviation, seen as jitter, and also slows down the mean intensity evolutions.

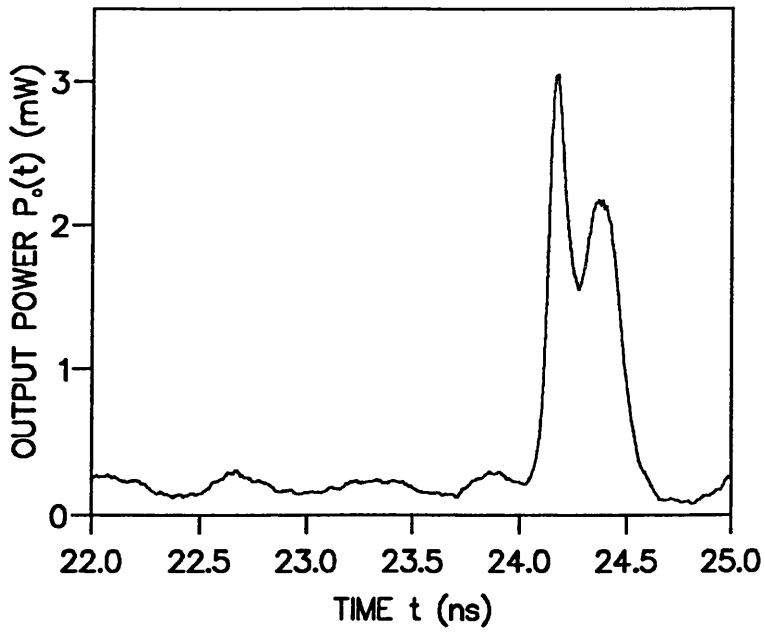

Fig. 2.6: Sample of Output Power $P_o(t)$ During an Individual Pulse for Independent Pulses Without Optical Feedback ($I=1.26I_{th}$).

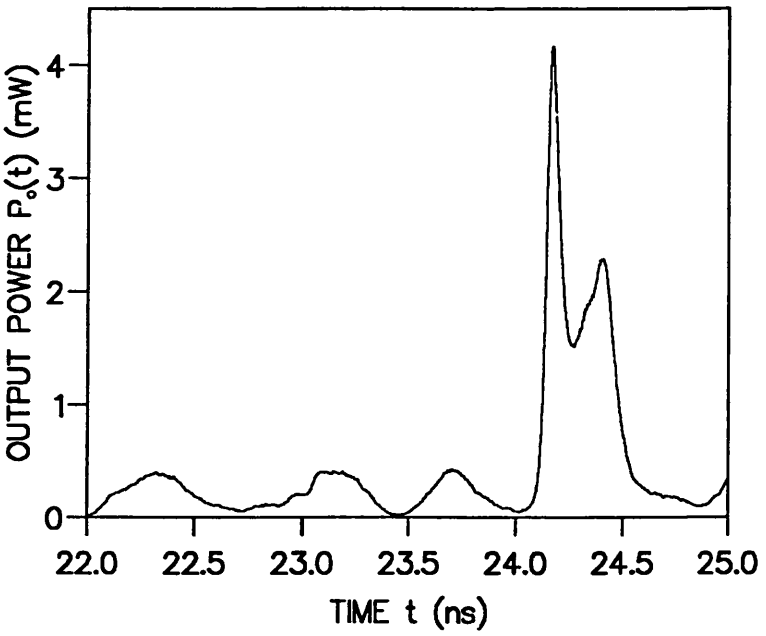

Fig. 2.7: Sample of Output Power $P_o(t)$ During an Individual Pulse for Independent Pulses With Optical Feedback ($R_{ext}=0.005$, $I=1.26I_{th}$).

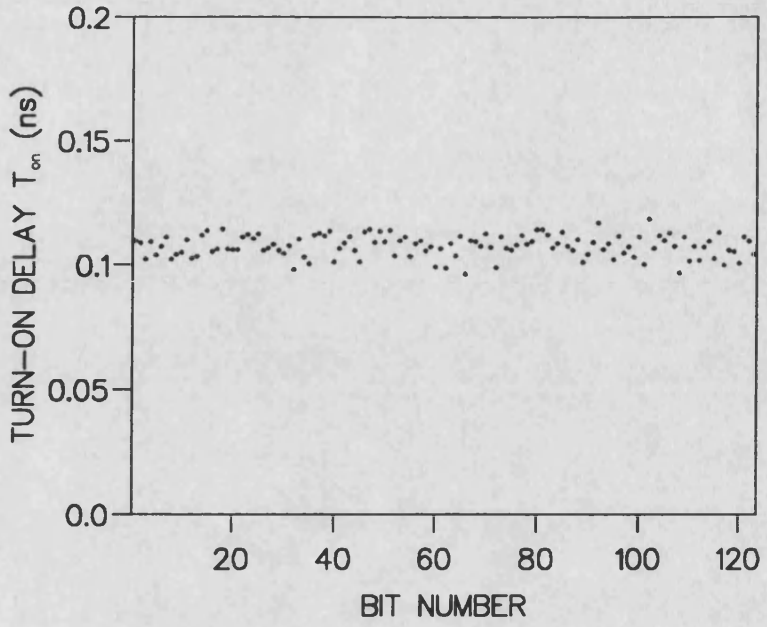

Fig. 2.8: Turn-on Delay Times for Each Modulation Bit for Independent Pulses Without Optical Feedback ($I=1.26I_{th}$).

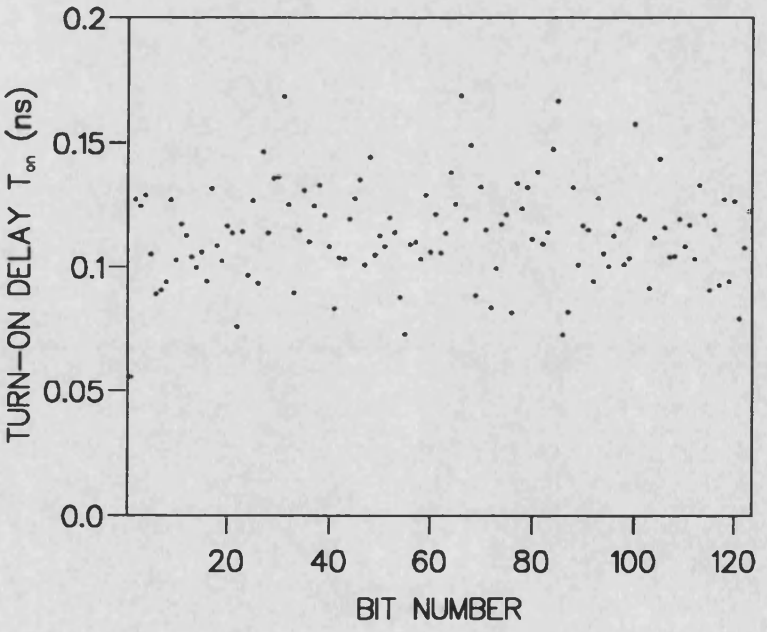

Fig. 2.9: Turn-on Delay Times for Each Modulation Bit for Independent Pulses With Optical Feedback ($R_{ext}=0.005, I=1.26I_{th}$).

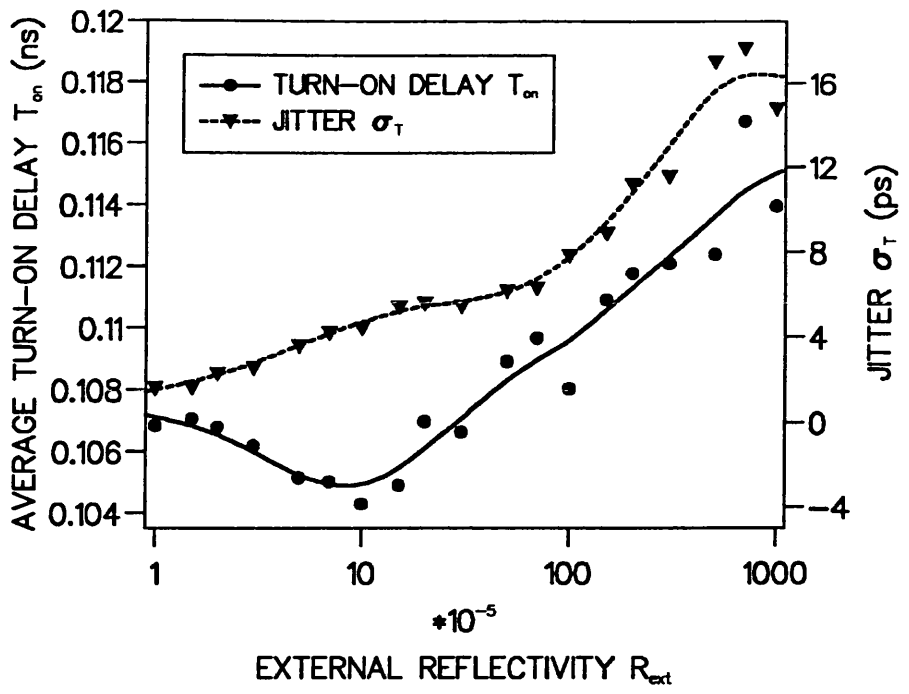

Fig. 2.10: Average Turn-on Delay T_{on} and Jitter σ_T for Increasing External Reflectivity R_{ext} for the Independent Pulses Modulation Format ($I=1.26I_{th}$).

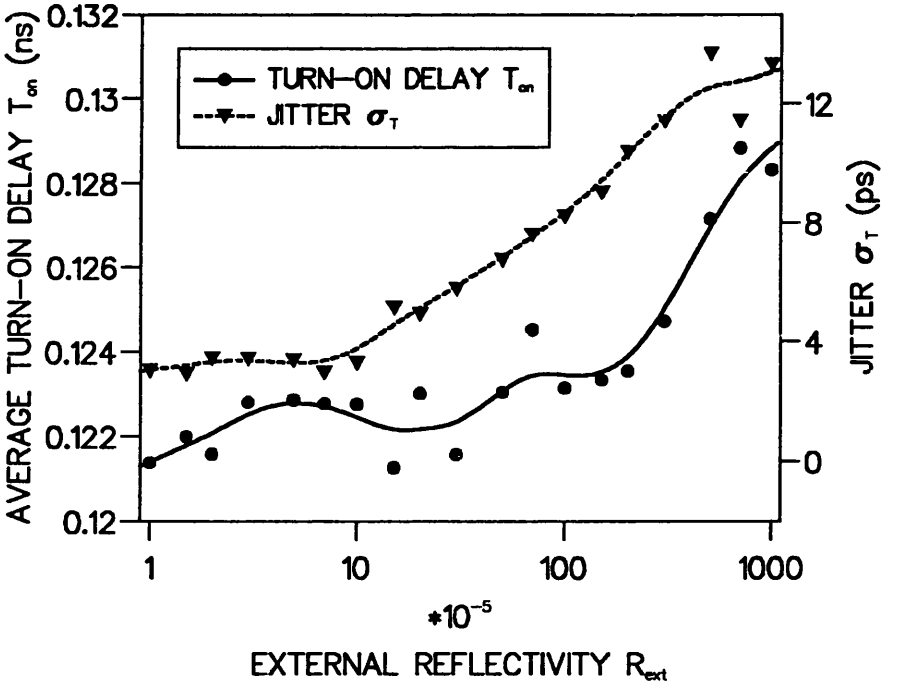

Fig. 2.11: Average Turn-on Delay T_{on} and Jitter σ_T for Increasing External Reflectivity R_{ext} for the Independent Pulses Modulation Format ($I=1.1I_{th}$).

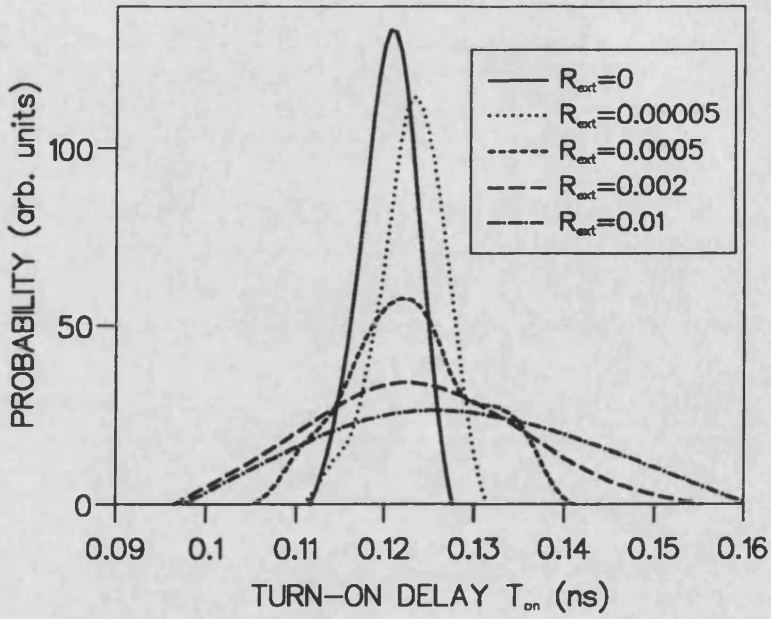

Fig. 2.12: Turn-on Delay Distribution for the Independent Pulses Modulation Format for Increasing External Reflectivity R_{ext} ($I=1.1I_{th}$).

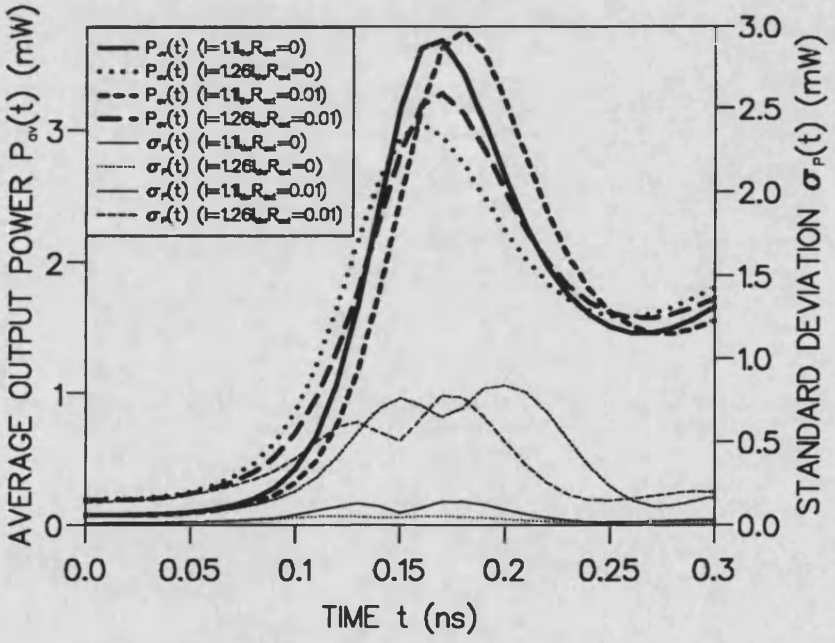

Fig. 2.13: Mean Intensity Evolutions $P_{av}(t)$ and the Standard Deviation $\sigma_P(t)$ of the Intensity Under the Independent Pulses Modulation without Optical Feedback and with Optical Feedback from an External Reflectivity of R_{ext}=0.01 at Bias Currents of 10% and 26% Above Threshold.

To explain these results it is recalled that optical feedback produces large amounts of intensity noise in the optical output power. The intensity noise is induced by the behaviour of the laser when external optical feedback is introduced. This causes the output power pdf to be wider. Hence the spread of possible starting points for the carrier and photon density rises during the turn-on process is wider also, resulting in a broader turn-on delay pdf, seen as an increase in the jitter. It is well known that optical feedback increases the average output power by a small amount. Therefore, on first inspection, the average turn-on time would be expected to be decreased by external optical feedback, due to the smaller increase in carrier and photon densities required for the output power to exceed the logic decision power. Fig. 2.14 shows the output power pdf for a bias current 26% above threshold, which corresponds to an average output power of 0.2 mW. When no optical feedback is present the output power pdf is approximately gaussian. The width of the output power pdf is approximately equal to the mean value, which agrees with experiments performed at relatively low output power [40]. However, the output power pdf is no longer approximately gaussian when reflections induce large output power fluctuations. This changed shape is because the time to recover to the average value is longer when the output light power is displaced below the average than when it is displaced above it. Hence the temporal power waveform appears to be spiked, as seen in fig. 2.15, with longer periods of below average power between the spikes, resulting in the non-gaussian output power pdf's in fig. 2.14 as external optical feedback increases. Therefore, since the average power has increased, the turn-on delay when starting from the average output power is decreased. However, since external optical feedback causes more time to be spent below the average output power than above it, the average turn-on delay is increased. The non-gaussian output power pdf at high optical feedback does not prevent the turn-on delay pdf from being approximately gaussian in shape. The sudden broadening of the turn-on delay pdf when the external reflectivity exceeds 10^{-4} is caused by the high levels of intensity noise that occur as the laser enters the coherence collapse regime.

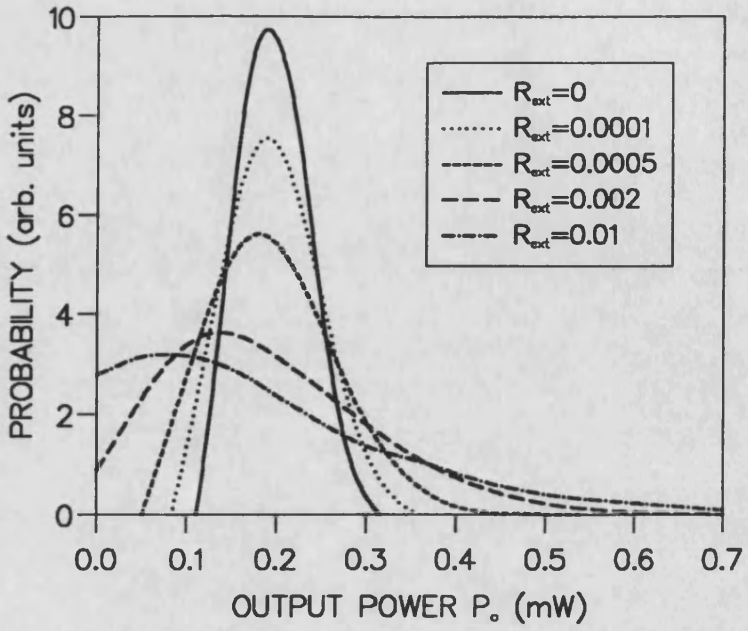

Fig. 2.14: Output Power Distribution for Increasing External Reflectivity R_{ext} at Constant Current ($I=1.26I_{th}$, $P_o=0.2$ mW).

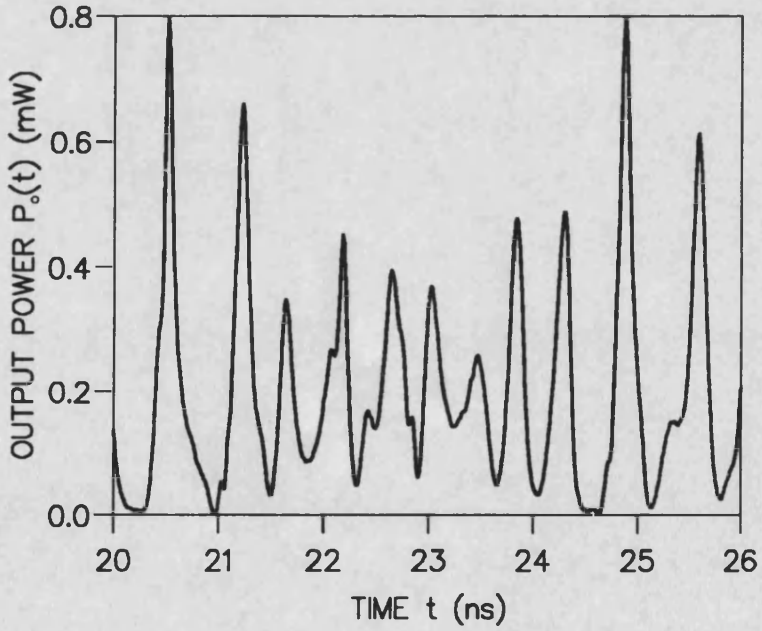

Fig. 2.15: Output Power Waveform for Constant Current and Moderate Optical Feedback ($I=1.26I_{th}$, $P_o=0.2$ mW, $R_{ext}=0.01$).

2.7 Turn-on Delay Jitter with External Feedback for Periodically Modulated Lasers.

For periodically modulated lasers a data stream of alternating logic zero and logic one data bits is used to modulate the laser. The starting point for the power rise in each optical pulse is determined by the relaxation oscillations from the previous pulse. Fig. 2.16 shows how the average turn-on delay T_{on} and jitter σ_T change with increasing external optical feedback, for a bias current 26% above threshold and a modulation frequency of 2 GHz. The average turn-on delay is increased by a few percent by the optical feedback. Fig. 2.18 shows the same parameters for 10% above threshold modulated at 2 GHz. At this lower bias current and also at higher modulation frequencies the average turn-on delay decreases as optical feedback increases, but the change from that where no optical feedback is present is not as large as in the high bias current, low modulation frequency case of fig. 2.16. Increasing the modulation frequency changes the initial starting point for the power increase in the next optical pulse by allowing less of the relaxation oscillation to occur between pulses. The turn-on delay jitter increases dramatically as the level of external optical feedback increases (fig. 2.18) [35]. The jitter increase is larger at higher bias currents (fig. 2.16). Further investigations show that the jitter increase is larger at higher modulation frequencies. The graphs of average turn-on delay and jitter do not show smooth changes as the level of optical feedback is increased. A possible reason for the peaks and troughs in the curves is that the optical feedback-induced intensity noise does not always increase smoothly as the external reflectivity increases [31]. This is also seen in the intensity noise investigations in chapter 5 and 6.

The above effects are seen in the changing shape of the turn-on delay probability distribution function (pdf) as optical feedback increases, shown in figs. 2.17 and 2.19, for a bias current 26% and 10% above threshold respectively. The modulation frequency is 2 GHz in both cases. The turn-on delay pdf remains approximately gaussian for low feedback levels but changes to a very wide gaussian pdf at high optical feedback levels. There appears to be a transition stage for moderate optical feedback levels where the turn-on delay pdf becomes highly non-gaussian in shape and can even become double peaked. The levels of optical feedback at which the turn-on delay pdf's are highly non-gaussian are the same at which the average turn-on delay and jitter graphs do not show smooth changes. Hence the two observations are likely to be linked. A multiple peaked pdf means that there is a an effect taking place which causes two or more most likely starting points for the power rise in the pulses. The increase in jitter caused by optical feedback is again resultant from the large amounts

of intensity noise that optical feedback introduces.

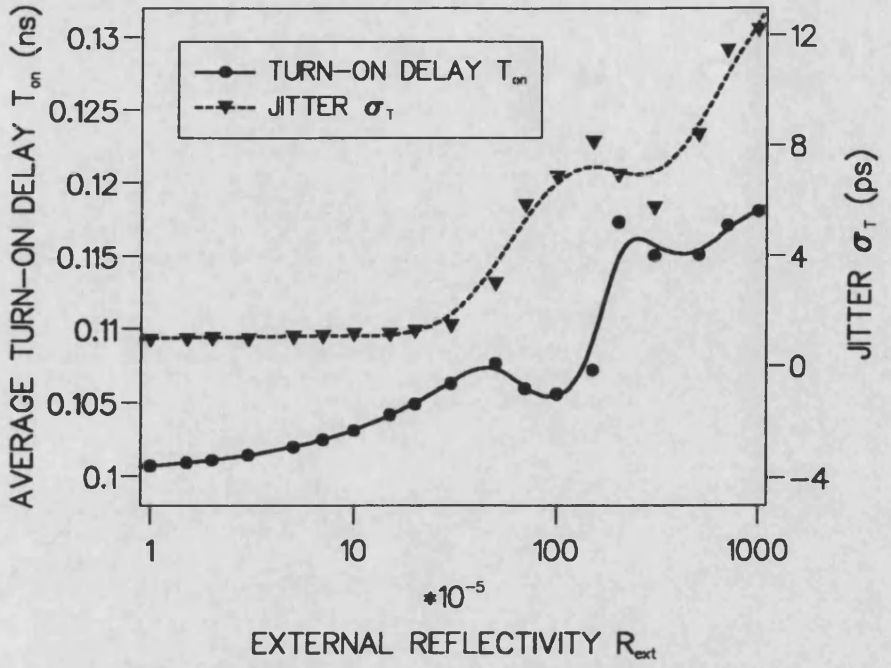

Fig. 2.16: Average Turn-on Delay T_{on} and Jitter σ_T for Increasing External Reflectivity R_{ext} for the Periodic Modulation Format ($I=1.26I_{th}$, $f_m=2$ GHz).

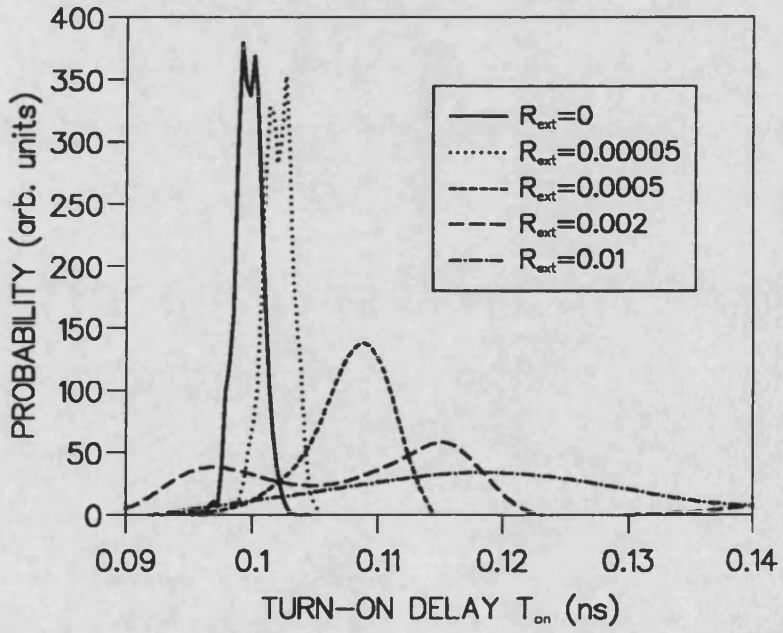

Fig. 2.17: Turn-on Delay Distribution for the Periodic Modulation Format for Increasing External Reflectivity R_{ext} ($I=1.26I_{th}$, $f_m=2$ GHz).

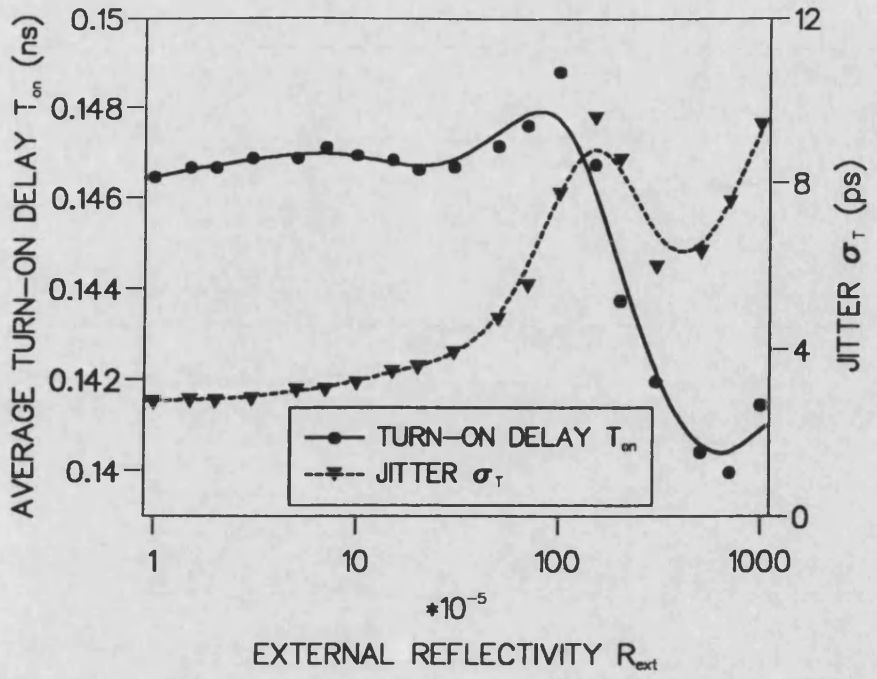

Fig. 2.18: Average Turn-on Delay T_{on} and Jitter σ_T for Increasing External Reflectivity R_{ext} for the Periodic Modulation Format ($I=1.1I_{th}$, $f_m=2$ GHz).

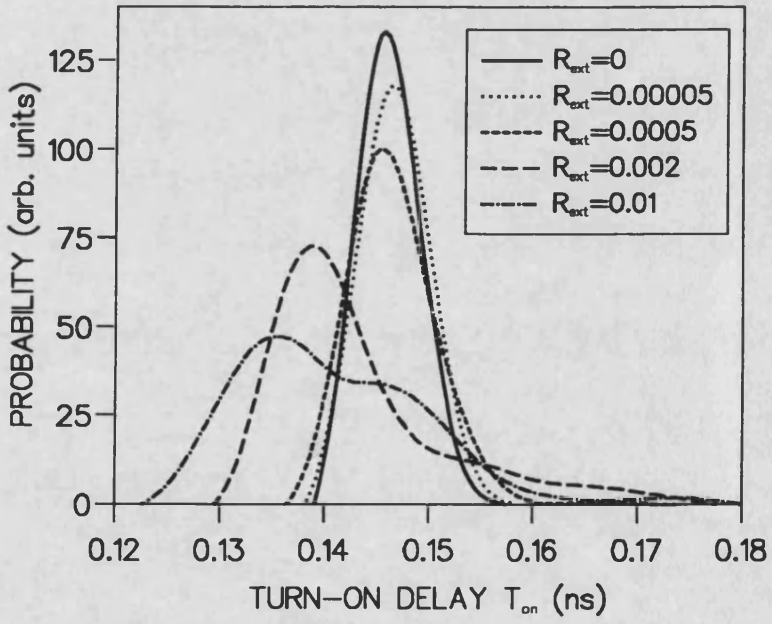

Fig. 2.19: Turn-on Delay Distribution for the Periodic Modulation Format for Increasing External Reflectivity R_{ext} ($I=1.1I_{th}$, $f_m=2$ GHz).

The mean intensity evolution $P_{av}(t)$ and the intensity standard deviation $\sigma_P(t)$ are shown in fig. 2.20 for bias currents 10% and 26% above threshold. The graph shows the evolutions with and without optical feedback and looks similar to that for the gain-switched modulation format, but the spread in the evolutions is wider. The intensity standard deviation during optical feedback has similar values to that under gain-switched modulation, even though the intensity standard deviation without optical feedback is larger in the periodic modulation regime.

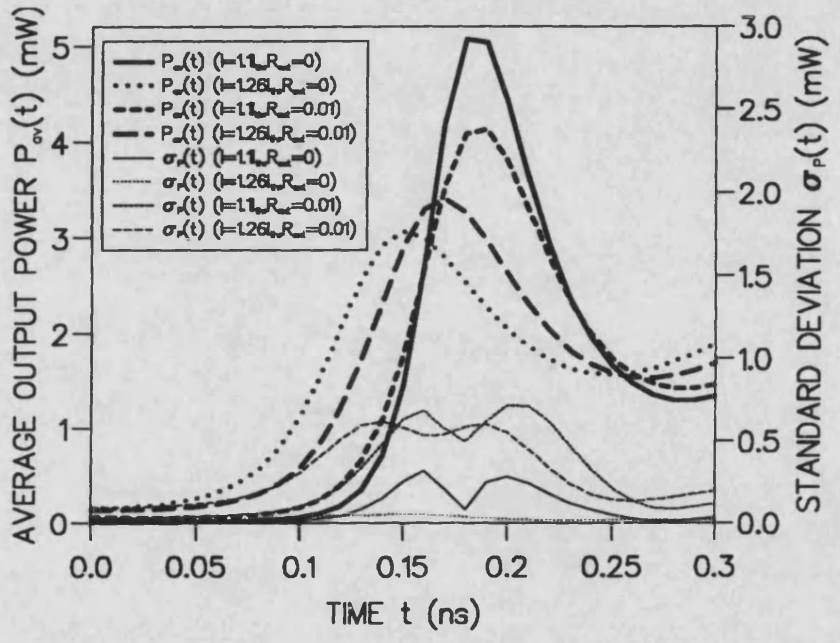

Fig. 2.20: Mean Intensity Evolutions $P_{av}(t)$ and the Standard Deviation $\sigma_P(t)$ of the Intensity Under Periodic Modulation without Optical Feedback and with Optical Feedback from an External Reflectivity of R_{ext}=0.01 at Bias Currents 10% and 26% Above Threshold (f_m=2 GHz).

2.8 Turn-on Delay Jitter with External Feedback for Pseudorandomly Modulated Lasers.

For pseudorandomly modulated lasers a data stream of random data bits is used to modulate the laser. Fig. 2.21 shows how the average turn-on delay and jitter change with increasing external optical feedback, for a bias current 26% above threshold and modulated at 2 GHz. Fig. 2.23 shows the same parameters for 10% above threshold modulated at 2 GHz. The average turn-on delay increases by a few percent for high bias current (fig. 2.21). At low bias currents the turn-on delay is virtually unchanged (fig. 2.23). At high bias currents the turn-on delay jitter increases dramatically as the level of optical feedback increases.

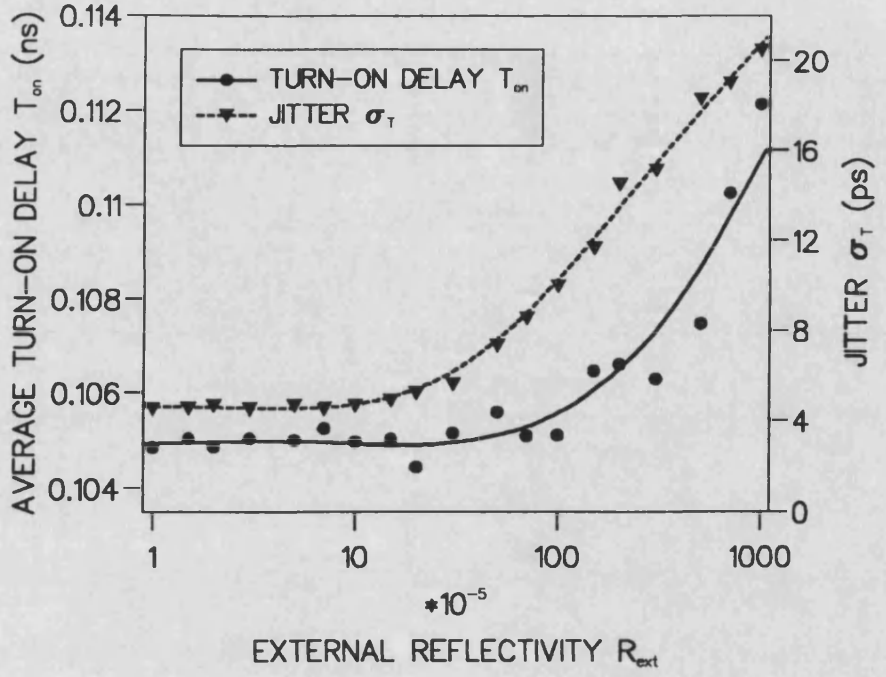

Fig. 2.21: Average Turn-on Delay T_{on} and Jitter σ_T for Increasing External Reflectivity R_{ext} for the Pseudorandom Modulation Format ($I=1.26I_{th}$, f_m=2 GHz).

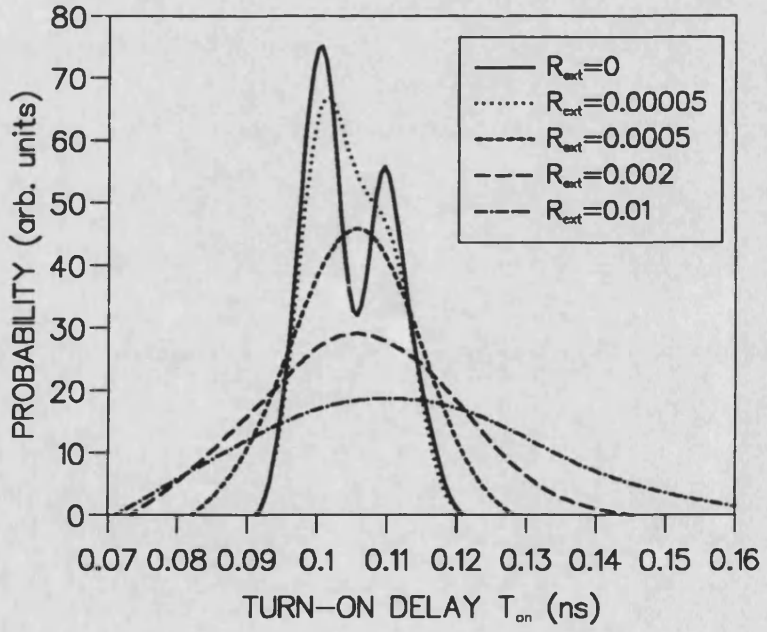

Fig. 2.22: Turn-on Delay Distribution for the Pseudorandom Modulation Format for Increasing External Reflectivity R_{ext} ($I=1.26I_{th}$, f_m=2 GHz).

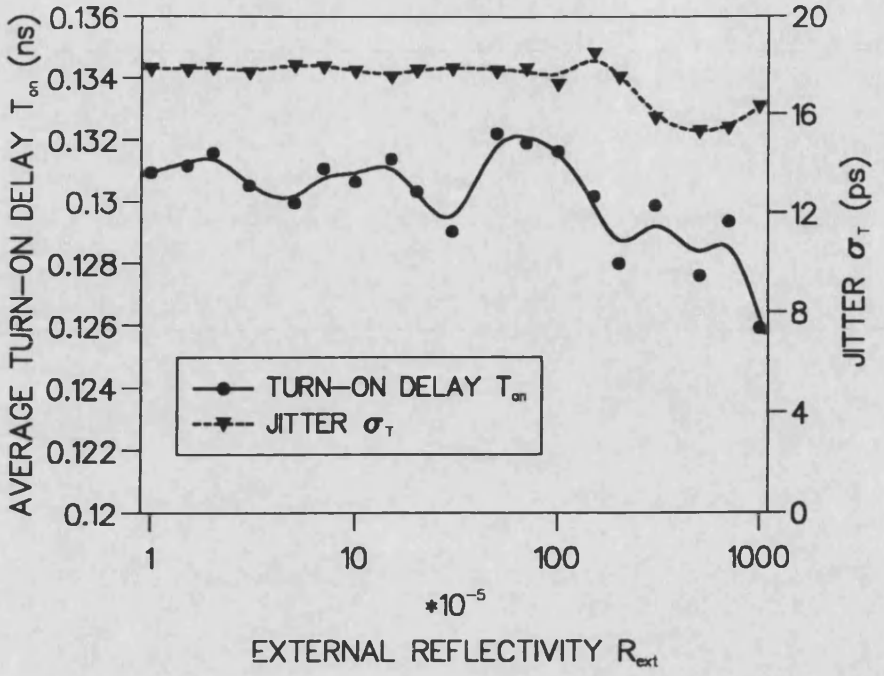

Fig. 2.23: Average Turn-on Delay T_{on} and Jitter σ_T for Increasing External Reflectivity R_{ext} for the Pseudorandom Modulation Format ($I=1.1I_{th}$, $f_m=2$ GHz).

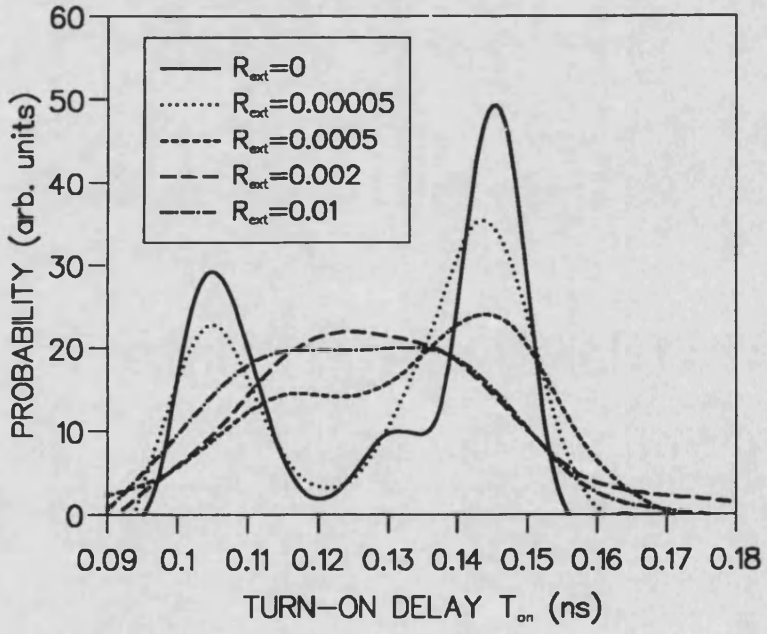

Fig. 2.24: Turn-on Delay Distribution for the Pseudorandom Modulation Format for Increasing External Reflectivity R_{ext} ($I=1.1I_{th}$, $f_m=2$ GHz).

The increase in jitter is greater at lower modulation frequency, and is less than in the gain-switching and periodic modulation regimes. At low bias currents the jitter remains virtually unchanged. The value of the jitter without any optical feedback at a bias current 10% above threshold is 19 ps. This can be compared to an experimental value of 32 ps [5], under pseudorandom modulation conditions at 1 GHz. The relatively lower value obtained in the simulation may be attributed to the presence of less spontaneous emission noise. This may occur by either using a lower value for the spontaneous emission factor, or by operating at a bias current further above threshold.

The above effects are seen in the changing shape of the turn-on delay probability distribution function (pdf) as optical feedback increases, shown in figs. 2.22 and 2.24. At the modulation conditions investigated the turn-on delay pdf is double peaked without external feedback. The double peaked distribution occurs because the modulation frequency is sufficiently high to prevent the carrier density relaxing to its steady state value during a single logic bit. Hence different turn-on delays occur, depending on the number of preceding zero bits, and double peaks known as pattern effects [11,14,19-21] are seen in the turn-on delay pdf without external optical feedback present. At lower modulation frequencies the carrier density reaches its steady state value during a single logic zero bit, thus preventing pattern effects and giving a single peaked turn-on delay pdf. Such pattern effects also depend upon the device parameters and particularly the carrier lifetime τ_{sp}. For shorter carrier lifetimes pattern effects will occur only at higher modulation frequencies. The two peaks are broadened by external optical feedback but remain distinguishable for low external reflectivities. For high external reflectivities the turn-on delay pdf is changed into an approximately gaussian shaped pdf because the peaks are broadened so much that they are destroyed, but at the expense of increased jitter. At low bias currents the jitter is already very large and hence optical feedback does not increase it significantly. Whether the average turn-on delay increases or decreases with optical feedback is dependent on whether the single peaked distribution that remains after the pattern effects have been destroyed lies nearer the faster or slower of the two original peaks. The increase in jitter caused by optical feedback is again resultant from the large amounts of intensity noise that optical feedback introduces. Therefore moderate amounts of optical feedback can be used to prevent the pattern effects which may occur at some combinations of modulation frequency and operating conditions [34,35].

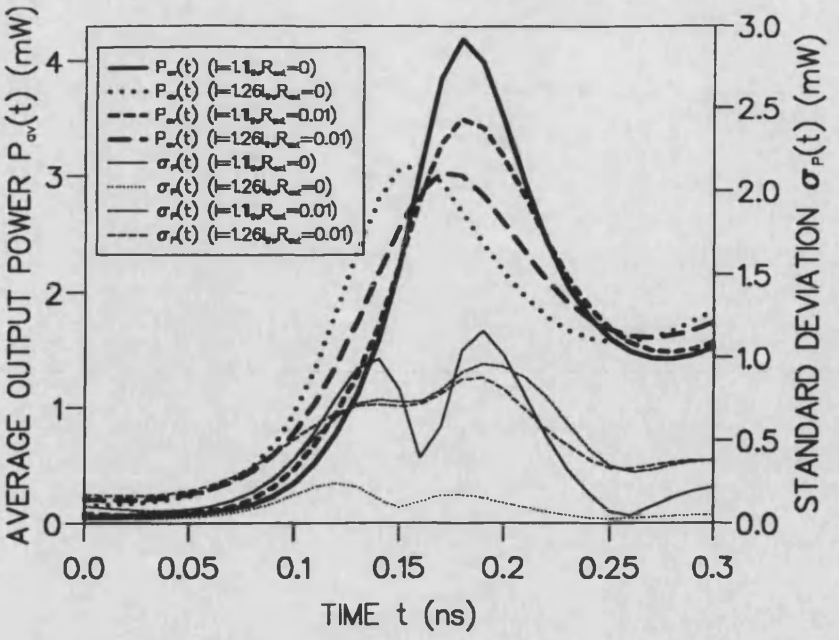

Fig. 2.25: Mean Intensity Evolutions $P_{av}(t)$ and the Standard Deviation $\sigma_P(t)$ of the Intensity Under Pseudorandom Modulation without Optical Feedback and with Optical Feedback from an External Reflectivity of R_{ext}=0.01 at Bias Currents of 10% and 26% Above Threshold (f_m=2 GHz).

The mean intensity evolution $P_{av}(t)$ and the intensity standard deviation $\sigma_P(t)$ are shown in fig. 2.25 for bias currents 10% and 26% above threshold. The graph shows the evolutions with and without optical feedback. The mean intensity evolutions show that optical feedback can increase or decrease the average turn-on delay. At the lower bias current of 10% above threshold the intensity standard deviation is already very large and is not altered very much by the addition of optical feedback. This agrees with the results of fig. 2.23. For the higher bias current of 26% above threshold the intensity standard deviation is small without optical feedback but increases when optical feedback is present. This is seen as an increase of the jitter in fig. 2.21.

At lower bias currents the jitter is already large due to spontaneous emission noise, therefore the increase in jitter due to optical feedback is less at lower bias currents. The effect of changing the logic zero state bias current is shown in fig. 2.26 for fixed optical feedback of external reflectivity, R_{ext}=0.005. The modulation frequency is 2 GHz. It can be seen that the average turn-on delay with optical feedback is usually larger than when no optical feedback is present. The jitter without optical feedback decreases as the bias current increases. However, the jitter with optical feedback increases as the bias current increases. At low bias currents the jitter is already relatively large due to spontaneous emission. Therefore the increase in jitter due to optical feedback is larger at high bias currents than at low bias currents. This leads to

the increasing difference between the jitter with and without optical feedback seen in fig. 2.26.

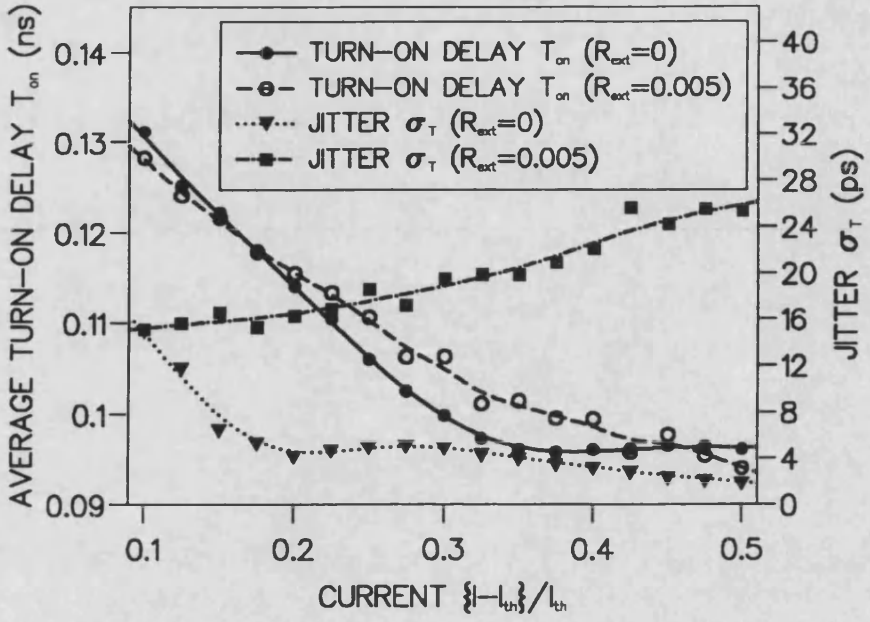

Fig. 2.26: Average Turn-on Delay T_{on} and Jitter σ_T with (R_{ext}=0.005) and Without Optical Feedback (R_{ext}=0) for Increasing Bias Current I (f_m=2 GHz).

2.9 Implications for Bit-Error-Rate and System Performance.

The bit-error-rate (BER) can be calculated from the turn-on delay probability distribution or the jitter. Errors in the transmitted data due to the turn-on delay jitter of the laser can occur when the turn-on delay is too long for the pulse to be detected by the receiver. This is illustrated in fig. 2.27. If a turn-on delay approaches or exceeds the modulation bit duration then an error is detected at the receiver. The error probability can alternatively be interpreted as a power penalty in the communication system. The probability of an error is represented as the shaded area in the long turn-on pdf delay tail of fig. 2.27. It is not strictly the shape of the turn-on delay pdf that is important. The jitter-induced error rate is dependent on the tails of the turn-on delay pdf. By approximating the turn-on delay pdf as a gaussian shape with easily calculated tails, it is possible to calculate the system performance degradation due to jitter [41-49].

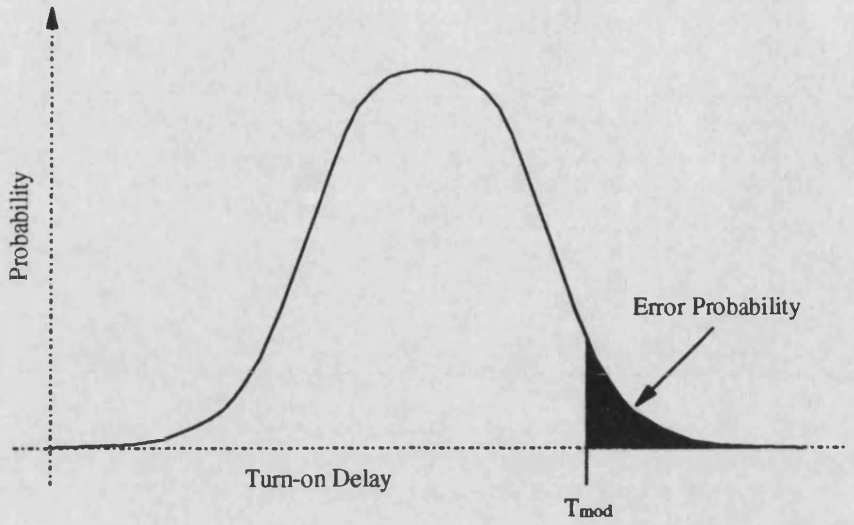

Fig 2.27: How Data Errors Occur from Turn-on Delay Jitter.

2.10 Conclusion.

This chapter has investigated the effect of external optical feedback on the turn-on delay characteristics of typical semiconductor lasers used in digital optical communications systems. Chaotic behaviour introduced by the external optical feedback introduces additional intensity noise to that caused by spontaneous emission. The result is increased turn-on delay jitter in all of the gain-switching, periodic and pseudorandom modulation formats. The jitter is increased dramatically by high external reflectivity. The average turn-on delay is increased by optical feedback during the gain-switching modulation format. During periodic modulation and the more practical pseudorandom modulation regime the effect on the average turn-on delay is dependant on the modulation conditions, with the average turn-on delay either increasing or decreasing as the optical feedback increases. The increase in jitter is greatest at higher bias currents. If under pseudorandom modulation the modulation conditions result in the turn-on delay pdf to be twin peaked without feedback, then moderate amounts of external optical feedback can change the pdf into a single peaked pdf. Thus optical feedback can prevent the pattern effect from occurring, but at the expense of a very large jitter. The increase in turn-on delay jitter caused by external optical feedback is less when the turn-on delay distribution is initially double peaked since in this case a large jitter is already exhibited.

Chapter 2 References.

[1] M M Choy, P L Liu, P W Shumate, T P Lee, and S Tsuji, "Measurements of Dynamic Photon Fluctuations in a Directly Modulated 1.5-μm InGaAsP Distributed Feedback Laser", Appl. Phys. Lett., Vol. 47, No. 5, pp. 448-450, 1985.

[2] E H Böttcher, K Ketterer, and D Bimberg, "Turn-on Delay Time Fluctuations in Gain-Switched AlGaAs/GaAs Multiple-Quantum-Well Lasers", J. Appl. Phys., Vol. 63, No. 7, pp. 2469-2471, 1988.

[3] W H Cheng, J M Dugan, J C Miller, D Renner, T C McDermott, and C B Su, "1.3 μm InGaAsP Fabry-Perot Lasers with Reduced Pulse Jitter and Power Penalty", Electron. Lett. Vol. 28, No. 14, pp. 1337-1338, 1992.

[4] A D'Ottavi, A Mecozzi, P Spano, and P Piazzolla, "Time Jitter in Multimode Fabry-Perot Laser Diodes", Appl. Phys. Lett., Vol. 53, No. 24, pp. 2362-2364, 1988.

[5] T M Shen, "Timing Jitter in Semiconductor Lasers Under Pseudorandom Word Modulation", IEEE J. Lightwave Tech., Vol. 7, No. 9, pp. 1394-1399, 1989.

[6] P Spano, A D'Ottavi, A Mecozzi, and B Daino, "Experimental Observation of Time Jitter in Semiconductor Laser Turn-on", Appl. Phys. Lett., Vol. 52, No. 26, pp. 2203-2204, 1988.

[7] A G Weber, W Ronghan, E H Böttcher, M Schell, and D Bimberg, "Measurement and Simulation of the Turn-on Delay Time Jitter in Gain-Switched Semiconductor Lasers", IEEE J. Quantum Electron., Vol. 28, No. 2, pp. 441-445, 1992.

[8] P Spano, A D'Ottavi, A Mecozzi, B Daino, and S Piazzolla, "Experimental Measurements and Theory of First Passage Time in Pulse-Modulated Semiconductor Lasers", IEEE J. Quantum Electron., Vol. 25, No. 6, pp. 1440-1449, 1989.

[9] E Sano, M Shinagawa, and R Takahashi, "Theoretical Analysis of Timing Jitter in Gain-Switched Semiconductor Lasers", Appl. Phys. Lett., Vol. 55, No. 6, pp. 522-524, 1989.

[10] P K Pepeljugoski, D M Cutrer and K Y Lau. "Parametric Dependence of Timing Jitter in Gain-Switched Semiconductor Lasers", Appl. Phys. Lett. Vol. 63, No. 26, pp. 3556-3558, 1993.

[11] A Sapia, P Spano, C R Mirasso, P Colet, and M San Miguel, "Pattern Effects in Time Jitter of Semiconductor Lasers", Appl. Phys. Lett., Vol. 61, No. 15, pp. 1748-1750, 1992.

[12] S E Miller, "Turn-on Jitter in Nearly Single-Mode Injection Lasers", IEEE J. Quantum Electron., Vol. 22, No. 1, pp. 16-19, 1986.

[13] C R Mirasso, P Colet, and M San Miguel, "Pulse Statistics in Single-Mode Semiconductor Lasers Modulated at Gigahertz Rates", Optics Lett., Vol. 16, No. 22, pp. 1753-1755, 1991.

[14] C R Mirasso, P Colet, and M San Miguel, "Dependence of Timing Jitter on Bias Level for Single-Mode Semiconductor Lasers Under High Speed Modulation", IEEE J. Quantum Electron., Vol. 29, No. 1, pp. 23-32, 1993.

[15] M Jinno, "Correlated and Uncorrelated Timing Jitter in Gain-Switched Laser Diodes", IEEE Phot. Technol. Lett., Vol. 5, No. 10, pp. 1140-1143, 1993.

[16] A Valle, M Rodriguez, and C R Mirasso, "Analytical Calculation of Timing Jitter in Single-Mode Semiconductor Lasers Under Fast Periodic Modulation", Optics Lett., Vol. 17, No. 21, pp. 1523-1525, 1992.

[17] S Balle, C R Mirasso, A Sapia and P Spano, "Analytical Results of the Switch on Statistics in Distributed Feedback Laser Diodes by Short Triangular Pulses", Appl. Phys. Lett., Vol. 63, No. 13, pp. 1721-1723, 1993.

[18] C R Mirasso and E Hernández-Garcia, "Effects of Current Modulation on Single-Mode Semiconductor Lasers in a Short External Cavity", Submitted to IEEE Phot. Technol. Lett., 1994.

[19] C R Mirasso, P Colet, and M San Miguel, "Pseudorandom Word Modulation of Single-Mode Semiconductor Lasers at GHz Rates", IEE Proc.-Part J, Vol. 140, No. 1, pp. 26-29, 1993.

[20] P Colet, C R Mirasso, and M San Miguel, "Memory Diagram of Single-Mode Semiconductor Lasers", IEEE J. Quantum Electron., Vol. 29, No. 6, pp. 1624-1630, 1993.

[21] C R Mirasso, A Valle, L Pesquera, and P Colet, "Simple Method for Estimating the Memory Diagram in Single Mode Semiconductor Lasers", IEE Proc.-Optoelectron., Vol. 141, No. 2, pp. 109-113, 1994.

[22] K Petermann, "Laser Diode Modulation and Noise", Kluwer Academic, 1988.

[23] R Lang and K Kobayashi, "External Optical Feedback Effects on Semiconductor Injection Laser Properties", IEEE J. Quantum Electron., Vol. 16, No. 3, pp. 347-355, 1980.

[24] R W Tkach and A R Chraplyvy, "Regimes of Feedback Effects in 1.5-μm Distributed Feedback Lasers", IEEE J. Lightwave Tech., Vol. 4, No. 11, pp. 1655-1661, 1986.

[25] N Schunk and K Petermann, "Numerical Analysis of the Feedback Regimes for a Single-Mode Semiconductor Laser with External Feedback", IEEE J. Quantum Electron., Vol. 24, No. 7, pp. 1242-1247, 1988.

[26] J Mørk, J Mark, and B Tromborg, "Route to Chaos and Competition Between Relaxation Oscillations for a Semiconductor Laser with Optical Feedback", Phys. Rev. Lett., Vol. 65, No. 16, pp. 1999-2002, 1990.

[27] T B Simpson, J M Liu, A Gavrielides, V Kovanis, and P M Alsing, "Period-Doubling Route to Chaos in a Semiconductor Laser Subject to Optical Injection", Appl. Phys. Lett., Vol. 64, No. 26, pp. 3539-3541, 1994.

[28] B Tromborg and J Mørk, "Stability Analysis and the Route to Chaos for Laser Diodes with Optical Feedback", IEEE Phot. Technol. Lett., Vol. 2, No. 8, pp. 549-552, 1990.

[29] J Mørk, B Tromborg, and J Mark, "Chaos in Semiconductor Lasers with Optical Feedback: Theory and Experiment", IEEE J. Quantum Electron., Vol. 28, No. 1, pp. 93-108, 1992.

[30] H Li, J Ye, and J G McInerney, "Detailed Analysis of Coherence Collapse in Semiconductor Lasers", IEEE J. Quantum Electron., Vol. 29, No. 9, pp. 2421-2432, 1993.

[31] B R Clarke, "The Effect of Reflections on the System Performance of Intensity Modulated Laser Diodes", IEEE J. Lightwave Tech., Vol. 9, No. 6, pp. 741-749, 1991.

[32] D M Byrne, D Maclean, and R Plumb, "Optical Feedback-Induced Noise in Pigtailed Laser Diode Modules", IEEE Phot. Technol. Lett., Vol. 3, No. 10, pp. 891-894, 1991.

[33] N Schunk and K Petermann, "Measured Feedback-Induced Intensity Noise for 1.3 μm DFB Laser Diodes", Electron. Lett., Vol. 25, No. 1, pp. 63-64, 1989.

[34] H J Wu and H C Chang, "Turn-on Jitter in Semiconductor Lasers with Moderate Reflecting Feedback", IEEE Phot. Technol. Lett., Vol. 4, No. 4, pp. 339-342, 1992.

[35] L N Langley and K A Shore, "The Effect of External Optical Feedback on Timing Jitter in Modulated Laser Diodes", IEEE J. Lightwave Technol., Vol. 11, No. 3, pp. 434-441, 1993.

[36] L N Langley and K A Shore, "The Effect of External Optical Feedback on the Turn-on Delay Statistics of Laser Diodes Under Pseudorandom Modulation", IEEE Phot. Technol. Lett., Vol. 4, No. 11, pp. 1207-1209, 1992.

[37] E Hernández-García, C R Mirasso, K A Shore, and M San Miguel, "Turn-on Jitter of External-Cavity Semiconductor Lasers", IEEE J. Quantum Electron., Vol. 30, No. 2, pp. 241-248, 1994.

[38] M Schell, W Utz, D Huhse, J Kässner, and D Bimberg, "Reduction of the Turn-On Delay Jitter of a Gain-Switched Semiconductor Laser by Self-Seeding", Submitted to Appl. Phys. Lett., 1994.

[39] N Schunk and K Petermann, "Noise Analysis of Injection-Locked Semiconductor Lasers", IEEE J. Quantum Electron., Vol. 22, No. 5, pp. 642-650, 1986.

[40] P L Liu, L E Fencil, J S Ko, P I Kaminow, T P Lee, and C A Burrus, "Amplitude Fluctuations and Photon Statistics of InGaAsP Injection Lasers", IEEE J. Quantum Electron., Vol. 19, No. 9, pp. 1348-1351, 1983.

[41] G P Agrawal and T M Shen, "Power Penalty Due to Decision-Time Jitter in Optical Communication Systems", Electron. Lett., Vol. 22, No. 9, pp. 450-451, 1986.

[42] J J O'Reilly, J R F da Rocha, and K Schumacher, "Influence of Timing Errors on the Performance of Direct-Detection Optical-Fibre Communication Systems", IEE Proc.-Part J, Vol. 132, No. 6, pp. 309-313, 1985.

[43] K Schumacher and J J O'Reilly, "Power Penalty Due to Jitter on Optical Communication Systems", Electron. Lett., Vol. 23, No. 14, pp. 718-719, 1987.

[44] A Cartaxo and A de Albuquerque, "Influence of the Various Types of Noise on Jitter Performance in Binary Direct Detection Optical Communications", IEE Proc.-Part J, Vol. 137, No. 6, pp. 375-378, 1990.

[45] K Schumacher and J J O'Reilly, "Distribution Free Bound on the Performance of Optical Communication Systems in the Presence of Jitter", IEE Proc.-Part J, Vol. 136, No. 2, pp. 129-136, 1989.

[46] G P Agrawal and T M Shen, "Effect of Fiber-Far-End Reflections on the Bit Error Rate in Optical Communication with Single-Frequency Semiconductor Lasers", IEEE J. Lightwave Tech., Vol. 4, No. 1, pp. 58-63, 1986.

[47] N A Olsson, W T Tsang, H Temkin, N K Dutta, and R A Logan, "Bit-Error-Rate Saturation Due to Mode-Partition Noise Induced by Optical Feedback in 1.5-μm Single Longitudinal-Mode C^3 and DFB Semiconductor Lasers", IEEE J. Lightwave Tech., Vol. 3, No. 2, pp. 215-218, 1985.

[48] M Shikada, S Takano, S Fujita, I Mito, and K Minemura, "Evaluation of Power Penalties Caused by Feedback Noise of Distributed Feedback Laser Diodes", IEEE J. Lightwave Tech., Vol. 6, No. 5, pp. 655-659, 1988.

[49] T M Shen and G P Agrawal, "Computer Simulation and Noise Analysis of the System Performance of 1.55-μm Single-Frequency Semiconductor Lasers", IEEE J. Lightwave Tech., Vol. 5, No. 5, pp. 653-659, 1987.

Chapter 3:

An Iterative Travelling Wave Model for External Cavity Laser Diodes.

3.1 Introduction to External Cavity Laser Diodes.

In this chapter a model to describe the dynamics of external cavity laser diodes is developed. The model is developed for the case of strong conventional optical feedback (sections 3.3-3.7), and is adapted for the cases of the external cavity FM diode laser (sections 3.8 and 3.9) and strong phase conjugate optical feedback (sections 3.10 and 3.11). In chapter 4 the various adaptations of the model for the above cases are used to investigate a variety of effects in external cavity laser diodes.

An external cavity laser diode is shown in fig. 3.1. In chapter 2 unwanted weak optical feedback in an optical communication system was considered. Here the case of light deliberately returned into the laser is studied. When the external reflectivity is large (say greater than 10%), the operating regime is known as strong optical feedback. The laser output can be monitored through the laser facet r_1 or through the external mirror if it is not 100% reflective. The facet r_2 forming the boundary between the laser internal cavity and the external cavity may or may not be anti-reflection (AR) coated. To form an anti-reflection coating a thin layer (one quarter of a wavelength thick) of a suitable material is placed on the laser facet such that the reflection is lowered to approximately zero. In this case, the optical feedback from the external mirror is strong enough so that the dominant lasing cavity is defined between the laser facet r_1 and the external mirror, hence the name External Cavity Diode Laser (ECDL) [1-13].

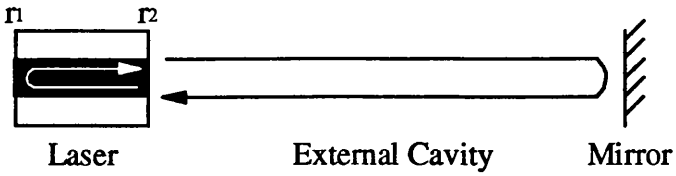

Fig. 3.1: An External Cavity Laser Showing Strong Optical Feedback From a Mirror.

Figs. 3.1 and 3.2 illustrate some possible configurations of external cavity laser diodes. An external grating can be used instead of a mirror [14-39], thus adding the benefit of wavelength selection of the feedback light to force the laser to operate in a specific longitudinal mode. Also, by rotating the grating the lasing wavelength can be tuned [29-39]. Integrated external cavity laser diodes [40-49] have been made with a short external cavity on the laser chip itself. The external cavity can also be formed by coupling the laser to an optical fibre with a high reflection coating on the fibre far end [50-53].

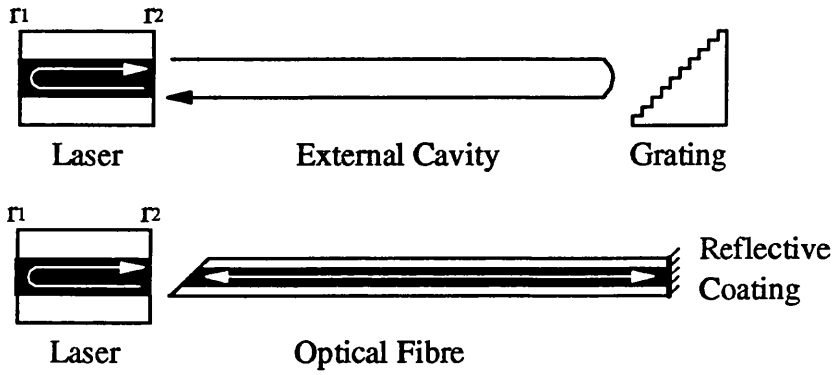

Fig. 3.2: External Cavity Formed Using a Grating or Optical Fibre.

Sometimes it is necessary to use a curved mirror to focus as much as possible of the feedback light back into the laser. For all but the shortest external cavities, lenses are usually required to collimate the light so as to increase the coupling between the laser and external mirror. It is also possible to use a phase conjugate mirror, as shown in fig. 3.3. Phase conjugate mirrors produce a reflected beam which is reversed in phase with respect to the incident beam. Thus there is no net external cavity round trip phase change. Also, since the phase conjugate mirror returns incident beams along their original path nearly all of the light is returned back into the laser without alignment problems. This gives the phase conjugate mirror the advantage of having a high reflectivity (of greater than unity if required). A more detailed discussion of optical feedback from phase conjugate mirrors is given in chapters 6 and 7. Strong optical feedback from a phase conjugate mirror is considered later in the present chapter.

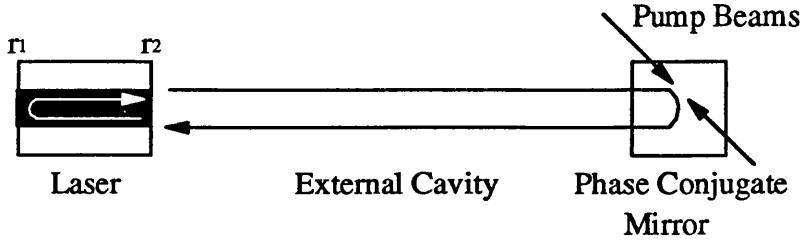

Fig. 3.3: External Cavity Laser Formed Using a Phase Conjugate Mirror.

The use of external cavity laser diodes brings the further benefit of allowing the insertion of optical elements into the laser cavity. In such a way modulation of the light within the lasing cavity can be accomplished. One such laser is the external cavity frequency modulated laser [54-56] described later in this chapter. External cavities are also used for resonant modulation (see chapter 4) and mode locking of diode lasers [57].

3.2 Characteristics of External Cavity Laser Diodes.

The addition of an external mirror can increase the effective reflectivity of the laser facet, causing more light to be fed back into the laser active region than would occur from the solitary laser facet alone. In this case, there is a smaller loss of light from the laser through the facets. Hence the gain required to reach the lasing threshold is less for an external cavity laser than for a solitary laser. Therefore the threshold current I_{th} is decreased, allowing operation of the external cavity laser at currents below that of the solitary device. The consequence of this is that for a fixed injection current the output power P_o of the external cavity laser can be considerably increased over that of the solitary laser. The decreasing of the threshold current and increasing of output power is shown in fig. 3.4, as a shifting to the left of the Light-Current characteristic [58]. It should also be noted that the Light-Current curve is also shifted by weak optical feedback but that the shift is so small that it can usually be ignored. If the length of the external cavity is longer than the coherence length of the laser then movement of the mirror has no effect on the laser behaviour. However, if the external cavity is shorter than the coherence length then the relative phase between the laser facet r_2 and the external mirror r_3 must be considered. Alternatively, A phase conjugate mirror ensures that the external reflection is always in phase with that from the laser facet, irrespective of any movement of the mirror.

The linewidth $\Delta\nu$ of solitary laser diodes is very large ($\approx$ 1 MHz) [58]. The linewidth is dependent on the level of the spontaneous noise processes within the laser, and is also inversely proportional to the output power of the device. An external cavity is often added to reduce the linewidth of the laser to considerably lower values ($\approx$10 kHz) [1-8,59-65]. For a given output power, the external cavity laser has many times more photons within it than a solitary laser. However, both lasers have the same size of active region, resulting in the same rate of spontaneous photon generation. Hence, the ratio of total photons with the laser to the spontaneously emitted photons is much

greater for an external cavity laser than for a solitary laser, resulting in a lower linewidth.

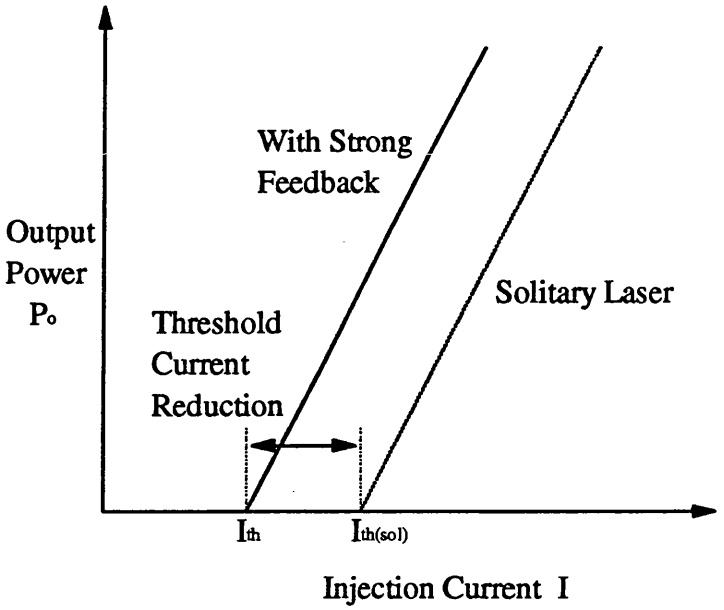

Fig. 3.4: The Changing of the Light-Current Characteristic Due to Strong Optical Feedback.

The intensity noise of the external cavity laser is also considerably different from that of the solitary laser. The external cavity causes resonances in the intensity noise at frequencies of multiples of $1/\tau_{ext}$ where τ_{ext} is the external cavity round trip delay. The intensity noise at other frequencies is suppressed. The intensity modulation response of the external cavity laser is also enhanced at multiples of $1/\tau_{ext}$ in exactly the same way as the intensity noise. This is the basis of resonant modulation beyond the relaxation oscillation frequency of the laser, which is discussed in chapter 4.

The characteristics of external cavity laser diodes result from the large levels of optical feedback from the external mirror. The optical feedback properties of laser diodes have been classified into five regions of behaviour denoted regimes I to V respectively, where strong optical feedback is denoted regime V [66,67]. These regimes have already been described in detail in chapter 1. Regimes I-IV encompass the low feedback properties of laser diodes including the so called "coherence collapse" [68-70] state of operation, and have been thoroughly investigated. Despite the fact that external cavity laser diodes are frequently used experimentally for their linewidth narrowing properties [1-8,59-65], much less work has been performed on the properties of laser diodes with strong optical feedback (regime V) [71-84]. The present work aims to rectify that deficiency.

3.3 Effective Reflectivity of Laser Facet and External Mirror.

In considering the effects of optical feedback on laser diodes, it is useful to combine the laser facet reflectivity r_2 and external mirror reflectivity r_3 into an effective reflectivity $r_R(\omega)$ as shown in fig. 3.5. In the case of strong optical feedback the contribution of many multiple reflections around the external cavity are of comparable magnitude to the first single round trip reflection. The effective reflectivity $r_R(\omega)$ takes into account the magnitudes of the facet reflectivity and the external mirror reflectivity, as well as the phase change between them. The effective reflectivity is written in terms of a summation of successive reflections around the external cavity,

$$r_R(\omega) = r_2 + r_3(1-r_2^2)\sum_{q=1}^{\infty}(-r_2 r_3)^{q-1} e^{-jq\omega\tau_{ext}}, \tag{3.1}$$

where $\omega\tau_{ext}$ is the phase change for a single trip around the external cavity, and q is the number of multiple reflections to be considered around the external cavity. The summation in (3.1) is a geometric progression with a first term of $a = e^{-j\omega\tau_{ext}}$ and a common ratio of $b = -r_2 r_3 e^{-j\omega\tau_{ext}}$. Using the sum to infinity of a converging geometric progression in the form

$$\sum_{q=0}^{\infty} ab^q = \frac{a}{1-b}, \tag{3.2}$$

gives

$$\sum_{q=1}^{\infty}(-r_2 r_3)^{q-1} e^{-jq\omega\tau_{ext}} = \frac{e^{-j\omega\tau_{ext}}}{1+r_2 r_3 e^{-j\omega\tau_{ext}}}. \tag{3.3}$$

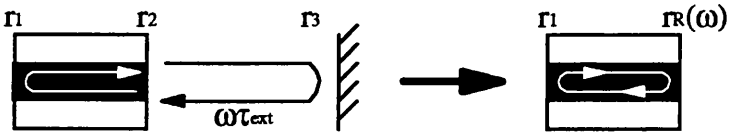

Fig. 3.5: How the Laser Facet r_2 and External Mirror r_3 can be Replaced by an Effective Reflectivity $r_R(\omega)$.

Substituting (3.3) into (3.1) and simplifying gives [73]

$$r_R(\omega) = \frac{r_2 + r_3 e^{-j\omega\tau_{ext}}}{1+r_2 r_3 e^{-j\omega\tau_{ext}}}. \tag{3.4}$$

The effective reflectivity $r_R(\omega)$ is frequency dependent. The magnitude and phase of $r_R(\omega)$ will oscillate as the distance to the external mirror is varied. Alternatively the magnitude and phase of $r_R(\omega)$ will also oscillate as the laser frequency is varied. This is due to r_2 and r_3 moving in and out of phase with each other in this case. If the external feedback is provided by a grating [14-39] then there will also be a frequency dependence of the external reflectivity $r_3(\omega)$ which can be incorporated into $r_R(\omega)$. In addition, if there is a modulator placed in the external cavity then a time dependence of the effective reflectivity $r_R(\omega,t)$ will result. This is the case for the frequency modulated external cavity laser discussed later in this chapter and also in chapter 4.

3.4 Limitations of the Weak Optical Feedback Rate Equations.

The standard Lang and Kobayashi rate equations [66,67,85] adequately describe the behaviour of the laser diode only for weak feedback regimes of operation. These rate equations for weak optical feedback (see chapter 2) require the condition $|2\Delta k\ell| \ll 1$ [73] where Δk is the dynamical change in the complex wave number and ℓ is the laser diode cavity length. The complex wave number $k(\omega,n)$ is given by [73]

$$k(\omega,n) = \frac{\omega}{c}\mu(\omega,n) + j\frac{1}{2}\{g(\omega,n) - \alpha_i\}, \tag{3.5}$$

where n is the carrier density, $\mu(\omega,n)$ is the refractive index, $g(\omega,n)$ is the modal gain per unit length and α_i is the laser internal losses per unit length. The above condition $|2\Delta k\ell| \ll 1$ is violated for the coherence collapse state at high feedback levels. When the above inequality is violated the laser emission frequency $\omega(t)$ has changed by so much that the laser wavelength will, in practice, have hopped to an adjacent longitudinal mode. Due to the single mode nature of the rate equation model this effect cannot be accommodated.

The weak feedback rate equation approach, due to the above condition, is only valid for modelling the laser at feedback levels up to a few percent [66,85], and is not able to model strong optical feedback or external cavity laser diodes. The rate equations also do not model multiple reflections from the external cavity. A strong optical feedback model must allow larger levels of external reflectivity to be modelled, as well as multiple reflections around the external cavity. The optical feedback rate equations have been modified to accommodate strong optical feedback [78-82]. The modifications include the addition of terms representing multiple reflections from the external cavity and the replacing of the facet reflectivity r_2 with the effective

reflectivity $r_R(\omega)$ developed in section 3.3. The modified rate equation models suffer from the problem of large computation times, due to the combination of the stiffness of the differential equations and the Runge-Kutta solution method usually used. As a result travelling wave descriptions have been developed [71-77]. These travelling wave models do not include differential equations and are hence much more efficient computationally. In particular a simple iterative travelling wave model [72-75] has been developed to describe the behaviour of semiconductor lasers subject to arbitrary levels of optical feedback. The model is described in the next section and accounts for strong optical feedback with multiple reflections around the external cavity.

3.5 The Iterative Travelling Wave Model for an External Cavity Laser Diode.

The following model is based on that of an iterative travelling wave model [72-74]. The left moving $E_\omega^-(z,t)$ and right moving $E_\omega^+(z,t)$ electric fields within the laser are shown in fig. 3.6. A reference plane is drawn just within the laser facet r_2. The right and left reflectivities seen at this reference plane are $r_L(\omega,n)$ and $r_R(\omega)$ respectively, and are frequency dependent. The left reflectivity at the reference plane is also dependent on the carrier density within the laser. The length of the laser is ℓ and that of the external cavity is L_{ext}. The total electric field $E_\omega(z)$ within the laser is given by the sum of the left and right moving electric fields,

$$E_\omega(z) = E_\omega^-(z) + E_\omega^+(z). \tag{3.6}$$

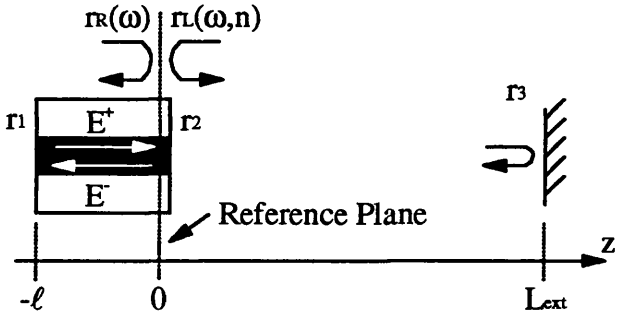

Fig. 3.6: The Frequency Dependent Right $r_R(\omega)$ and Left $r_L(\omega,n)$ Reflectivities Seen at the Reference Plane.

3.5.1 Boundary Conditions.

Firstly the reflection boundary conditions within the laser are considered, with reference to fig. 3.6. The boundary condition at the facet r_1,

$$E_\omega^+(-\ell) = r_1 E_\omega^-(-\ell), \tag{3.7}$$

is transformed into a boundary condition at the reference plane, i.e.

$$E_\omega^+(0) = r_L(\omega,n) E_\omega^-(0), \tag{3.8}$$

where $r_L(\omega,n)$ is the effective reflectivity of the left going field given by

$$r_L(\omega,n) = r_1 e^{-j2k(\omega,n)\ell}. \tag{3.9}$$

The boundary condition at the right facet is

$$E_\omega^-(0) = r_R(\omega) E_\omega^+(0), \tag{3.10}$$

where $r_R(\omega)$ is the effective right reflectivity given in (3.4).

The left moving field at the reference plane is written as a sum of multiple reflections of the right moving field in a similar way to the derivation of the effective right reflectivity $r_R(\omega)$, thus (by placing (3.1) into (3.10))

$$E_\omega^-(0) = r_2 E_\omega^+(0) + r_3\left(1-r_2^2\right)\left\{\sum_{q=1}^{\infty}\left(-r_2 r_3\right)^{q-1} e^{-jq\omega\tau_{ext}}\right\} E_\omega^+(0). \tag{3.11}$$

The boundary conditions (3.8) and (3.10) give the oscillation condition for the external cavity laser in the absence of spontaneous emission noise,

$$r_L(\omega_s, n_{th}) r_R(\omega_s) = 1. \tag{3.12}$$

This is the usual oscillation condition for a laser, where the net round trip gain (including losses) must be unity and a whole number of wavelengths must fit inside the cavity. The oscillation condition (3.12) defines the longitudinal modes and operating frequency of the external cavity laser diode. It enables the threshold carrier

density n_{th} and the steady state emission frequency ω_s to be found. In the presence of noise (3.12) is modified to

$$E_{\omega}^{+}(0) = r_L(\omega_s, n_{th}) r_R(\omega_s) E_{\omega}^{+}(0) + F_L(\omega). \tag{3.13}$$

where $F_L(\omega)$ is the noise. The preceding lasing conditions (3.6)-(3.13) have been developed in the frequency domain. A dynamic equation in the time domain is required for the model of strong optical feedback. This is performed by the introduction of slowly varying envelope functions $A^+(t)$ and $A^-(t)$ of the electric fields at the reference plane [73],

$$A^{+}(t)e^{j\omega_s t} = \frac{1}{2\pi}\int_{-\infty}^{\infty} E_{\omega}^{+}(0)e^{j\omega t}d\omega \tag{3.14}$$

and

$$A^{-}(t)e^{j\omega_s t} = \frac{1}{2\pi}\int_{-\infty}^{\infty} E_{\omega}^{-}(0)e^{j\omega t}d\omega. \tag{3.15}$$

3.5.2 Partial Derivatives of the Wave Vector.

To produce the iterative travelling wave model the left reflectivity $r_L(\omega,n)$ (3.9) is expanded about the stationary values of emission frequency ω_o and carrier density n_{th} of the solitary laser [73]. The expansion of the left reflectivity is achieved by the expansion of the wave vector $k(\omega,n)$ (3.5) about the same stationary values. To perform this operation the partial derivatives of $k(\omega,n)$ with respect to frequency ω and carrier density n are required. From (3.5)

$$\frac{\partial k}{\partial \omega} = \frac{1}{c}\left(\mu + \omega\frac{\partial \mu}{\partial \omega}\right) + j\frac{1}{2}\frac{\partial g}{\partial \omega}. \tag{3.16}$$

The group velocity v_g is given by

$$v_g = \frac{c}{\mu_g} = \frac{c}{\mu + \omega\dfrac{\partial \mu}{\partial \omega}}, \tag{3.17}$$

where μ_g is the group refractive index. Substituting (3.17) into the partial derivative (3.16) gives the partial derivative of the wave vector with respect to frequency,

$$\frac{\partial k}{\partial \omega} = \frac{1}{v_g} + j\frac{1}{2}\frac{\partial g}{\partial \omega}. \tag{3.18}$$

The wave vector (3.5) can be rewritten using a complex refractive index

$$\mu = \mu' + j\mu'', \tag{3.19}$$

to give

$$k(\omega, n) = \frac{\omega}{c}\mu' - j\frac{\omega}{c}\mu'', \tag{3.20}$$

where

$$\mu'' = -\frac{1}{2}\frac{c}{\omega}(g(\omega, n) - \alpha_i). \tag{3.21}$$

Also the partial derivative of the wave vector (3.20) with respect to carrier density is,

$$\frac{\partial k}{\partial n} = \frac{\omega}{c}\frac{\partial \mu'}{\partial n} - j\frac{\omega}{c}\frac{\partial \mu''}{\partial n}. \tag{3.22}$$

The linewidth enhancement factor [58] is introduced,

$$\alpha = \frac{\partial \mu' / \partial n}{\partial \mu'' / \partial n}, \tag{3.23}$$

and relates the changes in the real part of the refractive index to changes in the imaginary part of the refractive index. The partial derivative of (3.21) with respect to carrier density is

$$\frac{\partial \mu''}{\partial n} = -\frac{1}{2}\frac{c}{\omega}\frac{\partial g}{\partial n}, \tag{3.24}$$

which when placed into (3.22) together with (3.23) gives

$$\frac{\partial k}{\partial n} = j\frac{1}{2}(1 + j\alpha)\frac{\partial g}{\partial n}. \tag{3.25}$$

3.5.3 Modelling of the Electric Field.

Once the partial derivatives (3.18) and (3.25) are known, the left reflectivity $r_L(\omega,n)$ (3.9) can be expanded about the stationary solutions ω_o and n_{th} of the solitary laser [73] as

$$r_L(\omega,n) = r_1 e^{-j\{2k(\omega_o,n_{th})\ell+2\Delta k\ell\}}. \tag{3.26}$$

The term $2\Delta k\ell$ in (3.26) can be written as

$$2\Delta k\ell = 2\ell\left\{(\omega-\omega_o)\frac{\partial k}{\partial \omega}+(n-n_{th})\frac{\partial k}{\partial n}\right\}. \tag{3.27}$$

Substituting (3.18) and (3.25) into (3.27) gives

$$2\Delta k\ell = \tau_L\left\{\left(1+j\frac{1}{2}G_\omega\right)(\omega-\omega_o)+j\frac{1}{2}G_n(1+j\alpha)(n-n_{th})\right\}, \tag{3.28}$$

where τ_L is the laser internal cavity round trip time

$$\tau_L = \frac{2\ell}{v_g}, \tag{3.29}$$

G is the gain per unit time

$$G = gv_g, \tag{3.30}$$

G_ω is the rate of change of the gain with frequency

$$G_\omega = \frac{\partial G}{\partial \omega} = v_g\frac{\partial g}{\partial \omega}, \tag{3.31}$$

and G_n is the rate of change of gain with carrier density (gain slope)

$$G_n = \frac{\partial G}{\partial n} = v_g\frac{\partial g}{\partial n}. \tag{3.32}$$

Substituting (3.28) into (3.26) and assuming that G_ω=0 gives

$$r_L(\omega,n) = r_1 e^{j\frac{1}{2}G_n(1+j\alpha)(n-n_{th})\tau_L} e^{-j(\omega-\omega_o)\tau_L} e^{-j2k(\omega_o,n_{th})\ell}. \tag{3.33}$$

The term $e^{-j2k(\omega_o,n_{th})\ell}$ in (3.33) is equal to unity at the stationary values ω_o and n_{th}, and substituting the solitary laser condition,

$$r_L(\omega_o,n_{th})r_2 = r_1 r_2 = 1 \tag{3.34}$$

into (3.33) gives

$$r_L(\omega,n) = \frac{1}{r_2} e^{j\frac{1}{2}G_n(1+j\alpha)(n-n_{th})\tau_L} e^{-j(\omega-\omega_o)\tau_L}. \tag{3.35}$$

Inserting (3.35), (3.10) and (3.11) into (3.13) (with ω_s replaced by ω_o) results in [73]

$$E_\omega^+(0) = \frac{1}{r_2} e^{-j(\omega-\omega_o)\tau_L} e^{j\frac{1}{2}G_n(1+j\alpha)(n-n_{th})\tau_L} \times \left\{ r_2 E_\omega^+(0) + r_3\left(1-r_2^2\right)E_\omega^+(0)\sum_{q=1}^{\infty}\left(-r_2 r_3\right)^{q-1} e^{-jq\omega\tau_{ext}} \right\} + F_L(\omega), \tag{3.36}$$

which is simplified to

$$E_\omega^+(0) = \frac{1}{r_2^2} e^{-j(\omega-\omega_o)\tau_L} e^{j\frac{1}{2}G_n(1+j\alpha)(n-n_{th})\tau_L} \times \left\{ E_\omega^+(0) - \left(1-r_2^2\right)E_\omega^+(0)\sum_{q=0}^{\infty}\left(-r_2 r_3\right)^{q} e^{-jq\omega\tau_{ext}} \right\} + F_L(\omega). \tag{3.37}$$

Finally (3.37) is transformed into the time domain using (3.14) and (3.15),

$$A^+\left(t+\tau_L\right) = \frac{1}{r_2^2} e^{\frac{1}{2}(1+j\alpha)G_n(n(t)-n_{th})\tau_L} \times \left\{ A^+(t) - \left(1-r_2^2\right)\sum_{q=0}^{\infty}\left(-r_2 r_3 e^{-j\omega\tau_{ext}}\right)^q A^+\left(t-q\tau_{ext}\right) \right\} + F_L(t)\tau_L. \tag{3.38}$$

where an arbitrary time shift of $t \to t+\tau_L$ has been introduced to produce the iterative equation. The term $F_L(t)$ represents the Langevin noise processes to model the spontaneous emission noise. The iterative equation for the electric field envelope

(3.38) relates the right moving envelope $A^+(t+\tau_L)$ at intervals of the laser internal round trip time τ_L to the values of the right moving field one internal cavity round trip earlier $A^+(t)$ and also to the external cavity round trip reflections $A^+(t-q\tau_L)$.

3.5.4 Modelling of Carrier Density.

To complete the model an iterative equation for the carrier density is required also. It is chosen to use a Taylor series expansion up to the second derivative [73],

$$n(t+\tau_L)=n(t)+\frac{dn(t)}{dt}\tau_L+\frac{1}{2}\frac{d^2n(t)}{dt^2}\tau_L^2. \tag{3.39}$$

It has been found that a Taylor series up to terms in τ_L^2 is sufficient to keep numerical stability of the model [73]. The dn(t)/dt term in (3.39) is calculated from the usual rate equation for the carrier density

$$\frac{dn(t)}{dt}=\frac{I}{eV}-\frac{n(t)}{\tau_{sp}}-G_n(n(t)-n_o)s(t), \tag{3.40}$$

where I(t) is the injection current, V is the active region volume of the laser diode, e is the electronic charge, τ_{sp} is the carrier lifetime, G_n is the gain slope, n_o is the gain linearisation point and s(t) is the photon density. The second derivative of the carrier density is obtained by further differentiation of (3.40)

$$\frac{d^2n(t)}{dt^2}=\frac{1}{eV}\frac{dI(t)}{dt}-\left\{\frac{1}{\tau_{sp}}+G_n s(t)\right\}\frac{dn(t)}{dt}-G_n(n(t)-n_o)\frac{ds(t)}{dt}. \tag{3.41}$$

The model for a laser diode with strong optical feedback is thus described by the iterative equations (3.38) and (3.39) [73-75], and is represented in fig. 3.7. The laser is operating as an external cavity laser in which the dominant cavity is defined by the mirrors r_1 and r_3. In fig. 3.7 $A^+(t)$ is the right moving electric field leaving the laser facet, $A^-(t-\tau_{ext})$ is the left moving field returning into the laser, τ_{ext} is the external cavity round trip delay and τ_L is the laser internal round trip time. The effective reflectivity of the r_2 and r_3 combination is $r_R(\omega)$, and $\omega\tau_{ext}$ is the single pass external cavity round trip phase change.

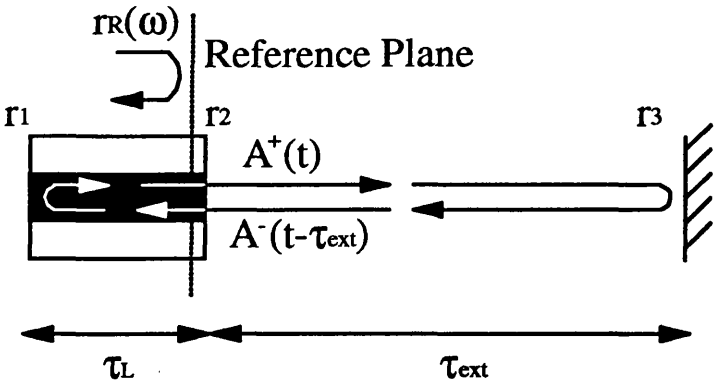

Fig. 3.7: Representation of the Iterative Travelling Wave Model for an External Cavity Laser.

3.5.5 Photon Density, Output Power and Spontaneous Emission Noise.

From a consideration of the relationship between the exponential intra-cavity variation of the photon densities and the emitted photon density s(t), it is found [72,73] that

$$s(t) = \sigma(\omega, n)\left|A^{+}(t)\right|^{2} \tag{3.42}$$

where

$$\sigma(\omega, n) = \frac{4\pi\varepsilon_o\mu\mu_g}{h\omega_s}\frac{1}{(g-\alpha_i)}\frac{1}{r_1}\left(|r_R|+r_1\right)\left(1-r_1|r_R|\right). \tag{3.43}$$

and g is the modal gain per unit length. The output power is then calculated from the photon density using the method in chapter 2,

$$P_o(t) = \frac{\eta_q \omega_s h s(t) V}{4\pi\Gamma\tau_{ph}}. \tag{3.44}$$

To complete the model the Langevin noise term to model spontaneous noise is added as in (3.38). A similar term is not added to the carriers (3.39) because the carrier Langevin noise is due to shot noise which can be neglected. The term $F_L(t)$ is calculated in a similar manner to (3.42) using

$$F_L(t) = \sqrt{\frac{F_s(t)}{\sigma(\omega, n)}}e^{jx2\pi}. \tag{3.45}$$

The photon Langevin noise term $F_s(t)$ in (3.45) is calculated as in appendix 2, using

$$F_s(t) = \sqrt{\frac{2s(t_i)\gamma n(t)\Gamma}{\tau_{sp}\tau_L}} x_1, \tag{3.46}$$

where the Langevin noise application interval Δt (see appendix 2) has been replaced by the iterative model time step of the laser internal cavity round trip time τ_L. The terms x_1 and x_2 are random variables, with x_1 having zero mean and unity variance, and x_2 being evenly distributed in the range $-1 \le x_2 \le 1$

3.6 Stationary Solutions.

Due to the strong optical feedback the stationary solutions at a given injection current are significantly altered from those of the solitary laser described in chapter 1. The effective reflectivity $r_R(\omega)$ is used instead of r_2 to calculate such parameters as the photon lifetime and threshold current. The photon lifetime is thus modified from τ_{ph} to $\tau_{ph,r}$

$$\tau_{ph,r} = \frac{\mu_g}{c\left(\alpha_i - \frac{\ln(r_1 |r_R(\omega)|)}{\ell}\right)}, \tag{3.47}$$

resulting in a modified threshold carrier density $n_{th,r}$, and threshold injection current $I_{th,r}$

$$n_{th,r} = n_o + \frac{1}{G_n \tau_{ph,r}}, \tag{3.48}$$

$$I_{th,r} = \frac{n_{th,r} eV}{\tau_{sp}}. \tag{3.49}$$

The stationary photon density s_o is then calculated as

$$s_o = \frac{\left(\frac{J}{J_{th,r}} - 1\right)}{G_n\left(n_{th,r} - n_o\right)} \frac{n_{th,r}}{\tau_{sp}}. \tag{3.50}$$

3.7 Numerical Solution.

The equations defining the behaviour of the laser (3.38)-(3.41) are solved iteratively to calculate the photon density s(t), output power $P_o(t)$, carrier density n(t) and emission frequency $\omega(t)$ at time steps of the laser internal cavity round trip time τ_L. To evaluate the reflections of the field $A^+(t-q\tau_{ext})$, all previous calculated values of the emitted field $A^+(t)$ are stored for later use. Langevin noise is added to model spontaneous emission noise, as described in the section 3.5.5. Simulation of the noise is achieved by random noise events at each iteration step. The values of the laser parameters used in the model are given in table 2.1. A more detailed description of the numerical solution of the iterative travelling wave model for a semiconductor laser subject to strong optical feedback is given in appendix 4. The model is used in chapter 4 to investigate the properties of external cavity laser diodes.

3.8 Frequency Modulated External Cavity Diode Laser.

As noted earlier in this chapter, an advantage of operating a semiconductor laser in an external cavity configuration is that optical elements can be placed within the lasing cavity. One example is the implementation of an external cavity frequency modulated (FM) laser diode [54-56]. An FM laser has a constant output power but has a sinusoidally sweeping emission frequency. An external cavity FM laser is shown in fig. 3.8. In this case, a phase modulator is placed between the laser and the external mirror. The phase modulator is controlled with an RF signal which induces a frequency modulation of the laser light output. In the time domain the laser appears to be sweeping its emission frequency backwards and forwards at the frequency of the RF signal. The maximum frequency displacement from the mean can, however, be much larger than the RF frequency [54].

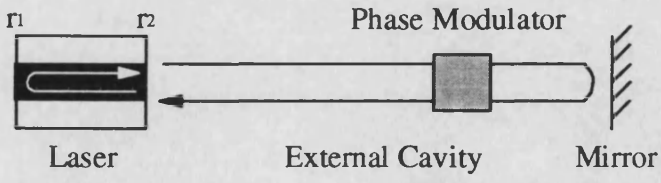

Fig. 3.8: An External Cavity Frequency Modulated (FM) Laser Diode.

The instantaneous phase of the FM laser output is given by

$$\phi(t) = \omega_s t + \Gamma_\phi \sin(\omega_m t), \tag{3.51}$$

where ω_m is the RF modulation frequency and Γ_ϕ is the peak phase deviation (modulation index) of the FM output signal. The instantaneous laser emission frequency is given in the usual way by

$$\omega(t) = \frac{d\phi(t)}{dt} = \omega_s + \Gamma_\phi \omega_m \cos(\omega_m t). \tag{3.52}$$

Therefore the laser emission frequency has a maximum displacement of $\Gamma_\phi\omega_m$ [54], which is known as the FM bandwidth. Fig 3.9 shows the emission spectra produced as the laser frequency sweeps sinusoidally back and forth. The emission spectra shows the typical shape for a sinusoidally swept frequency signal. The amplitudes of the individual modes within the spectra are given by Bessel functions [54],

$$E(t) = E_o \sum_{q=-\infty}^{\infty} J_q(\Gamma_\phi \omega_m) \cos\left\{(\omega_s - q\omega)t - \frac{q\pi}{2}\right\}. \tag{3.53}$$

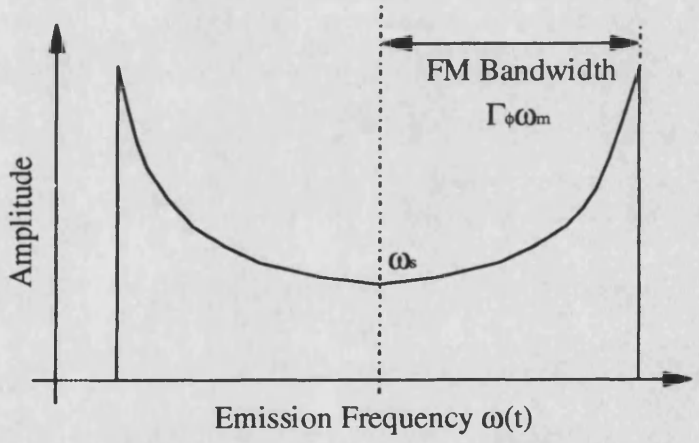

Fig. 3.9: Emission Spectra of an FM Laser.

The FM modulation index Γ_ϕ can be expressed in terms of the modulation index Δ_m of the phase modulator by [54]

$$\Gamma_\phi = \frac{1}{2\pi}\frac{\omega_m}{\omega_d}\Delta_m. \tag{3.54}$$

In (3.54) ω_d is the detuning between the RF signal and the longitudinal mode spacing, and Δ_m is the modulation index of the RF signal. The longitudinal mode spacing is equal to the inverse of the external cavity round trip delay $1/\tau_{ext}$. Thus, the FM bandwidth can be much larger than the modulation index of the RF signal by a large ratio (up to 100). The closer the RF signal to the axial mode spacing the larger the

FM bandwidth. However if the modulation frequency is equal to the longitudinal mode spacing the laser will become FM mode locked [57].

3.9 Iterative Travelling Wave Model for Frequency Modulated External Cavity Diode Laser.

To apply the iterative travelling wave model to the investigation of external cavity FM lasers the external cavity round trip phase change $\omega\tau_{ext}$ must be considered. To include the RF modulation of the phase, the external cavity round trip phase change is modified in the following way,

$$\omega\tau_{ext} \rightarrow \omega\tau_{ext} + \Delta_m \sin(\omega_m t). \tag{3.55}$$

where Δ_m is the modulation index of the RF signal. The external cavity round trip phase change has become time dependent due to the phase modulation. This results in the effective reflectivity $r_R(\omega)$ (3.4) also becoming time dependent,

$$r_R(\omega,t) = r_2 + r_3\left(1-r_2^2\right)\sum_{q=1}^{\infty}\left(-r_2 r_3\right)^{q-1} e^{-j\left\{q\omega\tau_{ext}+\sum_{p=1}^{q}\Delta_m \sin\left(\omega_m[t-(p-1)\tau_{ext}]\right)\right\}}. \tag{3.56}$$

The iterative equation for the right moving field (3.38) is modified in a similar manner to give the following

$$\begin{aligned} A^+\left(t+\tau_L\right) = \frac{1}{r_2^2} e^{\frac{1}{2}(1+j\alpha)G_n(n(t)-n_{th})\tau_L} \times \\ \left\{ A^+(t) - \left(1-r_2^2\right)\times \right. \\ \left. \sum_{q=0}^{\infty}\left(-r_2 r_3\right)^q e^{-j\left\{q\omega\tau_{ext}+\sum_{p=1}^{q}\Delta_m \sin\left(\omega_m[t-(p-1)\tau_{ext}]\right)\right\}} A^+\left(t-q\tau_{ext}\right) \right\}. \\ + F(t)\tau_L \end{aligned} \tag{3.57}$$

The second sum in (3.56) and (3.57) accounts for the different modulation induced phase changes for each round trip within the external cavity. The iterative equations for the carrier density (3.39)-(3.41) are unchanged from those used to describe a conventional external cavity laser diode.

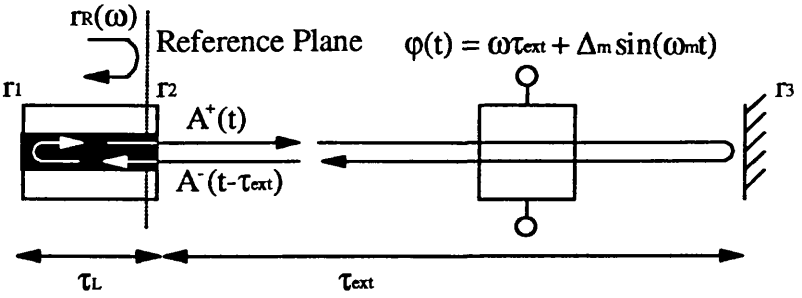

Fig. 3.10: Adaptation of the Iterative Travelling Wave Model for an External Cavity Frequency Modulated Laser Diode.

Fig. 3.10 represents the modifications to the iterative model for investigations of an external cavity FM laser diode. The model is numerically solved in exactly the same way as for the conventional external cavity laser. Investigations into the performance of external cavity FM laser diodes using this model are described in chapter 4.

3.10 Strong Phase Conjugate Optical Feedback.

A phase conjugate mirror can produce a very high reflectivity [86], possibly greater than unity. The iterative travelling wave model is also applicable for strong phase conjugate feedback into the laser diode. The conventional rate equations with appropriate modifications (see chapter 6) are applicable to weak phase conjugate feedback. A particular feature of strong phase conjugate feedback is illustrated in fig. 3.11. When considering strong optical feedback multiple reflections around the external cavity must be taken into account. However, with a phase conjugate mirror only the odd number round trip reflections consist of phase conjugate feedback (PCFB). The even number round trip reflections consist of conventional optical feedback (COF), due to the self-inverse property of the phase conjugation process. Therefore, true strong phase conjugate feedback cannot exist alone, and always contains an element of conventional mirror feedback within it. This is taken into account in the modification of the model described in the next section. Strong phase conjugate feedback is discussed further in chapter 4. Weak phase conjugate feedback is treated further in chapters 6 and 7.

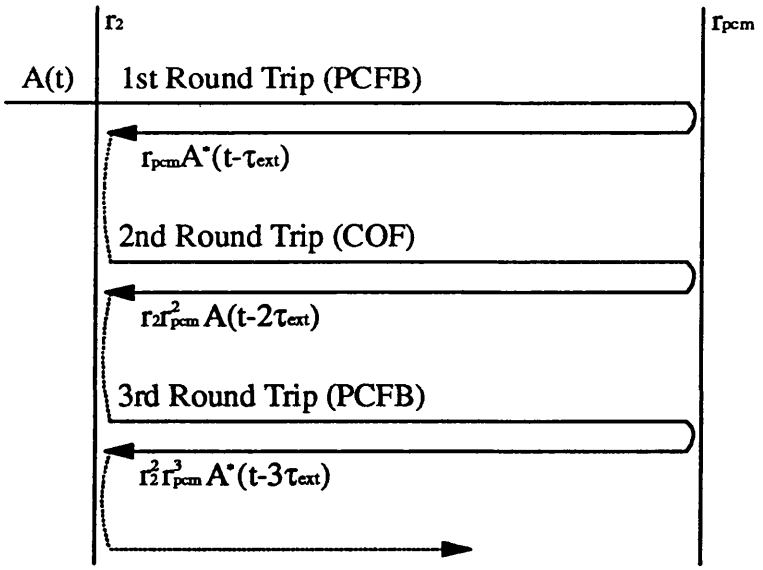

Fig. 3.11: Strong Phase Conjugate Feedback Consists of Both Phase Conjugate (PCFB) and Conventional Mirror (COF) Reflections.

3.11 Adaptation of Model for Strong Phase Conjugate Feedback.

As described in the previous section, strong phase conjugate feedback consists of both phase conjugate and conventional reflections. The iterative equation (3.38) must be modified accordingly as,

$$A^{+}(t+\tau_L)=\frac{1}{r_2^2}e^{\frac{1}{2}G_n(1+j\alpha)(n(t)-n_{th})\tau_L}\times \left\{\begin{array}{l} A^{+}(t)-(1-r_2^2)\sum_{q=0}^{\infty}(-r_2r_{pcm})^{2q}A(t-2q\tau_{ext}) \\ -(1-r_2^2)\sum_{q=0}^{\infty}(-r_2r_{pcm})^{2q+1}A^{*}(t-(2q+1)\tau_{ext}) \end{array}\right\}, \\ +F(t)\tau_L \qquad (3.58)$$

where $A(t-2q\tau_{ext})$ are the conventional reflections and $A^{*}(t-(2q+1)\tau_{ext})$ are the phase conjugate reflections. The result is to have two similar summations for both the types of optical feedback present in such a system. The numerical solution is exactly the same as for strong conventional optical feedback.

3.12 Conclusion.

An iterative travelling wave model for external cavity laser diodes has been developed. The model has been extended to include a time dependent reflectivity as encountered in external cavity FM laser diodes. The time dependent reflectivity is due to the modulation of the external cavity round trip phase change. The model has also been adapted to account for strong phase conjugate feedback which consists of both phase conjugate and conventional feedback. The iterative travelling wave model is used in chapter 4 to investigate the behaviour of laser diodes subject to strong optical feedback, external cavity FM laser diodes, and strong phase conjugate feedback.

Chapter 3 References.

[1] W F Sharfin, J Seppala, A Mooradian, B A Soltz, R G Waters, B J Vollmer, and K J Bystrom, "High-Power, Diffraction-Limited, Narrow-Band, External-Cavity Diode Laser", Appl. Phys. Lett., Vol. 54, No. 18, pp. 1731-1733, 1989.

[2] O Yamamoto, H Hayashi, N Miyauchi, S Maei, H Kawanishi, T Morimoto, S Yamamoto, S Yano, and T Hijikata, "Stable Single-Longitudinal-Mode Operation in Visible (AlGa)As Semiconductor Lasers Coupled with a Short External Cavity", J. Appl. Phys., Vol. 61, No. 3, pp. 870-874, 1987.

[3] A R Chraplyvy, K Y Liou, R W Tkach, G Eisenstein, Y K Jhee, T L Koch, P J Anthony, and U K Chakrabarti, "Simple Narrow-Linewidth 1.5 μm InGaAsP DFB External-Cavity Laser", Electron. Lett., Vol. 22, No. 2, pp. 88-90, 1986.

[4] T P Lee, S G Menocal, and H Matsumura, "Characteristics of Linewidth Narrowing of a 1.5 μm DFB Laser with a Short GRIN-ROD External Coupled Cavity", Electron. Lett., Vol. 21, No. 15, pp. 655-656, 1985.

[5] C Lin, C A Burrus, and L A Coldren, "Characteristics of Single-Longitudinal-Mode Selection in Short-Coupled-Cavity (SCC) Injection Lasers", IEEE J. Lightwave Tech., Vol. 2, No. 4, pp. 544-549, 1984.

[6] N K Dutta, N A Olsson, and K Y Liou, "Effect of External Optical Feedback on Spectral Properties of External Cavity Semiconductor Lasers", Electron. Lett., Vol. 20, No. 14, pp. 588-589, 1984.

[7] J P Van der Ziel and R M Mikulyak, "Single-Mode Operation of 1.3 μm InGaAsP/InP Buried Crescent Lasers Using a Short External Optical Cavity", IEEE J. Quantum Electron., Vol. 20, No. 3, pp. 223-229, 1984.

[8] K H Cameron, P J Chidgey, and K R Preston, "102 km Optical Fibre Transmission Experiments at 1.52 μm Using an External Cavity Controlled Laser Transmitter Module", Vol. 18, No. 15, pp. 650-651, 1982.

[9] J Zhang, P Ye, Y Xie, and S Tao, "Tunable Stabilized Single-Frequency GRINROD External Coupled Cavity Semiconductor Lasers", IEEE J. Lightwave Tech., Vol. 8, No. 10, pp. 1612-1619, 1990.

[10] K R Preston, K C Woollard, and K H Cameron, "External Cavity Controlled Single Longitudinal Mode Laser Transmitter Module", Electron. Lett., Vol. 17, No. 24, pp. 931-933, 1981.

[11] D T Cassidy, D M Bruce, and B F Ventrudo, "Short-External-Cavity Module for Enhanced Single-Mode Tuning of InGaAsP and AlGaAs Semiconductor Lasers", Rev. Sci. Instrum., Vol. 62, No. 10, pp. 2385-2388, 1991.

[12] Z M Chuang, D A Cohen, and L A Coldren, "Tuning Characteristics of a Tunable-Single-Frequency External-Cavity Laser", IEEE J. Quantum Electron., Vol. 26, No. 7, pp. 1200-1205, 1990.

[13] A Lidgard, T Tanbun-Ek, R A Logan, H Temkin, K W Wecht, and N A Olsson, "External-Cavity InGaAs/InP Graded Index Multiquantum Well Laser with a 200 nm Tuning Range", Appl. Phys. Lett., Vol. 56, No. 9, pp. 816-817, 1990.

[14] Z Ahmed, R S Tucker, and L Zhai, "Discontinuous Modulation Response of Grating-Assisted Extended-Cavity Semiconductor Lasers", Electron. Lett., Vol. 30, No. 4, pp. 305-306, 1994.

[15] P A Morton, V Mizrahi, T Tanbun-Ek, R A Logan, P J Lemaire, H M Presby, T Erdogan, S L Woodward, J E Sipe, M R Phillips, A M Sergent, and K W Wecht, "Stable Single Mode Hybrid Laser with High Power and Narrow Linewidth", Appl. Phys. Lett., Vol. 64, No. 20, pp. 2634-2636, 1994.

[16] H Sun, G Anderson, S Menhart, J Ma, and D Wilson, "Small-Signal Circuit Modeling for a Grating External-Cavity Semiconductor Laser", J. Opt. Soc. Am. B, Vol. 11, No. 4, pp. 574-579, 1994.

[17] H Asakura, K Hagiwara, M Iida, and K Eda, "External Cavity Semiconductor Laser with a Fourier Grating and an Aspheric Lens", Appl. Optics, Vol. 32, No. 12, pp. 2031-2038, 1993.

[18] O Ishida and H Toba, "200 kHz Absolute Frequency Stability in 1.5 μm External-Cavity Semiconductor Laser", Electron. Lett., Vol. 27, No. 12, pp. 1018-1019, 1991.

[19] J Wittmann and G Gaukel, "Narrow-Linewidth Laser with a Prism Grating/GRIN Rod Lens Combination Serving as External Cavity", Electron. Lett., Vol. 23, No. 10, pp. 524-525, 1987.

[20] C Y Kuo and J P Van der Ziel, "Linewidth Reduction of 1.5-μm Grating Loaded External Cavity Semiconductor Laser by Geometric Reconfiguration", Appl. Phys. Lett., Vol. 48, No. 14, pp. 885-887, 1986.

[21] R Wyatt, "Spectral Linewidth of External Cavity Semiconductor Lasers with Strong, Frequency-Selective Feedback", Electron. Lett., Vol. 21, No. 15, pp. 658-659, 1985.

[22] M R Mathews, K H Cameron, R Wyatt, and W J Devlin, "Packaged Frequency-Stable Tunable 20 kHz Linewidth 1.5 μm InGaAsP External Cavity Laser", Electron. Lett., Vol. 21, No. 3, pp. 113-115, 1985.

[23] H Sato, H Asakura, M Fukai, and N Suzuki, "Design of Nondispersion Optical Feedback System Using Diffraction Grating for Semiconductor Laser Multiple Longitudinal Modes Control", IEEE J. Quantum Electron., Vol. 18, No. 2, pp. 155-157, 1982.

[24] O Nilsson, S Saito, and Y Yamamoto, "Oscillation Frequency, Linewidth Reduction and Frequency Modulation Characteristics for a Diode Laser with External Grating Feedback", Electron. Lett., Vol. 17, No. 17, pp. 589-591, 1981.

[25] D Syvridis, G Guekos, R Dall'Ara, and H Melchior, "Sequential TE/TM Polarization Emission from a Tunable External Cavity Diode Laser", IEEE J. Quantum Electron., Vol. 11, No. 2, pp. 265-271, 1993.

[26] K C Harvey and C J Myatt, "External-Cavity Diode Laser Using a Grazing-Incidence Diffraction Grating", Optics Lett., Vol. 16, No. 12, pp. 910-912, 1991.

[27] P Gavrilovic, A V Chelnokov, M S O'Neill, and D M Beyea, "Narrow-Linewidth Operation of Broad-Stripe Single Quantum Well Laser Diodes in a Grazing Incidence External Cavity", Appl. Phys. Lett., Vol. 60, No. 24, pp. 2977-2979, 1992.

[28] P Zorabedian, "Characteristics of a Grating-External-Cavity Semiconductor Laser Containing Intracavity Prism Beam Expanders", IEEE J. Lightwave Tech., Vol. 10, No. 3, pp. 330-334, 1992.

[29] W R Trutna and L F Stokes, "Continuously Tuned External Cavity Semiconductor Laser", IEEE J. Lightwave Tech., Vol. 11, No. 8, pp. 1279-1286, 1993.

[30] D Mehuys, D Welch, and D Scifres, "1 W CW, Diffraction-Limited, Tunable External-Cavity Semiconductor Laser", Electron. Lett., Vol. 29, No. 14, pp. 1254-1255, 1993.

[31] C P Seltzer, M Bagley, D J Elton, S Perrin, and D M Cooper, "160 nm Continuous Tuning of an MQW Laser in an External Cavity Across the Entire 1.3 μm Communications Window", Electron. Lett., Vol. 27, No. 1, pp. 95-96, 1991.

[32] F Favre and D Le Guen, "82 nm of Continuous Tunability for an External Cavity Semiconductor Laser", Electron. Lett., Vol. 27, No. 2, pp. 183-184, 1991.

[33] A T Schremer and C L Tang, "External-Cavity Semiconductor Laser with 1000 GHz Continuous Piezoelectric Tuning Range", IEEE Phot. Technol. Lett., Vol. 2, No. 1, pp. 3-5, 1990.

[34] J O Binder, G D Cormack, and A Somani, "Intermodal Tuning Characteristics of an InGaAsP Laser with Optical Feedback from an External-Grating Reflector", IEEE J. Quantum Electron., Vol. 26, No. 7, pp. 1191-1199, 1990.

[35] P Zorabedian and W R Trutna, "Alignment-Stabilized Grating-Tuned External-Cavity Semiconductor Laser", Optics Lett., Vol. 15, No. 9, pp. 483-485, 1990.

[36] R X Min, Z L Tao, and Y P Da, "Achievement of 6 GHz Wide, Continuous and Pure Frequency Tuning of 1.3 μm External Cavity Semiconductor Laser and its Application in High Resolution Spectral Measurement", Electron. Lett., Vol. 24, No. 15, pp. 961-962, 1988.

[37] B Glance, C A Burrus, and L W Stulz, "Fast Frequency-Tunable External-Cavity Laser", Electron. Lett., Vol. 23, No. 3, pp. 98-100, 1987.

[38] F Favre, D Le Guen, J C Simon, and B Landousies, "External-Cavity Semiconductor Laser with 15 nm Continuous Tuning Range", Electron. Lett., Vol. 22, No. 15, pp. 795-796, 1986.

[39] R Wyatt and W J Devlin, "10 kHz Linewidth 1.5 μm InGaAsP External Cavity Laser with 55 nm Tuning Range", Electron. Lett., Vol. 19, No. 3, pp. 110-112, 1983.

[40] T Miyazawa, H Iwamura, and M Naganuma, "Integrated External-Cavity InGaAs/InP Lasers Using Cap-Annealing Disordering", IEEE Phot. Technol. Lett., Vol. 3, No. 5, pp. 421-423, 1991.

[41] J Helms, N Schunk, and K Petermann, "Stable Operation Range for Laser Diodes with an Integrated Passive Cavity in the Presence of External Optical Feedback", IEEE Phot. Technol. Lett., Vol. 1, No. 12, pp. 409-411, 1989.

[42] J Werner, E Kapon, N G Stoffel, E Colas, S A Schwarz, C L Schwartz, and N Andreadakis, "Integrated External Cavity GaAs/AlGaAs Lasers Using Selective Quantum Well Disordering", Appl. Phys. Lett., Vol. 55, No. 6, pp. 540-542, 1989.

[43] B C De Cooman, G L A Van der Hofstad, P I Kuindersma, C K Wong, W Scheepers, and L F Tiemeyer, "Fabrication and Spectral Characteristics of a 1.55-μm Distributed Feedback Laser with a Tunable Integrated External Cavity", J. Appl. Phys., Vol. 66, No. 4, pp. 1525-1529, 1989.

[44] N K Dutta, T Cella, A B Piccirilli, R L Brown, and C Green, "Chirp and CW Linewidth Measurements of Integrated External Cavity Lasers", Appl. Phys. Lett., Vol. 52, No. 2, pp. 91-92, 1988.

[45] A B Piccirilli, N K Dutta, S G Napholtz, T Cella, and R L Brown, "1.3-μm Integrated External Cavity Distributed Bragg Reflector Laser", J. Appl. Phys., Vol. 62, No. 1, pp. 307-309, 1987.

[46] N K Dutta, T Cella, J L Zilko, A B Piccirilli, R L Brown, and S G Napholtz, "Integrated External Cavity Distributed Bragg Reflector Laser", Appl. Phys. Lett., Vol. 50, No. 11, pp. 644-646, 1987.

[47] S Murata, S Yamazaki, I Mito, and K Kobayashi, "Spectral Characteristics for 1.3 μm Monolithic External Cavity DFB Lasers", Electron. Lett., Vol. 22, No. 22, pp. 1197-1198, 1986.

[48] N K Dutta, T Cella, A B Piccirilli, and R L Brown, "Integrated External Cavity Laser", Appl. Phys. Lett., Vol. 49, No. 19, pp. 1227-1229, 1986.

[49] T Fujita, J Ohya, K Matsuda, M Ishino, H Sato, H Serizawa, "Narrow Spectral Linewidth Characteristics of Monolithic Integrated-Passive-Cavity InGaAsP/InP Semiconductor Lasers", Electron. Lett., Vol. 21, No. 9, pp. 374-376, 1985.

[50] K Y Liou, Y K Jhee, G Eisenstein, R S Tucker, R T Ku, T M Shen, U K Chakrabarti, and P J Anthony, "Linewidth Characteristics of Fibre-Extended-Cavity Distributed-Feedback Lasers", Appl. Phys. Lett., Vol. 48, No. 16, pp. 1039-1041, 1986.

[51] P L Liu, G Eisenstein, R S Tucker, and I P Kaminow, "Measurements of Intensity Fluctuations of an InGaAsP External Cavity Laser", Appl. Phys. Lett., Vol. 44, No. 5, pp. 481-483, 1984.

[52] K Y Liou, Y K Jhee, C A Burrus, and K L Hall, "Narrow-Linewidth Fibre-External-Cavity Injection Lasers", Electron. Lett., Vol. 21, No. 20, pp. 933-934, 1985.

[53] K Y Liou, R T Ku, T M Shen, and P J Anthony, "Oscillation Frequency Tuning Characteristics of Fiber-Extended-Cavity Distributed-Feedback Lasers", Appl. Phys. Lett., Vol. 50, No. 7, pp. 380-382, 1987.

[54] A E Siegman, "Lasers", University Science Books, 1986.

[55] A P Willis and D M Kane, "Modulation Induced Coherence Collapse in FM Diode Lasers", Opt. Comm., Vol. 107, No. 1-2, pp. 65-70, 1994.

[56] S E Harris and O P McDuff, "Theory of FM Laser Oscillation", IEEE J. Quantum Electron., Vol. 1, No. 6, pp. 245-262, 1965.

[57] K Y Lau, "Narrow-Band Modulation of Semiconductor Lasers at Millimeter Wave Frequencies (> 100 GHz) by Mode Locking", IEEE J. Quantum Electron., Vol. 26, No. 2, pp. 250-261, 1990.

[58] K Petermann, "Laser Diode Modulation and Noise", Kluwer Academic, 1988.

[59] E Patzak, A Sugimura, S Saito, T Mukai, and H Olesen, "Semiconductor Laser Linewidth in Optical Feedback Configurations", Electron. Lett., Vol. 19, No. 24, pp. 1026-1027, 1983.

[60] H Sato and J Ohya, "Theory of Spectral Linewidth of External Cavity Semiconductor Lasers", IEEE J. Quantum Electron., Vol. 22, No. 7, pp. 1060-1063, 1986.

[61] M W Fleming and A Mooradian, "Spectral Characteristics of External-Cavity Controlled Semiconductor Lasers", IEEE J. Quantum Electron., Vol. 17, No. 1, pp. 44-59, 1981.

[62] R Q Hui, S P Tao, Y Wu, and H Peng, "An Experimental Study on Stable Single-Frequency Semiconductor Lasers with External Cavity", IEEE Phot. Technol. Lett., Vol. 1, No. 9, pp. 255-257, 1989.

[63] T P Lee, S G Menocal, S Sakano, V Valster, and S Tsuji, "Linewidth and FM Characteristics of a Distributed Feedback Laser Monolithically Integrated with a Tunable External Cavity", Electron. Lett., Vol. 23, No. 4, pp. 153-154, 1987.

[64] S Tai, K Kyuma, and T Nakayama, "Spectral Linewidth of an External-Cavity Laser Diode Stabilized by a Fiber-Optic Ring Resonator", Appl. Phys. Lett., Vol. 47, No. 5, pp. 439-440, 1985.

[65] J Buus, "Linewidth of Monolithic External Cavity DFB Lasers", Electron. Lett., Vol. 24, No. 4, pp. 197-198, 1988.

[66] N Schunk and K Petermann, "Numerical Analysis of the Feedback Regimes for a Single-Mode Semiconductor Laser With External Feedback", IEEE J. Quantum Electron., Vol. 24, No. 7, pp. 1242-1247, 1988.

[67] R Tkach and A Chraplyvy, "Regimes of Feedback Effects in 1.5-μm Distributed Feedback Lasers", IEEE J. Lightwave Tech., Vol. 4, No. 11, pp. 1655-1661, 1986.

[68] H Li, J Ye, and J G McInerney, "Detailed Analysis of Coherence Collapse in Semiconductor Lasers", IEEE J. Quantum Electron., Vol. 29, No. 9, pp. 2421-2432, 1993.

[69] D Lenstra, B H Verbeek, and A J Den Boef, "Coherence Collapse in Single-Mode Semiconductor Lasers Due to Optical Feedback", IEEE J. Quantum Electron., Vol. 21, No. 6, pp. 674-679, 1985.

[70] J Mørk, B Tromborg, and J Mark, "Chaos in Semiconductor Lasers with Optical Feedback: Theory and Experiment", IEEE J. Quantum Electron., Vol. 28, No. 1, pp. 93-108, 1992.

[71] L A Glasser, A Linearized Theory for the Diode Laser in an External Cavity", IEEE J. Quantum Electron., Vol. 16, No. 5, pp. 525-531, 1980.

[72] B Tromborg, H Olesen, X Pan, and S Saito, "Transmission Line Description of Optical Feedback and Injection Locking for Fabry-Perot and DFB Lasers", IEEE J. Quantum. Electron., Vol. 23, No. 11, pp. 1875-1889, 1987.

[73] J Mørk, "Nonlinear Dynamics and Stochastic Behaviour of Semiconductor Lasers with Optical Feedback", Ph.D. Thesis, Report No. S48, Danish Center for Applied Mathematics and Mechanics, Technical University of Denmark, 1989.

[74] F Sporleder, "Travelling Wave Line Model for Laser Diodes with External Optical Feedback", Proc. URSI Int. Symp. on Electromagn. Theory, Santiago de Compostela, Spain, pp. 585-588, 1983.

[75] L N Langley, K A Shore, and J Mørk, "Dynamical and Noise Properties of Laser Diodes Subject to Strong Optical Feedback", accepted for publication in Optics Lett., 1994.

[76] A J Lowery, "New Dynamic Multimode Model for External Cavity Semiconductor Lasers", IEE Proc.-J, Vol. 136, No. 4, pp. 229-237, 1989.

[77] M F Ferreira, J F Rocha, and J L Pinto, "Noise and Modulation Performance of Fabry-Perot and DFB Semiconductor Lasers with Arbitrary External Optical Feedback", IEE Proc.-J, Vol. 137, No. 6, pp. 361-369, 1990.

[78] L A Coldren and T L Koch, "External-Cavity Laser Design", IEEE J. Lightwave Tech., Vol. 2, No. 6, pp. 1045-1051, 1984.

[79] D R Hjelme and A R Mickelson, "On the Theory of External Cavity Operated Single-Mode Semiconductor Lasers", IEEE J. Quantum Electron., Vol. 23, No. 6, pp. 1000-1004, 1987.

[80] J M Hammer, "Closed Form Theory of Multicavity Reflectors and the Output Power of External Cavity Diode Lasers", IEEE J. Quantum Electron., Vol. 20, No. 11, pp. 1252-1259, 1984.

[81] R Q Hui and S P Tao, "Improved Rate Equations for External Cavity Semiconductor Lasers", IEEE J. Quantum Electron., Vol. 25, No. 6, pp. 1580-1584, 1989.

[82] G P Agrawal, "Generalise Rate Equations and Modulation Characteristics of External-Cavity Semiconductor Lasers", J. Appl. Phys., Vol. 56, No. 11, pp. 3110-3115, 1984.

[83] P J Probert and J E Carroll, "Lumped Circuit Model for Prediction of Linewidth in Fabry-Perot and DFB Lasers, Including External Cavity Devices", IEE Proc.-Part J, Vol. 136, No. 1, pp. 22-32, 1989.

[84] R Hui and Y Wu, "Noise and Frequency Chirping in External-Cavity Semiconductor Lasers", Optics Lett., Vol. 14, No. 13, pp. 668-670, 1989.

[85] R Lang and K Kobayashi, "External Optical Feedback Effects on Semiconductor Injection Laser Properties", IEEE J. Quantum Electron., Vol. 16, No. 3, pp. 347-355, 1980.

[86] R A Fisher, "Optical Phase Conjugation", Academic Press, 1983.

Chapter 4:

Intensity Noise and Dynamics of External Cavity Laser Diodes.

4.1 Introduction to External Cavity Laser Diodes.

In this chapter the intensity noise and dynamics of external cavity laser diodes are investigated. The iterative travelling wave model, developed in chapter 3, for a diode laser with strong optical feedback is used to perform investigations into intensity noise, resonant modulation, dynamics, and transitions between optical feedback regimes. An external cavity laser is shown in fig. 4.1. A mirror is placed in the path of the light output of the laser such that much of the light is returned into the laser. The light output is obtained through the laser facet r_1 or through the external mirror if its reflectivity is less than 100%. The laser facet r_2 may or may not be antireflection (AR) coated. Laser diodes in this external cavity configuration are known as External Cavity Diode Lasers (ECDL's). Other configurations of external cavity diode lasers have been described in chapter 3.

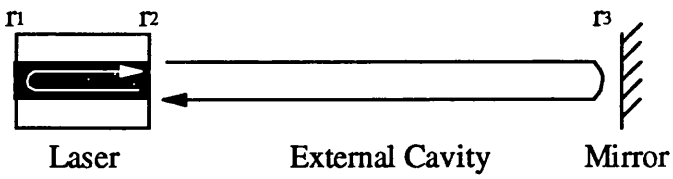

Fig. 4.1: An External Cavity Laser Showing Strong Optical Feedback From a Mirror.

4.2 Introduction to the Behaviour of External Cavity Laser Diodes.

As has been described in chapter 3, a typical external cavity laser has a dramatically reduced linewidth and a reduced threshold current. The optical feedback properties of laser diodes have been classified into five regions of behaviour denoted regimes I - V respectively [1,2], where stable external cavity operation is known as regime V. These

regimes have been described in more detail in chapter 1. Regimes I - IV encompass the low feedback properties of laser diodes, and have been thoroughly investigated. The regime denoted IV is the "Coherence Collapse" state of operation at moderate feedback levels [3-5]. The present chapter considers regimes IV and V and the transitions between them.

The intensity noise of an external cavity laser is considerably different to that of a solitary laser. The external cavity causes resonances of the intensity noise at frequencies of multiples of $1/\tau_{ext}$, where τ_{ext} is the external cavity round trip delay. The intensity noise at other frequencies is suppressed. The modulation response of the external cavity laser is also enhanced at multiples of $1/\tau_{ext}$. Thus, the use of external cavities allows the resonant modulation of laser diodes [6-13]. The modulation must be narrow band due to the $1/\tau_{ext}$ peaks in the modulation response, but can be of frequencies much larger than the relaxation oscillation frequency f_r of the solitary laser. This is similar to modelocking of lasers using external cavities [14].

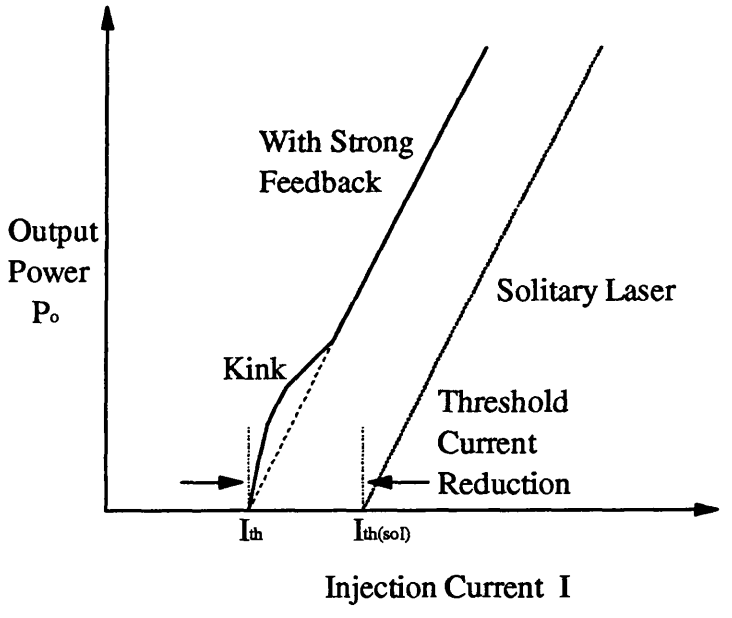

Fig. 4.2: The Changing of the Light-Current Characteristic Due to Strong Optical Feedback and the Formation of the "Kink".

When a laser with strong optical feedback is operated close to or below the solitary laser threshold current the output power evolves into a regime of behaviour known as Low Frequency Fluctuations (LFF) [15-28]. The Low Frequency Fluctuations are associated with the kink in the Light-Current characteristic as shown in fig. 4.2 [18,27]. A sudden drop in output intensity occurs followed by a stepwise increase, as shown in fig. 4.3, with the steps being of duration τ_{ext}. The process repeats with seemingly random periods T_{LFF}, which typically last fifty to several hundred

nanoseconds. The average period is known as the laminar length $T_{LAM(AV)}$. The Low Frequency Fluctuations are similar to the intensity drop outs seen in a more general delayed feedback situation, known as Ikeda rifts [29,30].

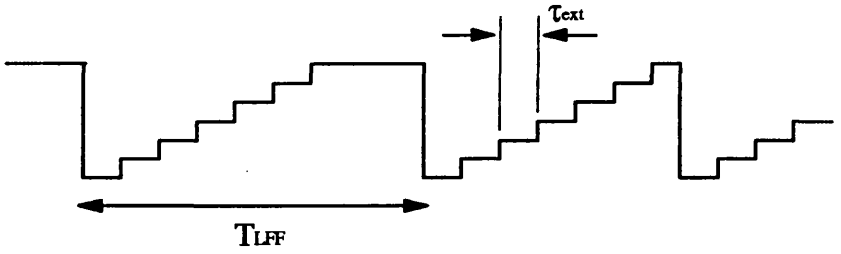

Fig. 4.3: An Example of a Low Frequency Fluctuation (LFF) Showing the Random Period T_{LFF} and the Step Duration of the External Cavity Round Trip Delay τ_{ext}.

Lastly, the external cavity provides an easy way of inserting optical elements into the lasing cavity. An external cavity frequency modulated FM laser diode [31-34] can be designed in this way, as described in section 3.8. A phase modulator is placed in the external cavity and produces a frequency modulation of the laser light. The result is a sinusoidally varying output frequency but at constant output power.

4.3 Use of the Iterative Travelling Wave Model to Describe External Cavity Laser Diodes.

The Investigations into the behaviour of external cavity laser diodes are performed using the iterative travelling wave model for strong optical feedback described in chapter 3 [15,25,35,36]. The iterative equations (3.38)-(3.41) are given again here for completeness,

$$A^+(t+\tau_L) = \frac{1}{r_2^2} e^{\frac{1}{2}(1+j\alpha)G_n(n(t)-n_{th})\tau_L} \times \left\{ A^+(t) - (1-r_2^2)\sum_{q=0}^{\infty} \left(-r_2 r_3 e^{-j\omega\tau_{ext}}\right)^q A^+(t-q\tau_{ext}) \right\}, + F_L(t)\tau_L \tag{4.1}$$

$$n(t+\tau_L) = n(t) + \frac{dn(t)}{dt}\tau_L + \frac{1}{2}\frac{d^2n(t)}{dt^2}\tau_L^2, \tag{4.2}$$

$$\frac{dn(t)}{dt} = \frac{I}{eV} - \frac{n(t)}{\tau_{sp}} - G_n(n(t)-n_o)s(t), \tag{4.3}$$

$$\frac{d^2n(t)}{dt^2} = \frac{1}{eV}\frac{dI(t)}{dt} - \left\{\frac{1}{\tau_{sp}} + G_n s(t)\right\}\frac{dn(t)}{dt} - G_n(n(t)-n_o)\frac{ds(t)}{dt}. \qquad (4.4)$$

The iterative model is represented by fig. 4.4. In equations (4.1)-(4.4) $A^+(t)$ is the right moving electric field and n(t) is the carrier density. All other terms are described in chapter 3. The iterative equations are solved at time steps of the laser internal cavity round trip time τ_L. The photon density s(t), output power $P_o(t)$, and emission frequency $\omega(t)$ are calculated as described in chapter 3. A more detailed description of the iterative solution of equations (4.1)-(4.4) is given in appendix 4. The values of the diode laser parameters used in the model are given in table 2.1.

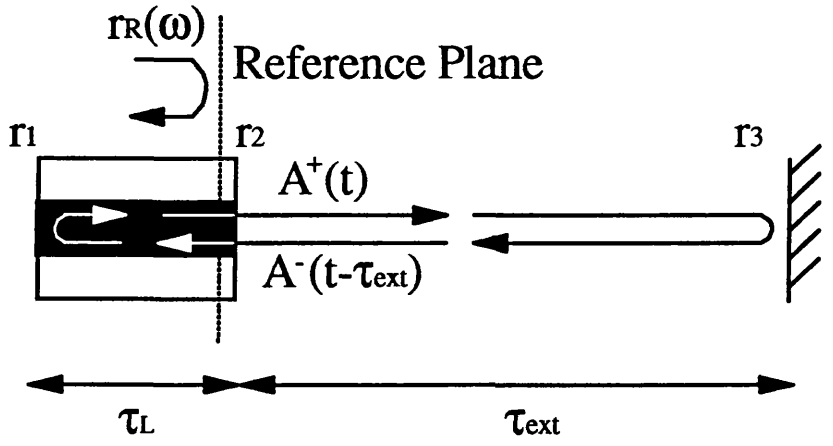

Fig. 4.4: Representation of the Iterative Travelling Wave Model for an External Cavity Laser.

4.4 Output Power Fluctuations.

The iterative travelling wave model for an external cavity diode laser allows the investigation of all five of the optical feedback regimes. Here regimes IV (Coherence Collapse) and V (stable external cavity operation) will be investigated. Fig. 4.5 shows output power $P_o(t)$ time series for different combinations of laser facet reflectivity r_2 and external reflectivity r_3. Spontaneous emission noise is included in the simulations. The upper left waveform shows that without feedback the laser behaves in a stable manner with the intensity noise oscillations being predominantly determined by the relaxation oscillation frequency f_r. The top right waveform is for weak feedback (within optical feedback regimes I - III) and shows a slightly enhanced level of noise. The middle two waveforms show the coherence collapse operation state (regime IV), with very large levels of noise consisting of high power spikes. The top four traces could be generated using a weak feedback rate equation model such as is used in chapter 2. However, the iterative travelling wave model developed in chapter 3 can

also investigate strong optical feedback where the laser operates in regime V. Such regime V operation is shown in the bottom two traces. The laser is anti-reflection (AR) coated. The intensity noise is seen to repeat predominantly at the round trip time of the external cavity τ_{ext}. For a lower laser facet reflectivity the intensity noise consists of smaller spikes. Thus, fig. 4.5 shows that the iterative travelling wave model is suitable for investigating all five of the optical feedback regimes.

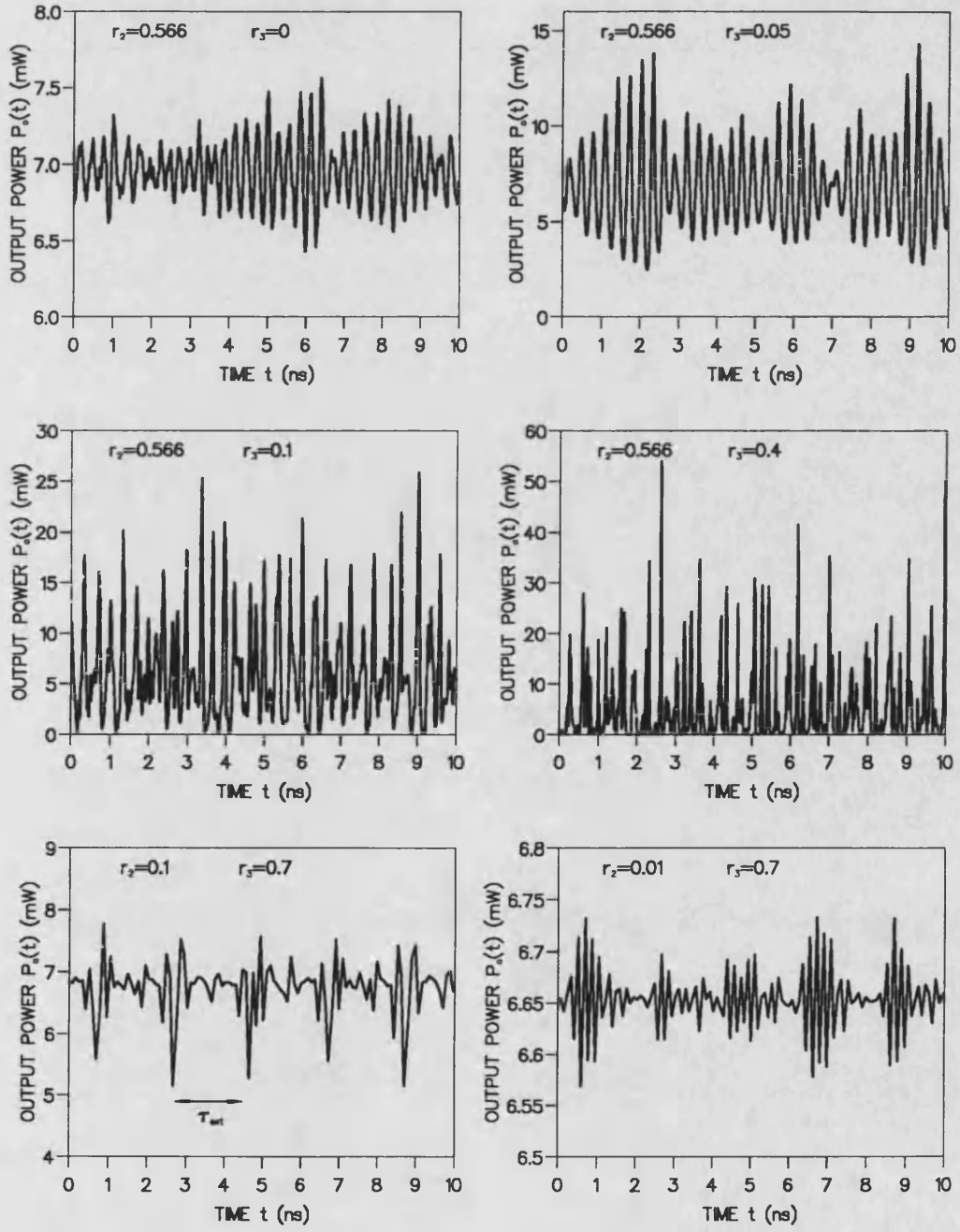

Fig. 4.5: Output Power $P_o(t)$ Waveforms for Different Combinations of Laser Facet Reflectivity r_2 and External Reflectivity r_3. The Graphs Show Zero Feedback (top left), Weak Feedback (top right), Coherence Collapse (middle), and External Cavity AR-Coated Operation (bottom) ($I=2I_{th}$, $\tau_{ext}=2$ ns).

4.5 Intensity Noise.

The Relative Intensity Noise (RIN) of the laser, defined by

$$RIN = \frac{\overline{P_o(t)^2} - \overline{P_o(t)}^2}{\overline{P_o(t)}^2}, \tag{4.5}$$

is shown in fig. 4.6 for external reflectivities ranging from weak feedback (regimes I-IV) to external cavity operation (regime V). The RIN increases in the coherence collapse regime as expected [37,38] (approximately between $r_3=10^{-3}$ and $r_3=0.1$), and decreases as the laser enters regime V at high levels of feedback [39,40]. Fig. 4.7 shows the RIN spectra at three different combinations of the laser facet and external mirror reflectivities. Without feedback the intensity noise peaks at the relaxation oscillation frequency. At weak feedback the noise has peaks at multiples of the inverse external cavity round trip delay $1/\tau_{ext}$ but still under an envelope that has a maximum at the relaxation frequency f_r. For stable external cavity operation with an AR-coated laser facet there are many multiples of the inverse cavity round trip delay in the intensity noise spectrum.

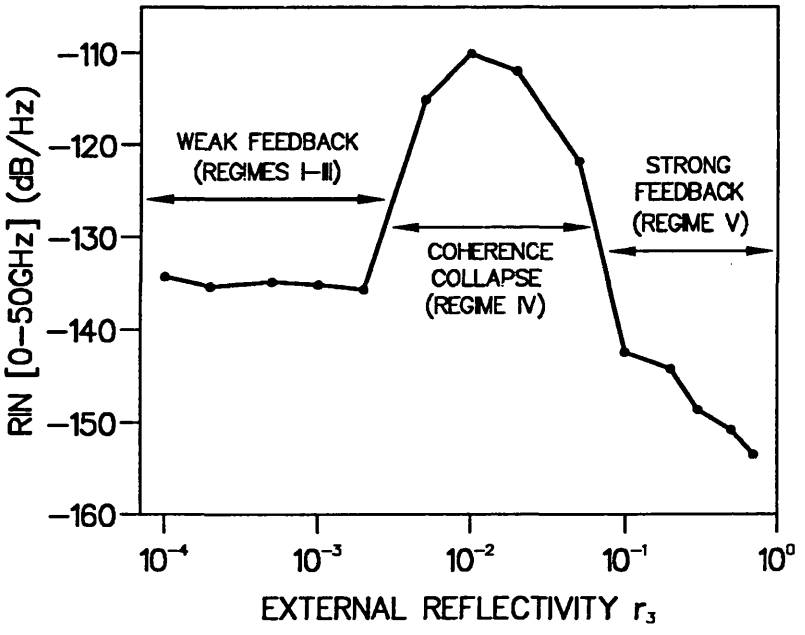

Fig. 4.6: Relative Intensity Noise (RIN) for Optical Feedback Levels Ranging from Weak Feedback Through to Stable External Cavity Operation ($I=2I_{th}$, $r_2=0.2$, $\tau_{ext}=0.9$ ns).

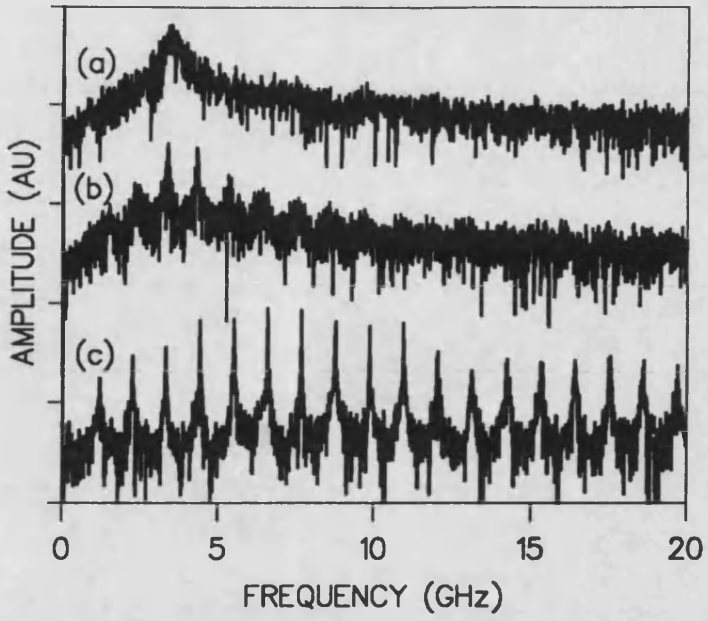

Fig. 4.7: RIN Spectra for {a} Low Feedback (r_2=0.566, r_3=0.001), {b} Strong Feedback Causing Coherence Collapse (r_2=0.566, r_3=0.7), and {c} AR-Coated Operation (r_2=0.01, r_3=0.7). τ_{ext}=0.9 ns for all Three Graphs. The Graphs are Shifted Vertically for Clarity.

4.6 Resonantly Enhanced Modulation.

Fig. 4.7 has shown that the intensity noise spectrum of an external cavity laser consists of peaks at multiples of $1/\tau_{ext}$. This property can be put to use to resonantly modulate the laser at microwave frequencies [6-13], for which a relatively short external cavity is required. Fig. 4.8 shows the intensity noise spectrum of such a laser with a short external cavity. There are strong intensity noise peaks at frequencies of many tens of GHz. Therefore, it is expected that the resonances of the external cavity can be used to modulate the laser at very high frequencies. The modulation response under the same operating conditions is shown in fig. 4.9, and also shows resonances at multiples of $1/\tau_{ext}$. Therefore, the laser can be modulated at microwave frequencies, providing that the signal is narrow-band, so that the modulation frequency remains within the resonance peaks of the external cavity. In such a way it is possible to modulate the laser at frequencies far in excess of the relaxation oscillation frequency f_r [6-13]. Figs. 4.8 and 4.9 should be compared to the corresponding intensity noise spectrum and modulation response for a solitary laser shown in figs. 4.10 and 4.11 respectively.

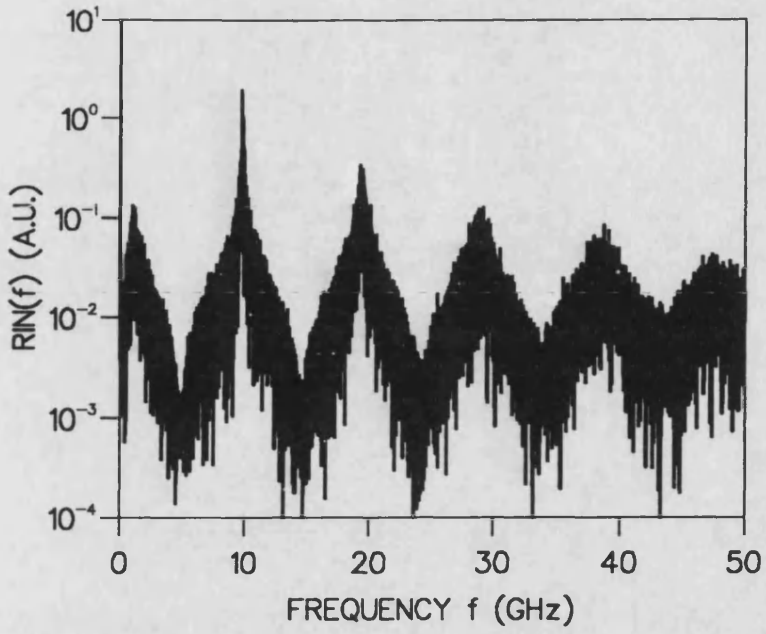

Fig. 4.8: Intensity Noise Spectrum of a Resonantly Enhanced AR-Coated Laser (r_2=0.01, r_3=0.7, I=2I_{th}).

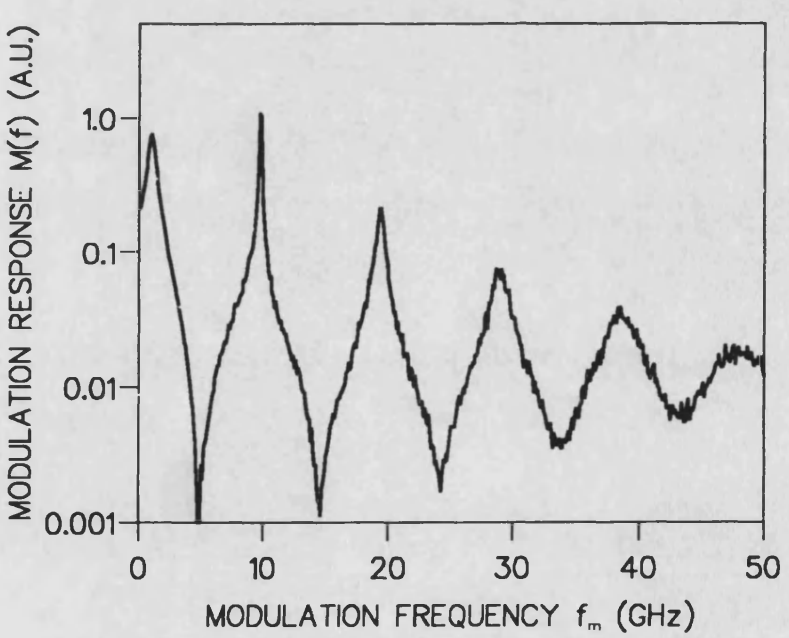

Fig. 4.9: Modulation Frequency Response of a Resonantly Enhanced AR-Coated Laser (r_2=0.01, r_3=0.7, τ_{ext}=10.5τ_L, I=2I_{th}, m=0.01).

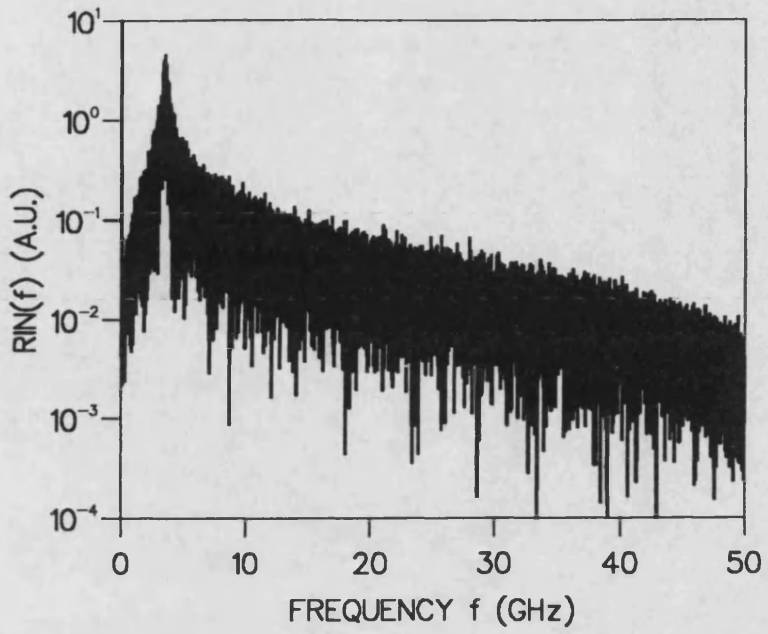

Fig. 4.10: Intensity Noise Spectrum of a Solitary Laser ($I=2I_{th}$).

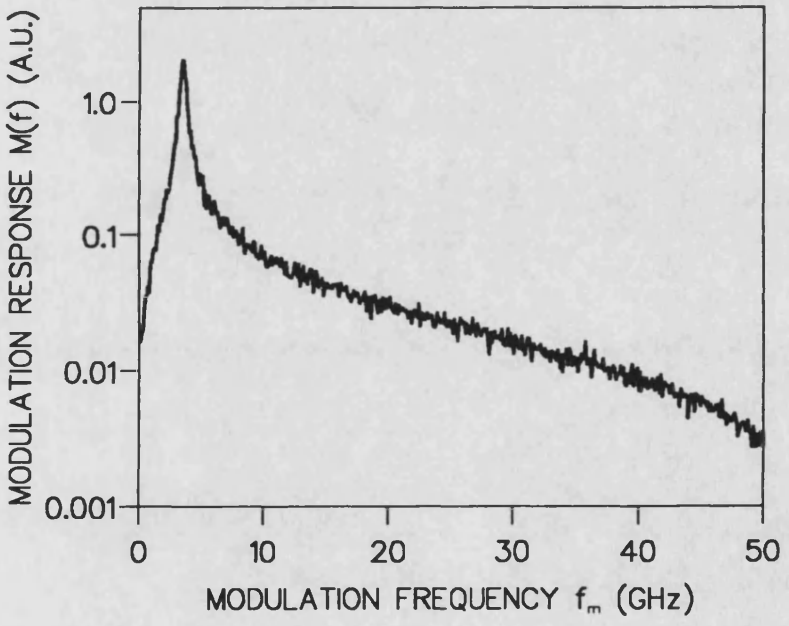

Fig 4.11: Modulation Frequency Response of a Solitary Laser ($I=2I_{th}$, m=0.01).

4.7 Low Frequency Fluctuations.

When the laser with optical feedback is biased close to threshold Low Frequency Fluctuations (LFF) occur [15-28]. Strong optical feedback is not required to produce Low Frequency Fluctuations. However, the iterative travelling wave model has been used due to the speed of the model in calculating the very long timescale dynamics required. The same calculations performed using a rate equation model would be much more computationally expensive.

The Low Frequency Fluctuations consist of drop-outs of the laser output, followed by a stepwise increase, as depicted in fig. 4.3. The steps have a duration of the external cavity round trip delay τ_{ext} and there is a random number of steps in each period. The LFF's appear in the kink region of the light-current characteristic of fig. 4.2. A typical LFF generated using the iterative model is shown in fig. 4.12, with two periods being shown in more detail in fig. 4.13. The stepwise increase in the output power at time intervals of τ_{ext} are clearly seen. The output power for figs 4.12 and 4.13 is averaged over 100 iteration steps or 0.9 ns. Without this averaging the steps are difficult to see as the actual output consists of intensity spikes as shown in fig. 4.14 [27]. The averaging is not required if looking at the carrier density as is shown in fig. 4.15 [15].

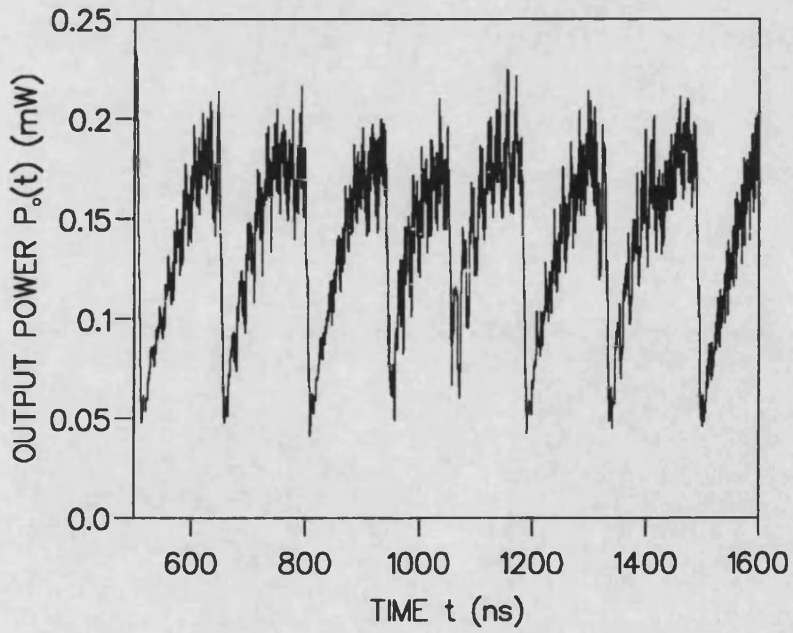

Fig. 4.12: Output Power $P_o(t)$ During Low Frequency Fluctuations Showing Eight LFF Periods. The Output is Averaged Using a 0.9 ns Running Average ($I=1.01I_{th}$, $r_2=0.566$, $r_3=0.1$, $\tau_{ext}=15$ ns).

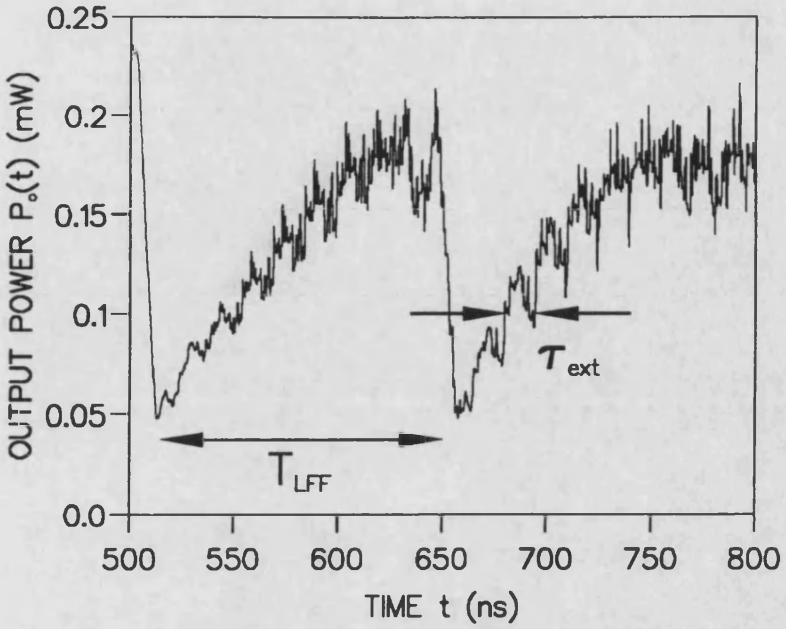

Fig. 4.13: Detail of Fig 4.12 Showing a Particular Low Frequency Fluctuation Period T_{LFF} and the External Cavity Round Trip Delay τ_{ext} ($I=1.01I_{th}$, $r_2=0.566$, $r_3=0.1$, $\tau_{ext}=15$ ns).

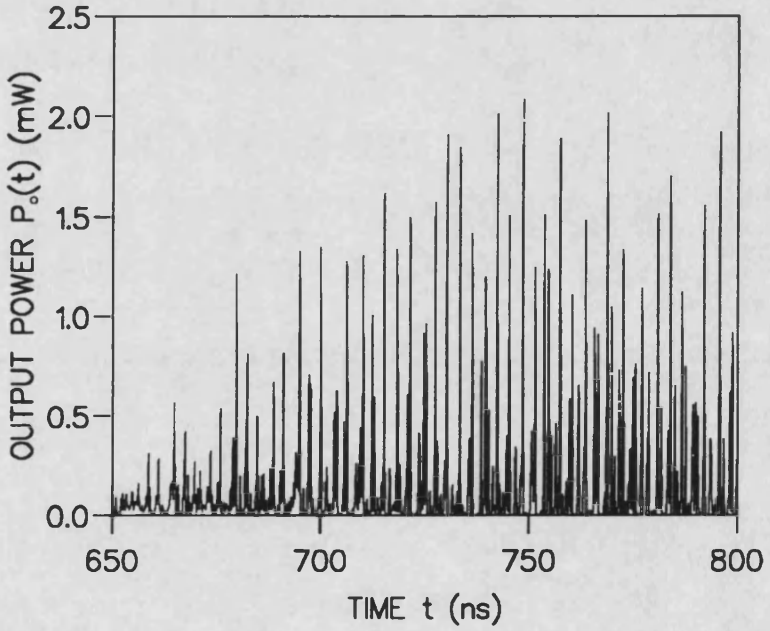

Fig. 4.14: Detail without Averaging of a Single Period of a Low Frequency Fluctuation Showing that the LFF Consists of Many Output Power $P_o(t)$ Spikes ($I=1.01I_{th}$, $r_2=0.566$, $r_3=0.1$, $\tau_{ext}=15$ ns).

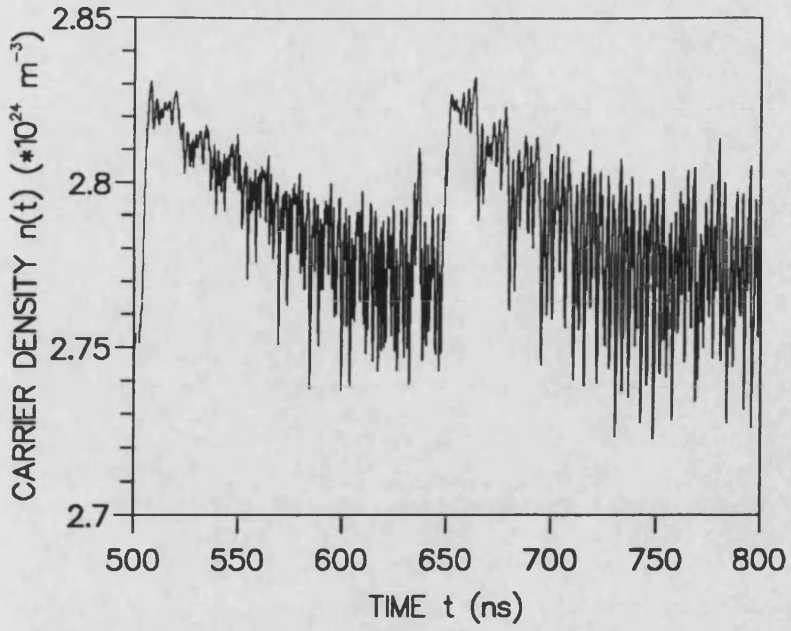

Fig. 4.15: The Corresponding Carrier Density n(t) for Fig. 4.14. No Averaging is Performed ($I=1.01I_{th}$, $r_2=0.566$, $r_3=0.1$, $\tau_{ext}=15$ ns).

The intensity noise frequencies present during the LFF are shown in fig. 4.16. Three frequencies are easily identified. They are the frequency of the LFF itself f_{LFF}, the inverse of the external cavity round trip delay $1/\tau_{ext}$, and the laser diode relaxation oscillation frequency f_r. The LFF peak is broad due to the variation in the number of steps present in each LFF period. The intensity noise peaks at multiples of the inverse cavity round trip delay are contained within an envelope which has a maximum at the relaxation oscillation frequency f_r. The relaxation oscillation frequency seen in fig. 4.16 is f_r=480 MHz. This value is close to that of f_r=550 MHz calculated at the same bias current using [41]

$$f_r = \frac{1}{2\pi}\left\{\frac{S_o G_n}{\tau_{ph}} - \frac{1}{4}\left(\frac{1}{\tau_{sp}} + S_o G_n\right)^2\right\}, \tag{4.7}$$

where s_o is the stationary value of the photon density. It can also be seen in fig. 4.16 that the intensity noise peaks at multiples of the inverse external cavity round trip delay split into double peaks due to the presence of the Low Frequency Fluctuations. This splitting of the intensity noise peaks has been seen experimentally [15] but no clear explanation for this phenomena has yet been given.

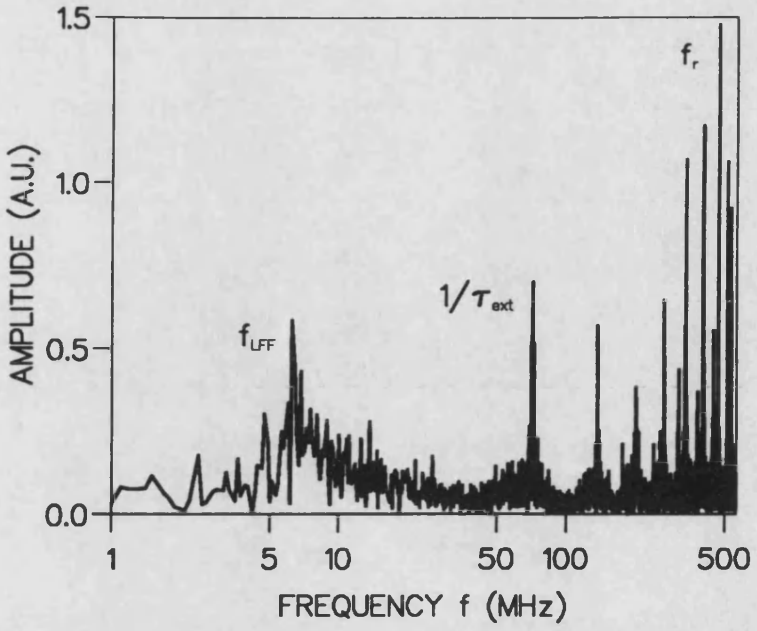

Fig. 4.16: RIN Spectra During Low Frequency Fluctuations Isolating the Three Characteristic Frequencies ($I=1.01I_{th}$, $r_2=0.566$, $r_3=0.1$, $\tau_{ext}=15$ ns).

The emission spectra during each step of the LFF of fig. 4.13 are shown in fig 4.17. Step 0 is the step immediately preceding the sudden drop in intensity. It is seen that the emission spectrum changes rapidly after the drop-out and slowly returns to its former state during the subsequent steps. This process is an indication that jumping between external cavity modes is occurring. The LFF has recently been shown to be the result of such an external cavity mode jumping [27]. Several external cavity modes exist which have slightly different gains. The laser jumps to the adjacent external cavity mode, trying to reach the mode of maximum gain, as shown in fig. 4.18. Since each mode has a different gain, the output power in each step is different, giving the stepwise increase. This process continues, but the laser never reaches the mode of maximum gain. An unstable mode is reached and the laser falls back to a low gain external cavity mode and so is quenched, leaving no output power. The process then repeats again.

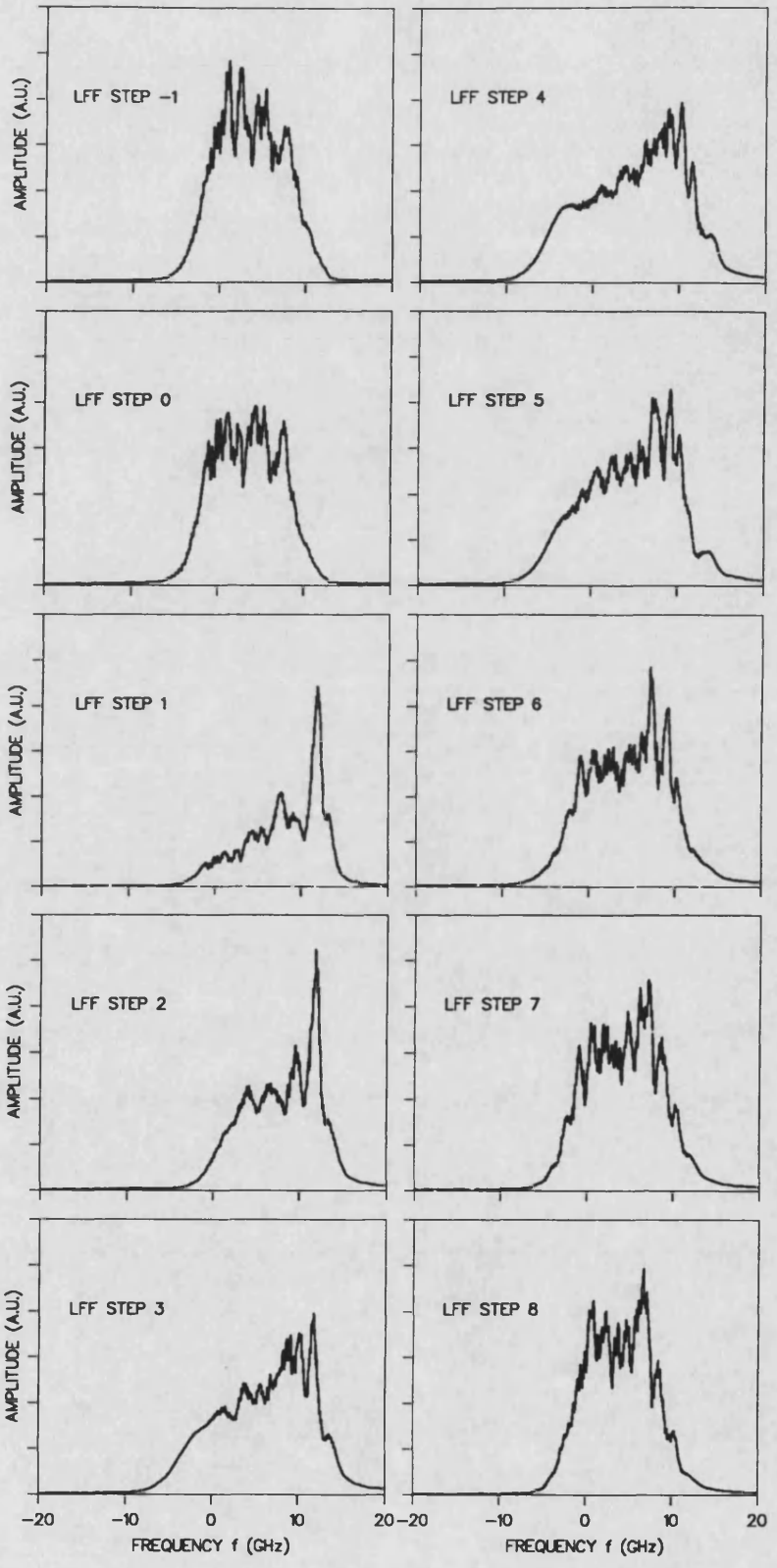

Fig. 4.17: Emission Spectra of the Laser During Each Step of the Low Frequency Fluctuation ($I=1.01I_{th}$, $\tau_{ext}=15$ ns, $r_2=0.566$, $r_3=0.1$).

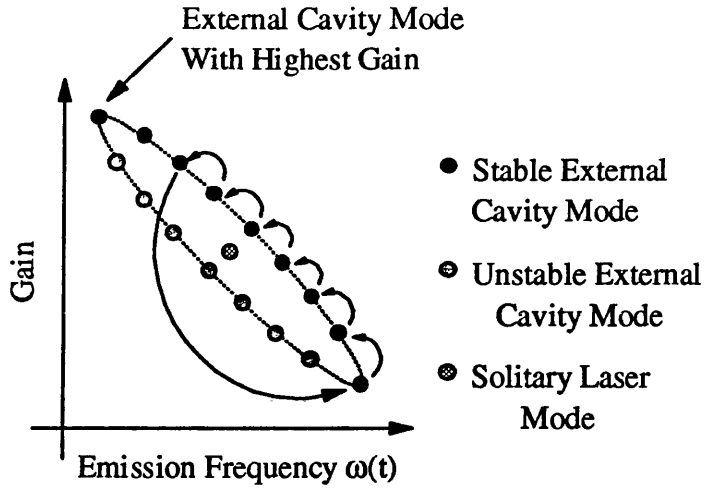

Fig. 4.18: The Evolution of the Low Frequency Fluctuation Described as a Successive External Cavity Mode Jumping.

4.8 Laminar Lengths of Low Frequency Fluctuations.

The average period of the LFF is described as the laminar length $T_{LAM(AV)}$. The term laminar length is taken from chaos theory where it is used to characterise the intermittent appearance of complex dynamics [42]. Fig 4.19. shows a series of samples of the LFF period T_{LFF}. The period is seen to be random. A distribution of the LFF periods is shown in fig. 4.20, with a steep rise for low periods and a long tail at high periods. The type of intermittency can be ascertained by plotting the laminar length $T_{LAM(AV)}$ against the fraction of injection current above the modified laser threshold with feedback. A plot such as this is shown in fig. 4.21. and has a slope of approximately -1, indicating either type II or type III intermittency [42].

Fig 4.22 shows that the average laminar length $T_{LAM(AV)}$ is proportional to the external cavity round trip delay. Therefore the external cavity round trip time does not affect the dynamics of the intermittency process. The dependency of the average laminar length $T_{LAM(AV)}$ on the external reflectivity is shown in fig. 4.23. The average laminar length increases with external reflectivity (and hence output power).

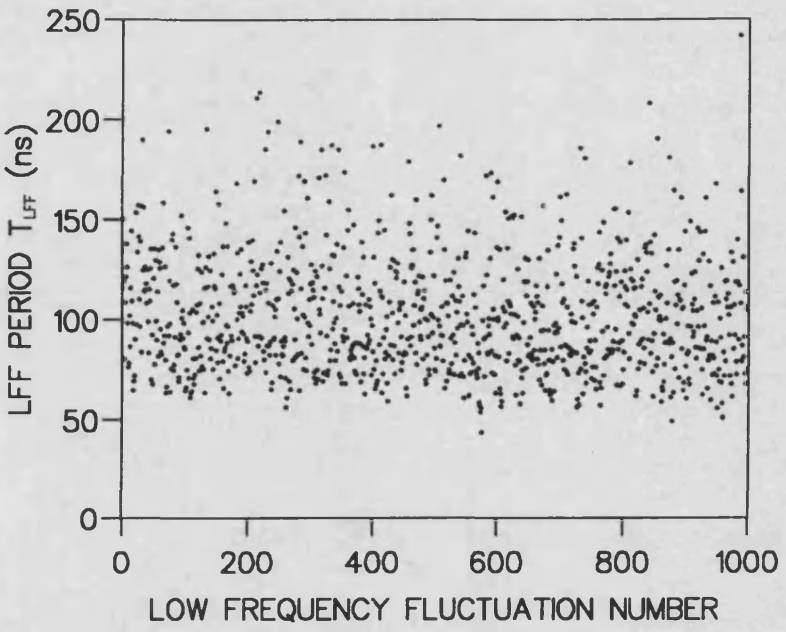

Fig. 4.19: Samples of the Period T_{LFF} of the Low Frequency Fluctuations ($I=1.01I_{th}$, $\tau_{ext}=6$ ns, $r_2=0.566$, $r_3=0.2$).

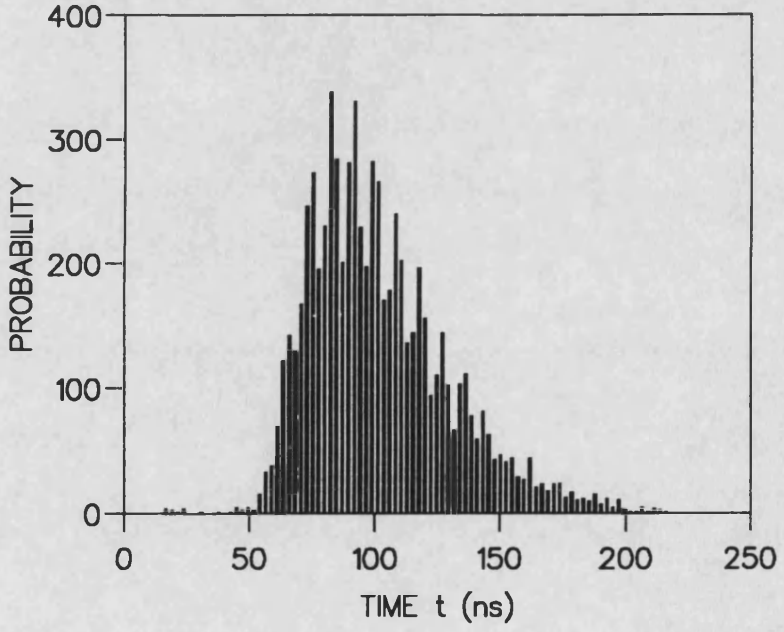

Fig. 4.20: Probability Distribution of the Period T_{LFF} of the Low Frequency Fluctuations ($I=1.01I_{th}$, $\tau_{ext}=6$ ns, $r_2=0.566$, $r_3=0.2$).

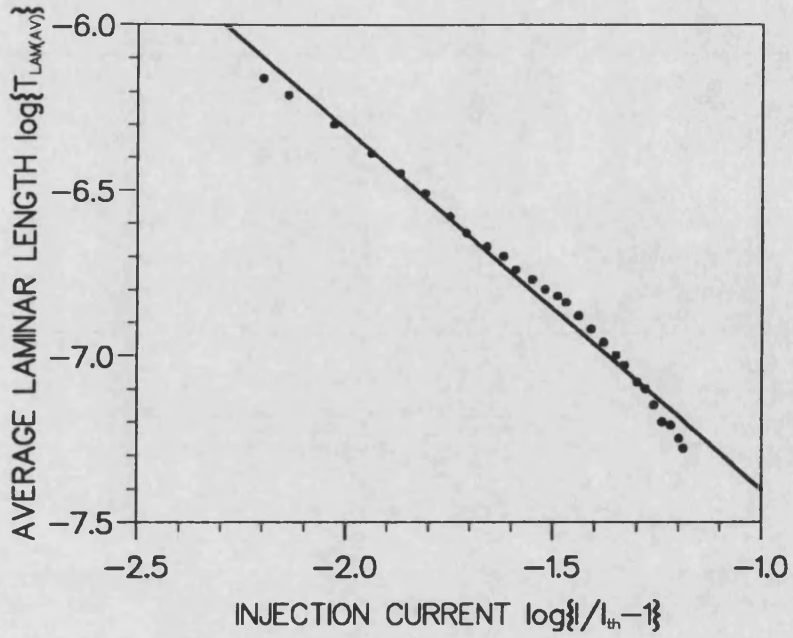

Fig. 4.21: Dependency of the Average Laminar Length $T_{LAM(AV)}$ of the Low Frequency Fluctuations with Injection Current I (r_2=0.566, r_3=0.2, τ_{ext}=6 ns).

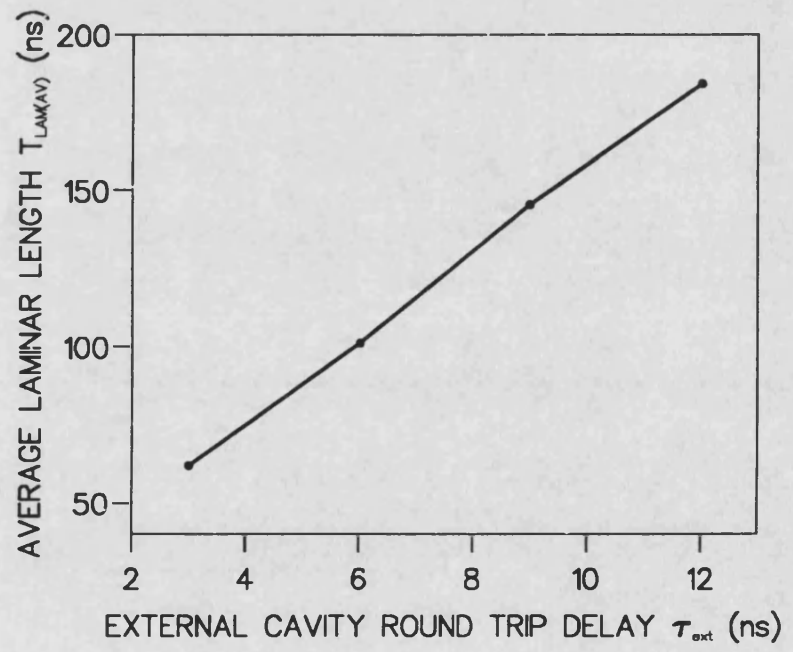

Fig. 4.22: Dependency of the Average Laminar Length $T_{LAM(AV)}$ of the Low Frequency Fluctuations with External Cavity Round Trip Delay τ_{ext} (r_2=0.566, r_3=0.2, I=1.01I_{th}).

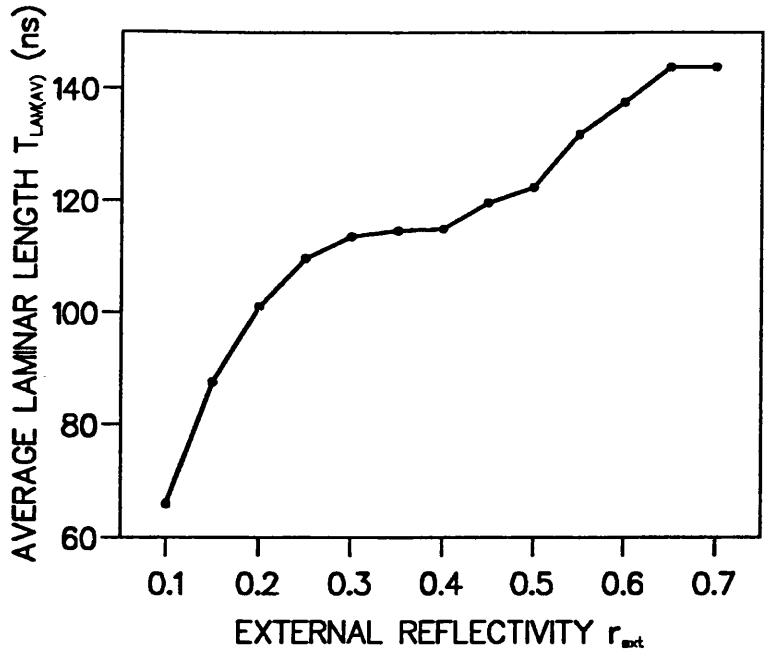

Fig. 4.23: Dependency of Average Laminar Length $T_{LAM(AV)}$ of the Low Frequency Fluctuations with External Reflectivity r_3 (τ_{ext}=6 ns, r_2=0.566, I=1.01I_{th}).

4.9 Experimental Investigations into Low Frequency Fluctuations.

Experimental measurements on the laminar length of the LFF's have been performed [43,44]. The experimental apparatus is shown in fig 4.24. The laser diode used was a Toshiba TOLD 9140. The laser diode was coupled to a Barium Titanate ($BaTiO_3$) crystal, producing a photorefractive phase conjugate mirror [45]. Investigations have shown that all the LFF phenomena seen in the experiments also occur for conventional optical feedback. Therefore, the LFF experimental results are compared to the numerical results produced using conventional optical feedback in the previous section. The experimental apparatus allowed the use of external reflectivities of between 15% and 40%. The external cavity length was 80 cm giving an external cavity round trip delay of 5.3 ns.

A typical experimentally observed LFF is shown in fig. 4.25. The experimental LFF period T_{LFF} probability distribution is shown in fig. 4.26. The distribution has a long tail at high periods, as found with numerical investigations using the iterative travelling wave model in section 4.9. The experimentally observed average laminar length $T_{LAM(AV)}$ is plotted against injection current in fig. 4.27. The slope of the

graph is again approximately -1, confirming the deduction in section 4.8 that the LFF is an intermittency phenomenon of type II or type III [42-44].

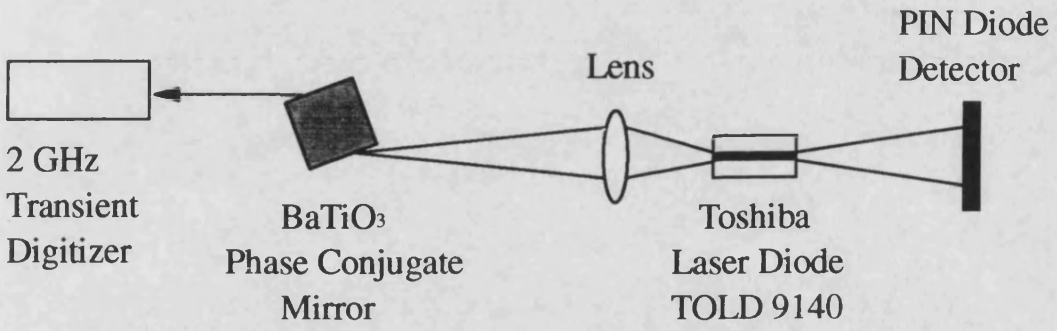

Fig. 4.24: Experimental Apparatus for the Investigation of Low Frequency Fluctuations.

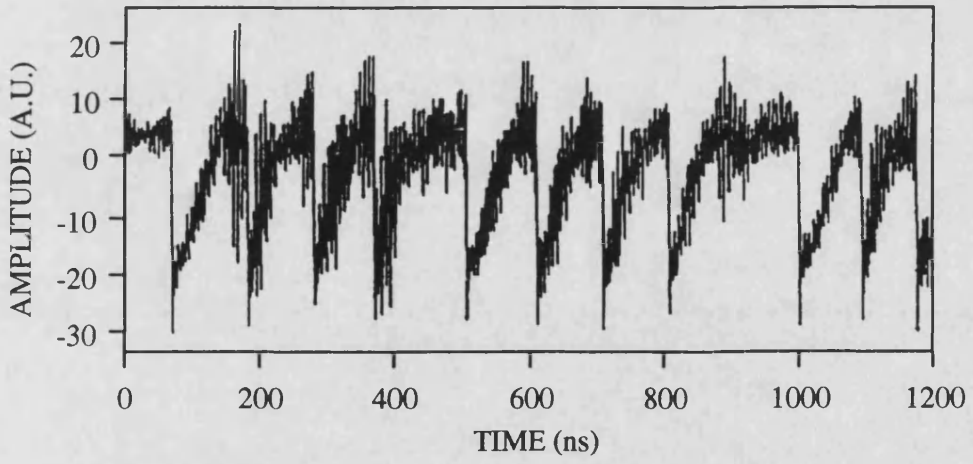

Fig. 4.25: Experimental Observation of Low Frequency Fluctuations (P_o=4.5 mW, τ_{ext}=5.3 ns).

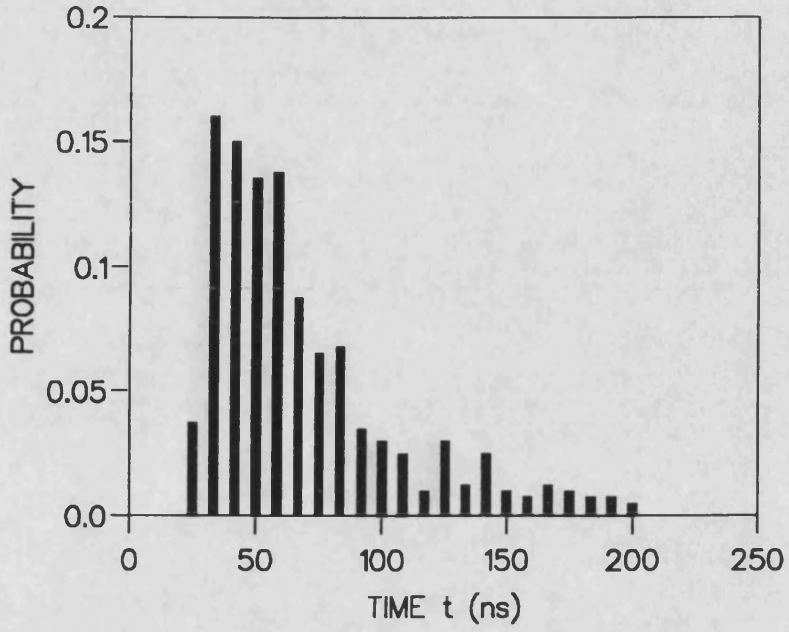

Fig. 4.26: Experimental Probability Distribution of the Period T_{LFF} of the Low Frequency Fluctuations (r_3=0.15, τ_{ext}=5.3 ns).

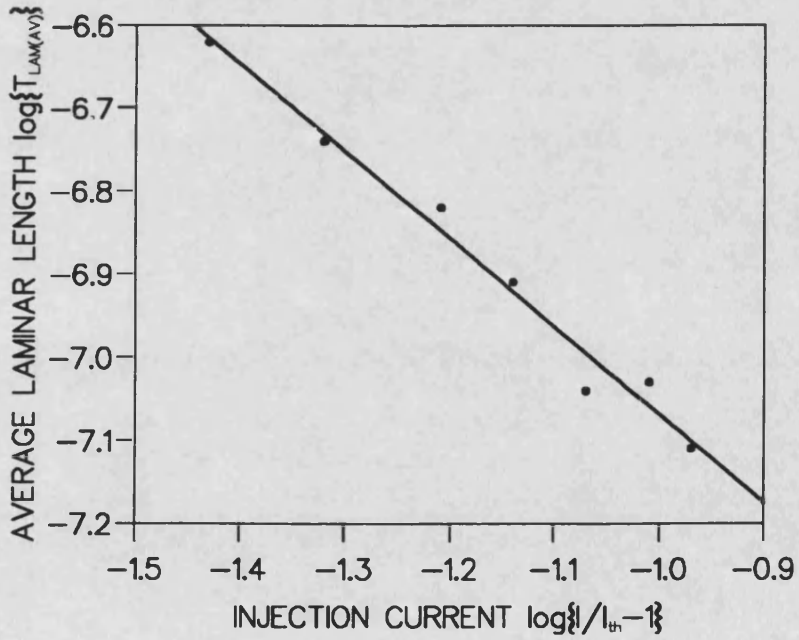

Fig. 4.27: Experimental Dependency of the Average Laminar Length $T_{LAM(AV)}$ of the Low Frequency Fluctuations with Injection Current I (r_3=0.15, τ_{ext}=5.3 ns).

4.10 Dynamics and Bifurcation Diagrams.

Bifurcation diagrams have been used to investigate the behaviour of the laser diode as the optical feedback is *increased* [3] from zero. The iterate travelling wave model has been used here to calculate bifurcation diagrams for *decreasing* [25,26] levels of strong optical feedback starting from the stable external cavity operation regime. Each time the output power $P_o(t)$ crosses its steady state value, the carrier density n(t) is recorded as a normalised value given by

$$\frac{n}{n_{th,r}} - 1 \rightarrow n, \tag{4.6}$$

where $n_{th,r}$ is the threshold carrier density with feedback. The number of different values of this normalised carrier density indicates the number of frequency components present in the laser output intensity fluctuations. Fig. 4.28 shows a bifurcation diagram of the normalised carrier density for increasing levels of reflectivity of the laser facet r_2. The external mirror reflectivity r_3 is fixed at a high value of 0.7. The left of the diagram corresponds to stable external cavity operation (regime V) with an anti-reflection (AR) coated laser diode and the right of the diagram corresponds to the noisy coherence collapse regime (regime IV) with an uncoated laser diode. The sudden increase in the width of the bifurcation diagram shows the point at which the laser facet reflectivity is too large to prevent the laser from entering the noisy coherence collapse regime [22,46]. For r_2 in the range 0.01-0.2, the laser output tends to repeat at a frequency $1/\tau_{ext}$ [47,48] determined by the external cavity round trip delay. The output power waveform $P_o(t)$, as seen in fig. 4.5, is quite complicated in contrast to the simple periodic oscillation at the relaxation frequency obtained with weak optical feedback. The laser output is also seen to repeat on timescales of τ_{ext} in an experimental trace of fig. 4.29 [43]. The experimental apparatus was the same as described in section 4.9. Also in contrast with the weak feedback regime, no bifurcation sequence is found in the present case. Fig. 4.30 shows the bifurcation diagram of the normalised carrier density for decreasing levels of the external mirror reflectivity r_3 for a constant AR-coated laser facet reflectivity r_2. The diagram shows the level of external feedback required to prevent noisy laser output, which has been previously identified as the transition into coherence collapse [46].

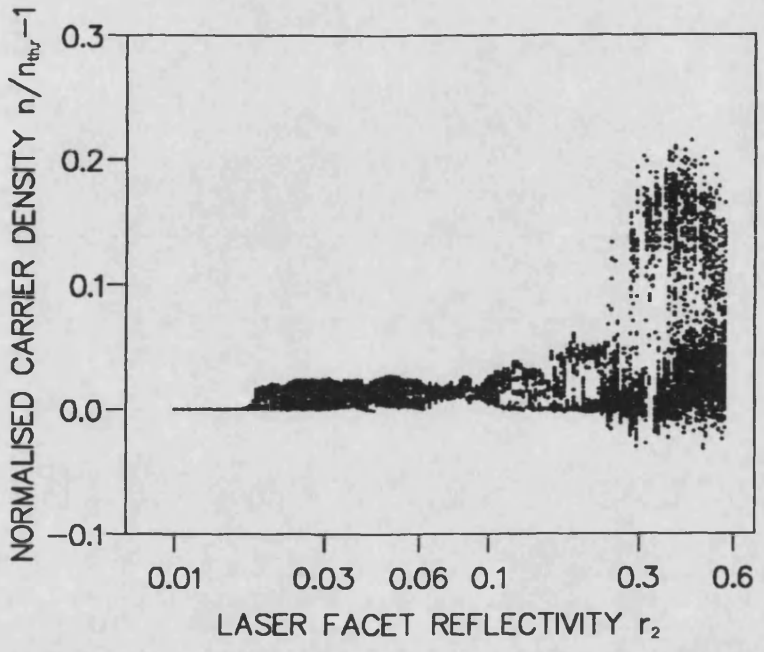

Fig. 4.28: Bifurcation Diagram for Normalised Carrier Density $n/n_{th,r}-1$ for Increasing Laser Facet Reflectivity r_2 in the Strong Feedback Operating Regime ($I=2I_{th}$, $r_3=0.7$, $\tau_{ext}=2$ ns).

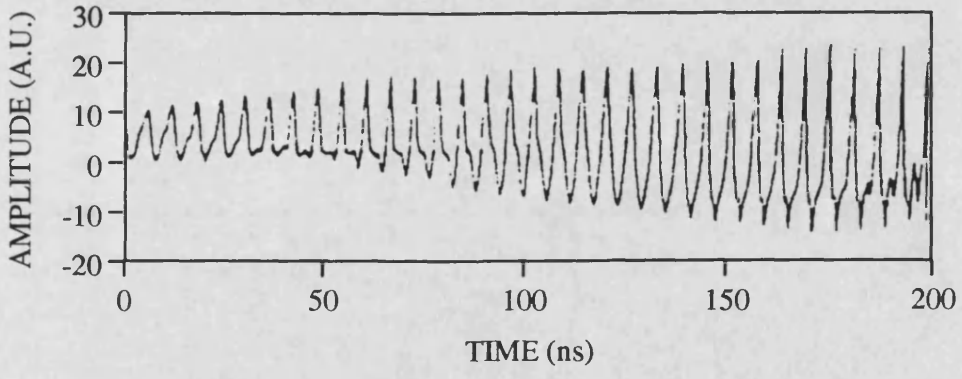

Fig. 4.29: Experimental Observation of the Output of an External Cavity Laser Diode Repeating at the External Cavity Round Trip Delay ($P_o=1$ mW, $\tau_{ext}=5.3$ ns).

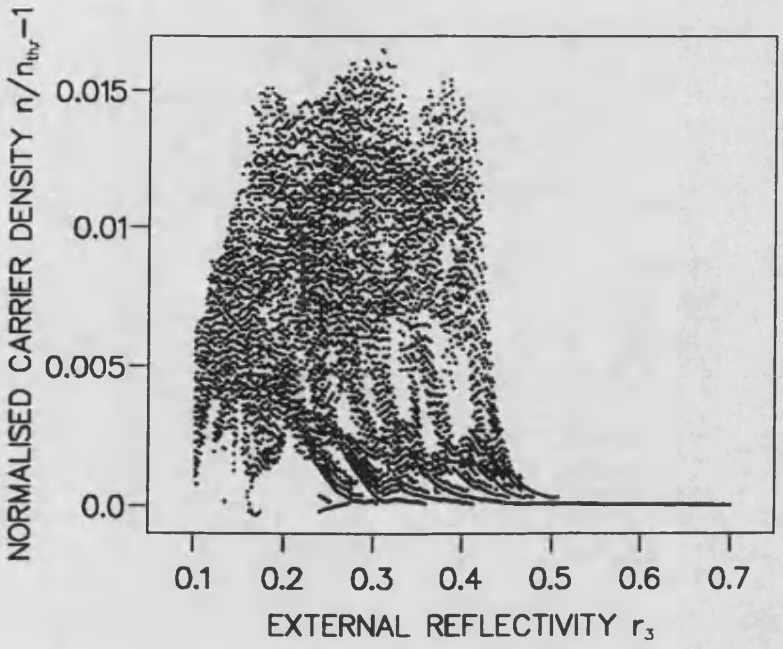

Fig. 4.30: Bifurcation Diagram for Normalised Carrier Density $n/n_{th,r}$-1 for Increasing Levels of Strong Optical Feedback ($I=2I_{th}$, $r_2=0.01$, $\tau_{ext}=2$ ns).

4.11 External Cavity Frequency Modulated FM Laser Diodes.

The model developed for external cavity frequency modulated (FM) diode lasers in section 3.9 is used in the present section. The right moving field $A^+(t)$ is given by (3.57), with the carrier iterative equations remaining as for the conventional external cavity diode laser model. The emission frequency of the external cavity FM laser calculated using the iterative travelling wave model is shown in fig. 4.31, showing the sinusoidal oscillation due to the RF phase modulation within the external cavity. However, the sinusoidal oscillation of the emission frequency is contained within an envelope of the detuning frequency f_m-$1/\tau_{ext}$, as shown in fig. 4.32, which should not be present. The output power is constant as expected. The sinusoidal modulation of the emission frequency that should be seen results in a characteristic emission spectra with the form of fig. 3.9. The envelope seen with the output of the external cavity FM laser diode model destroys this characteristic emission spectra giving a central peak at the steady state laser frequency. The envelope of the detuning frequency is not seen in practice [31-34] for FM lasers and so it is concluded that further development of the external cavity FM diode laser model is required.

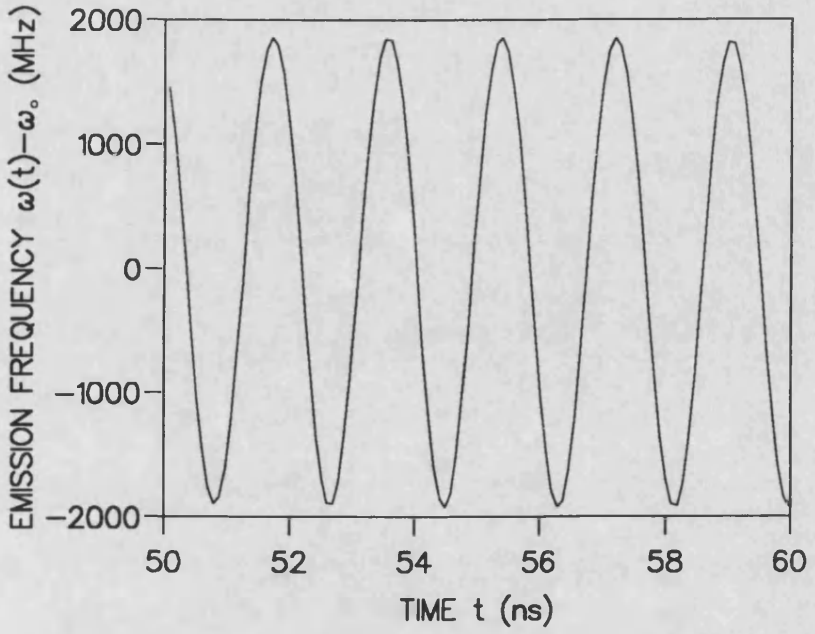

Fig. 4.31: Emission Frequency Output From the External Cavity Frequency Modulated (FM) Diode Laser Model (f_m-$1/\tau_{ext}$=10 MHz, r_3=0.7, r_2=0.1, Δ_m=0.1 rad).

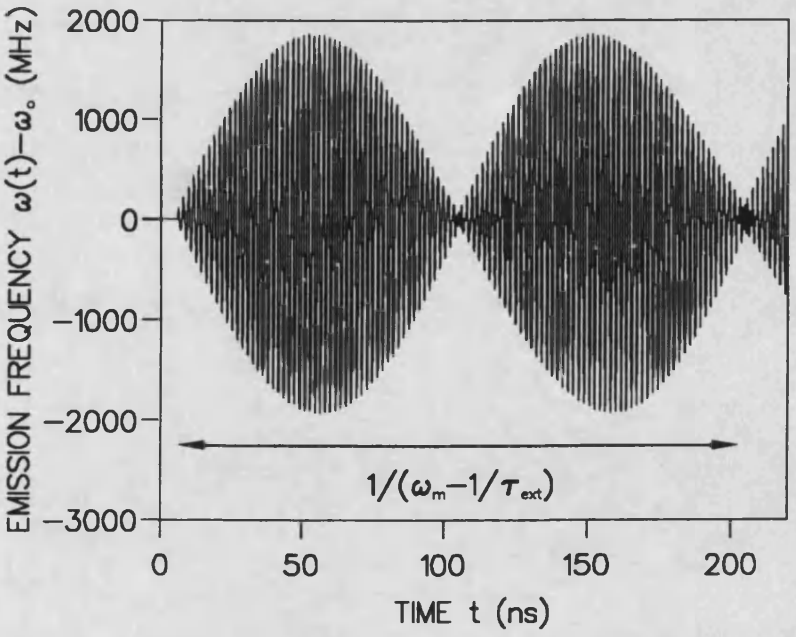

Fig. 4.32: A Longer Time Trace of Fig. 4.31 Showing the Unexpected Modulation of the Emission Frequency at a Frequency of the Detuning (f_m-$1/\tau_{ext}$=10 MHz, r_3=0.7, r_2=0.1, Δ_m=0.1 rad).

4.12 Experimental Investigations into External Cavity Frequency Modulated FM Laser Diodes.

Experimental measurements on the external cavity frequency modulated FM laser diode have been performed [32,34]. The experimental apparatus is shown in fig. 4.33. The laser diode was an STC Defence Systems STC LT50-03U and had a front facet reflectivity of approximately 4 % (r_2=0.2). The external cavity is formed by a mirror with 96.5 % (r_3=0.982) reflectivity. The external cavity length is 32 cm giving a longitudinal mode spacing $1/\tau_{ext}$ of 472 MHz. A Lithium Niobate ($LiNbO_3$) crystal is used to implement the external cavity phase modulation. The crystal is coupled to an inductor to make the resonance of the circuit close to the longitudinal mode spacing. RF powers of up to 0.5 W were applied to the phase modulator. The output of the laser was observed using a CCD camera, a variable Fabry-Perot interferometer to measure the optical frequency spectrum, a RF spectrum analyser to measure the intensity noise spectrum, and a sampling oscilloscope to monitor the time behaviour.

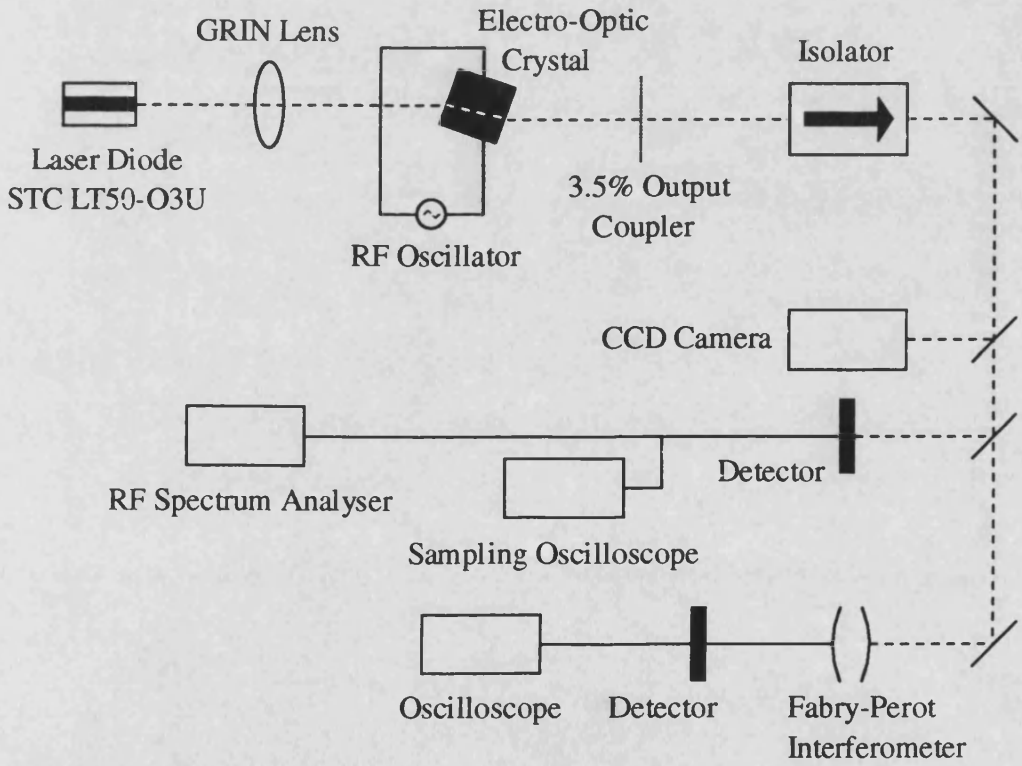

Fig. 4.33: Experimental Apparatus for the Investigation of External Cavity Frequency Modulated (FM) Laser Diodes.

The emission spectra for a single pass phase modulation Δ_m of 0.5 rad is shown in fig. 4.34 for decreasing detuning of the RF modulation from the longitudinal mode spacing $1/\tau_{ext}$. The characteristic emission spectrum for an FM laser is seen. The

appropriate Bessel function sidebands are drawn next to the emission spectra. If the single pass phase modulation is further increased the laser eventually moves into a regime in which there is a very broad linewidth emission [32]. This could be considered to be modulation induced coherence collapse. This transition into coherence collapse has not been investigated using the iterative travelling wave model because of the problem with the envelope of the detuning frequency, as described in the previous section.

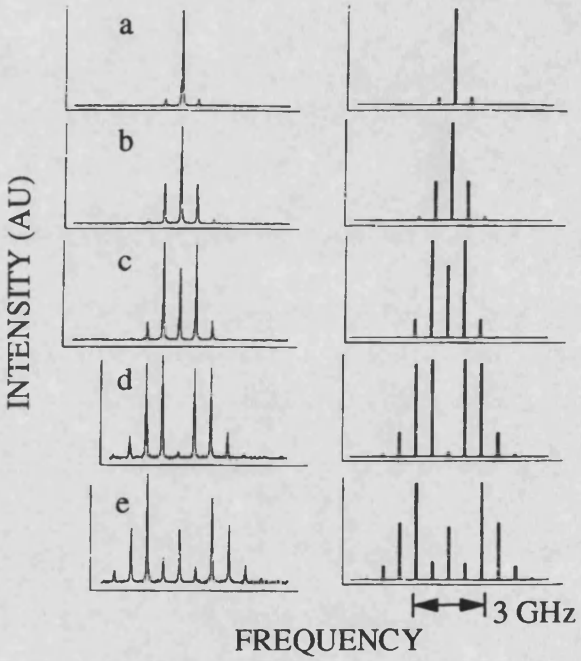

Fig. 4.34: Emission Frequency of External Cavity Frequency Modulated (FM) Laser Diode. The detuning f_m-$1/\tau_{ext}$ is respectively {a} 18.4, {b} 9.4, {c} 6.4, {d} 3.4, {e} 2.4 MHz (Δ_m=0.5 rad, R_2=4 % {r_2=0.2}, R_{ext}=96.5 % {r_3=0.982}). Graphs on the Right are the Corresponding Bessel Function Spectra.

4.13 Conclusion.

In summary, the iterative travelling wave model for a laser diode subject to strong optical feedback, developed in chapter 3, has been used to investigate strong optical feedback into laser diodes. The dynamics and intensity noise characteristics of the transition from stable external cavity operation to the coherence collapse regime have been investigated. It has been found that the model is suitable for all five of the regimes used to describe optical feedback behaviour. Large amounts of intensity noise is predicted in the coherence collapse regime under moderate optical feedback, and

low levels of intensity noise in the stable external cavity operation for strong optical feedback conditions. Bifurcation diagrams indicate the laser facet reflectivity required to prevent coherence collapse for a fixed level of strong feedback. Resonant modulation at microwave frequencies has also been demonstrated. Low Frequency Fluctuations (LFF) are exhibited by the model. The results have identified that the LFF is an intermittency phenomena and that it is of type II or type III. Experimental work confirms this deduction. The laminar length of the LFF's increases with external reflectivity, and decreases with increasing current. An adaptation of the model has been applied to the case of an external cavity frequency modulated laser diode. Experiments indicate that at a critical level of single pass phase modulation the FM laser moves into the coherence collapse regime. It has not been possible to investigate this modulation induced coherence collapse with the model because the instantaneous emission frequency is modulated by the detuning frequency, something which does not occur in the experiments.

Chapter 4 References.

[1] R Tkach and A Chraplyvy, "Regimes of Feedback Effects in 1.5 μm Distributed Feedback Lasers", IEEE J. Lightwave Tech., Vol. 4, No. 11, pp. 1655-1661, 1986.

[2] N Schunk and K Petermann, "Numerical Analysis of the Feedback Regimes for a Single-Mode Semiconductor Laser With External Feedback", IEEE J. Quantum Electron., Vol. 24, No. 7, pp. 1242-1247, 1988.

[3] H Li, J Ye, and J G McInerney, "Detailed Analysis of Coherence Collapse in Semiconductor Lasers", IEEE J. Quantum Electron., Vol. 29, No. 9, pp. 2421-2432, 1993.

[4] D Lenstra, B H Verbeek, and A J Den Boef, "Coherence Collapse in Single-Mode Semiconductor Lasers Due to Optical Feedback", IEEE J. Quantum Electron., Vol. 21, No. 6, pp. 674-679, 1985.

[5] J Mørk, B Tromborg, and J Mark, "Chaos in Semiconductor Lasers with Optical Feedback: Theory and Experiment", IEEE J. Quantum Electron., Vol. 28, No. 1, pp. 93-108, 1992.

[6] J B Georges, M H Kiang, K Heppel, M Sayed, and K Y Lau, "Optical Transmission of Narrow-Band Millimeter-Wave Signals by Resonant Modulation of Monolithic Semiconductor Lasers", IEEE Phot. Technol. Lett., Vol. 6, No. 4, pp. 568-570, 1994.

[7] R Nagarajan, S Levy, and J E Bowers, "Millimeter Wave Narrowband Optical Fiber Links Using External Cavity Semiconductor Lasers", IEEE J. Lightwave Tech., Vol. 12, No. 1, pp. 127-136, 1994.

[8] S Levy, R Nagarajan, R J Helkey, P Humphrey, and J E Bowers, "Millimetre Wave Fibre-Optic PSK Subcarrier Transmission at 35 GHz Over 6.3 km Using a Grating External Cavity Semiconductor Laser", Electron. Lett., Vol. 29, No. 8, pp. 690-691, 1993.

[9] K Y Lau and J B Georges, "On the Characteristics of Narrow-Band Resonant Modulation of Semiconductor Lasers Beyond Relaxation Oscillation Frequency", Appl. Phys. Lett., Vol. 63, No. 11, pp. 1459-1461, 1993.

[10] R Nagarajan, S Levy, A Mar, and J E Bowers, "Resonantly Enhanced Semiconductor Lasers for Efficient Transmission of Millimeter Wave Modulated Light", IEEE Phot. Technol. Lett., Vol. 5, No. 1, pp. 4-6, 1993.

[11] S Levy, R Nagarajan, A Mar, P Humphrey, and J E Bowers, "Fibre-Optic PSK Subcarrier Transmission at 35 GHz Using a Resonantly Enhanced Semiconductor Laser", Electron. Lett., Vol. 28, No. 22, pp. 2103-2104, 1992.

[12] K Y Lau, "Efficient Narrow-Band Direct Modulation of Semiconductor Injection Lasers at Millimeter Wave Frequencies of 100 GHz and Beyond", Appl. Phys. Lett., Vol. 52, No. 26, pp. 2214-2216, 1988.

[13] K Y Lau and A Yariv, "Direct Modulation and Active Mode Locking of Ultrahigh Speed GaAlAs Lasers at Frequencies up to 18 GHz", Appl. Phys. Lett., Vol. 46, No. 4, pp. 326-328, 1985.

[14] K Y Lau, "Narrow-Band Modulation of Semiconductor Lasers at Millimeter Wave Frequencies (> 100 GHz) by Mode Locking", IEEE J. Quantum Electron., Vol. 26, No. 2, pp. 250-261, 1990.

[15] J Mørk, "Nonlinear Dynamics and Stochastic Behaviour of Semiconductor Lasers with Optical Feedback", Ph.D. Thesis, Report No. S48, Danish Center for Applied Mathematics and Mechanics, Technical University of Denmark, 1989.

[16] T Sato, "Antimode Dynamics and Chaotic Itinerancy in the Coherence Collapse of Semiconductor Lasers with Optical Feedback", SPIE Vol. 2039: Chaos in Optics, pp. 58-64, 1993.

[17] J Mørk, B Tromborg, J Mark, and V Velichansky, "Instabilities in a Laser Diode with Strong Optical Feedback", SPIE Vol. 1837: Frequency-Stabilized Lasers and Their Applications, 1992.

[18] J Mørk, B Tromborg, and P L Christiansen, "Bistability and Low-Frequency Fluctuations in Semiconductor Lasers with Optical Feedback: A Theoretical Analysis", IEEE J. Quantum Electron., Vol. 24, No. 2, pp. 123-133, 1988.

[19] J O'Gorman, B J Hawdon, J Hegarty, and D M Heffernan, "Feedback Induced Instabilities in External Cavity Injection Lasers", Electron. Lett., Vol. 25, No. 2, pp. 114-115, 1989.

[20] M Fujiwara, K Kubota, and R Lang, "Low-Frequency Intensity Fluctuation in Laser Diodes with External Optical Feedback", Appl. Phys. Lett., Vol. 38, No. 4, pp. 217-220, 1981.

[21] J Sacher, W Elsässer, and E O Göbel, "Intermittency in the Coherence Collapse of a Semiconductor Laser with External Feedback", Phys. Rev. Lett., Vol. 63, No. 20, pp. 2224-2227, 1989.

[22] H Temkin, N A Olsson, J H Abeles, R A Logan, and M B Panish, "Reflection Noise in Index-Guided InGaAsP Lasers", IEEE J. Quantum. Electron., Vol. 22, No. 2, pp. 286-293, 1986.

[23] C H Henry and R F Kazarinov, "Instability of Semiconductor Lasers Due to Optical Feedback from Distant Reflectors", IEEE J. Quantum Electron., Vol. 22, No. 2, pp. 294-301, 1986

[24] G van Tartwijk, "Semiconductor Laser Dynamics with Optical Injection and Feedback", Ph.D. Thesis, Free University, Amsterdam, 1994.

[25] L N Langley, K A Shore, and J Mørk, "Dynamical and Noise Properties of Laser Diodes Subject to Strong Optical Feedback", accepted for publication in Optics Lett., 1994.

[26] L N Langley, K A Shore, and J Mørk, "Dynamics of Laser Diodes Subject to Strong Optical Feedback", CLEO Europe '94, paper QTuE3, 1994.

[27] G H M van Tartwijk, A M Levine, and D Lenstra, "Low-Frequency Fluctuations in Diode Lasers: A True Sisyphus Effect", CLEO Europe '94, paper QWI1, 1994

[28] J Sacher, W Elsässer, and E Göbel, "Nonlinear Dynamics of Semiconductor Laser Emission Under Variable Feedback Conditions", IEEE J. Quantum Electron., Vol. 27, No.3, pp. 373-379, 1991.

[29] K Ikeda, "Delay-Differential Equations Modeling Nonlinear Optical Resonators", in "Optical Instabilities", R W Boyd, M G Rayner, and L M Narducci (Eds), Cambridge University Press, 1986.

[30] K A Shore, "Static and Dynamic Bifurcations in Semiconductor Lasers for Device Applications", Opt. and Quantum Electron., Vol. 19, pp. S113-S119, 1987.

[31] A E Siegman, "Lasers", University Science Books, 1986.

[32] A P Willis and D M Kane, "Modulation Induced Coherence Collapse in FM Diode Lasers", Opt. Comm., Vol. 107, No. 1-2, pp. 65-70, 1994.

[33] S E Harris and O P McDuff, "Theory of FM Laser Oscillation", IEEE J. Quantum Electron., Vol. 1, No. 6, pp. 245-262, 1965.

[34] A P Willis, D M Kane, L N Langley, and K A Shore, "Frequency Modulated External Cavity Diode Lasers: A Theoretical and Experimental Study, CLEO Europe '94, paper CTuK15, 1994

[35] B Tromborg, H Olesen, X Pan, and S Saito, "Transmission Line Description of Optical Feedback and Injection Locking for Fabry-Perot and DFB Lasers", IEEE J. Quantum. Electron., Vol. 23, No. 11, pp. 1875-1889, 1987.

[36] F Sporleder, "Travelling Wave Line Model for Laser Diodes with External Optical Feedback", Proc. URSI Int. Symp. on Electromagn. Theory, Santiago de Compostela, Spain, pp. 585-588, 1983.

[37] D M Byrne, D MacLean, and R Plumb, "Optical Feedback-Induced Noise in Pigtailed Laser Diode Modules", IEEE Phot. Technol. Lett., Vol. 3, No. 10, pp. 891-894, 1991.

[38] N Schunk and K Petermann, "Measured Feedback-Induced Intensity Noise for 1.3 μm DFB Laser Diodes", Electron. Lett., Vol. 25, No. 1, pp. 63-64, 1989.

[39] X S Zhou and P Ye, "Intensity Noise of Semiconductor Laser in Presence of Arbitrary Optical Feedback", Electron. Lett., Vol. 25, No. 7, pp. 446-447, 1989.

[40] T Fujita, J Ohya, H Serizawa, H Sato, and K Fujito, "Correlation Between Intensity Noise and Longitudinal Modes of a Semiconductor Laser Coupled to an External Cavity", J. Appl. Phys., Vol. 57, No. 5, pp. 1753-1756, 1985.

[41] K Petermann, "Laser Diode Modulation and Noise", Kluwer Academic, 1988.

[42] E Ott, "Chaos in Dynamical Systems", Cambridge University Press, 1993.

[43] E Miltényi, W Elsässer, and E Göbel, "Intensity Dynamics of a Semiconductor Laser with Phase-Conjugate Feedback", EQEC '93, Florence, 1994.

[44] E Miltényi, W Elsässer, and E Göbel, "Intensity Dynamics of Semiconductor Lasers with Phase-Conjugate Feedback", Dynamics Days '94, Budapest, 1994.

[45] R A Fisher, "Optical Phase Conjugation", Academic Press, 1983.

[46] J Mørk, P Christiansen, and B Tromborg, "Limits of Stable Operation of AR-Coated Semiconductor Lasers with Strong Optical Feedback", Electron. Lett., Vol. 24, No. 17, pp. 1065-1066, 1988.

[47] A A Tager, "Mode Competition and Mode Locking in Compound Cavity Semiconductor Lasers", IEEE Phot. Technol. Lett., Vol. 6, No. 2, pp. 164-166, 1994.

[48] A A Tager and B B Elenkrig, "Stability Regimes and High-Frequency Modulation of Laser Diodes with Short External Cavity", IEEE J. Quantum Electron., Vol. 29, No. 12, pp. 2886-2890,1993.

Chapter 5:

The Effect of Optical Feedback on Vertical Cavity Surface Emitting Lasers.

5.1 The Structure and Facet Reflectivity of VCSEL's.

A Vertical Cavity Surface Emitting Laser (VCSEL) has a structure that is radically different from conventional edge emitting lasers, as shown in fig. 5.1 [1]. In an edge emitting laser the light output is emitted through a cleaved facet on the edge of the laser chip, with the lasing cavity being located horizontally in the plane of the growth layers. In contrast, a VCSEL has its lasing cavity located on a vertical axis, perpendicular to the growth layers. The mirrors in a VCSEL are implemented on the laser chip by growing many alternating layers of two materials with different refractive indices. The combined reflections from the interfaces of the layers gives the required facet reflectivity. VCSEL's are usually circular in cross section. The lateral confinement of the carriers is provided by fabricating the laser as an air post, giving the VCSEL a cylindrical geometry. The lasing cavity of VCSEL's is much shorter than edge emitting lasers, with the aim of achieving a single longitudinal mode output. However, the large area of the active region often results in high order transverse modes being present. Due to the short cavity length, the light encounters less gain in a single round trip of the cavity in VCSEL's than in edge emitting lasers. As a result a very high facet reflectivity is required to prevent excessive loss of light and to keep the threshold current low. Despite the high facet reflectivity (typically 99%) the photon lifetime of VCSEL's is very similar to that of edge emitting lasers. The high facet reflectivity is balanced out by the short cavity length. This can be confirmed by looking at the photon lifetime τ_{ph},

$$\tau_{ph} = \frac{\mu_g}{c\left(\alpha_i - \frac{\ln(R_2)}{\ell}\right)}, \qquad (5.1)$$

where μ_g is the group refractive index, c is the speed of light, α_i is the laser internal losses, R_2 is the facet reflectivity and ℓ is the laser cavity length. The high facet reflectivity requires many layers to be grown in the mirror stacks. The number of layers in the stacks is usually greater than twenty. Electrical contact is made via a circular contact on the top mirror stack and the substrate below the bottom stack. Light output can be arranged to be through the top or bottom stack.

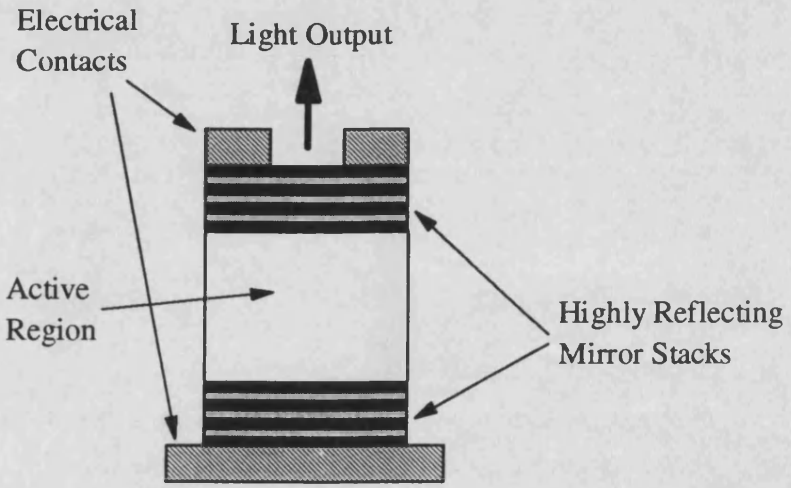

Fig. 5.1: Structure of a Vertical Cavity Surface Emitting Laser (VCSEL).

5.2 Optical Feedback into VCSEL's.

Only a small proportion of any feedback from the external reflection re-enters the VCSEL due to its extremely high facet reflectivity. Thus, it might be thought that this would give VCSEL's a very good immunity to optical feedback. However, it has been found both experimentally [2-7] and numerically [7] that VCSEL's have a similar sensitivity to optical feedback as that of conventional edge emitting lasers. This similarity in feedback sensitivity is linked to the similar photon lifetimes in the two types of devices. The feedback rate into the laser is given as k_{ext}/τ_L with k_{ext} being given by

$$k_{ext} = \frac{(1-R_2)\sqrt{R_{ext}}\eta}{\sqrt{R_2}}, \qquad (5.2)$$

where R_{ext} is the external reflectivity, and η is the coupling between the external mirror and the laser. The value of k_{ext}/τ_L is the same for VCSEL's and for edge emitting lasers [6]. Any benefit gained from the high facet reflectivity of VCSEL's is effectively cancelled by the small cavity round trip time. The amount of external light

injection per round trip of the internal laser cavity is the same for both types of lasers, hence the similar feedback sensitivities.

The high facet reflectivity of VCSEL's precludes their use in an external cavity laser configuration. To operate as an external cavity laser the external mirror must dominate over the laser facet reflectivity, which is not possible in the case of a VCSEL. Conventional edge emitting lasers can be configured into an external cavity structure by anti-reflection (AR) coating the front facet. However, by partially reducing the reflectivity of one of the facets, VCSEL's have been made to operate as an external cavity laser [8-10]. The external cavity is short and has been added to give single transverse mode operation [8,9] and to provide tuning of the lasing wavelength [10].

5.3 Modelling Optical Feedback into VCSEL's.

The rate equations used to model optical feedback are the same as those used in chapter 2 for conventional edge emitting lasers [7,11-14]. They are given below for clarity.

$$\frac{dn(t)}{dt}=\frac{I(t)}{eV}-\frac{n(t)}{\tau_{sp}}-s(t)G_n\{n(t)-n_o\}\left\{\frac{1}{1+\varepsilon s(t)}\right\}+F_n(t), \tag{5.3}$$

$$\begin{aligned}\frac{ds(t)}{dt}=&\frac{\gamma n(t)\Gamma}{\tau_{sp}}-\frac{s(t)}{\tau_{ph}}+s(t)G_n\{n(t)-n_o\}\Gamma\left\{\frac{1}{1+\varepsilon s(t)}\right\}\\&+\frac{k_{ext}}{\tau_L}\sqrt{s(t)}\sqrt{s(t-\tau_{ext})}\cos(\theta(t))+F_s(t)\end{aligned}, \tag{5.4}$$

$$\frac{d\phi(t)}{dt}=\frac{1}{2}\alpha G_n\{n(t)-n_{th}\}\Gamma-\frac{k_{ext}}{\tau_L}\frac{\sqrt{s(t-\tau_{ext})}}{\sqrt{s(t)}}\sin(\theta(t))+F_\phi(t), \tag{5.5}$$

where

$$\theta(t)=\phi(t)-\phi(t-\tau_{ext})+\omega_{th}\tau_{ext}. \tag{5.6}$$

The values and descriptions of the VCSEL parameters used in (5.3)-(5.6) are given in table 5.1. The parameters should be compared to those for an edge emitting laser in table 2.1. The numerical solution of the rate equations with optical feedback (5.3)-

(5.6) is described in chapter 2 and in appendix 3. Langevin noise sources (see appendix 2) [12,15] are added to model spontaneous emission noise,

$$F_n(t) = -\sqrt{\frac{2s(t_i)\gamma n(t)\Gamma}{\tau_{sp}\Delta t}}x_s + \sqrt{\frac{2n(t_i)}{\tau_{sp}\Delta t V}}x_n, \tag{5.7}$$

$$F_s(t) = \sqrt{\frac{2s(t_i)\gamma n(t)\Gamma}{\tau_{sp}\Delta t}}x_s, \tag{5.8}$$

$$F_\phi(t) = \frac{1}{s(t)}\sqrt{\frac{s(t_i)\gamma n(t)\Gamma}{2\tau_{sp}\Delta t}}x_\phi, \tag{5.9}$$

where $s(t_i)$ is the photon density at the start of the time interval Δt, $n(t_i)$ is the carrier density at the start of the interval Δt, V is the active region volume, and x_n, x_s, x_ϕ are gaussian distributed random variables with zero mean and unity variance.

Symbol	Description	Value
d	Active Region Diameter	4 μm
ℓ	Active Region Length	5 μm
V	Active Region Volume	1.3×10^{-16} m^3
τ_{sp}	Carrier Lifetime	2 ns
G_n	Gain Slope	2.125×10^{-12} m^{3}s^{-1}
n_{th}	Threshold Carrier Density	9.9×10^{23} m^{-3}
ε	Saturation Parameter	3×10^{-23} m^3
γ	Spontaneous Emission Factor	10^{-5}
Γ	Confinement Factor	0.4
τ_{ph}	Photon Lifetime	2.7 ps
α	Linewidth Broadening Factor	5.5
n_o	Transparency Carrier Density	4×10^{23} m^{-3}
R_2	Laser Facet Reflectivity	0.99
η	Laser to Fibre Coupling Efficiency	0.4
τ_L	Laser Cavity Round Trip Delay	0.15 ps
η_q	Quantum Efficiency	0.4

Table 5.1: Laser Parameters for Vertical Cavity Surface Emitting Lasers.

5.4 Relative Intensity Noise.

A simple way of investigating the feedback sensitivity of VCSEL's is to calculate the Relative Intensity Noise (RIN)

$$RIN = \frac{\overline{P_o(t)^2 - \overline{P_o(t)}^2}}{\overline{P_o(t)}^2}, \tag{5.10}$$

as the optical feedback increases. The Relative Intensity Noise can then be compared to that of edge emitting lasers for the same levels of optical feedback. The Relative Intensity Noise of VCSEL's due to optical feedback will also give an indication as to their performance in optical communication systems. Conventional edge emitting lasers exhibit a sudden increase in intensity noise when the level of optical feedback reaches a level sufficient to force the laser to operate in the coherence collapse regime [15-18] (regime IV). Fig. 5.2 shows the increase in RIN of a VCSEL as the level of external reflectivity R_{ext} is increased. The RIN is shown for several facet reflectivities R_2. It is seen that the onset of coherence collapse is dependent on the facet reflectivity R_2. Fig. 5.3 shows the RIN increase for increasing optical feedback into a conventional edge emitting laser.

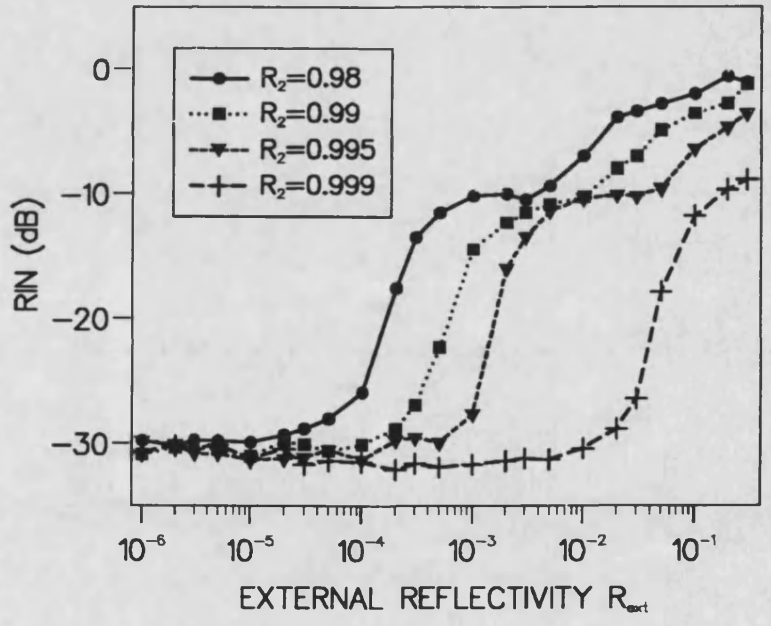

Fig. 5.2: The Relative Intensity Noise (RIN) Dependence for Increasing External Reflectivity R_{ext} at Different Levels of the VCSEL Facet Reflectivity R_2 (τ_{ext}=2 ns, I=2I_{th}).

By comparing figs. 5.2 and 5.3 it is seen that for a typical value of the VCSEL facet reflectivity (R_2=0.99) the transition into a very noisy operation state takes place at approximately the same level of optical feedback as for conventional edge emitting lasers. This can be explained by the similar values of the feedback rate k_{ext}/τ_L for both types of lasers. Only for very high levels of facet reflectivity R_2=0.999 does the VCSEL have a better immunity to feedback than the edge emitting laser. In this case the photon lifetime has increased significantly to almost 4 ps.

The dependence of the RIN on the VCSEL facet transmissivity T_2 is shown for fixed levels of external reflectivity in fig. 5.4. If we consider that an external reflectivity of R_{ext}=0.01 is the maximum accidental feedback expected to be encountered in an optical communication system, then the facet reflectivity needs to be greater than 0.995 to prevent significant increase of the RIN from the solitary VCSEL value.

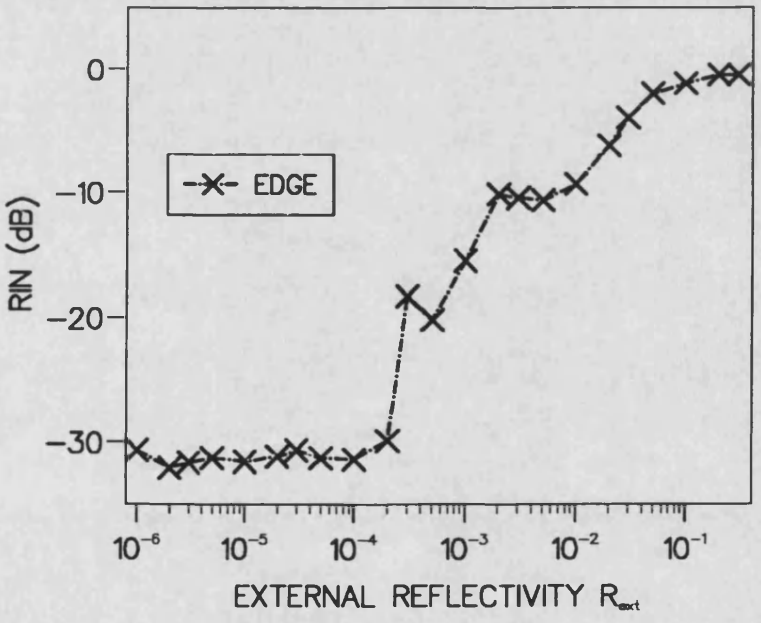

Fig. 5.3: The Relative Intensity Noise (RIN) Dependence for Increasing External Reflectivity R_{ext} of a Conventional Edge Emitting Laser (R_2=0.566, τ_{ext}=2 ns, $I=2I_{th}$).

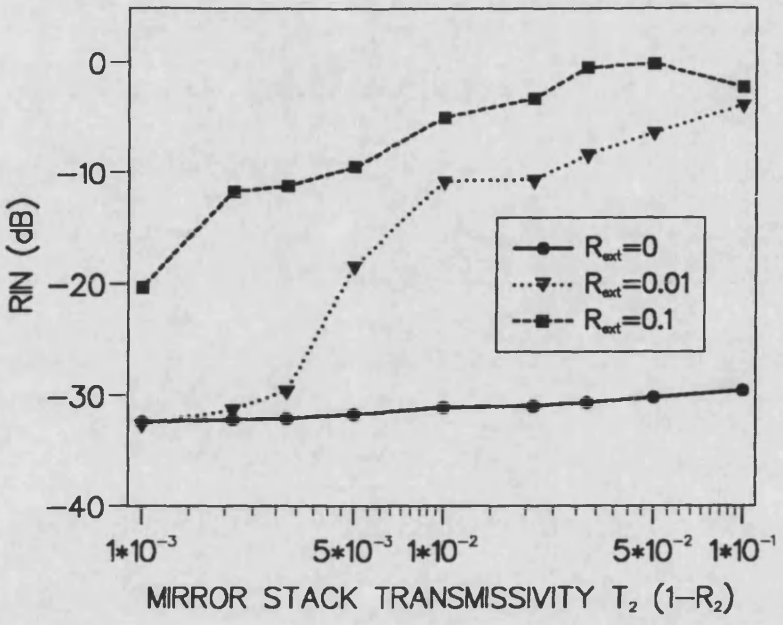

Fig. 5.4: The Relative Intensity Noise (RIN) Dependence on the VCSEL Facet Reflectivity R_2 for Different Levels of External Reflectivity R_{ext} (τ_{ext}=2 ns, I=2I_{th}).

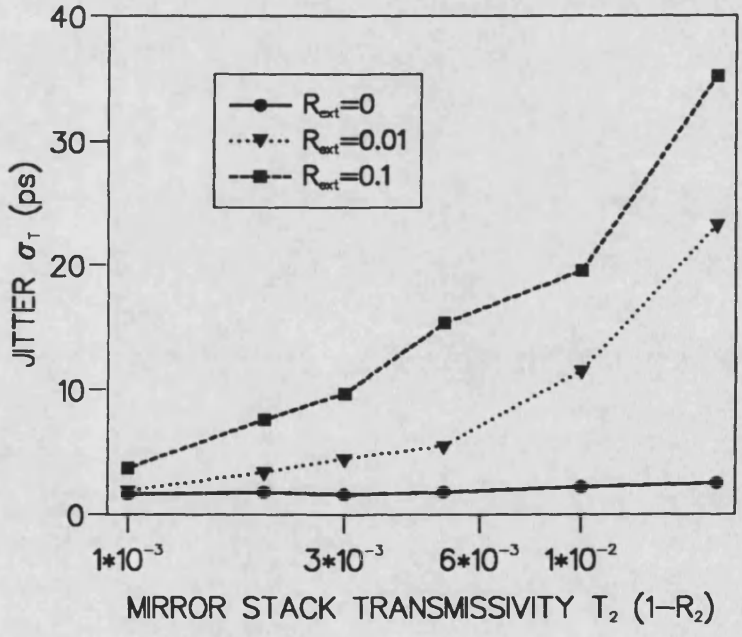

Fig. 5.5: The Turn-on Delay Jitter σ_T Dependence on the VCSEL Facet Reflectivity R_2 for Different Levels of External Reflectivity R_{ext} (τ_{ext}=2 ns, I=2I_{th}).

5.5 Turn-on Delay Jitter.

The performance of a laser in an optical communication system with optical feedback can be evaluated using the turn-on delay jitter (see chapter 2) [19-22]. The dependence of the turn-on delay jitter σ_T on the VCSEL facet transmissivity T_2 is shown for fixed levels of external reflectivity in fig. 5.4. If we consider that an external reflectivity of R_{ext}=0.01 is the maximum accidental feedback expected to be encountered in an optical feedback system, then the facet reflectivity needs to be greater than 0.995 to prevent significant increase of the of the jitter from the solitary VCSEL value. This agrees with the deduction from the intensity noise analysis of section 5.4.

5.6 Bifurcation Diagrams and Sensitivity to Feedback.

Bifurcation diagrams are a useful tool for indicating the feedback behaviour of lasers with increasing feedback [23-25]. A time series of the output power $P_o(t)$ is generated. Each time the output power crosses its steady state value without feedback, the carrier density n(t) is recorded. A single value of the carrier density indicates a single frequency oscillation in the laser output, no crossings of the steady state value indicates a stable output, and many values of the carrier density indicate chaotic behaviour. Figs. 5.6 to 5.8 show the bifurcation diagrams of the normalised carrier density n/n_{th}-1 for increasing feedback into VCSEL's for three different levels of facet reflectivity R_2. Comparison should be made with the bifurcation diagram of the normalised carrier density for increasing reflectivity into a conventional edge emitting laser shown in fig. 5.9. As noted in section 5.4, the feedback sensitivity is dependent on the facet reflectivity of the VCSEL. For typical values of the VCSEL facet reflectivity the feedback sensitivity is similar to conventional edge emitting lasers. This is seen in figs. 5.6 and 5.7, in which the transition to chaos occurs at approximately the same level of feedback as for the edge emitting laser of fig. 5.9. Only for extremely high facet reflectivity does the VCSEL have a greater feedback immunity than conventional edge emitting lasers. For the extremely high facet reflectivity of R_2=0.999 of fig. 5.7 it has not been possible to drive the VCSEL into coherence collapse.

The critical external reflectivity to force the laser into the coherence collapse regime in which the intensity noise increases has been calculated for semiconductor lasers [26-32]. A simple expression for the critical feedback strength k_{crit} is given in [26] as

$$k_{crit} = \tau_L \frac{\sqrt{2}\omega_r}{\sqrt{1+\alpha^2}}, \tag{5.11}$$

where ω_r is the relaxation oscillation frequency given by [12]

$$\omega_r = \frac{S_o G_n}{\tau_{ph}} - \frac{1}{4}\left(\frac{1}{\tau_{sp}} + S_o G_n\right)^2. \tag{5.12}$$

The critical reflectivity R_{crit} is evaluated using

$$k_{crit} = \frac{(1-R_2)\sqrt{R_{crit}}\eta}{\sqrt{R_2}}. \tag{5.13}$$

More complicated forms for R_{crit} for DFB laser diodes are given in [29-31]. The value of the critical reflectivity is evaluated as R_{crit}=4 % for both the VCSEL and the edge emitting laser. This value of the critical reflectivity to cause coherence collapse should be compared to figs. 5.7 and 5.9. It is difficult to decide from the bifurcation diagrams when coherence collapse begins because of the many windows of periodic output within the chaotic behaviour. However, the final transition to chaos occurs at approximately the same value as is calculated from equations (5.11)-(5.13).

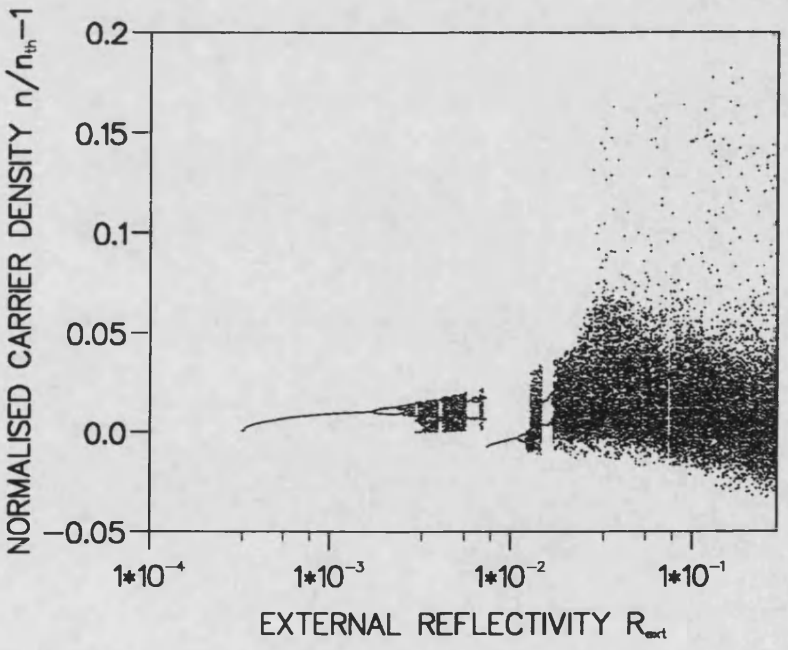

Fig 5.6: Bifurcation Diagram of Normalised Carrier Density for Increasing Levels of Optical Feedback into a VCSEL (R_2=0.98, τ_{ext}=0.23 ns, I=2I_{th}).

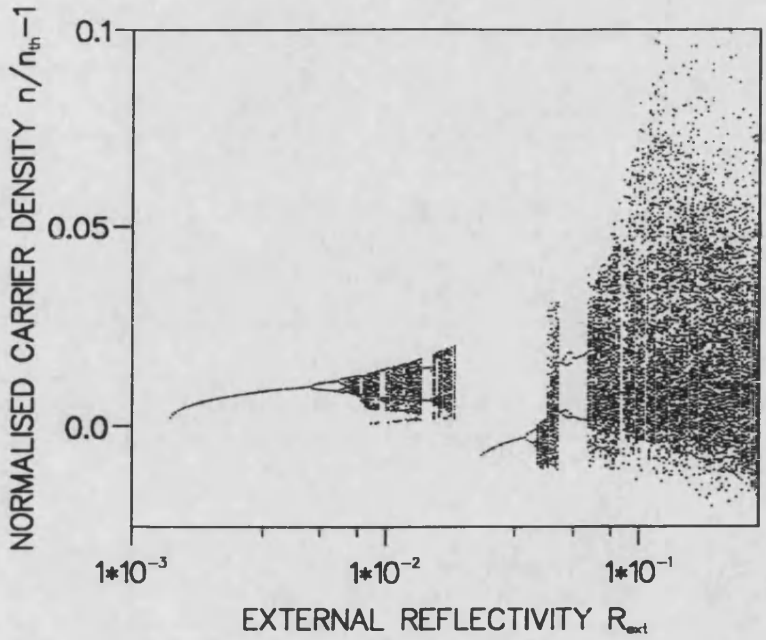

Fig. 5.7: Bifurcation Diagram of Normalised Carrier Density for Increasing Levels of Optical Feedback into a VCSEL (R_2=0.99, τ_{ext}=0.23 ns, I=2I_{th}).

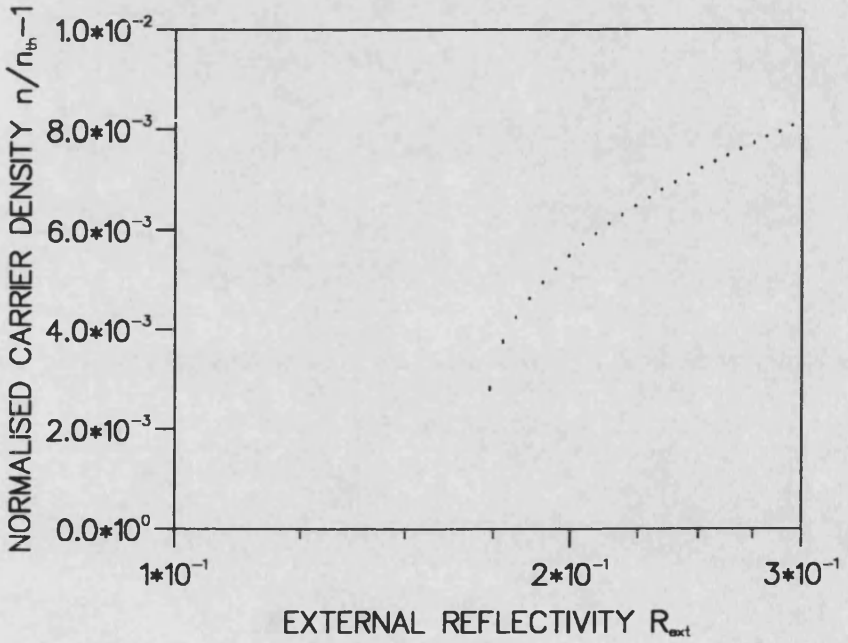

Fig 5.8: Bifurcation Diagram of Normalised Carrier Density for Increasing Levels of Optical Feedback into a VCSEL (R_2=0.999, τ_{ext}=0.23 ns, I=2I_{th}).

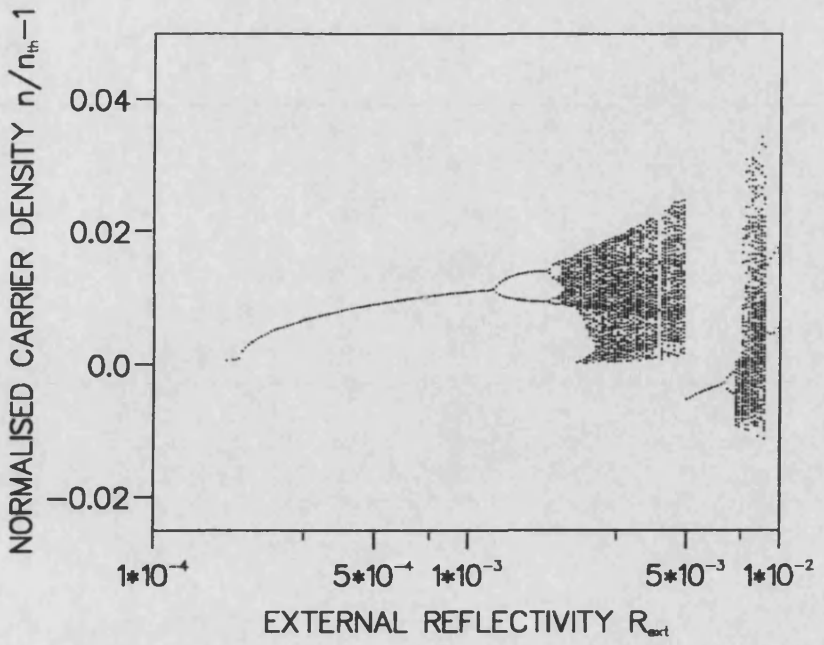

Fig 5.9: Bifurcation Diagram of Normalised Carrier Density for Increasing Levels of Optical Feedback into a Conventional Edge Emitting Laser (R_2=0.566, τ_{ext}=0.23 ns, $I=2I_{th}$).

5.7 Conclusion.

The feedback sensitivity of VCSEL's has been compared to that of edge emitting lasers. This has been achieved by investigating the Relative Intensity Noise as the feedback level is increased, and also by calculating bifurcation diagrams. The feedback sensitivity of VCSEL's is comparable to edge emitting lasers for typical values of the VCSEL facet reflectivity. Only for very high facet reflectivity are VCSEL's less sensitive to feedback than edge emitting lasers. The similarity in the feedback sensitivity of the two types of lasers can be attributed to their similar photon lifetimes despite their very different structures. The comparable photon lifetimes and feedback sensitivity results from the high facet reflectivity of VCSEL's being cancelled out by their short cavity length.

Chapter 5 References.

[1] G A Evans and J M Hammer, "Surface Emitting Semiconductor Lasers and Arrays", Academic Press, 1993.

[2] S Jiang, Z Pan, M Dagenais, R A Morgan, and K Kojima, "Influence of External Optical Feedback on Threshold and Spectral Characteristics of Vertical-Cavity Surface-Emitting Lasers", IEEE Phot. Technol. Lett., Vol. 6, No. 1, pp. 34-36, 1994.

[3] K H Hahn, M R Tan, and S Y Wang, "Intensity Noise of Large Area Vertical Cavity Surface Emitting Lasers in Multimode Optical Fibre Links", Electron. Lett., Vol. 30, No. 2, pp. 139-140, 1994.

[4] K P Ho, J D Walker, and J M Kahn, "External Optical Feedback Effects on Intensity Noise of Vertical-Cavity Surface-Emitting Lasers", IEEE Phot. Technol. Lett., Vol. 5, No. 8, pp. 892-895, 1993.

[5] J W Bae, H Temkin, S E Swirhun, W E Quinn, P Brusenbach, C Parsons, M Kim, and T Uchida, "Reflection Noise in Vertical Cavity Surface Emitting Lasers", Appl. Phys. Lett., Vol. 63, No. 11, pp. 1480-1482, 1993.

[6] Y C Chung and Y H Lee, "Spectral Characteristics of Vertical-Cavity Surface-Emitting Lasers with External Optical Feedback", IEEE Phot. Technol. Lett., Vol. 3, No. 7, pp. 597-599, 1991.

[7] H M Chen, K Tai, K F Huang, Y H Kao, and J D Wynn, "Instability in Surface Emitting Lasers due to External Optical Feedback", J. Appl. Phys., Vol. 73, No. 1, pp. 16-20, 1993.

[8] G C Wilson, M A Hadley, J S Smith, and K Y Lau, "High Single-Mode Output Power from Compact External Microcavity Surface-Emitting Laser Diode", Appl. Phys. Lett., Vol. 63, No. 24, pp. 3265-3267, 1993.

[9] M A Hadley, G C Wilson, K Y Lau, and J S Smith, "High Single-Transverse-Mode Output from External-Cavity Surface-Emitting Laser Diodes", Appl. Phys. Lett., Vol. 63, No. 12, pp. 1607-1609, 1993.

[10] N Yokouchi, T Miyamoto, T Uchida, Y Inaba, F Koyama, and T Iga, "40 Å Continuous Tuning of a GaInAsP/InP Vertical-Cavity Surface-Emitting Laser Using an External Mirror", IEEE Phot. Technol. Lett., Vol. 4, No. 7, pp. 701-703, 1992.

[11] B Clarke, "The Effect of Reflections on the System Performance of Intensity Modulated Laser Diodes", IEEE J. Lightwave Tech., Vol. 9, No. 6, pp. 741-749, 1991.

[12] K Petermann, "Laser Diode Modulation and Noise", Kluwer Academic, 1988.

[13] K D LaViolette and P L Liu, "Photon Statistics and Noise Modeling of Surface-Emitting Lasers", IEEE Phot. Technol. Lett., Vol. 3, No. 2, pp. 110-111, 1991.

[14] N Schunk and K Petermann, "Noise Analysis of Injection-Locked Semiconductor Injection Lasers", IEEE J. Quantum Electron., Vol. 22, No. 5, pp. 642-650, 1986.

[15] N Schunk and K Petermann, "Numerical Analysis of the Feedback Regimes for a Single-Mode Semiconductor Laser With External Optical Feedback", IEEE J. Quantum Electron., Vol. 24, No. 7, pp. 1242-1247, 1988.

[16] N Schunk and K Petermann, "Measured Feedback-Induced Intensity Noise for 1.3 μm DFB Laser Diodes", Electron. Lett., Vol. 25, No. 1, pp. 63-64, 1989.

[17] D M Byrne, D MacLean, and R Plumb, "Optical Feedback-Induced Noise in Pigtailed Laser Diode Modules", IEEE Phot. Technol. Lett., Vol. 3, No. 10, pp. 891-894, 1991.

[18] R Tkach and A Chraplyvy, "Regimes of Feedback Effects in 1.5-μm Distributed Feedback Lasers", IEEE J. Lightwave Tech., Vol. 4, No. 11, pp. 1655-1661, 1986.

[19] H J Wu and H C Chang, "Turn-on Jitter in Semiconductor Lasers with Moderate Reflecting Feedback", IEEE Phot. Technol. Lett., Vol. 4, No. 4, pp. 339-342, 1992.

[20] L N Langley and K A Shore, "The Effect of External Optical Feedback on Timing Jitter in Modulated Laser Diodes", IEEE J. Lightwave Technol., Vol. 11, No. 3, pp. 434-441, 1993.

[21] L N Langley and K A Shore, "The Effect of External Optical Feedback on the Turn-on Delay Statistics of Laser Diodes Under Pseudorandom Modulation", IEEE Phot. Technol. Lett., Vol. 4, No. 11, pp. 1207-1209, 1992.

[22] P Pepeljugoski, J Lin, J Gamelin, M Hong, and K Y Lau, "Ultralow Timing Jitter in Electrically Gain-Switched Vertical Cavity Surface Emitting Lasers", Appl. Phys. Lett., Vol. 62, No. 14, pp. 1588-1590, 1993.

[23] E Ott, "Chaos in Dynamical Systems", Cambridge University Press, 1993.

[24] H Li, J Ye, and J G McInerney, "Detailed Analysis of Coherence Collapse in Semiconductor Lasers", IEEE J. Quantum Electron., Vol. 29, No. 9, pp. 2421-2432, 1993.

[25] J Mørk, B Tromborg, and J Mark, "Chaos in Semiconductor Lasers with Optical Feedback: Theory and Experiment", IEEE J. Quantum Electron., Vol. 28, No. 1, pp. 93-108, 1992.

[26] B Tromborg and J Mørk, "Nonlinear Injection Locking Dynamics and the Onset of Coherence Collapse in External Cavity Lasers", IEEE J. Quantum Electron., Vol. 26, No. 4, pp. 642-654, 1990.

[27] J Helms and K Petermann, "A Simple Analytic Expression for the Stable Operation Range of Laser Diodes with Optical Feedback", IEEE J. Quantum Electron., Vol. 26, No. 5, pp. 833-836, 1990.

[28] J S Cohen and D Lenstra, "The Critical Amount of Optical Feedback for Coherence Collapse in Semiconductor Lasers", IEEE J. Quantum Electron., Vol. 27, No. 1, pp. 10-12, 1991.

[29] M Suhara, S Islam, and M Yamada, "Criterion of External Feedback Sensitivity in Index-Coupled and Gain-Coupled DFB Semiconductor Lasers to be Free from Excess Intensity Noise", IEEE J. Quantum Electron., Vol. 30, No. 1, pp. 3-9, 1994.

[30] T Hirono, T Kurosaki, and M Fukuda, "A Novel Analytical Expression of Sensitivity to External Optical Feedback for DFB Semiconductor Lasers", IEEE J. Quantum Electron., Vol. 28, No. 12, pp. 2674-2677, 1992.

[31] J L Beylat and J Jacquet, "Analysis of DFB Semiconductor Lasers with External Optical Feedback", Electron. Lett., Vol. 24, No. 9, pp. 509-510, 1988.

[32] F Favre, "Theoretical Analysis of External Optical Feedback on DFB Semiconductor Lasers", IEEE J. Quantum Electron., Vol. 23, No. 1, pp. 81-88, 1987.

Chapter 6:

Intensity Noise and Linewidth Characteristics of Laser Diodes with Phase Conjugate Optical Feedback.

6.1 Introduction to Phase Conjugate Feedback.

The use of phase conjugate feedback with semiconductor lasers has attracted attention recently [1-22]. Phase conjugate mirrors have the property of reversing the phase of the light incident upon them so that the reflected beam is the conjugate of the incident beam [23]. If an incident beam E_i is written as a wave moving in the positive z direction,

$$E_i = Ae^{j(-kz+\varphi)}e^{j\omega t} \tag{6.1}$$

then the phase conjugate wave will take the form

$$E_c = E_i^* = Ae^{j(kz-\varphi)}e^{j\omega t}. \tag{6.2}$$

The conjugated wave E_c contains the complex conjugate of only the spatial dependence, leaving the temporal dependence unchanged. The conjugate signal then corresponds to a wave moving in the opposite direction to the incident wave with its phase reversed. Alternatively conjugation is equivalent to leaving the spatial part of the incident wave unchanged and reversing the sign of t, hence the process can be considered to produce the "time reversal" of the incident beam. This chapter investigates the effect of phase conjugate feedback on the properties of semiconductor lasers, giving emphasis to the intensity noise and linewidth of the device. Deductions are made about which of the conventional mirror feedback regimes (described in chapter 1) are applicable to phase conjugate feedback.

Theoretical work has investigated the noise and dynamic properties of semiconductor lasers with phase conjugate feedback [1-6], showing that the laser properties are different to those with conventional mirror optical feedback. Linewidth properties have also been investigated [6,7]. The intensity noise in a gas laser has been significantly reduced using phase conjugate feedback [8]. In semiconductor lasers phase conjugate feedback has been used to narrow the laser linewidth [9-11]. Phase conjugate mirrors (PCM) have also attracted attention as a means of coupling the individual laser elements in laser arrays [15-22], and for phase locking of two laser diodes [24-26].

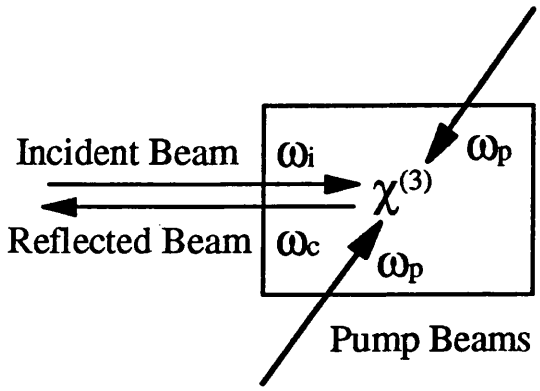

Fig. 6.1: Phase Conjugation Implemented by the Four Wave Mixing (FWM) Process.

Phase conjugate mirrors used to provide optical feedback into semiconductor lasers have been implemented in two ways. Both methods use the process of multiwave mixing [23] to generate the phase conjugate reflection. The first method is to use a non-linear crystal (usually Barium Titanate, $BaTiO_3$) [9,11-15] to generate the reflected phase conjugate beam. The second is to perform the phase conjugation process within another semiconductor laser [10,11]. The phase conjugate beam is generated by the Four-Wave-Mixing (FWM) process [23], illustrated in fig. 6.1. In this process two pump beams ω_p and a signal beam ω_i interact to produce a phase conjugate beam ω_c. The interaction is through the third order susceptibility $\chi^{(3)}$ (non-linear polarisation). The phase conjugation process can be thought of as the formation of gratings within the material. The material is described as Kerr-like because the refractive index is dependent on the light intensity. Thus the process is called Kerr-like Four-Wave-Mixing. The interference pattern formed between the signal and pump beam causes a grating in the refractive index, off which the other pump beam scatters to form the phase conjugate beam. This occurs for both pump beams. The Four-Wave-Mixing process is defined as Degenerate Four-Wave-Mixing (DFWM) if the frequency of the incident and pump beams are the same, resulting in a reflected phase conjugate beam of the same frequency as the incident beam, i.e. $\omega_c=\omega_i=\omega_p$. If the

frequency of the incident beam ω_i differs from the pump beam frequency ω_p then the reflected phase conjugate beam will be of a frequency ω_c where $\omega_c-\omega_p=\Delta\omega=\omega_p-\omega_i$. This is known as Non-Degenerate Four-Wave-Mixing (NDFWM).

6.2 Fundamental Differences Between Phase Conjugate Feedback and Conventional Optical Feedback.

Conventional mirror feedback, even at very low levels, can significantly affect the performance of semiconductor lasers [27-34]. Chapter 2 has already shown how unwanted optical feedback from components in an optical communication system can degrade the laser performance by increasing the intensity noise and turn-on delay jitter. Dramatic changes in the noise characteristics of semiconductor lasers occur under the influence of optical feedback. Unwanted optical feedback, such as may occur from components in optical communications systems, can increase the intensity noise [27,28], resulting in higher error rates. Five distinct regimes, denoted I-V, of the operating characteristics of semiconductor lasers with conventional optical feedback have been identified and investigated [29,30]. These optical feedback regimes are described in chapter 1. Factors influencing the laser with optical feedback are the external cavity round trip delay τ_{ext}, the external reflectivity R_{ext}, and the external cavity round trip phase change $\omega_{th}\tau_{ext}$. With phase conjugate feedback the external cavity round trip phase change is absent. See section 6.3 for a full explanation of the external cavity round trip phase change with phase conjugate and conventional mirror optical feedback.

Conventional mirrors are restricted to reflectivities of 100%. In phase conjugate mirrors the pump beam (or beams) provide an energy source for the reflected phase conjugate beam. Therefore it is possible to get a very large reflectivity far greater than 100%. This has been shown theoretically [35-37], and demonstrated experimentally [38-43].

Another difference between phase conjugate and conventional mirror optical feedback lies in the coupling between the laser and the external mirror. Fig. 6.2 shows a diverging beam (as from a laser) reflecting off both types of mirrors. For a conventional mirror the diverging beam continues to diverge after reflection. With a phase conjugate mirror, however, each ray within the beam retraces the path it took to arrive at the mirror. This results in a diverging beam being transformed into a converging beam. Thus all of the light that leaves the laser and strikes the phase

conjugate mirror will be returned exactly on its incident path, resulting in a 100% coupling efficiency. Also the orientation of a conventional mirror needs to be perpendicular to the light to reflect the light back into the laser, whereas the orientation of the phase conjugate mirror is unimportant. As a consequence of this property the difficulties which occur when trying to align a laser and conventional mirror so the reflection passes back into the laser are overcome with a phase conjugate mirror.

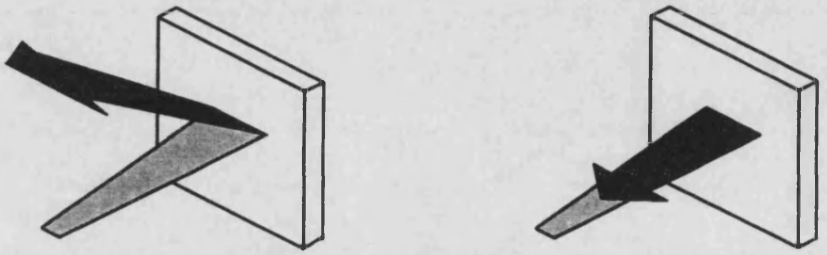

Fig. 6.2: Comparison of How Light Diverges from Conventional Mirrors but Retraces its Original Path from Phase Conjugate Mirrors.

6.3 Zero External Cavity Round Trip Phase Change.

Due to the phase reversal process, the external cavity round trip phase change when a phase conjugate mirror is used to provide optical feedback into a laser is zero [1]. Thus it is to be expected that a semiconductor laser with phase conjugate feedback will behave differently to that with conventional mirror feedback. This difference is illustrated in figs. 6.3 and 6.4. Fig. 6.3 shows that with a conventional mirror the feedback signal has undergone a phase change of $\omega_{th}\tau_{ext}$ after one round trip of the external cavity, whereas fig. 6.4 shows that there is zero phase change around the external cavity with a phase conjugate mirror. The phase change due to the outward path has been cancelled by the phase change due to the return path.

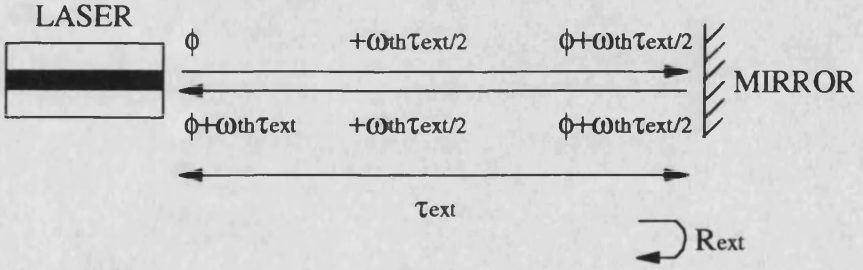

Fig. 6.3: External Cavity Round Trip Phase Change for Conventional Optical Feedback.

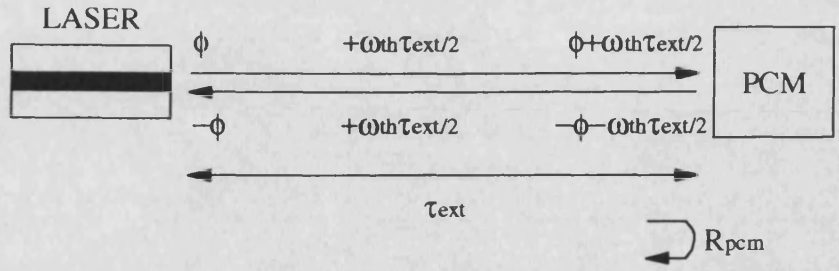

Fig. 6.4: Explanation of Zero Round External Cavity Trip Phase Change for Phase Conjugate Optical Feedback.

6.4 Numerical Model of Phase Conjugate Optical Feedback.

The laser model used in this investigation is similar to that used in chapter 2 to describe conventional optical feedback. The system configuration is shown in fig. 6.5.

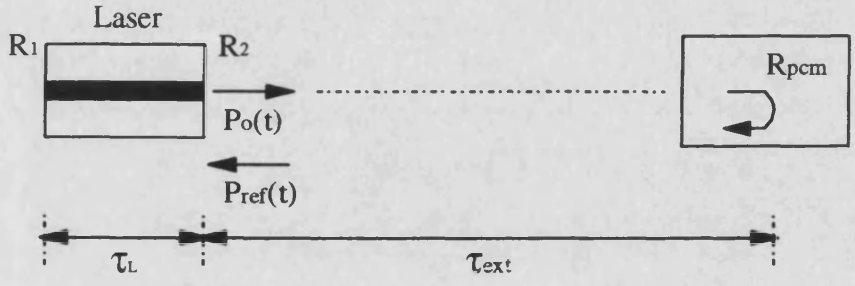

Fig. 6.5: Schematic Diagram of the Laser with Optical Feedback from a Phase Conjugate Mirror (PCM).

The rate equations are single-mode and include optical feedback terms. The field rate equation for conventional optical feedback (2.1) is modified to contain phase conjugate optical feedback terms [1-4],

$$\frac{dE(t)}{dt} = \left\{ j(\omega - \omega_{th}) + \frac{1}{2}\left\{ G_n(n(t) - n_o) - \frac{1}{\tau_{ph}} \right\} \right\} E(t) + \frac{k_{pcm}}{\tau_L} E^*(t - \tau_{ext}) \quad , \tag{6.3}$$

and must be manipulated into rate equations for photon density and phase in order for ease of numerical solution. This process is similar to that followed in chapter 2 for conventional optical feedback. Note the absence of a phase term for the reflected phase conjugate field. In (6.3) E(t) is the field and $E^*(t-\tau_{ext})$ is the reflected phase

conjugate field. All other parameters in (6.3) are described in chapter 2. The feedback strength is calculated from

$$k_{pcm} = \frac{(1-R_2)\sqrt{R_{pcm}}\eta}{\sqrt{R_2}}, \tag{6.4}$$

where R_2 is the laser facet reflectivity, R_{pcm} is the phase conjugate mirror reflectivity and η is the laser to phase conjugate mirror coupling efficiency. The method for finding the photon density s(t) and electric field phase $\phi(t)$ rate equations follows the same steps as in chapter 2 for the laser rate equations with conventional optical feedback.

Two simple relationships between the photon density s(t) and the electric field E(t) are

$$E(t) = \sqrt{s(t)}e^{j\phi(t)} \tag{6.5}$$

and

$$s(t) = E(t)E(t) = E(t)E^*(t). \tag{6.6}$$

The photon rate equation is calculated as in chapter 2 (2.5) using

$$\frac{ds(t)}{dt} = \frac{d}{dt}\{E(t)E^*(t)\}. \tag{6.7}$$

Inserting (6.3) into (6.7) gives

$$\begin{aligned}\frac{ds(t)}{dt} &= E(t)E^*(t)\left\{G_n(n(t)-n_o)-\frac{1}{\tau_{ph}}\right\} \\ &+\frac{k_{pcm}}{\tau_L}\{E(t)E(t-\tau_{ext})+E^*(t)E^*(t-\tau_{ext})\}\end{aligned} \tag{6.8}$$

Using (6.5) and (6.6) in (6.8) gives

$$\frac{ds(t)}{dt} = s(t)\left\{G_n(n(t)-n_o)-\frac{1}{\tau_{ph}}\right\} + \frac{k_{pcm}}{\tau_L}\sqrt{s(t)}\sqrt{s(t-\tau_{ext})}\left\{e^{j(\phi(t)+\phi(t-\tau_{ext}))}+e^{-j(\phi(t)+\phi(t-\tau_{ext}))}\right\}, \tag{6.9}$$

which can be further simplified as in chapter 2 using (2.8), resulting in the rate equation for the photon density in the presence of phase conjugate optical feedback.

$$\frac{ds(t)}{dt} = -\frac{s(t)}{\tau_{ph}} + s(t)G_n(n(t)-n_o) + \frac{2k_{pcm}}{\tau_L}\sqrt{s(t)}\sqrt{s(t-\tau_{ext})}\cos(\phi(t)+\phi(t-\tau_{ext})). \tag{6.10}$$

The electric field phase rate equation is calculated using the following relationship

$$\frac{d\phi(t)}{dt} = \frac{1}{s(t)}\mathrm{Im}\left\{E^*(t)\frac{dE(t)}{dt}\right\}. \tag{6.11}$$

Inserting (6.3) into (6.11) gives

$$\frac{d\phi(t)}{dt} = \frac{1}{s(t)}\mathrm{Im}\left\{\begin{array}{l} E^*(t)E(t)\left\{j(\omega-\omega_{th})+\frac{1}{2}\left\{G_n(n(t)-n_o)-\frac{1}{\tau_{ph}}\right\}\right\} \\ +\frac{k_{pcm}}{\tau_L}E^*(t)E^*(t-\tau_{ext}) \end{array}\right\}. \tag{6.12}$$

Using (6.6) results in

$$\frac{d\phi(t)}{dt} = \mathrm{Im}\left\{\begin{array}{l} j(\omega-\omega_{th})+\frac{1}{2}\left\{G_n(n(t)-n_o)-\frac{1}{\tau_{ph}}\right\} \\ +\frac{k_{pcm}}{\tau_L}\frac{\sqrt{s(t-\tau_{ext})}}{\sqrt{s(t)}}e^{-j(\phi(t-\tau_{ext})+\phi(t))} \end{array}\right\}. \tag{6.13}$$

Taking the imaginary part (as in chapter 2 (2.13)) of the exponential term in (6.13) gives

$$\frac{d\phi(t)}{dt} = (\omega-\omega_{th})-\frac{k_{pcm}}{\tau_L}\frac{\sqrt{s(t-\tau_{ext})}}{\sqrt{s(t)}}\sin(\phi(t)+\phi(t-\tau_{ext})). \tag{6.14}$$

From appendix 1 it is seen that in the absence of optical feedback [27]

$$\omega-\omega_{th}=\frac{1}{2}\alpha G_n(n(t)-n_{th}). \tag{6.15}$$

Substituting (6.15) for ω-ω_{th} in (6.14) results in the final rate equation for the phase of the electric field in the presence of phase conjugate feedback

$$\frac{d\phi(t)}{dt}=\frac{1}{2}\alpha G_n(n(t)-n_{th})-\frac{k_{ext}}{\tau_L}\frac{\sqrt{s(t-\tau_{ext})}}{\sqrt{s(t)}}\sin(\phi(t)+\phi(t-\tau_{ext})). \tag{6.16}$$

To complete the model a confinement factor Γ, gain saturation ε and spontaneous emission are included as in chapter 2, giving the final rate equation for a semiconductor laser with weak phase conjugate optical feedback. A carrier rate equation is added and is unchanged from that of a solitary laser described in appendix 1. The rate equations are single-mode and include Langevin noise terms (see appendix 2) as follows:

$$\frac{dn(t)}{dt}=\frac{I(t)}{eV}-\frac{n(t)}{\tau_{sp}}-s(t)G_n\{n(t)-n_o\}\left\{\frac{1}{1+\varepsilon s(t)}\right\}+F_n(t), \tag{6.17}$$

$$\begin{aligned}\frac{ds(t)}{dt}=&\frac{\gamma n(t)\Gamma}{\tau_{sp}}-\frac{s(t)}{\tau_{ph}}+s(t)G_n\{n(t)-n_o\}\Gamma\left\{\frac{1}{1+\varepsilon s(t)}\right\}\\&+\frac{k_{pcm}}{\tau_L}\sqrt{s(t)}\sqrt{s(t-\tau_{ext})}\cos(\theta(t))+F_s(t)\end{aligned}, \tag{6.18}$$

$$\frac{d\phi(t)}{dt}=\frac{\alpha}{2}G_n\{n(t)-n_{th}\}\Gamma-\frac{k_{pcm}}{\tau_L}\frac{\sqrt{s(t-\tau_{ext})}}{\sqrt{s(t)}}\sin(\theta(t))+F_\phi(t), \tag{6.19}$$

where

$$\theta(t)=\phi(t)+\phi(t-\tau_{ext}). \tag{6.20}$$

The values of the laser diode parameters used in (6.17)-(6.20) are given in table 2.1.

Equation (6.20) for θ(t) should be contrasted with that for conventional optical feedback (2.22), i.e.

$$\theta(t) = \phi(t) - \phi(t - \tau_{ext}) + \omega_{th}\tau_{ext}. \tag{6.21}$$

The significant difference between the two types of feedback is the term $\omega_{th}\tau_{ext}$ in (6.21). This is the external cavity round trip phase change. Fig. 6.4 shows why $\omega_{th}\tau_{ext}$ does not appear in the model for phase conjugate feedback [1]. The nature of the phase conjugate mirror is to reverse the phase of the incident light as it is reflected. Hence any phase shift acquired by the light due to the outward path length is exactly cancelled by the phase shift acquired during the return path length. Therefore the dependence of the laser characteristics on the external cavity round trip phase change is eliminated. The phase conjugate feedback is, however, still retarded by the external cavity round trip delay, plus any delay or response time due to the phase conjugate mirror itself (see chapter 7).

If non-degenerate four-wave-mixing (NDFWM) is used to generate the phase conjugate reflection then $\theta(t)$ has an additional term containing the detuning, $\Delta\omega$, between the pump and signal beams [3],

$$\theta(t) = \phi(t) + \phi(t - \tau_{ext}) + 2\Delta\omega\left(t - \frac{\tau_{ext}}{2}\right), \tag{6.22}$$

where $\Delta\omega$ is the detuning between the incident beam (laser output) and pump beams. The detuning of the phase conjugate beam from the pump beams takes the same value, i.e.

$$\Delta\omega = \omega_c - \omega_p = \omega_p - \omega_i. \tag{6.23}$$

The detuning term $\Delta\omega$ arises due to the mismatch between the laser frequency and the phase conjugate mirror pump beam frequency. The total frequency change between the incident beam and the phase conjugate beam is $2\Delta\omega$ as in (6.22). The time delay of half the external cavity round trip time $\tau_{ext}/2$ is due to the frequency change occurring when the light has passed half way around the external cavity path back to the laser (i.e. at the phase conjugate mirror).

The Langevin noise terms used in the rate equations (6.17)-(6.20), are described in appendix 2. The are written below for completeness:

$$F_n(t) = -\sqrt{\frac{2s(t_i)\gamma n(t)\Gamma}{\tau_{sp}\Delta t}}x_s + \sqrt{\frac{2n(t_i)}{\tau_{sp}\Delta t V}}x_n, \tag{6.24}$$

$$F_s(t) = \sqrt{\frac{2s(t_i)\gamma n(t)\Gamma}{\tau_{sp}\Delta t}}x_s, \tag{6.25}$$

$$F_\phi(t) = \frac{1}{s(t)}\sqrt{\frac{s(t_i)\gamma n(t)\Gamma}{2\tau_{sp}\Delta t}}x_\phi, \tag{6.26}$$

where $s(t_i)$ is the photon density at the start of the interval Δt, $n(t_i)$ is the carrier density at the start of the interval Δt, and x_n, x_S, x_ϕ are gaussian distributed random variables with zero mean and unity variance. The Langevin noise in the photon and electric field phase rate equations is due to the random nature of the spontaneous emission process. The Langevin noise in the carrier rate equation is due to the shot noise nature of the injection current and spontaneous and stimulated recombination.

The rate equations with phase conjugate feedback (6.17)-(6.20) and Langevin noise terms (6.24)-(6.26) are solved numerically using a variable-step, variable-order Runge-Kutta algorithm, as described in chapter 2 and appendix 3. Interest in this chapter is restricted to the static properties of the system where the injection current is held constant, particularly the intensity noise and linewidth.

6.5 Intensity Noise Properties of Phase Conjugate Feedback.

Firstly, noise properties of laser diodes in the case of constant injection current are considered for optical feedback from both conventional and phase conjugate mirrors. The noise properties are characterised by relative intensity noise, (RIN), and is calculated from the expression,

$$RIN = \frac{\overline{P_o(t)^2} - \overline{P_o(t)}^2}{\overline{P_o(t)}^2} \tag{6.27}$$

where $P_o(t)$ are the output power samples. Fig. 6.6 shows the behaviour of the RIN for various injection currents as the external reflectivity is increased. It can be seen that optical feedback from a conventional mirror increases the intensity noise as the external reflectivity increases [27-34]. The sudden increase in the intensity noise corresponds to the laser entering the coherence collapse feedback regime. In contrast, with optical feedback from a phase conjugate mirror the increase in intensity noise is much more gradual. Lower levels of phase conjugate feedback are required to increase the intensity noise above that of the solitary laser than is required for

conventional mirror feedback. At low external reflectivity the intensity noise with phase conjugate feedback is larger than that caused by conventional mirror feedback of the same strength. The situation is reversed at higher external reflectivity where the intensity noise is greatest for conventional mirror feedback. In the transition to coherence collapse the increase in the RIN occurs at all frequencies to some extent but particularly at the relaxation oscillation frequency of the solitary laser and at multiples of the inverse external cavity round trip delay. These results show that the laser becomes unstable and develops output power fluctuations (i.e. intensity noise) at lower external reflectivity for phase conjugate feedback than occurs with conventional mirror feedback [6].

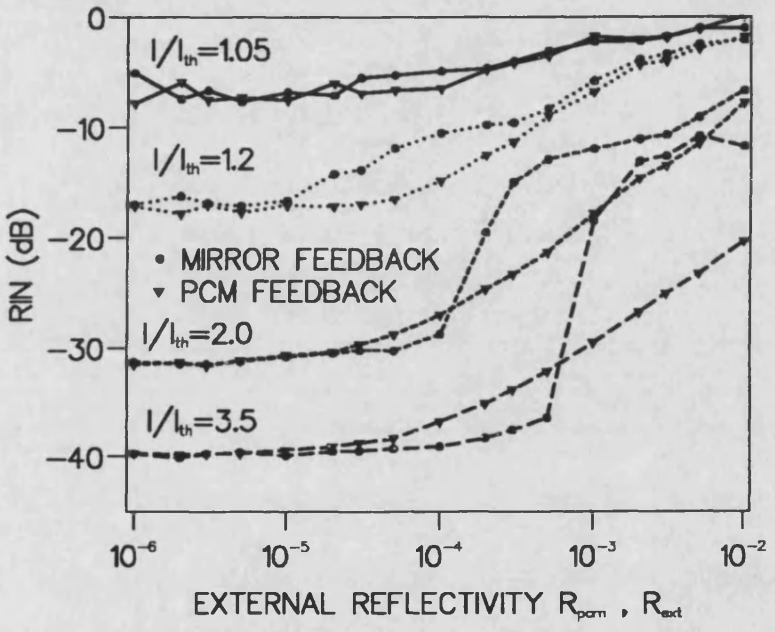

Fig. 6.6: Relative Intensity Noise (RIN) for Increasing Levels of Conventional Mirror R_{ext} and Phase Conjugate Feedback R_{pcm}, at Several Injection Currents from $I=1.05I_{th}$ to $I=3.5I_{th}$ (τ_{ext}=2 ns).

The output power probability distribution functions (pdf's), as shown in figure 6.7, give a clearer indication of the effect of lower levels of optical feedback from a phase conjugate mirror on the intensity noise properties of the laser. The laser is operated at twice the threshold current and with a phase conjugate reflectivity $R_{pcm}=2x10^{-6}$. The output power pdf for the solitary laser corresponds to a RIN value of -30.4 dB. The output power pdf with phase conjugate optical feedback is narrower than that of the solitary laser, corresponding to a RIN of -31.7 dB, a small decrease in intensity noise. Hence phase conjugate optical feedback has narrowed the output power pdf by reducing the intensity noise in the laser output. Further investigations show that the

noise reduction properties of the phase conjugate optical feedback are independent of the external cavity round trip delay.

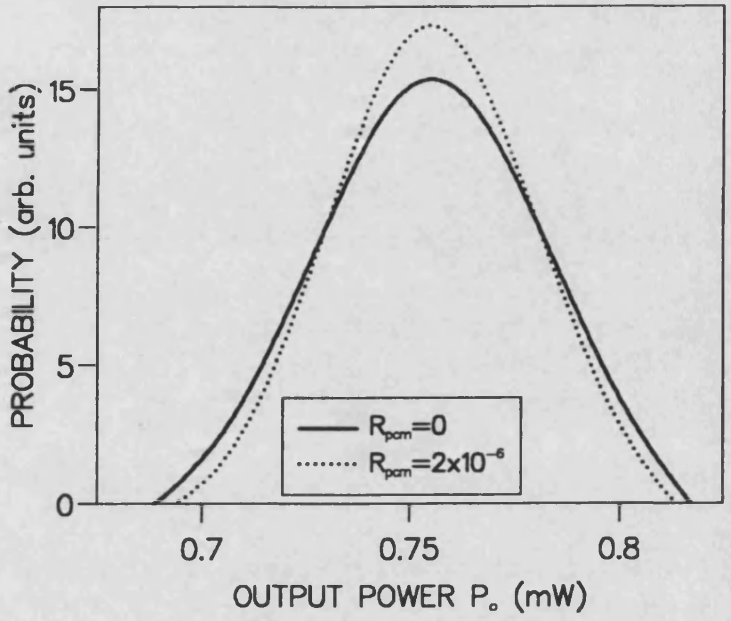

Fig. 6.7: Output Power PDF's with and without Phase Conjugate Optical Feedback ($I=2I_{th}$, $R_{pcm}=2\times10^{-6}$, $\tau_{ext}=2$ ns).

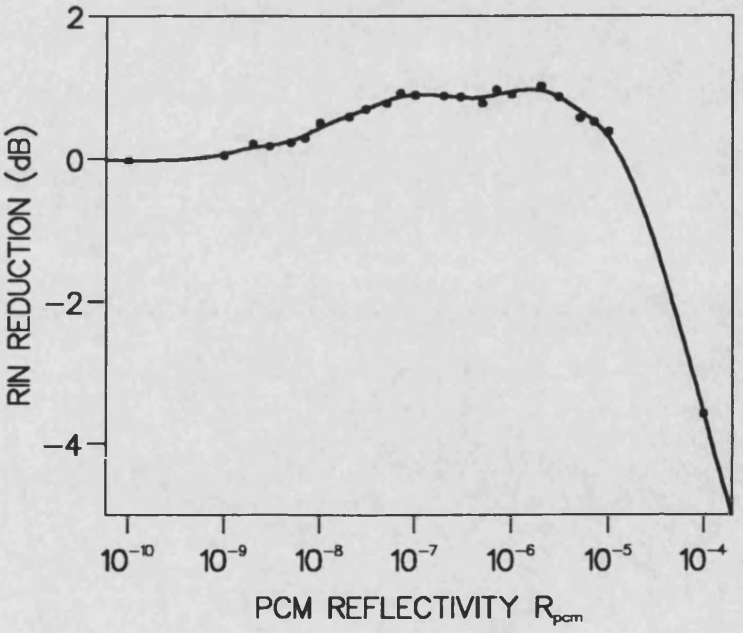

Fig. 6.8: Reduction of RIN Due to Phase Conjugate Optical Feedback ($I=2I_{th}$, $\tau_{ext}=2$ ns).

Fig. 6.7 has shown that it is possible for phase conjugate feedback to cause a small decrease in the intensity noise in the laser output power. Figure 6.8 shows the noise reduction dependence on the level of phase conjugate optical feedback. The intensity noise is reduced for an phase conjugate reflectivity R_{pcm} between 10^{-9} and 10^{-5}. For values of external reflectivity greater than $R_{pcm}=10^{-5}$ the intensity noise is increased. It has been found that the phase conjugate optical feedback can significantly reduce the low frequency intensity noise [2] (up to a few hundred MHz). There is very little reduction of the higher frequency intensity noise. Since most intensity noise will be of frequencies around the relaxation oscillation frequency and above, the overall intensity noise reduction will be small, as shown in this work.

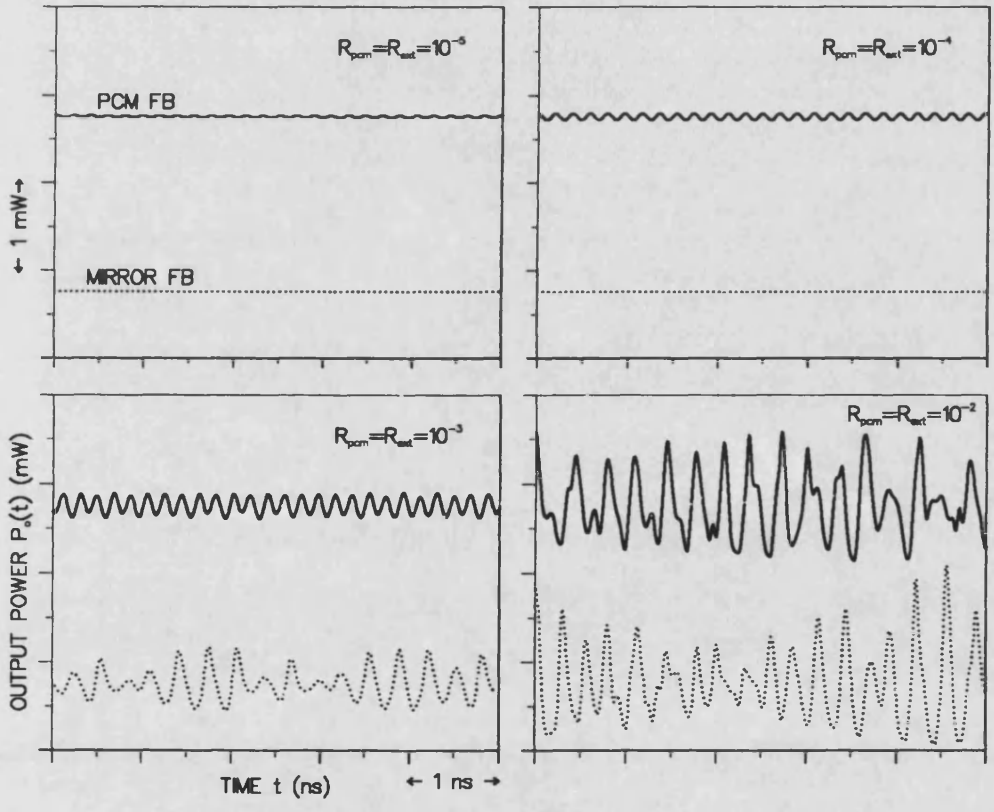

Fig. 6.9: Comparison of Optical Output Power Fluctuations $P_o(t)$ for Several Levels of Phase Conjugate R_{pcm} and Conventional Mirror Feedback R_{ext} ($I=2I_{th}$, $\tau_{ext}=2$ ns). The Power Levels are Displaced for Clarity.

6.6 Output Power Waveforms.

The output power waveforms $P_o(t)$ at four different levels of external reflectivity are shown in fig. 6.9 for phase conjugate and conventional mirror feedback. The Langevin noise sources have been removed from the numerical solution to obtain a clearer picture of the effects of optical feedback. The results agree with the observations from fig. 6.6 that output power fluctuations occur at lower levels of external reflectivity with phase conjugate than for conventional mirror feedback. At low phase conjugate reflectivity R_{pcm} from 10^{-5} to 10^{-4} the phase conjugate feedback causes a single frequency oscillation in the output power. The frequency of the oscillation is twice the relaxation oscillation frequency of the solitary laser. At the same low levels of external reflectivity for conventional mirror feedback the output power waveform is stable. At a high reflectivity of 10^{-2} the waveforms with both types of optical feedback appear to be chaotic. However the output power waveform at a moderate reflectivity of 10^{-3} for conventional mirror feedback appears to be almost chaotic, whilst that for phase conjugate feedback still has a regular period. Hence the transition to a chaotic output occurs at higher levels of external reflectivity for phase conjugate feedback.

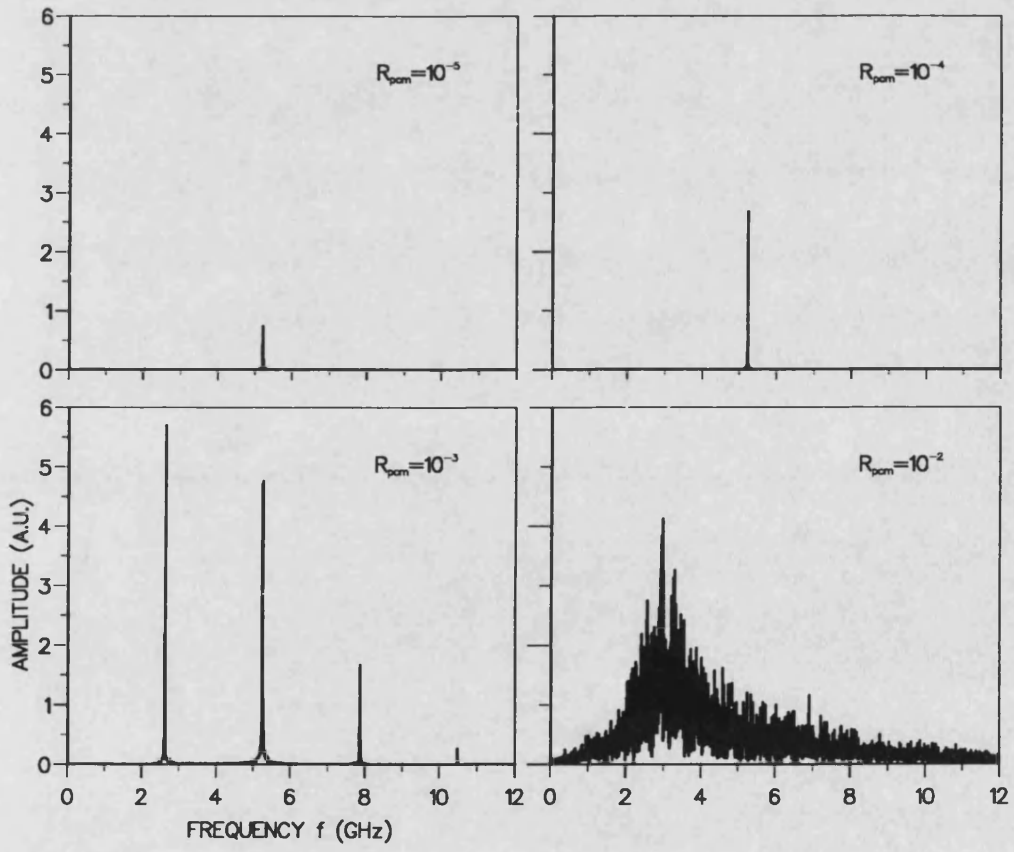

Fig. 6.10: Optical Output Power Fluctuation Frequency Components for Several Levels of Phase Conjugate Feedback R_{pcm} ($I=2I_{th}$, $\tau_{ext}=2$ ns).

6.7 Output Power Fluctuation Frequency Spectrum.

The output power fluctuation frequency spectra corresponding to fig. 6.9 are shown in figs. 6.10 and 6.11 for phase conjugate and conventional mirror feedback respectively. These graphs show the intensity noise spectra due to optical feedback only, plotted on a linear vertical axis. At low feedback levels of 10^{-5} to 10^{-4} phase conjugate feedback results in a single frequency oscillation that is twice the relaxation oscillation frequency. No output power fluctuation frequency spectra are shown for conventional mirror feedback at low external reflectivities from 10^{-5} to 10^{-4} because the laser output is stable at such levels of conventional optical feedback. At a moderate external reflectivity of 10^{-3} it is seen that phase conjugate feedback causes only a few frequency components at integer multiples of the relaxation oscillation frequency. Conventional mirror feedback of the same strength causes many frequencies to be present in the output power fluctuations, with spacing corresponding to the inverse of the external cavity round trip delay.

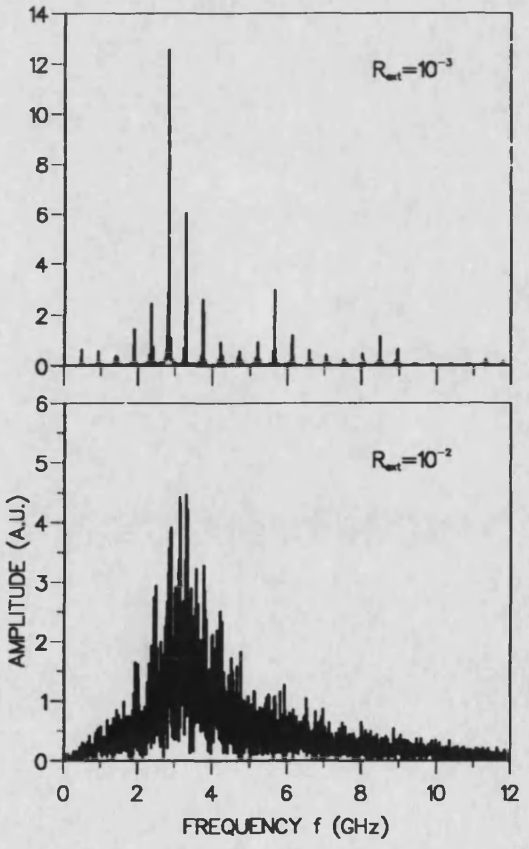

Fig. 6.11: Optical Output Power Fluctuation Frequency Components for Several Levels of Conventional Mirror Feedback R_{ext} ($I=2I_{th}$, $\tau_{ext}=2$ ns).

Large numbers of frequency components indicate that the laser is tending towards chaotic behaviour [29-33]. For high levels of external reflectivity of 10^{-2} both types of feedback cause chaotic fluctuations, as seen from the very large number of frequency components present in the output power fluctuations. At this high reflectivity both types of feedback cause the laser to operate in feedback regime IV, i.e. coherence collapse (see chapter 1). The output power fluctuation frequency spectra confirm that phase conjugate optical feedback causes output power fluctuations at lower levels of external reflectivity than conventional mirror feedback; and that the transition to chaotic output power fluctuations is at a higher external reflectivity for phase conjugate than for conventional mirror feedback.

Fig. 6.12 shows the levels of RIN at different frequencies, for a phase conjugate reflectivity $R_{pcm}=10^{-6}$. This graph is similar to that of figs. 6.10 and 6.11 but with spontaneous emission noise included. At low levels of phase conjugate feedback the intensity noise can be reduced [2,4]. The reduction is a very small one, only becoming significant at very low frequencies of a few hundred MHz [2]. The intensity noise reduction is much less than that which has been achieved with phase conjugate feedback into a gas laser [8], and is not large enough to be of practical use.

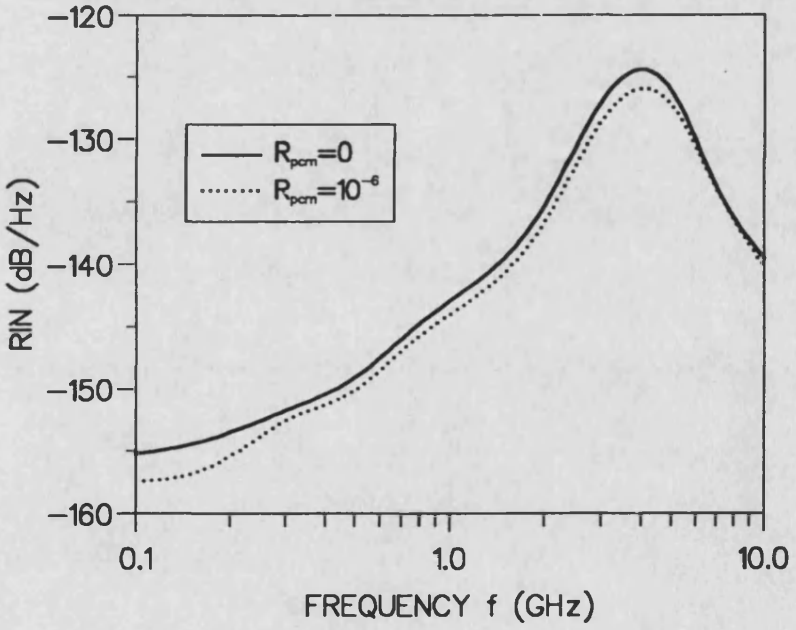

Fig. 6.12: Variation of Relative Intensity Noise (RIN) with Frequency for Solitary Laser and for Phase Conjugate Optical Feedback R_{pcm} ($I=2I_{th}$, $R_{pcm}=10^{-6}$, $\tau_{ext}=2$ ns).

The phase difference between the reflected and emitted light plays an important part in determining the intensity noise properties of an external cavity laser. With optical feedback from a conventional mirror the round trip phase change, $\omega_{th}\tau_{ext}$, due to the external cavity path length is very unlikely to be a multiple of 2π radians. Therefore the reflected light is not in phase with the emitted light. A phase conjugate mirror ensures that there is zero phase change due to the external cavity path length. The reflected light is, thus, in phase with the emitted light, and hence a different intensity noise behaviour results for the two types of optical feedback. The difference in the intensity noise behaviour of a semiconductor laser induced by phase conjugate and conventional mirror feedback can thus be attributed to the round trip phase cancelling property of the phase conjugate mirror.

6.8 Linewidth Behaviour and Optical Feedback Regimes.

The linewidth, $\Delta\nu$, of a semiconductor laser can be determined from the two-sided spectral density of the frequency fluctuations S_ϕ [27],

$$\Delta\nu = \frac{S_\phi}{2\pi}. \tag{6.28}$$

The two sided spectral density of the frequency fluctuations is calculated using a Fast Fourier Transform (FFT) of the instantaneous frequency variations $\omega(t)-\omega_{th}=d\phi/dt$. The two sided spectral density of the frequency fluctuations $S_\phi(\omega)$ is defined by

$$S_\phi(\omega) = \left\langle \left|\dot{\phi}(\omega)\right|^2 \right\rangle = \left\langle \left|\frac{d\phi(\omega)}{dt}\right|^2 \right\rangle \tag{6.29}$$

or

$$S_\phi(\omega) = \int_{-\infty}^{\infty} \left\langle \dot{\phi}(t)\dot{\phi}(t-T) \right\rangle e^{-j\omega T} dT. \tag{6.30}$$

The relation (6.28) is defined for a white frequency noise spectrum. Optical feedback causes the frequency noise spectrum to be very unlike a white noise spectrum, as seen in fig. 6.13. However, (6.28) holds for a non-white frequency noise spectrum if S_ϕ is replaced by $S_\phi(\omega\rightarrow 0)$ [34]. Thus

$$\Delta\nu = \frac{S_\phi(\omega \to 0)}{2\pi}. \tag{6.31}$$

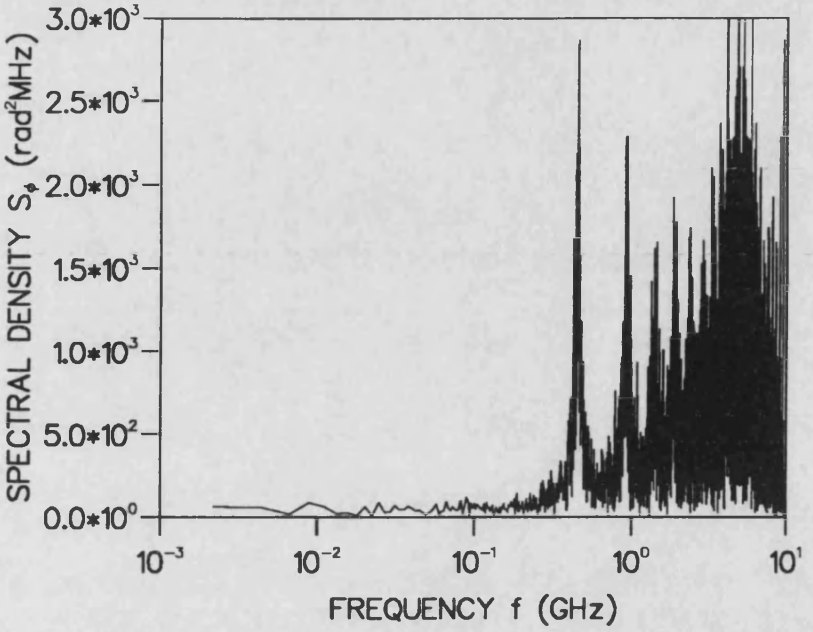

Fig. 6.13: Two-Sided Spectral Density S_ϕ of the Frequency Fluctuations ($I=3.5I_{th}$, $R_{pcm}=10^{-3}$, $\tau_{ext}=2$ ns).

The behaviour of the linewidth as the external reflectivity is increased is shown in fig. 6.14. The graph shows linewidth for increasing levels of phase conjugate feedback. The linewidth for increasing levels of conventional mirror feedback with two different external cavity round trip phase changes, $\omega_{th}\tau_{ext}$, is also shown. It can be seen that the linewidth behaves differently as the strength of the phase conjugate feedback and conventional mirror feedback increases. The feedback regimes I-IV [29,30] as described in chapter 1 are shown for conventional mirror feedback. At low levels of conventional mirror feedback (regimes I and II) the linewidth is increased or decreased depending on the phase of the reflected light. At higher levels of conventional mirror feedback (regime III) the linewidth is reduced and is independent of the phase of the reflected light. For very high levels of conventional mirror feedback the laser enters regime IV, and the linewidth is dramatically increased. Since there is zero round trip phase change with phase conjugate feedback, it is anticipated that feedback regimes I and II do not exist. Fig. 6.14 confirms this. Quite large levels of phase conjugate feedback are required before the linewidth is altered from that of the solitary laser compared to conventional mirror feedback. The reduced linewidth regime III can be obtained with phase conjugate feedback but occurs at higher levels of external reflectivity than for conventional mirror feedback. A transition to regime

IV, coherence collapse, is found for phase conjugate feedback as for conventional mirror feedback.

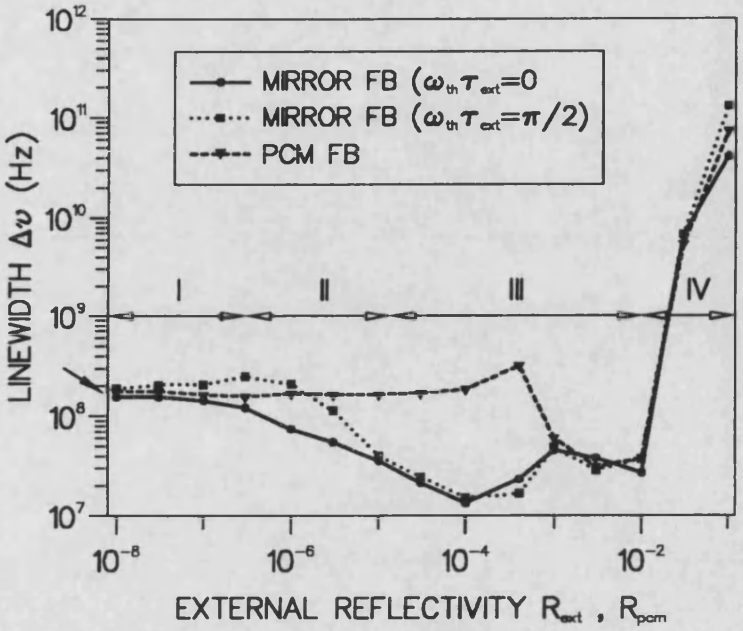

Fig. 6.14: Linewidth Δν for Phase Conjugate R_{pcm} and Conventional Mirror Optical Feedback R_{ext} ($I=3.5I_{th}$, τ_{ext}=2 ns). Roman Numerals Indicate the Conventional Mirror Optical Feedback Regimes. The Solid Arrow Indicates the Solitary Laser Linewidth.

Phase conjugate feedback has a different effect on the linewidth behaviour of semiconductor lasers to that of conventional mirror feedback as the level of external reflectivity is increased. The feedback regimes I and II do not exist for phase conjugate optical feedback due to the zero external cavity round trip phase change. Feedback regime III has a smaller range for phase conjugate than for conventional mirror feedback. Feedback regime IV is unchanged between the two types of optical feedback.

6.8 Conclusion.

The intensity noise and linewidth characteristics of a semiconductor laser with phase conjugate feedback have been investigated. The results show that different intensity noise behaviour occurs with the two types of optical feedback. At very low levels of phase conjugate feedback the intensity noise can be lowered slightly. Output power fluctuations occur at lower levels of phase conjugate external reflectivity than for conventional mirror feedback. However, the transition to the chaotic coherence

collapse laser output state occurs at a higher level of external reflectivity for phase conjugate than for conventional mirror feedback. Low levels of phase conjugate feedback have the effect of reducing low frequency intensity noise, up to a few hundred MHz. The behaviour of the laser linewidth with increasing external reflectivity is also qualitatively different for the two types of optical feedback. Higher levels of external reflectivity are required to decrease the linewidth with phase conjugate feedback than for conventional mirror feedback. The feedback regimes III and IV are applicable to describe phase conjugate feedback effects in semiconductor lasers but regimes I and II cannot be used as they have a dependence on an external cavity phase change, which is eliminated by phase conjugate feedback. Phase conjugate mirrors fabricated from semiconductor optical amplifiers are quite capable of generating a very large external reflectivity [35-43]. The behaviour of semiconductor lasers with high levels of phase conjugate feedback will be analogous to feedback regime V for conventional mirror feedback, as investigated in chapter 4.

Chapter 6 References.

[1] G P Agrawal and J T Klaus, "Effect of Phase-Conjugate Feedback on Semiconductor Laser Dynamics", Optics Lett., Vol. 16, No. 17, pp. 1325-1327, 1991.

[2] G P Agrawal and G R Gray, "Effect of Phase-Conjugate Feedback on the Noise Characteristics of Semiconductor Lasers", Phys. Rev. A., Vol. 46, No. 9, pp. 5890-5898, 1992.

[3] G H M Tartwijk, H J C Van der Linden, and D Lenstra, "Theory of a Diode Laser with Phase Conjugate Feedback", Optics Lett., Vol. 17, No. 22, pp. 1590-1592, 1992.

[4] G R Gray, D Huang, and G P Agrawal, "Chaotic Dynamics of Semiconductor Lasers with Phase Conjugate Feedback", Phys. Rev. A, Vol. 49, No. 3, pp. 2096-2105, 1994.

[5] L N Langley and K A Shore, "The Effect of Phase Conjugate Optical Feedback on the Intensity Noise in Laser Diodes", Optics Lett., Vol. 18, No. 17, pp. 1432-1434, 1993.

[6] L N Langley and K A Shore, "Intensity Noise and Linewidth Characteristics of Laser Diodes with Phase Conjugate Optical Feedback", IEE Proc.-Optoelectron., Vol. 141, No. 2, pp. 103-108, 1994.

[7] L Petersen, U Gliese, and T N Nielsen, "Phase Noise Reduction by Self Phase Locking in Semiconductors Lasers using Phase Conjugate Feedback", to be published, IEEE J. Quantum Electron., 1994.

[8] N McCarthy and D Gay, "Noise Reduction in an Argon Laser with a Phase-Conjugating External Cavity", Optics Lett., Vol. 16, No. 13, pp. 1004-1006, 1991.

[9] K Vahala, K Kyuma, A Yariv, S K Kwong, M Cronin-Golomb, and K Y Lau, "Narrow Linewidth Single Frequency Semiconductor Laser with a Phase Conjugate External Cavity Mirror", Appl. Phys. Lett., Vol. 49, No. 23, pp. 1563-1565, 1986.

[10] M Ohtsu, I Koshishi, and Y Teramachi, "A Semiconductor Laser as a Stable Phase Conjugate Mirror for Linewidth Reduction of Another Semiconductor Laser", Jap. J. Appl. Phys., Vol. 29, No. 11, pp. L2060-L2062, 1990.

[11] R R Stephens, R C Lind, and C R Giuliano, "Phase Conjugate Master Oscillator-Power Amplifier Using $BaTiO_3$ and AlGaAs Semiconductor Diode Lasers", Appl. Phys. Lett., Vol. 50, No. 11, pp. 647-649, 1987.

[12] Y Champagne, N McCarthy, and R Tremblay, "Optical Phase-Conjugate Feedback Effects in Gain-Guided Diode Laser Characteristics", IEEE J. Quantum Electron., Vol. 25, No. 3, pp. 595-601, 1989.

[13] M Cronin-Golomb and A Yariv, "Self-Induced Frequency Scanning and Distributed Bragg Reflection in Semiconductor Lasers with Phase Conjugate-Feedback", Optics Lett., Vol. 11, No. 7, pp. 455-457, 1986.

[14] E J Bochove, "Transverse-Mode Instability and Chaos in an Optical Cavity with Phase-Conjugate Mirror", Optics Lett., Vol. 11, No. 11, pp. 727-729, 1986.

[15] S MacCormack and R W Eason, "Near-Diffraction-Limited Single-Lobe Emission from a High-Power Diode-Laser Array Coupled to a Photorefractive Self-Pumped Phase-Conjugate Mirror", Optics Lett., Vol. 16, No. 10, pp. 705-707, 1991.

[16] S Weiss, M Segev, and B Fischer, "Line Narrowing and Self Frequency Scanning of Laser Diode Arrays Coupled to a Photorefractive Oscillator", IEEE J. Quantum Electron, Vol. 24, No. 5, pp. 706-708, 1988.

[17] S MacCormack and J Feinberg, "High-Brightness Output from a Laser-Diode Array Coupled to a Phase-Conjugating Mirror", Optics Lett., Vol. 18, No. 3, pp. 211-213, 1993.

[18] M Segev, S Weiss, and B Fischer, "Coupling of Diode Laser Arrays with Photorefractive Passive Phase Conjugate Mirrors", Appl. Phys. Lett., Vol. 50, No. 20, pp. 1397-1399, 1987.

[19] M Cronin-Golomb, A Yariv, and I Ury, "Coherent Coupling of Diode Lasers by Phase Conjugation", Appl. Phys. Lett., Vol. 48, No. 19, pp. 1240-1242, 1986.

[20] M Segev and B Fischer, "Laser Diode Arrays with Apertured Phase Conjugate Feedback", IEEE J. Quantum Electron., Vol. 26, No. 8, pp. 1318-1322, 1990.

[21] M Segev, Y Ophir, B Fischer, and G Eisenstein, "Mode Locking and Frequency Tuning of a Laser Diode Array in an Extended Cavity with a Photorefractive Phase Conjugate Mirror", Appl. Phys. Lett., Vol. 57, No. 24, pp. 2523-2525, 1990.

[22] S MacCormack, J Feinberg, and M H Garrett, "Injection-Locking a Laser-Diode Array with a Phase-Conjugate Beam", Optics Lett., Vol. 19, No. 2, pp. 120-122, 1994.

[23] R A Fisher, "Optical Phase Conjugation", Academic Press, 1983.

[24] P D Hillman and M Marciniak, "Phase Locking Laser Diodes Using Photorefractive Coupling", J. Appl. Phys., Vol. 66, No. 12, pp. 5731-5737, 1989.

[25] J Feinberg and G D Bacher, "Phase-Locking Lasers with Phase Conjugation", Appl. Phys. Lett., Vol. 48, No. 9, pp. 570-572, 1986.

[26] T Shimura, M Tamura, and K Kuroda, "Injection Locking and Mode Switching of a Diode Laser with a Double Phase-Conjugate Mirror", Optics Lett., Vol. 18, No. 19, pp. 1645-1647, 1993.

[27] K Petermann, "Laser Diode Modulation and Noise", Kluwer Academic, 1988.

[28] B R Clarke, "The Effect of Reflections on the System Performance of Intensity Modulated Laser Diodes", IEEE J. Lightwave Tech., Vol. 9, No. 6, pp. 741-749, 1991.

[29] R W Tkach and A R Chraplyvy, "Regimes of Feedback Effects in 1.5-μm Distributed Feedback Lasers", IEEE J. Lightwave Technol., Vol. 4, No. 11, pp. 1655-1661, 1986.

[30] N Schunk and K Petermann, "Numerical Analysis of the Feedback Regimes for a Single-Mode Semiconductor Laser with External Feedback", IEEE J. Quantum Electron., Vol. 24, No. 7, pp. 1242-1247, 1988.

[31] D Lenstra, B H Verbeek, and A J Den Boef, "Coherence Collapse in Single-Mode Semiconductor Lasers due to Optical Feedback", IEEE. J. Quantum Electron, Vol. 24, No. 6, pp. 674-679, 1985.

[32] H Li, J Ye, and J G McInerney, "Detailed Analysis of Coherence Collapse in Semiconductor Lasers", IEEE J. Quantum Electron., Vol. 29, No. 9, pp. 2421-2432, 1993.

[33] J Mørk, B Tromborg, and J Mark, "Chaos in Semiconductor Lasers with Optical Feedback: Theory and Experiment", IEEE J. Quantum Electron., Vol. 28, No. 1, pp. 93-108, 1992.

[34] N Schunk and K Petermann, "Minimum Bit Rate of DPSK Transmission for Semiconductor Laser with a Long External Cavity and Strong Linewidth Reduction", IEEE J. Lightwave Technol., Vol. 5, No. 9, pp. 1309-1314, 1987.

[35] W M Yee and K A Shore, "Nearly Degenerate Four-Wave Mixing in Laser Diodes with Nonuniform Longitudinal Gain Distribution", J. Opt. Soc. Am. B, Vol. 11, No. 7, pp. 1221-1228, 1994.

[36] H Nakajima and R Frey, "Collinear Nearly Degenerate Four-Wave Mixing in Intracavity Amplifying Media", IEEE J. Quantum Electron., Vol. 22, No. 8, pp. 1349-1354, 1986.

[37] H Nakajima and R Frey, "Intracavity Nearly Degenerate Four-Wave Mixing in a (GaAl)As Semiconductor Laser", Appl. Phys. Lett., Vol. 47, No. 8, pp. 769-771, 1985.

[38] Z Zhang, Y Zhu, C Yang, and P Fu, "A High Efficiency Double 45°-cut Mutually Pumped Phase Conjugate Mirror", J. Appl. Phys., Vol. 74, No. 3, pp. 2137-2139, 1993.

[39] Y Zhu, C Yang, M Hui, X Niu, J Zhang, T Zhou, and X Wu, "Phase Conjugation of $BaTiO_3$:Ce by Backward Stimulated Photorefractive Scattering", Appl. Phys. Lett., Vol. 64, No. 18, pp. 2341-2343, 1994.

[40] G W Ross and R W Eason, "Double Phase-Conjugate Mirror with Sixfold Gain in Photorefractive $BaTiO_3$ at Near-Infrared Wavelengths", Optics Lett., Vol. 18, No. 8, pp. 571-573, 1993.

[41] Y Ishii and I Uehira, "Laser-Diode Phase-Shifting Interferometry with a Self-Pumped Phase-Conjugate Mirror", Optics Lett., Vol. 18, No. 17, pp. 1459-1461, 1993.

[42] Y Awaji, S Sayama, H Suzuki, M Ohtsu, and Y Teramachi, "Generation of Phase Conjugate Wave from a Visible InGaAlP Laser", Jap. J. Appl. Phys., Vol. 32, pt. 1, Vol. 3A, pp. 1107-1111, 1993.

[43] X Gao, A Sasaki, and Y Zheng, "Stable High-Efficiency Double-Phase-Conjugate Mirror in a Cu-Doped Potassium Sodium Strontium Barium Niobate Crystal", Jap. J. Appl. Phys., Vol. 32, Pt. 2, No. 11B, pp. L1654-1656, 1993.

Chapter 7:

External Cavity Nonlinear Dynamics of Laser Diodes.

7.1 Introduction to External Cavity Dynamics.

This chapter examines two topics which relate to the novel practical applications of external cavity semiconductor lasers. First of all, a further aspect of laser diodes subject to phase conjugate feedback is examined where the finite time response of the medium giving rise to phase conjugate feedback is taken into account. The influence of such "sluggish" phase conjugate feedback is discussed in sections 7.2-7.6. In section 7.5 the appearance of chaotic dynamics in this configuration is noted. The second topic which is examined arises from recent interest in the control of nonlinear and chaotic dynamics. Here attention is focussed on targetting nonlinear dynamics of lasers subject to feedback from conventional or phase conjugate mirrors.

7.2 Introduction to Sluggish Phase Conjugate Feedback.

Recent work has considered, both theoretically [1-7] and experimentally [8,9], the effect of phase conjugate feedback (PCF) on semiconductor laser diodes. It is well known that conventional optical feedback (COF) can cause dramatic changes in the dynamical behaviour and noise properties of laser diodes [10,11]. Of particular importance in such cases is the phase of the light returned to the laser after the round trip of the external cavity. Phase conjugate mirrors have the property of reversing the phase of light incident upon them. Consequently there is a zero round trip phase change in an external cavity formed with a phase conjugate mirror, as discussed in chapter 6.

The dynamics of laser diodes with phase conjugate feedback have been investigated [1-3], as have the intensity noise [4-6] and linewidth properties [6-9]. In the previous

theoretical work it has been assumed that the phase conjugate mirror has an instantaneous response time. Processes for generation of phase conjugate feedback are described in chapter 6. In those cases, finite response times of the material can be expected, giving rise to changes in the input beam intensity [12-14]. The rise time of the response of the phase conjugate mirror is expected to be of the order of nanoseconds. The reflected pulse from a phase conjugate mirror will thus be delayed and spread out in time compared to the incident pulse [12]. This slow response is shown in fig. 7.1 and is known as sluggish phase conjugate feedback. The phase conjugate reflectivity can only achieve its steady state value if the input pulse duration is far greater then the round trip transit time of the phase conjugate mirror [12].

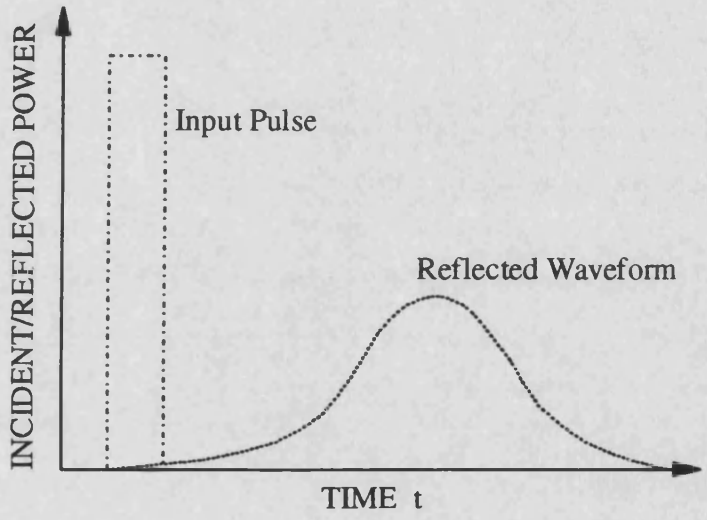

Fig. 7.1: Sluggish Response from a Phase Conjugate Mirror Showing the Delaying and Spreading of the Reflected Pulse.

The nanosecond response times of phase conjugate mirrors are comparable to both the external cavity round trip delay and the inverse of the relaxation oscillation frequency $1/f_r$. Therefore the behaviour of the laser is expected to be modified by the sluggish response of the phase conjugate mirror. The following sections consider how the sluggishness of the phase conjugate mirror affects the behaviour of laser diodes with phase conjugate feedback. The investigation is not concerned with the slow build up of the phase conjugate reflectivity when the phase conjugate mirror is initially turned on, which can be as long as seconds or minutes for photorefractive phase conjugate mirrors [15-17]. The aim of this chapter is to gain some insights into the effect of a sluggish phase conjugate mirror on the behaviour of the semiconductor laser, without detailing the dynamic processes within the phase conjugate mirror itself.

7.3 Rate Equation Model for Sluggish Phase Conjugate Feedback.

A single mode laser diode model is used to investigate the effect on diode lasers of sluggish phase conjugate feedback. The configuration is shown in fig. 7.2.

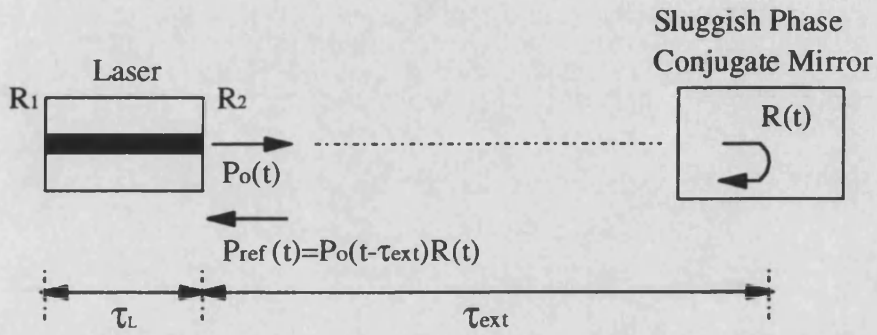

Fig 7.2: Laser Diode with Feedback from a Sluggish Phase Conjugate Mirror.

The phase conjugate mirror is assumed to respond with an exponential rise time. This representation is considered adequate for an initial investigation into sluggish phase conjugate feedback. An additional rate equation [18] is introduced into the model to account for the time dependent phase conjugate reflectivity R(t),

$$\frac{ds_{ref}(t)}{dt} = -\frac{1}{T_r}\left(s_{ref}(t) - R_{pcm}s(t)\right), \tag{7.1}$$

where R_{pcm} is the steady state phase conjugate mirror reflectivity and T_r is the rise time of the phase conjugate mirror. Equation (7.1) is a simple model of a sluggish phase conjugate mirror for the present initial investigation. A more detailed rate equation containing the sluggish response could be obtained from equation (6.3) by incorporating R(t) into k_{pcm}. The rise time T_r depends on the incident power in principle, but is treated as a constant for simplicity. The extra rate equation increases the flexibility of the model by including time dependent external reflectivities.

The rate equation (7.1) for the sluggish response is used in addition to those already used in chapter 6 to describe instantaneous phase conjugate feedback [1-7]. They are given below for completeness together with the Langevin noise terms to model the spontaneous emission noise. Note that $s(t-\tau_{ext})$ has been replaced by $s_{ref}(t-\tau_{ext})$,

$$\frac{dn(t)}{dt} = \frac{I(t)}{eV} - \frac{n(t)}{\tau_{sp}} - s(t)G_n\{n(t)-n_o\}\left\{\frac{1}{1+\varepsilon s(t)}\right\} + F_n(t), \tag{7.2}$$

$$\frac{ds(t)}{dt} = \frac{\gamma n(t)\Gamma}{\tau_{sp}} - \frac{s(t)}{\tau_{ph}} + s(t)G_n\{n(t)-n_o\}\Gamma\left\{\frac{1}{1+\varepsilon s(t)}\right\} + \frac{k_{pcm}}{\tau_L}\sqrt{s(t)}\sqrt{s_{ref}(t-\tau_{ext})}\cos(\theta(t)) + F_s(t), \tag{7.3}$$

$$\frac{d\phi(t)}{dt} = \frac{\alpha}{2}G_n\{n(t)-n_{th}\}\Gamma - \frac{k_{pcm}}{\tau_L}\frac{\sqrt{s_{ref}(t-\tau_{ext})}}{\sqrt{s(t)}}\sin(\theta(t)) + F_\phi(t), \tag{7.4}$$

where

$$\theta(t) = \phi(t) + \phi(t-\tau_{ext}), \tag{7.5}$$

and

$$F_n(t) = -\sqrt{\frac{2s(t_i)\gamma n(t)\Gamma}{\tau_{sp}\Delta t}}x_s + \sqrt{\frac{2n(t_i)}{\tau_{sp}\Delta t V}}x_n, \tag{7.6}$$

$$F_s(t) = \sqrt{\frac{2s(t_i)\gamma n(t)\Gamma}{\tau_{sp}\Delta t}}x_s, \tag{7.7}$$

$$F_\phi(t) = \frac{1}{s(t)}\sqrt{\frac{s(t_i)\gamma n(t)\Gamma}{2\tau_{sp}\Delta t}}x_\phi. \tag{7.8}$$

The values and descriptions of the laser diode parameters used in (7.2)-(7.8) are given in table 2.1. The rate equations (7.1)-(7.8) have been solved numerically for weak levels of sluggish phase conjugate feedback following the same methods described in chapters 2, 6 and appendix 3. The intensity noise and dynamics of the laser diode have been investigated.

7.4 Intensity Noise with Sluggish Phase Conjugate Feedback.

The sluggish response means that the phase conjugate mirror acts like a filter on the intensity noise frequency components in the laser output. The laser intensity noise components of frequency greater than approximately $1/T_\Gamma$ are filtered out and are absent from the reflected light. Thus the reflected light is a smoothed version of the light emitted from the laser.

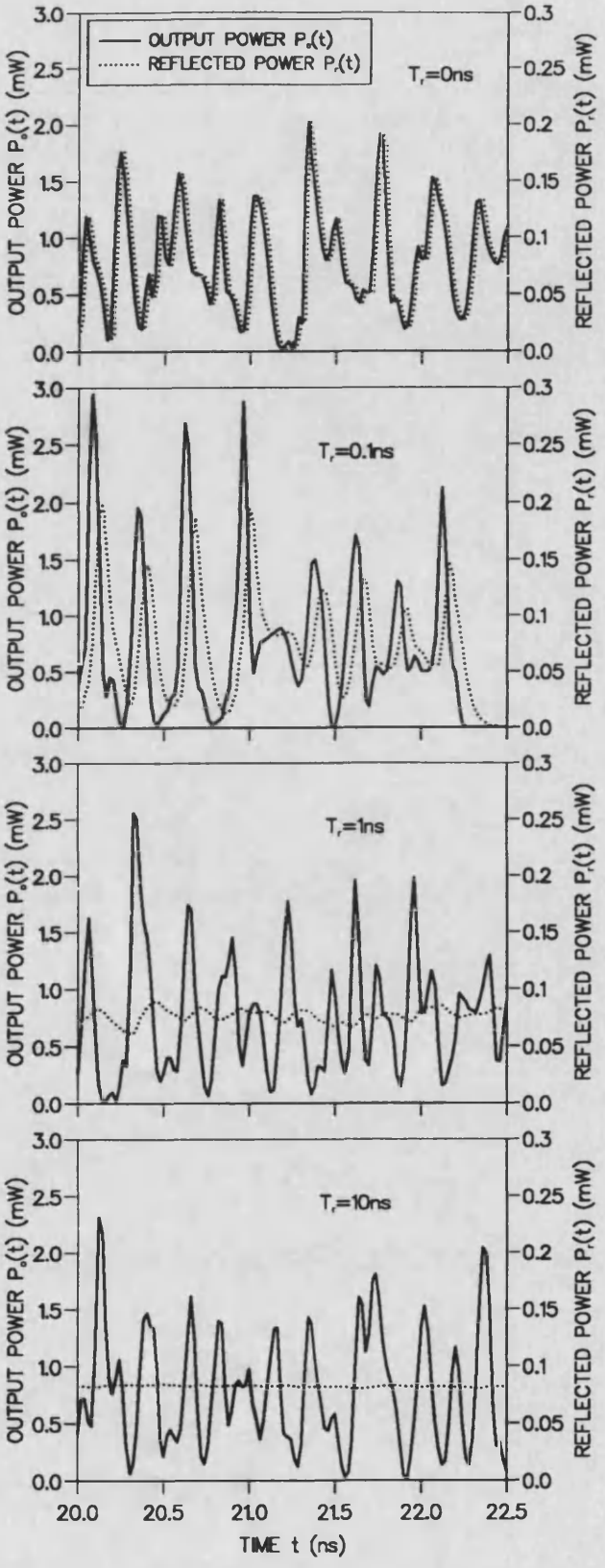

Fig. 7.3: Output Power $P_o(t)$ and Reflected Power $P_r(t)$ Waveforms for Sluggish Phase Conjugate Mirrors with Rise Times T_r up to 10 ns (R_{ext}=0.1, I=2I_{th}, τ_{ext}=2 ns).

Any sharp noise spikes in the laser output are not reflected by the phase conjugate mirror. Fig. 7.3 shows the output power $P_o(t)$ and reflected power $P_r(t)$ waveforms for a sluggish phase conjugate mirror with rise times T_r up to 10 ns. For large T_r (very sluggish phase conjugate feedback) the intensity spikes in the laser output do not appear in the reflected light. In noisy operating regimes (such as coherence collapse caused by moderate optical feedback) noise peaks at frequencies corresponding to multiples of $1/\tau_{ext}$ appear in the intensity noise spectrum. The noise peaks are due to pulses of light propagating around the external cavity at its characteristic delay τ_{ext}. A sluggish phase conjugate mirror does not allow noise spikes to propagate around the external cavity due to the filtering action of its sluggish response. The absence of spikes in the feedback light results in less intensity noise in noisy operating regimes (such as coherence collapse at moderate feedback levels) with sluggish phase conjugate feedback as compared to instantaneous phase conjugate feedback. Fig. 7.4 shows the intensity noise spectrum of sluggish phase conjugate feedback where the peaks corresponding to multiples of the inverse external cavity round trip delay $1/\tau_{ext}$ are absent. The laser is operating in the coherence collapse regime with a phase conjugate reflectivity R_{pcm}=0.1 and a bias current $I=2I_{th}$. Fig. 7.4 should be compared to the intensity noise spectrum of instantaneous phase conjugate feedback in Fig. 7.5 for the same feedback strength, where the intensity noise peaks at multiples of the inverse external cavity round trip delay $1/\tau_{ext}$ are more prominent.

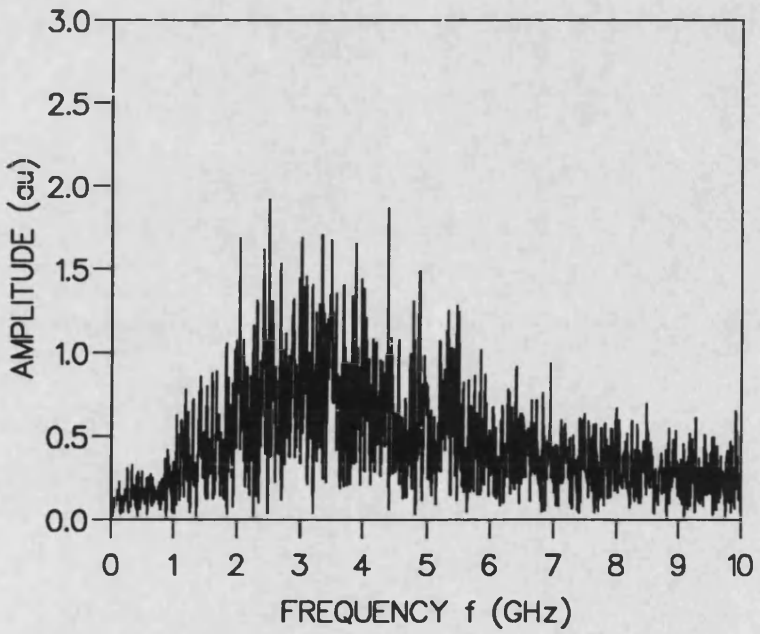

Fig. 7.4: Intensity Noise Spectrum for Optical Feedback from a Sluggish Phase Conjugate Mirror (T_r=1 ns, R_{pcm}=0.1, $I=2I_{th}$, τ_{ext}=2 ns).

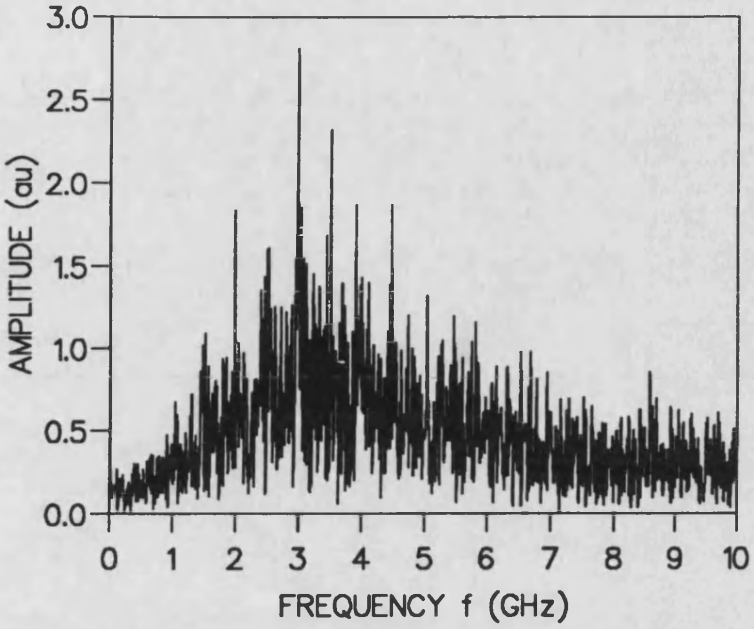

Fig. 7.5: Intensity Noise Spectrum for Optical Feedback from an Instantaneous Phase Conjugate Mirror (T_r=0 ns, R_{pcm}=0.1, I=2I_{th}, τ_{ext}=2 ns).

When a diode laser is subject to optical feedback the majority of the intensity noise generated is around the relaxation oscillation frequency f_r of the laser [19]. This is shown in figs. 7.4 and 7.5 where $f_r \approx 3$ GHz. Since the relaxation oscillation frequency changes with bias current it is expected that the small intensity noise reduction due to the sluggish response of the phase conjugate mirror will also change with bias current. The level of the intensity noise, defined by

$$RIN = \frac{\overline{P_o(t)^2} - \overline{P_o(t)}^2}{\overline{P_o(t)}^2}, \tag{7.9}$$

as the response time T_r of the sluggish phase conjugate mirror is increased is shown in Fig. 7.6 for several bias currents. Again the laser is operating in the noisy coherence collapse regime at moderate optical feedback levels of R_{pcm}=0.1 and I=2I_{th}. As the response becomes less sluggish, the phase conjugate mirror begins to reflect the higher frequency components of the intensity noise in the laser output and consequently the laser intensity noise increases. At higher bias currents the intensity noise spectrum contains higher frequency components. Therefore, for higher bias currents a faster response time can be tolerated before the transition to a higher level of intensity noise, as shown in Fig. 7.6.

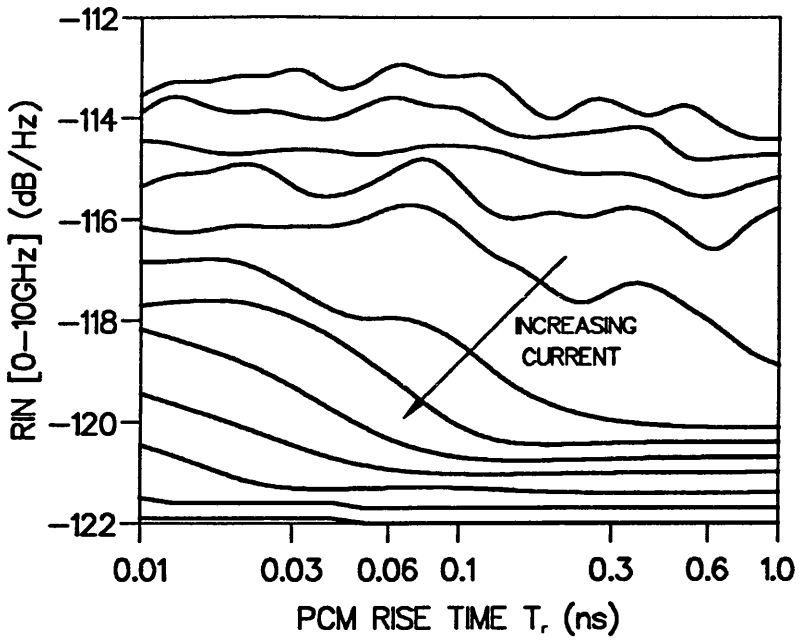

Fig. 7.6: Relative Intensity Noise (RIN) Variation with Sluggish Phase Conjugate Mirror Response Time for Varying Bias Current from 2.7 to 3.8 times I_{th} (R_{pcm}=0.1, τ_{ext}=2 ns).

7.5 Bifurcation Diagrams and Route to Chaos.

Further insight into the dynamics of laser diodes subject to sluggish phase conjugate feedback can be gained from bifurcation diagrams for increasing phase conjugate reflectivity. Bifurcation diagrams are produced by generating a long time series of the laser output power $P_o(t)$ at each feedback level. The carrier density n(t) is noted at each time the output power crosses its steady state solitary laser output power P_{sol}. The values of carrier density are then normalised using

$$\frac{n}{n_{th}} - 1 \rightarrow n, \tag{7.10}$$

where n_{th} is the threshold carrier density of the solitary laser. At a particular external reflectivity: (i) no crossings of the steady state laser output power P_{sol} indicates a stable laser output, (ii) a single value of the carrier density at the crossing indicates a single frequency oscillation in the laser output, (iii) multiple values of the carrier density at the crossings indicates a few frequency components in the oscillations of the laser output, and (iv) large numbers of the value of the carrier density at the crossings (blending into a continuous line) indicates chaotic fluctuations in the laser output.

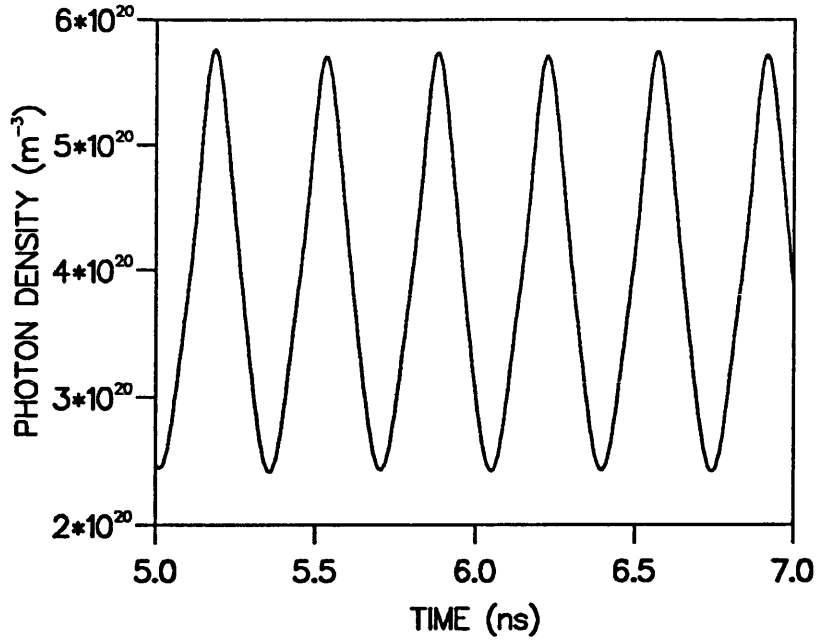

Fig. 7.7: Output Power Time Series for a Reflectivity Just Below a Period Doubling Bifurcation ($I=2I_{th}$, $\tau_{ext}=2$ ns).

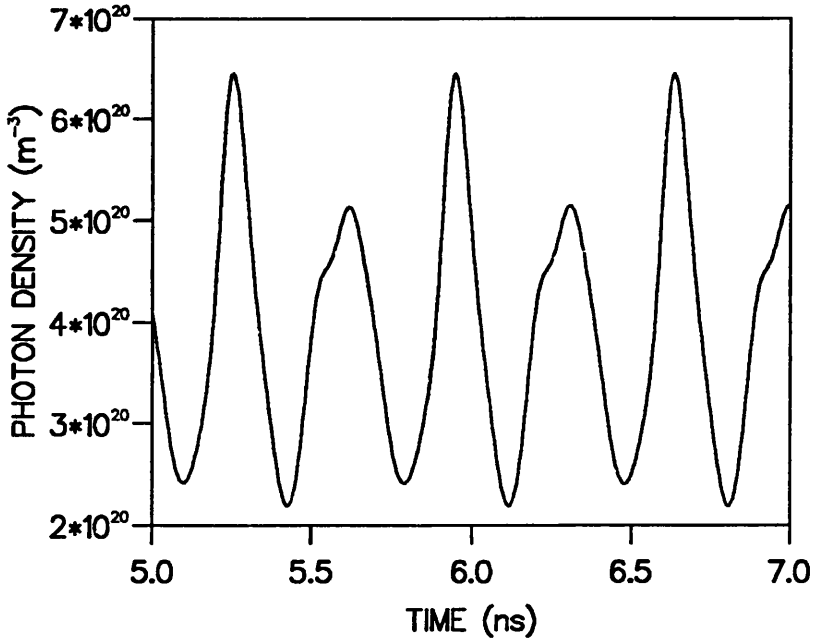

Fig. 7.8: Output Power Time Series for a Reflectivity Just Above a Period Doubling Bifurcation ($I=2I_{th}$, $\tau_{ext}=2$ ns).

When the number of values of the carrier density (at crossings of the steady state solitary laser output power) doubles it is called a period doubling bifurcation [20,21] because the output power waveform has twice as many frequency components (i.e.

the period has doubled). The process can continue indefinitely leading to an aperiodic or chaotic waveform. This is known as a period doubling route to chaos [20-24]. If a time series of the laser output were plotted at a reflectivity just below the period doubling bifurcation then the output would consist of a single frequency oscillation, as seen in fig 7.7. In comparison, an equivalent time series for a reflectivity just above the period doubling bifurcation is shown in fig 7.8, where the laser output consists of an oscillation which has a period twice as long as the period of the oscillation for a reflectivity below the bifurcation point. Hence, bifurcation diagrams are useful for comparing the route to chaos for the different types of feedback.

The bifurcation diagram of the normalised carrier density n/n_{th}-1 for sluggish phase conjugate feedback, with a rise time of T_r=10 ns and an external cavity round trip delay τ_{ext}=0.23 ns, is shown in Fig. 7.9. The laser bias current is $I=2I_{th}$. When compared to the bifurcation diagram for instantaneous phase conjugate feedback (T_r=0 ns) of the same external cavity round trip delay in Fig. 7.10 it can be seen that the dynamics are more complex for sluggish phase conjugate feedback, as there are more regions of periodic and chaotic behaviour before the final transition into chaos.

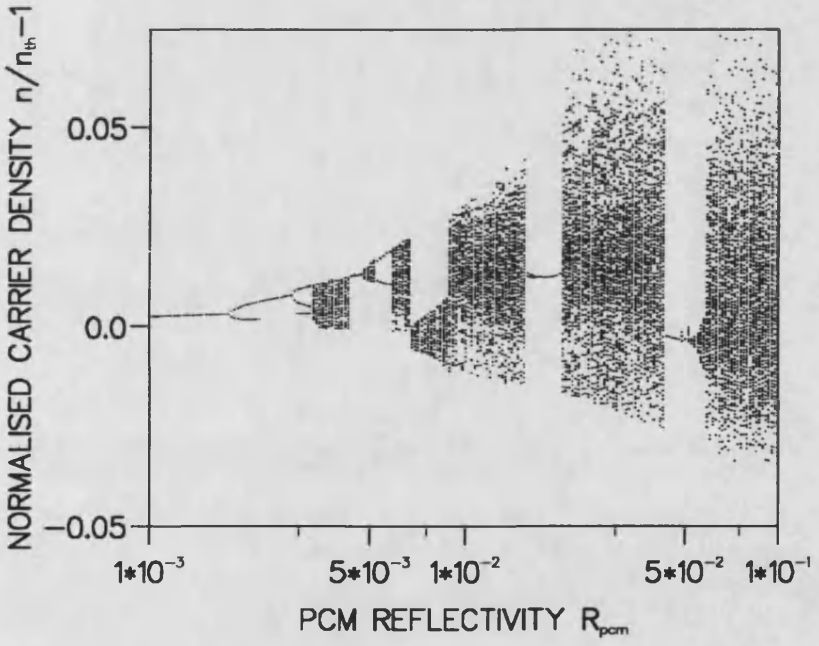

Fig. 7.9: Bifurcation Diagram of Normalised Carrier Density (n/n_{th}-1) for Increasing Feedback from a Sluggish Phase Conjugate Mirror (T_r=10 ns, τ_{ext}=0.23 ns, $I=2I_{th}$).

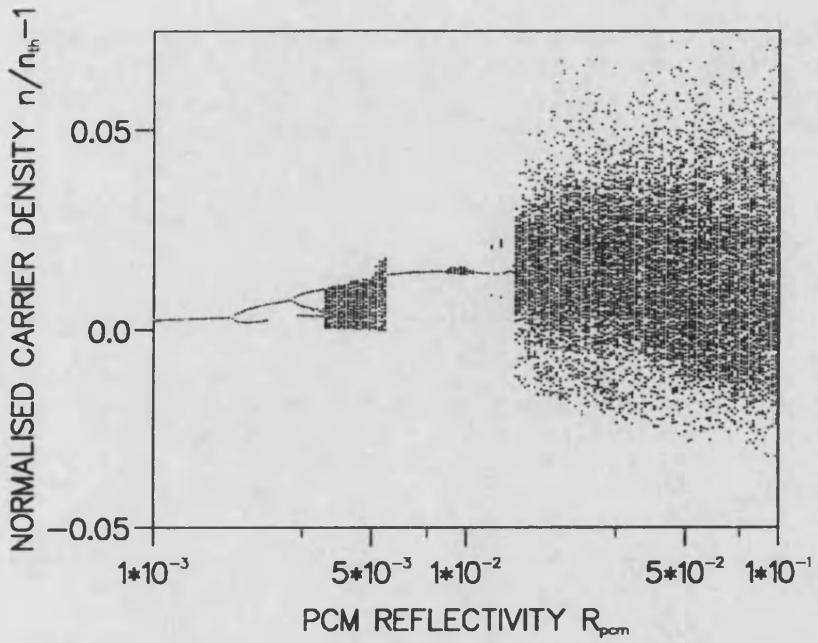

Fig. 7.10: Bifurcation Diagram of Normalised Carrier Density (n/n_{th}-1) for Increasing Feedback from an Instantaneous Phase Conjugate Mirror (T_r=0 ns, τ_{ext}=0.23 ns, I=2I_{th}).

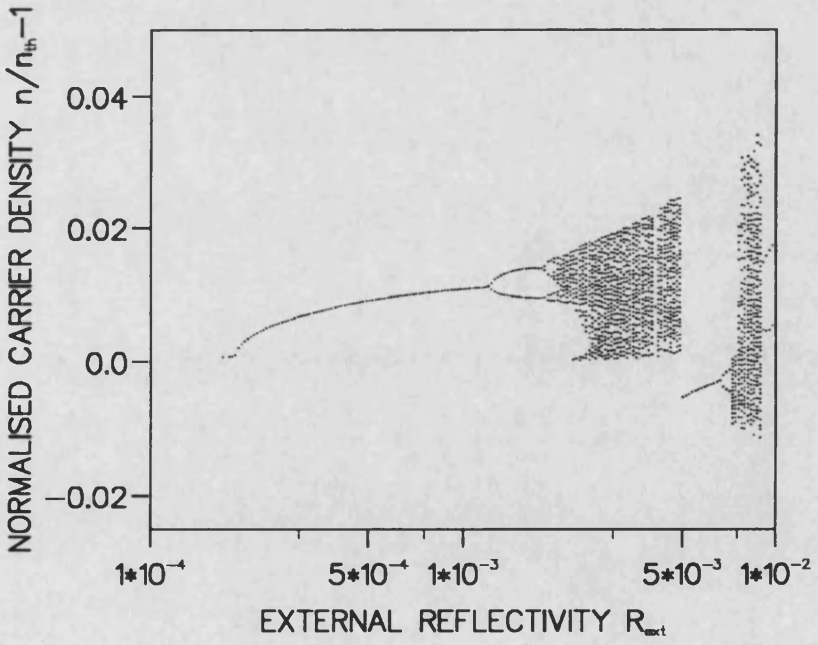

Fig. 7.11: Bifurcation Diagram of Normalised Carrier Density (n/n_{th}-1) for Increasing Conventional Optical Feedback (τ_{ext}=0.23 ns, I=2I_{th}).

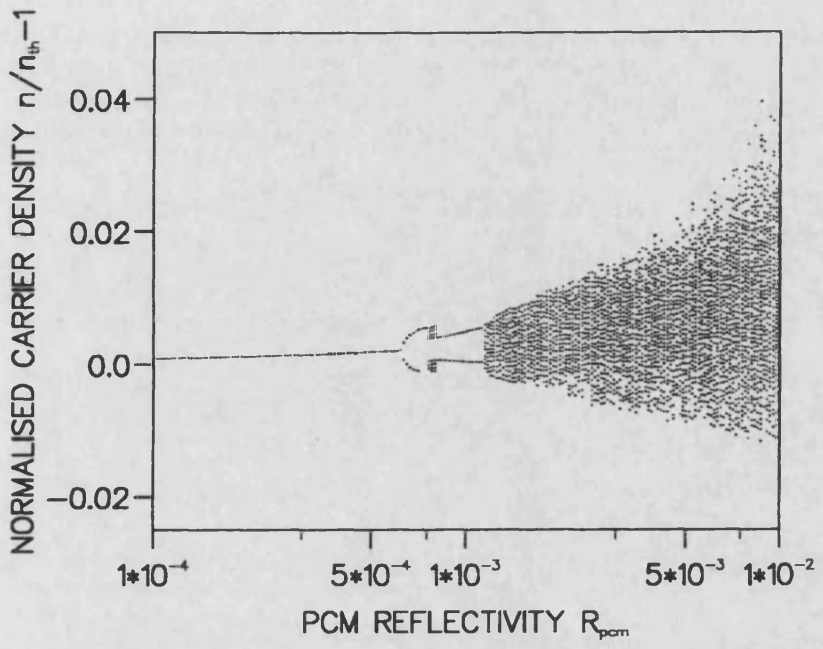

Fig. 7.12: Bifurcation Diagram of Normalised Carrier Density (n/n_{th}-1) for Increasing Feedback from a Sluggish Phase Conjugate Mirror (T_r=10 ns, τ_{ext}=2.3 ns, I=2I_{th}).

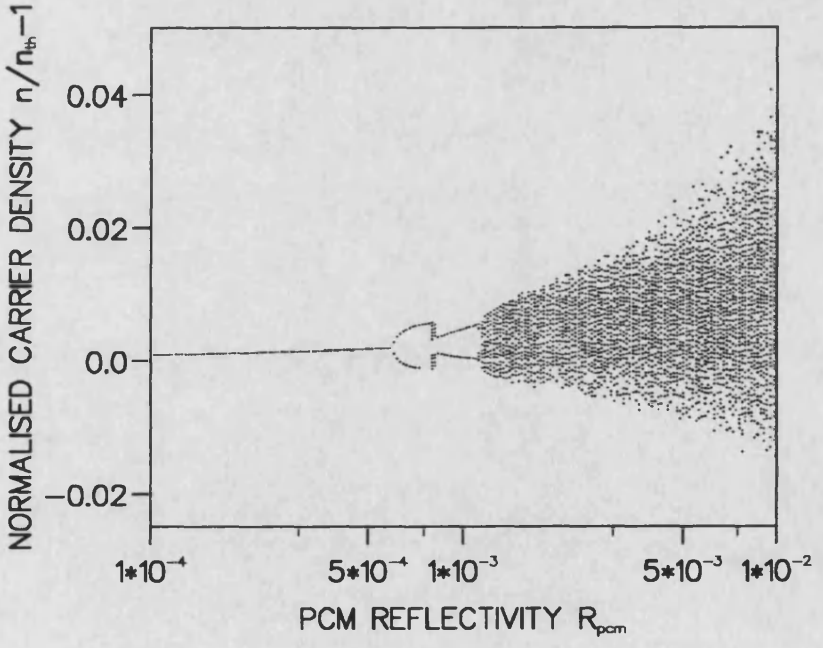

Fig. 7.13: Bifurcation Diagram of Normalised Carrier Density (n/n_{th}-1) for Increasing Feedback from an Instantaneous Phase Conjugate Mirror (T_r=0 ns, τ_{ext}=2.3 ns, I=2I_{th}).

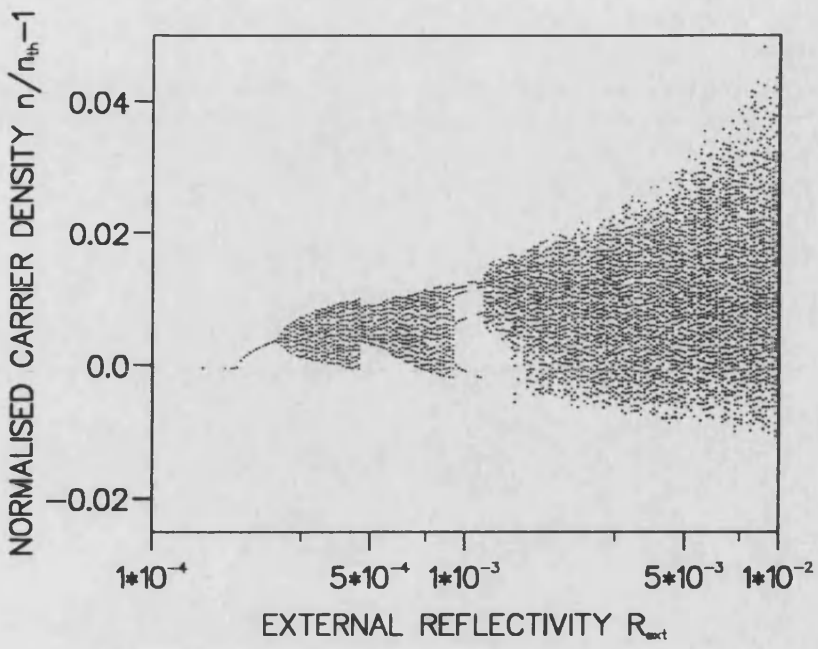

Fig. 7.14: Bifurcation Diagram of Normalised Carrier Density (n/n_{th}-1) for Increasing Conventional Optical Feedback (τ_{ext}=2.3 ns, $I=2I_{th}$).

The bifurcation diagrams for sluggish and instantaneous phase conjugate feedback should both be compared to that of conventional optical feedback for the same external cavity round trip delay in Fig. 7.11. For conventional optical feedback (fig. 7.11) the laser output oscillation is seen to double in period at the bifurcation points on its route to chaos. For instantaneous phase conjugate feedback (fig. 7.10) the bifurcation diagram is more complex, showing other structures as well as period doubling bifurcations. For sluggish phase conjugate feedback (fig. 7.9) it is still more complex, with many windows of single frequency oscillations in the output power. Also the complexity (i.e. the number of windows of periodic and regions of chaotic behaviour) increases as the sluggish phase conjugate mirror rise time T_r increases. However the first bifurcation point occurs at the same reflectivity for sluggish and instantaneous phase conjugate feedback.

Further calculations at longer external cavities show that the difference in complexity between sluggish and instantaneous phase conjugate feedback is reduced for a larger external cavity round trip delay. Fig. 7.12 shows the bifurcation diagram for sluggish phase conjugate feedback (T_r=10 ns) for a longer external cavity round trip delay of 2.3 ns and a bias current $I=2I_{th}$. Fig. 7.12 is not very different from that for instantaneous phase conjugate feedback shown in Fig. 7.13. Therefore changes in the dynamics of the laser with phase conjugate feedback caused by a sluggish phase

conjugate mirror are more pronounced for shorter external cavities. This behaviour is similar to the reduced differences at longer external cavities between the behaviour of instantaneous phase conjugate feedback (fig. 7.13) and conventional optical feedback shown in Fig 7.14 [4].

7.6 Linewidth Behaviour of Sluggish Phase Conjugate Feedback.

Weak levels of optical feedback may be used to reduce the linewidth $\Delta\nu$ of a semiconductor laser [25]. The linewidth is calculated as in chapter 6 (6.31) from

$$\Delta\nu = \frac{S_\phi(\omega \to 0)}{2\pi} \tag{7.11}$$

where S_ϕ is the two sided spectral density of the frequency fluctuations. Phase conjugate feedback has also been used for linewidth reduction [7,8]. It is relevant to investigate whether the use of a sluggish phase conjugate mirror affects the linewidth narrowing properties.

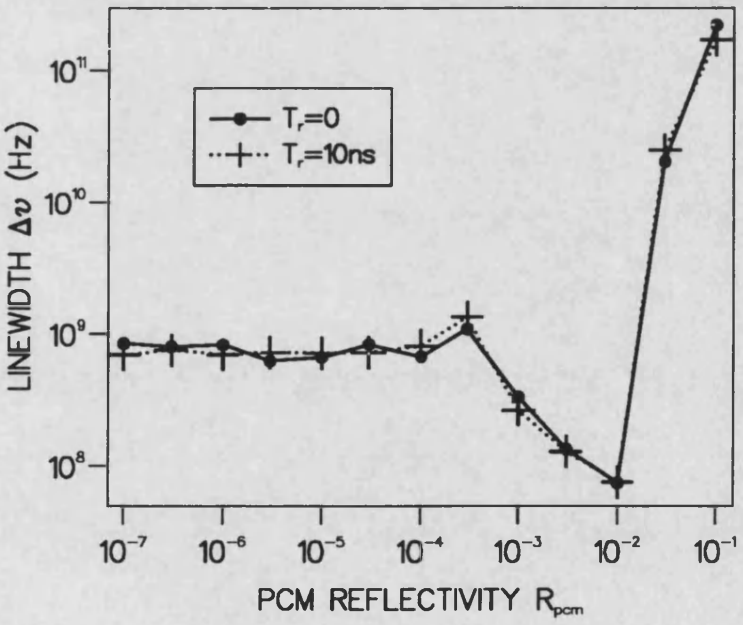

Fig.7.15: Linewidth for Increasing Levels of Sluggish (T_r=10 ns) and Instantaneous (T_r=0 ns) Phase Conjugate Feedback ($I=3.5I_{th}$, τ_{ext}=2 ns).

Fig. 7.15 shows the linewidth as the feedback level is increased for sluggish (T_r=10 ns) and instantaneous phase conjugate mirror (T_r=0 ns). The bias current is fixed at $I=2I_{th}$ and the external cavity round trip delay is taken to be τ_{ext}=2 ns. The linewidth reduction behaviour (in optical feedback regime III) due to sluggish phase conjugate feedback is no different from that of instantaneous phase conjugate feedback. The linewidth increase as the laser enters the noisy coherence collapse regime is also unchanged with sluggish phase conjugate feedback. A description of the linewidth narrowing optical feedback regime III has been given in chapter 1, and in chapter 6 the linewidth narrowing properties of phase conjugate feedback compared to conventional mirror optical feedback have been described.

7.7 Introduction to Targetting in Nonlinear Dynamics.

The following sections of this chapter describe a simple method of targeting periodic and chaotic dynamics appearing in a semiconductor laser subject to optical feedback. Practical applications for chaotic dynamics have been proposed in laser physics and in communications [26-29]. A major advance which has facilitated these efforts is the development of techniques for controlling chaotic dynamics [26] which have led, in particular, to the proposal of secure communication systems which exploit the properties of chaotic dynamical systems [27]. The idea is to control the chaotic dynamics to produce the desired information carrying signal. Any portion of a chaotic signal can be represented in terms of symbolic dynamics as some binary sequence [27]. Hence, the wanted binary sequence can be considered as truly chaotic and can be written with the help of an appropriate control technique. The engineering advantage of such a method of data encryption is that extremely low amplitudes of the controlling signal are required, due to the high sensitivity on the initial conditions. Techniques for the control of chaos permit the selection and stabilisation of one of the almost stable periodic orbits which are available within the dynamics of a chaotic system. Thus to send information, a targetting signal is used to direct trajectories within a chaotic attractor in a prescribed sequence. The transmitted information is then recovered from the transmitted "perturbed" chaos. Chaotic communications may also be produced by mixing the message signal with the output from a chaotic transmitter and then recovering the message from the received transmitted chaos using a rather different concept of chaos synchronisation [28]. An efficient algorithm for improving the locking rate between receiver and transmitter has been reported recently [29].

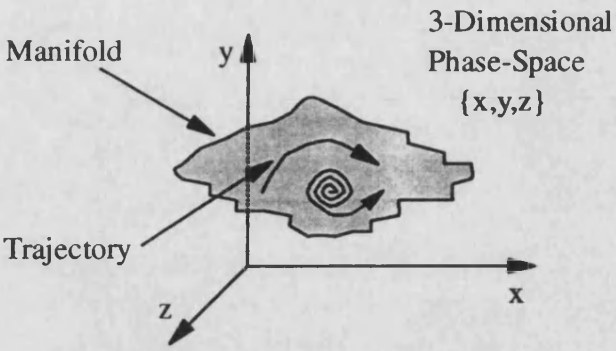

Fig. 7.16: A Trajectory on a Manifold in Phase-Space can be Used to Describe the Dynamics of a System.

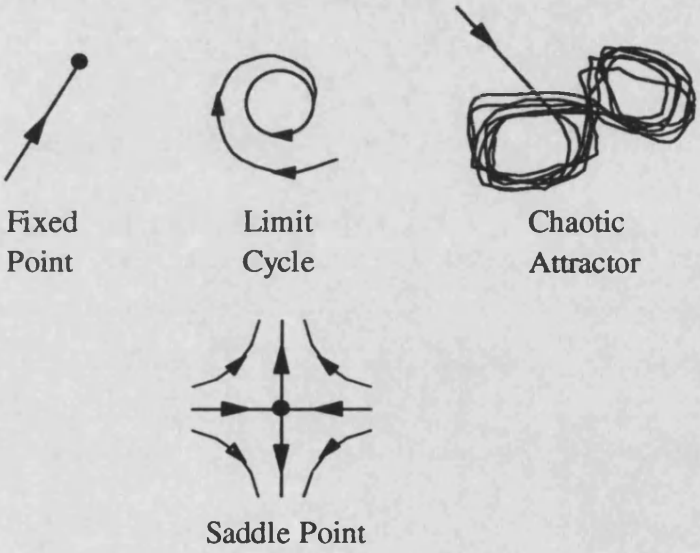

Fig. 7.17: Different Types of Attractors in Phase-Space.

To explain the results in the following sections a few concepts about nonlinear dynamics must be introduced. The dynamics of a system can be represented by a trajectory (as time varies) in phase-space. The trajectory shows how the output parameters of the system change with time. The phase-space is n-dimensional, where n is the number of system parameters being investigated. The trajectories may be restricted to regions of phase-space called manifolds. For example, a manifold for a 3-dimensional phase-space {x,y,z} might be a surface, as shown in fig. 7.16. The trajectories show the dynamics of the system, by moving from unstable areas of phase-space to stable areas. These stable features are called attractors [30,31], as shown in fig. 7.17. An attractor can be a fixed point (steady state output), a limit cycle (periodic solution), or a chaotic attractor (chaotic output). A saddle point is a point in phase-space that behaves as an attractor in one direction but is unstable in another. In a chaotic system two trajectories from initially close points will separate exponentially. The rate of exponential separation is called the Lyapunov exponent λ_L. If the

Lyapunov exponent is large and positive then there is a very sensitive dependence on the initial conditions and the system is described as chaotic.

An essential ingredient in controlling chaotic dynamics is the procedure for targetting [32] to the desired periodic or steady state orbit. Stabilising a system by small correcting signals is usually very effective once the system comes close to the desired state. The latter is guaranteed by the ergodicity of chaotic motion. That is to say a chaotic trajectory inevitably must visit some neighbourhood of any point embedded in a chaotic attractor. But, if the system starts far enough from the desired state unacceptably long transients can result. So, in general, a first stage in chaos control techniques requires a fast identification of the target orbit or trajectory. The usual method for identification of the target [26,32] is relatively complex algorithmically and thus practical applications may take advantage of simpler methods.

7.8 Chaos Control in Laser Diodes.

Based upon the availability of an improved chaos control algorithm, consideration has been given to the development of practical laser diode chaotic transmitters for use in optical fibre communications systems. For that purpose it is required that generation and control of laser diode chaotic dynamics be easily implemented. Laser diodes subject to phase conjugate optical feedback offer one possible method for implementing a controllable chaotic transmitter by varying the level of the feedback. The required controllable phase conjugate feedback would itself be generated via enhanced multiwave mixing in laser diode structures [33]. The response of laser diodes subject to phase conjugate optical feedback has already been demonstrated as giving rise to a transition to chaos [5,6] (see figs. 7.10 and 7.13). Account has also been taken of practical effects arising due to a finite response time of the phase conjugate mirror [18] (see sections 7.2-7.6). The first investigations of controlling chaotic dynamics in models of laser diodes have also been reported recently [34,35], using a technique known as Occasional Proportional Feedback (OPF). In the Occasional Proportional feedback method a control parameter is slightly varied at discrete time intervals to correct the motion to the required trajectory. The OPF method has also been used experimentally for the control of chaos in a laser diode interferometer [36]. The combination of an efficient control algorithm and a practical chaotic optical transmitter offers an opportunity for a novel secure communications system based upon chaotic encryption. In addition, chaos control techniques can be applied to avoid the coherence collapse caused by conventional residual feedback in

the hybrid integration and packaging of commercial laser diodes. The degradation in laser performance due to unwanted optical feedback has been investigated in chapter 2.

In earlier work [37,38] it has been shown, using the example of a CO_2 laser, that periodic orbits as well as a general target in phase-space can be targetted using additional loss modulation applied at an optimal phase [39]. This was one of the first well controlled experimental demonstrations of the observability of unstable states in laser dynamics. Recently an alternative scheme which can be readily realised experimentally has been proposed [40], based on the idea of step-wise Q-switching from a non-lasing regime. It is worth noting that although the changes in parameters are relatively large, they are short-lived, so an initial parameter set is completely re-established (at least after a single targetting correction) in a reversible manner. Both these methods can be used to steer bifurcating semiconductor lasers to unstable states by modulating the injection current. It is noted that loss modulation is also a practical option in some laser diode structures such as Vertical Cavity Surface Emitting Lasers (VCSEL's) [41]. In the following sections an investigation is performed into the possibility of directing trajectories to an unstable steady state in chaotic laser diodes subject to conventional optical feedback by using simple off/on manipulations.

7.9 Targetting Laser Diode Dynamics.

The key idea of targetting to unstable states is similar to that proposed in [40] in the context of models for conventional lasers with periodically modulated parameters or incorporating a saturable absorber. By targetting it is meant that a system parameter (in this case the feedback strength) is varied to achieve a specific output. The following procedure is considered. A single mode rate equation model (see chapter 2) for a diode laser subject to optical feedback is considered. The laser is initially biased below threshold ($I=0.9I_{th}$) for a time period of sufficient duration to ensure that all relaxation processes are over. Thus avoiding any pattern effects (see chapter 2) so that the laser has "forgotten" any previous history. The laser is then switched on abruptly using a step function increment in the injection current ($I=2I_{th}$). The subsequent time evolution of the laser can be described from a dynamical systems viewpoint in the following way. The unstable manifold of the non-lasing steady saddle point is attracting for neighbouring trajectories and is connected with an unstable lasing steady state [40]. In consequence it is possible to observe these unstable states during some time intervals of the transient dynamics. In general the duration of these

intervals strongly depends on the intrinsic noise level, as has been shown for a modulated class B laser [42]. In this present first study of the technique we have, however, restricted interest to noise-free (deterministic) simulations.

7.10 Targetting Periodic Motion.

As the level of feedback is increased the laser dynamics undergoes a sequence of period-doubling bifurcations culminating in chaotic behaviour, as has been seen in fig. 7.11. For the lowest levels of feedback shown the laser has entered a regime of periodic motion. At a reflectivity of about $R_{ext}=1.3x10^{-3}$ the period of the oscillations is doubled. This value of the reflectivity may be termed the first period doubling bifurcation point. A second period doubling bifurcation point is also visible before the dynamics becomes very complex. Such a bifurcation diagram is typical for laser diodes in a short external cavity as well as in other nonlinear dynamical systems. The targetting procedure exploits the availability of the various periodic and chaotic motions whose existence are revealed via the bifurcation diagram (fig. 7.11).

The results of targeting the system to the vicinity of the unstable steady state when the laser is operated just below the first period doubling bifurcation point ($R_{ext}=10^{-3}$) are shown in figs. 7.18-7.21. The laser injection current is increased from $I=0.9I_{th}$ in a step to $I=2I_{th}$. It is seen from the time dependence of the optical output power in fig. 7.18 that the targeting indeed takes place. After the turn-on delay a first large optical pulse is emitted, then the system relaxes (as for the case of a solitary laser) to the steady state and stays there for about 2 ns before the laser settles into a periodic output. In fig. 7.19 a photon-carrier density {s(t),n(t)} phase-plane representation of the dynamics is shown. The initial turn-on transient is seen as the phase portrait spirals towards the supposed steady state and then the dynamics evolves along a trajectory leading to the stable limit cycle which represents the final periodic motion [43-45]. In order to explain this effect account must be taken of the high dimension of phase space of the system under consideration. In a two-dimensional phase space such behaviour would not be possible since the uniqueness of the solution means that trajectories are not allowed to intersect themselves in a plane. For instance, the only way to approach the limit cycle in two-dimensional models of lasers with a saturable absorber is to spiral onto it from outside [40]. This type of approach path is not shown in the two-dimensional projection of phase space shown in fig. 7.19. Due to the time delay term there is an infinite number of degrees of freedom in an optical feedback system, and thus the trajectory can avoid self-intersections by moving in

other dimensions. This behaviour is illustrated in fig. 7.20 and in greater detail in fig. 7.21.

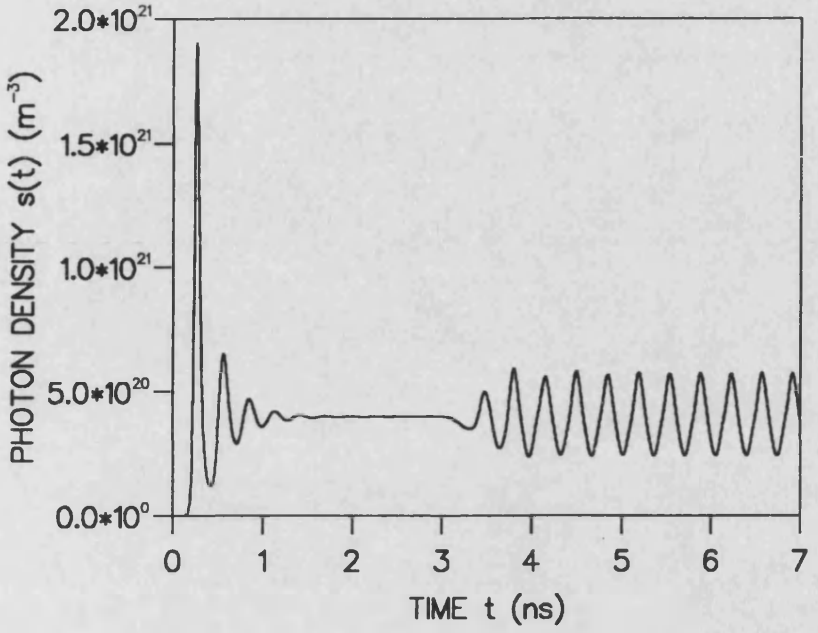

Fig. 7.18: Time Evolution of the Photon Density s(t) of a Laser Operated Below the First Period Doubling Bifurcation ($R_{ext}=10^{-3}$, $\tau_{ext}=2$ ns, $I(t<0)=0.9I_{th}$, $I(t\geq 0)=2I_{th}$).

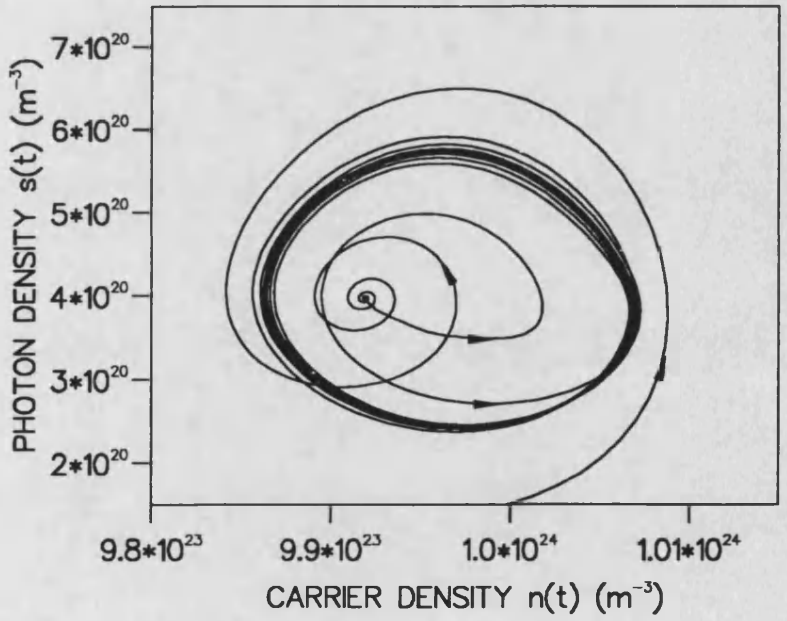

Fig. 7.19: Photon-Carrier Density {s(t), n(t)} Phase-Space Representation of the Dynamics of the Laser Operated Below the First Period Doubling Bifurcation ($R_{ext}=10^{-3}$, $\tau_{ext}=2$ ns, $I(t<0)=0.9I_{th}$, $I(t\geq 0)=2I_{th}$).

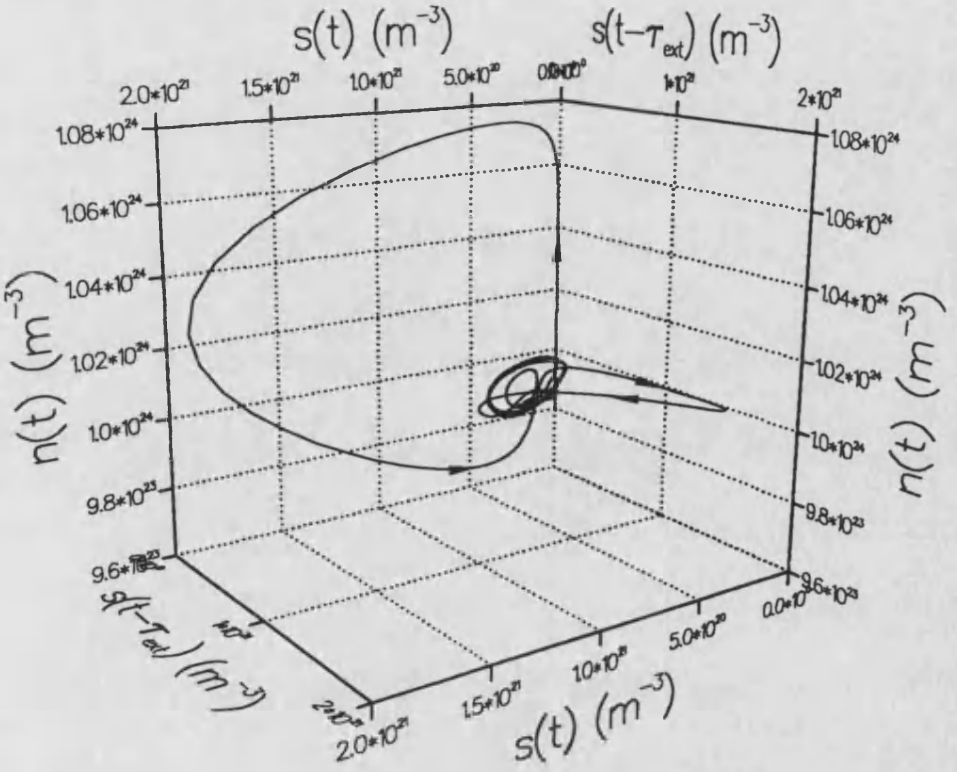

Fig. 7.20: Photon-Feedback-Carrier Density {s(t), s(t-τ_{ext}), n(t)} Phase-Space of the Laser Dynamics Below the First Period Doubling Bifurcation ($R_{ext}=10^{-3}$, $\tau_{ext}=2$ ns, $I(t<0)=0.9I_{th}$, $I(t\geq 0)=2I_{th}$).

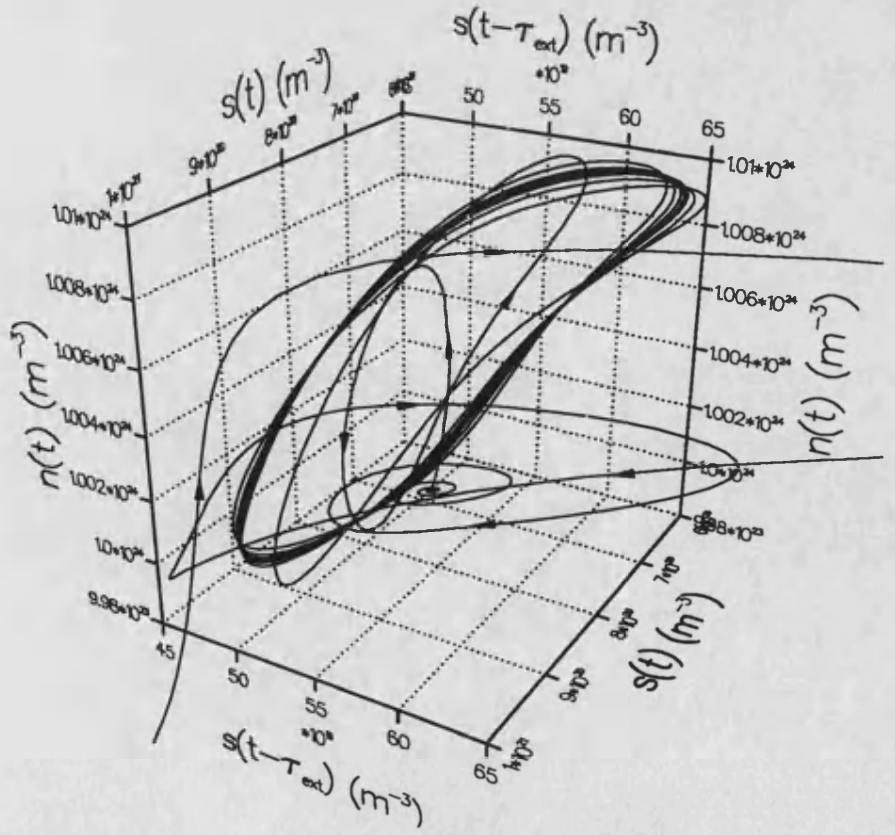

Fig. 7.21: Exploded View of the Laser Approaching the Limit Cycle of Fig. 7.20.

7.11 Dynamical Systems Description.

A more formal explanation of the behaviour is as follows. The saddle steady state lasing point, being embedded in high dimensional space, may have nontrivial combination of stable and unstable manifolds. For example, among the three-dimensional saddle points there is a so called node-unstable focus (e.g. the inverse Shilnikov geometry [46]). In this case we have a saddle point which can be properly represented only in at least four-dimensional phase space: the two-dimensional stable manifold (relaxation oscillations) and the two-dimensional unstable one (the dimension of a Hopf bifurcation normal form). So the present case is a complex saddle of kind of a double stable-unstable focus. Indeed, the three-dimensional phase portraits in figs. 7.20 and 7.21 resemble those of the Shilnikov homoclinic bifurcation [46]. It should be added that a similar Shilnikov orbit structure has been observed earlier in the CO_2 laser with a saturable absorber. The presence of the sharply pronounced undulations at both sides of pulses has been reproduced only in the framework of the four-dimensional theoretical model incorporating the finite relaxation rate of the lower laser level [44]. The tracing of this special kind of trajectory is only possible due to the specifically set initial conditions which belong to the stable manifold of the desired stationary point.

7.12 Feedback Effects and Chaotic Dynamics.

As the optical feedback is increased the period-one motion becomes unstable and a bifurcation to period-two dynamics occurs followed eventually by chaotic motion. The laser dynamics in the cases of a laser operated above the first period doubling bifurcation point (R_{ext}=1.5x10^{-3}) and also in the coherence collapse regime (R_{ext}=2.5x10^{-3}) are illustrated in figs. 7.22-7.24 and 7.25-7.27 respectively. The period-two periodic motion is clearly visible in the time series of fig. 7.22 as well as in the limit cycle of figs. 7.23-7.24. The complexity of the dynamics for higher feedback levels is apparent in figs. 7.25-7.27 but again, the required dynamical state has been correctly targeted [43-45]. From these results it is seen that the technique advocated here is robust to the strength of the optical feedback.

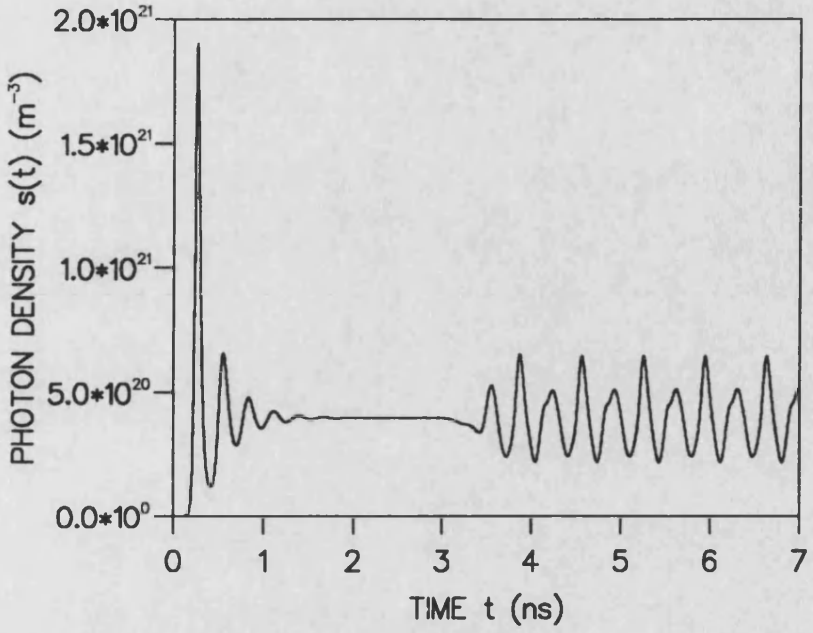

Fig. 7.22: Time Evolution of the Photon Density s(t) of a Laser Operated Above the First Period Doubling Bifurcation (R_{ext}=1.5x10^{-3}, τ_{ext}=2 ns, I(t<0)=0.9I_{th}, I(t≥0)=2I_{th}).

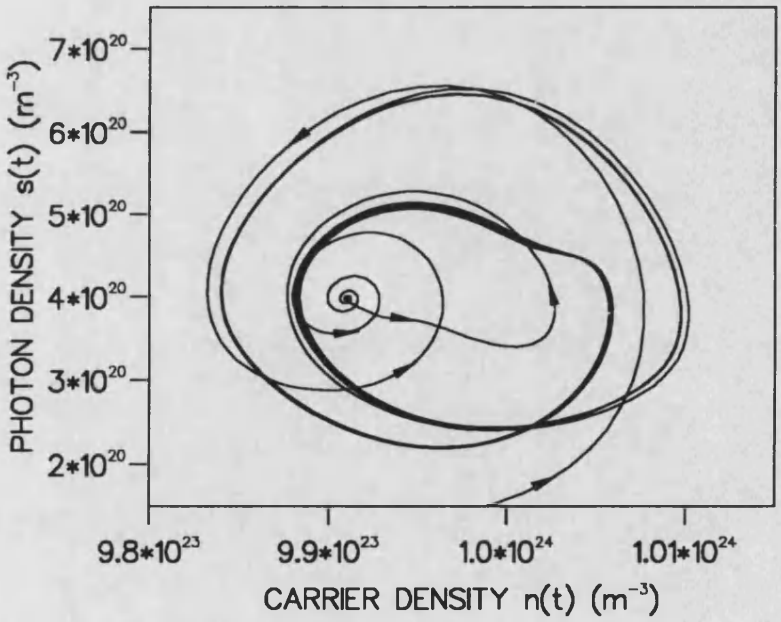

Fig. 7.23: Photon-Carrier Density {s(t), n(t)} Phase-Space Representation of the Laser Dynamics of the Laser Operated Above the First Period Doubling Bifurcation (R_{ext}=1.5x10^{-3}, τ_{ext}=2 ns, I(t<0)=0.9I_{th}, I(t≥0)=2I_{th}).

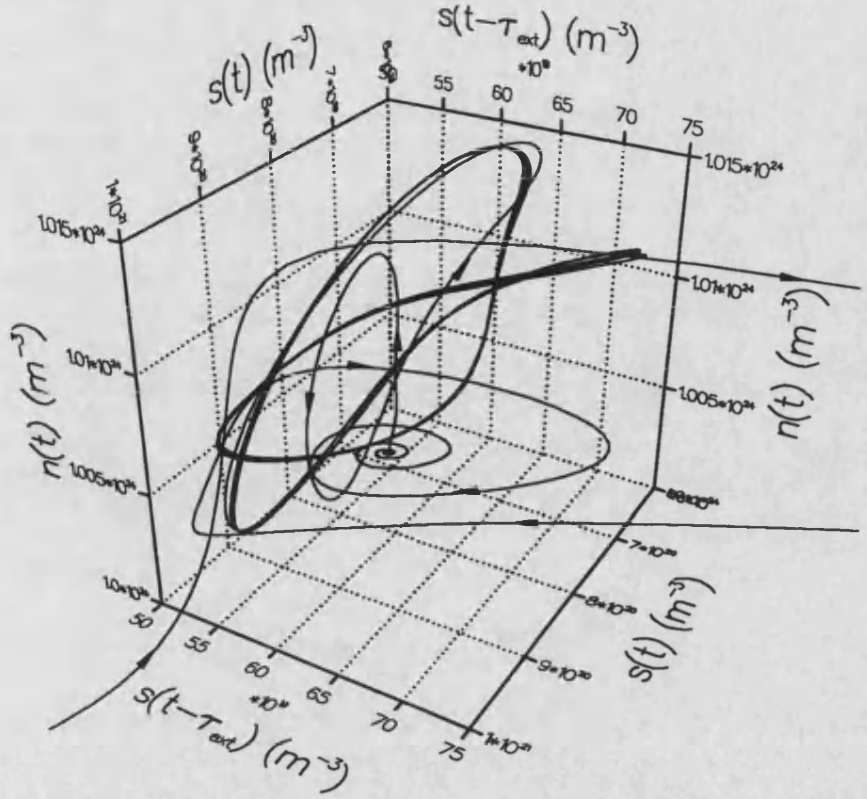

Fig. 7.24: Photon-Feedback-Carrier Density {s(t), s(t-τ_{ext}), n(t)} Phase-Space Representation of the Dynamics of the Laser Operated Above the First Period Doubling Bifurcation (R_{ext}=1.5x10^{-3}, τ_{ext}=2 ns, I(t<0)=0.9I_{th}, I(t≥0)=2I_{th}).

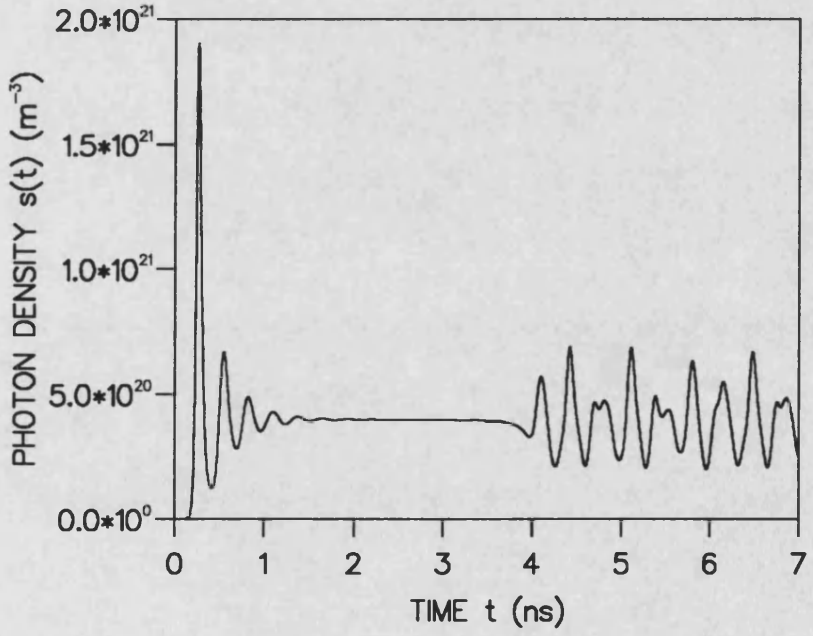

Fig. 7.25: Time Evolution of the Photon Density s(t) of a Laser Operated in the Coherence Collapse Regime (R_{ext}=2.5x10^{-3}, τ_{ext}=2 ns, I(t<0)=0.9I_{th}, I(t≥0)=2I_{th}).

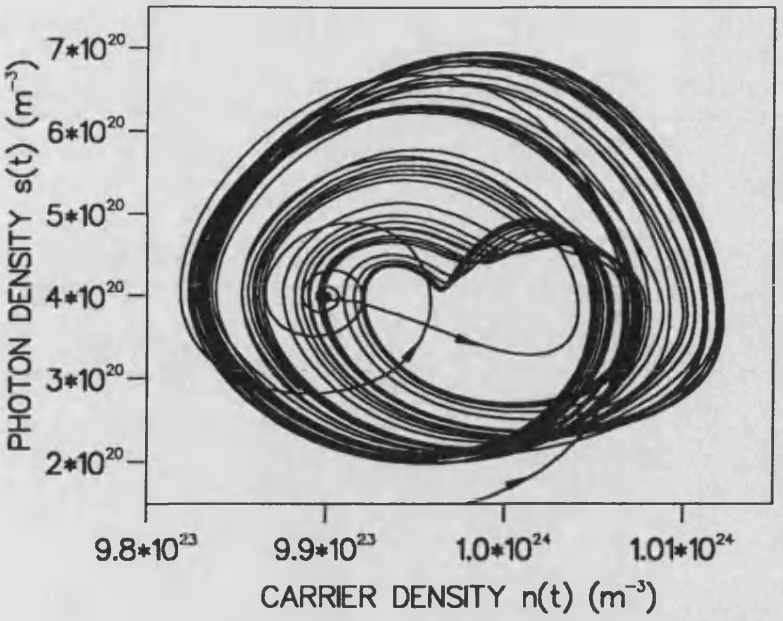

Fig. 7.26: Photon-Carrier Density {s(t), n(t)} Phase-Space Representation of the Laser Dynamics Operated in the Coherence Collapse Regime (R_{ext}=2.5x10^{-3}, τ_{ext}=2 ns, I(t<0)=0.9I_{th}, I(t≥0)=2I_{th}).

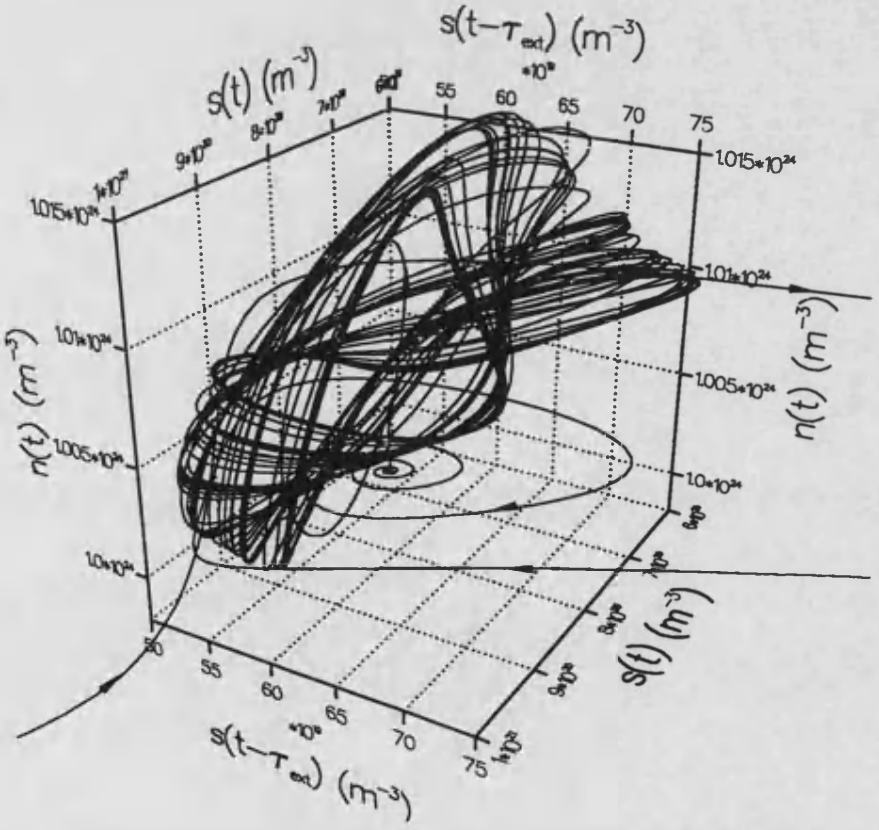

Fig. 7.27: Photon-Feedback-Carrier Density {s(t), s(t-τ_{ext}), n(t)} Phase-Space Representation of the Dynamics of the Laser Operated in the Coherence Collapse Regime (R_{ext}=1.5x10^{-3}, τ_{ext}=2 ns, I(t<0)=0.9I_{th}, I(t≥0)=2I_{th}).

Evidence of an intermediate portion of the trajectory visiting the unstable period-one cycle during the transients of the period-two dynamics (figs. 7.22-7.24) has not been observed. This is explained by the fact that due to the high positive values of the Lyapunov exponent λ_L in the unstable states, the system stays there only for a short period of time (~ $1/\lambda_L$) which is of order the oscillation period. It is expected that this unstable one-periodic orbit may become apparent when the laser is just above the bifurcation point where the positive exponent is small. Finally, it is interesting to point out (see fig. 7.27) that in spite of its chaotic nature the structure of the strange attractor in the coherence collapse regime may be readily characterised. A chaotic generator of such a sort will produce a seemingly random sequence of single and double-peaked pulses with different heights which can be associated with a binary sequence. In this way the present configuration is similar to the case of a double scroll oscillator [27] and thus can be considered for use in chaotic communications.

7.13 Conclusion.

In early sections of this chapter, the intensity noise behaviour and dynamics of laser diodes subject to sluggish phase conjugate feedback have been investigated and compared to those of instantaneous phase conjugate feedback. During the chaotic coherence collapse regime the intensity noise is slightly reduced by the sluggish phase conjugate feedback compared to instantaneous phase conjugate feedback. The reduction is dependent on the bias current due to the relationship between the relaxation oscillation frequency and the rise time of the sluggish phase conjugate mirror. Most intensity noise is centred around the relaxation oscillation frequency of the laser. Hence if the response time of the sluggish phase conjugate mirror is slower than the inverse of the relaxation oscillation frequency some of the intensity noise is removed from the feedback signal. Bifurcation diagrams of the normalised carrier density have shown that the complexity of the dynamics of the diode laser with sluggish phase conjugate feedback is greater for sluggish phase conjugate feedback than for instantaneous phase conjugate feedback and conventional optical feedback. This complexity with sluggish phase conjugate feedback is greater for shorter external cavities. The linewidth properties of phase conjugate feedback are not altered by the use of a sluggish phase conjugate mirror.

In the latter sections of this chapter targetting to the steady state of periodic and chaotic outputs of semiconductor lasers subject to weak optical feedback has been demonstrated. Control of chaos techniques may offer an opportunity for ensuring that

laser diodes are immune from coherence collapse. Such a technique would appear to be of some practical interest in respect to the hybrid optical integration and packaging of commercial semiconductor lasers.

Chapter 7 References.

[1] G R Gray, D Huang, and G P Agrawal, "Chaotic Dynamics of Semiconductor Lasers with Phase Conjugate Feedback", Phys. Rev. A, Vol. 49, No. 3, pp. 2096-2105, 1994.

[2] G P Agrawal and J T Klaus, "Effect of Phase-Conjugate Feedback on Semiconductor Laser Dynamics", Optics Lett., Vol. 16, No. 17, 19, pp. 1325-1327, 1991.

[3] G H M Tartwijk, H J C Van der Linden, and D Lenstra, "Theory of a Diode Laser with Phase Conjugate Feedback", Optics Lett., Vol. 17, No. 22, pp. 1590-1592, 1992.

[4] G P Agrawal and G R Gray, "Effect of Phase-Conjugate Feedback on the Noise Characteristics of Semiconductor Lasers", Phys. Rev. A., Vol. 46, No. 9, pp. 5890-5898, 1992.

[5] L N Langley and K A Shore, "The Effect of Phase Conjugate Optical Feedback on the Intensity Noise in Laser Diodes", Optics Lett., Vol. 18, No. 17, pp. 1432-1434, 1993.

[6] L N Langley and K A Shore, "Intensity Noise and Linewidth Characteristics of Laser Diodes with Phase Conjugate Optical Feedback", IEE Proc.-Optoelectron., Vol. 141, No. 2, pp. 103-108, 1994.

[7] L Petersen, U Gliese, and T N Nielsen, "Phase Noise Reduction by Self Phase Locking in Semiconductor Lasers Using Phase Conjugate Feedback", to be published in IEEE J. Quantum Electron., 1994.

[8] K Vahala, K Kyuma, A Yariv, S K Kwong, M Cronin-Golomb, and K Y Lau, "Narrow Linewidth Single Frequency Semiconductor Laser with a Phase Conjugate External Cavity Mirror", Appl. Phys. Lett., Vol. 49, No. 23, pp. 1563-1565, 1986.

[9] M Ohtsu, I Koshishi, and Y Teramachi, "A Semiconductor Laser as a Stable Phase Conjugate Mirror for Linewidth Reduction of Another Semiconductor Laser", Jap. J. Appl. Phys., Vol. 29, No. 11, pp. L2060-L2062, 1990.

[10] R Tkach and A Chraplyvy, "Regimes of Feedback Effects in 1.5-μm Distributed Feedback Lasers", IEEE J. Lightwave Tech., Vol. 4, No. 11, pp. 1655-1661, 1986.

[11] N Schunk and K Petermann, "Numerical Analysis of the Feedback Regimes for a Single-Mode Semiconductor Laser with External Feedback", IEEE J. Quantum Electron., Vol. 24, No. 7, pp. 1242-1247, 1988.

[12] R A Fisher, "Optical Phase Conjugation", Academic Press, 1983.

[13] G Reiner, P Meystre, and E M Wright, "Transverse Dynamics of a Phase-Conjugate Resonator. I: Sluggish Nonlinear Medium", J. Opt. Soc. Am. B, Vol. 4, No. 5, pp. 675-686, 1987.

[14] M Segev, D Engin, A Yariv, and G C Valley, "Temporal Evolution of Photorefractive Double Phase-Conjugate Mirrors", Optics Lett., Vol. 18, No. 21, pp. 1828-1830, 1993.

[15] X Gao, A Sasaki, and Y Zheng, "Enhancement of Time Response of Self-Pumped Phase-Conjugate Mirror in KNSBN:Cu Crystal Using Cylindrical Lenses", Jap. J. Appl. Phys., Vol. 32, pt. 1, No. 9B, pp. 4303-4306, 1993.

[16] T Suzuki and T Sato, "Improvement of Response Time with an Additional Bias Beam in a $BaTiO_3$ Self-Pumped Phase-Conjugate Mirror", Appl. Optics. Vol. 32, No. 21, pp. 3959-3961, 1993.

[17] N I Bel'dyugina, A V Mamaev, and V V Shkunov, "Dynamics of the Self-Starting Generation of a Phase-Conjugate Semilinear Mirror", Appl. Optics, Vol. 32, No. 21, pp. 3962-3965, 1993.

[18] L N Langley, K A Shore, and G P Agrawal, "Effect of Sluggish Phase Conjugate Feedback on Laser Diode Dynamics, CLEO Europe '94, paper CMH4, 1994.

[19] K Petermann, "Laser Diode Modulation and Noise", Kluwer Academic, 1988.

[20] H Li, J Ye, and J G McInerney, "Detailed Analysis of Coherence Collapse in Semiconductor Lasers", IEEE J. Quantum Electron., Vol. 29, No. 9, pp. 2421-2432, 1993.

[21] J Mørk, B Tromborg, and J Mark, "Chaos in Semiconductor Lasers with Optical Feedback", IEEE J. Quantum Electron., Vol. 28, No. 1, pp. 93-108, 1992.

[22] J Mørk, J Mark, and B Tromborg, "Route to Chaos and Competition between Relaxation Oscillations for a Semiconductor Laser with Optical Feedback", Phys. Rev. Lett., Vol. 65, No. 16, pp. 1999-2002, 1990.

[23] B Tromborg and J Mørk, "Stability Analysis and Route to Chaos for Laser Diodes with Optical Feedback", IEEE Phot. Technol. Lett., Vol. 2, No. 8, pp. 549-552, 1990.

[24] T B Simpson, J M Liu, A Gavrielides, V Kovanis, and P M Alsing, "Period-Doubling Route to Chaos in a Semiconductor Laser Subject to Optical Injection", Appl. Phys. Lett., Vol. 64, No. 26, pp. 3539-3541, 1994.

[25] N Schunk and K Petermann, "Minimum Bit Rate of DPSK Transmission for Semiconductor Laser with a Long External Cavity and Strong Linewidth Reduction", IEEE J. Lightwave Tech., Vol. 5, No. 9, pp. 1309-1314, 1987.

[26] E Ott, C Grebogi, and J A Yorke, "Controlling chaos", Phys. Rev. Lett., Vol. 64, No. 11, pp. 1196-1199, 1990.

[27] S Hayes, C Grebogi, and E Ott, "Communicating with Chaos", Phys. Rev. Lett., Vol. 70, No. 20, pp. 3031-3034, 1993.

[28] K M Cuomo and A V Oppenheim, "Circuit Implementation of Synchronised Chaos with Applications in Communications", Phys. Rev. Lett., Vol. 71, No. 1, pp. 65-68, 1993.

[29] K A Shore and D T Wright, "Improved Synchronisation Algorithm for Chaotic Communications Systems", Electron. Lett., Vol. 30, No. 15, pp. 1203-1204, 1994.

[30] A E Jackson, "Perspectives of Non-Linear Dynamics", Cambridge University Press, 1991

[31] P W Milloni, M L Shih, and J R Ackerhalt, "Chaos in Laser-Matter Interactions", World Scientific, 1987.

[32] T Shinbrot, E Ott, C Grebogi, and J A Yorke, "Using Chaos to Direct Trajectories to Targets", Phys. Rev. Lett., Vol. 65, No. 26, pp. 3215-3218, 1990.

[33] W M Yee and K A Shore, "Nearly Degenerate Four-Wave Mixing in Laser Diodes with Non-Uniform Longitudinal Gain Distribution", J. Opt. Soc. Am. B, Vol. 11, No. 7, pp. 1221-1228, 1994.

[34] G R Gray, A T Ryan, G P Agrawal, and E C Gage, "Optical-Feedback-Induced Chaos and its Control in Semiconductor Lasers", SPIE Vol. 2039: "Chaos in Optics", pp. 45-57, 1993.

[35] A T Ryan, G P Agrawal, G R Gray, and E C Gage, "Optical-Feedback-Induced Chaos and its Control in Multimode Semiconductor Lasers", IEEE J. Quantum Electron., Vol. 30, No. 3, pp. 668-679. 1994.

[36] Y Liu and J Ohtsubo, "Experimental Control of Chaos in a Laser-Diode Interferometer with Delayed Feedback", Optics Lett., Vol. 19, No. 7, pp. 448-450, 1994.

[37] A M Samson, S I Turovets, V N Chizhevsky, and V V Churakov, "Nonlinear Dynamics of a Loss-Switched CO_2 Laser", Sov. Phys. JETP, Vol. 74, No. 4, pp. 628-639, 1992.

[38] V N Chizhevsky and S I Turovets, "Modulated CO_2 Laser as an Optical Phase and Amplitude Multitrigger", Phys. Rev. A, Vol. 50, No. 2, pt. B, pp. 1840-1843, 1994.

[39] V N Chizhevsky and S I Turovets, "Small Pulsed Signal Amplification and Classical Squeezing in a Modulated CO_2 Laser", Opt. Comm., Vol. 102, No. 1-2, pp. 175-182, 1993.

[40] L A Kotomtseva, A V Naumenko, A M Samson, and S I Turovets, "On Observability of Unstable Orbits in Lasers with a Step-Wise Q-Switching", EQEC'94, paper QThG41, 1994.

[41] E A Avrutin, V B Gorfinkel, S Luryi, and K A Shore, "Control of Surface Emitting Laser Diodes by Modulating the Distributed Bragg Mirror Reflectivity: Small Signal Analysis", Appl. Phys. Lett., Vol. 63, No. 18, pp. 2460-2462, 1993.

[42] A Valle and S I Turovets, "Effects of Noise on the Turn-on Delay Jitter of a Modulated Class B Laser in the Generalized Multistability Domain", in preparation.

[43] L N Langley, S Turovets, and K A Shore, "Targetting in Nonlinear Dynamics of Laser Diodes", Optik '94, Berlin, 1994.

[44] L N Langley, S Turovets, and K A Shore, "Targetting in Nonlinear Dynamics of Laser Diodes", Accepted by IEE Proc.-Optoelectron., 1994.

[45] L N Langley, S Turovets, and K A Shore, "Targetting Periodic Oscillations of External Cavity Laser Diodes", Accepted by Optics Lett., 1994.

[46] C O Weiss and R Vilaseca, "Dynamics of Lasers", VCH, 1991.

Chapter 8:

Conclusions and Further Work.

8.1 Conclusions.

This thesis has investigated the effect of optical feedback on semiconductor lasers. Weak optical feedback from within a communication system has been investigated. Strong optical feedback occurring in external cavity laser diodes has also been characterised. Both conventional and phase conjugate optical feedback has been considered.

The effect of external optical feedback on the turn-on delay characteristics of typical semiconductor lasers used in digital optical communications systems has been investigated. The investigation was performed using a single mode rate equation model for a semiconductor laser with optical feedback. The external optical feedback introduces additional intensity noise to that caused by spontaneous emission. The additional intensity noise is due to the chaotic nature of the laser output with moderate optical feedback, resulting in increased turn-on delay jitter in all of the gain-switching, periodic and pseudorandom modulation formats. The jitter is increased dramatically by a moderate external reflectivity. The increase in jitter is greatest at higher bias currents. The average turn-on delay is increased by optical feedback during the gain-switching modulation format. During periodic modulation and the more practical pseudorandom modulation regime the effect on the average turn-on delay is dependant on the modulation conditions, with the average turn-on delay either increasing or decreasing as the optical feedback increases. If, under pseudorandom modulation the modulation conditions result in the turn-on delay distribution being twin peaked without feedback due to pattern effects, then large amounts of external optical feedback can change the turn-on delay distribution into a single peaked one. Thus optical feedback can prevent the pattern effects from occurring, but at the expense of a very large jitter. The increase in turn-on delay jitter caused by external optical feedback is less when the turn-on delay distribution is initially double peaked since in this case a large jitter is already exhibited.

An iterative travelling wave model for a laser diode subject to strong optical feedback has been developed and used to investigate strong optical feedback into laser diodes. The dynamics and intensity noise characteristics of the transition from stable external cavity operation to the coherence collapse regime have been investigated. It has been found that the model is suitable for all five of the regimes used to describe the behaviour of laser diodes with optical feedback. Large amounts of intensity noise is correctly predicted in the coherence collapse regime under moderate optical feedback. The model also predicts the low levels of intensity noise in the stable external cavity operation for strong optical feedback conditions. Bifurcation diagrams indicate the laser facet reflectivity required to prevent coherence collapse for a fixed level of strong feedback. Thus, a critical level of an anti-reflection coating (if applied) can be identified. Resonant modulation at microwave frequencies has also been demonstrated. Low Frequency Fluctuations (LFF) are exhibited by the model. The results have identified that the LFF is an intermittency phenomenon and that it is of type II or type III. Experimental work confirms this deduction. The laminar length of the LFF's increases with external reflectivity, and decreases with increasing current.

An adaptation of the iterative travelling wave model has been applied to the case of an external cavity frequency modulated (FM) laser diode. The adaptations involve the addition of a time dependent external cavity phase change. Experiments indicate that at a critical level of single pass phase modulation the FM laser moves into the coherence collapse regime. It has not been possible to investigate this modulation induced coherence collapse with the model because the instantaneous emission frequency is modulated by the detuning frequency, something which does not occur in the experiments.

The feedback sensitivity of VCSEL's has been compared to that of edge emitting lasers using the single mode rate equations for a diode laser with optical feedback. This has been achieved by investigating the Relative Intensity Noise as the feedback level is increased, and also by calculating bifurcation diagrams showing the route to chaos. Therefore the transition to coherence collapse can be identified and compared for the two types of laser diode. The feedback sensitivity of VCSEL's is comparable to edge emitting lasers for typical values of the VCSEL facet reflectivity. Only for very high facet reflectivity are VCSEL's less sensitive to feedback than edge emitting lasers. The similarity in the feedback sensitivity of the two types of lasers can be attributed to their similar photon lifetimes despite their very different structures. The comparable photon lifetimes and feedback sensitivity results from the high facet reflectivity being cancelled out by the short cavity length.

The single mode rate equation model for a laser diode with optical feedback has been adapted to include phase conjugate feedback. With the phase conjugate feedback model the intensity noise and linewidth characteristics of a semiconductor laser due phase conjugate feedback have been investigated, and compared to that due to conventional optical feedback. The results show that different intensity noise behaviour occurs with the two types of optical feedback. At very low levels of phase conjugate feedback the intensity noise can be lowered slightly. Output power fluctuations occur at lower levels of phase conjugate external reflectivity than for conventional mirror feedback. However, the transition to the chaotic coherence collapse laser output state occurs at a higher level of external reflectivity for phase conjugate than for conventional mirror feedback. Low levels of phase conjugate feedback have the effect of reducing low frequency intensity noise, up to a few hundred MHz. The behaviour of the laser linewidth with increasing external reflectivity is also qualitatively different for the two types of optical feedback. Higher levels of external reflectivity are required to decrease the linewidth with phase conjugate feedback than for conventional mirror feedback. The linewidth reduction feedback regime III and coherence collapse regime IV are applicable to describe phase conjugate feedback effects in semiconductor lasers but regimes I and II cannot be used as they have a dependence on an external cavity phase change, which is eliminated by phase conjugate feedback.

The single mode rate equation for laser diodes with phase conjugate reflectivity has also been extended to include the effects of sluggish phase conjugate feedback. This involves the addition of an extra rate equation governing the time dependent reflectivity of the phase conjugate mirror. The intensity noise behaviour and dynamics of laser diodes subject to sluggish phase conjugate feedback have been investigated and compared to those of instantaneous phase conjugate feedback. During the chaotic coherence collapse regime the intensity noise is slightly reduced by the sluggish phase conjugate feedback compared to instantaneous phase conjugate feedback. The reduction is dependent on the bias current due to the relationship between the relaxation oscillation frequency and the rise time of the sluggish phase conjugate mirror. Most intensity noise is centred around the relaxation oscillation frequency of the laser. Hence if the response time of the sluggish phase conjugate mirror is slower than the inverse of the relaxation oscillation frequency some of the intensity noise is removed from the feedback signal. Bifurcation diagrams of the normalised carrier density have shown that the complexity of the dynamics of the diode laser with sluggish phase conjugate feedback is greater for sluggish phase conjugate feedback than for instantaneous phase conjugate feedback and conventional optical feedback.

This complexity with sluggish phase conjugate feedback is greater for shorter external cavities. The linewidth properties of phase conjugate feedback are not altered by the use of a sluggish phase conjugate mirror.

Targetting to the steady state of periodic and chaotic outputs of semiconductor lasers subject to weak optical feedback has been demonstrated using the single mode rate equation model. Control of chaos techniques may offer an opportunity for ensuring that laser diodes are immune from coherence collapse. Such a technique would appear to be of some practical interest in respect to the hybrid optical integration and packaging of commercial semiconductor lasers.

8.2 Further Work.

The investigations into the turn-on delay statistics of a laser diode subject to optical feedback can be advanced by considering the effect of the feedback on the system performance. To estimate the system performance degradation due to jitter the bit-error-rate (BER) or the system power penalty needs to be calculated. The bit-error-rate cannot be directly calculated from the bits which are in error during a numerical simulation of the rate equations, due to the vast number of bits required. Instead, the turn-on delay distributions gained from the rate equation model are used directly to find the proportion of pulses which have a turn-on delay which is too slow. An error in a modulation bit occurs if the turn-on delay is of a similar value to the modulation period, resulting in the laser turning off before a light pulse is emitted. A simpler method is to fit a known mathematical distribution to the turn-on delay distribution, and use an analytical method for estimating the bit-error-rate. A discussion of the system performance degradation that can be calculated from the jitter is given in section 2.9.

The optical feedback phenomena known as Low Frequency Fluctuations (LFF) occurring close to threshold have been identified experimentally and numerically as consisting of type II or type III intermittency. This has been discovered by considering the scaling of the average laminar length of the LFF's as the diode laser injection current is increased. To discover whether the LFF's are type II or type III the distribution of the LFF periods must be calculated with sufficient number of periods such that the distribution is very smooth. The type of intermittency can be deduced from the slope of the tails of the LFF period distribution.

The iterative travelling wave model for strong optical feedback has been adapted with the addition of a time dependent external cavity phase change to investigate external cavity frequency modulated (FM) laser diodes. The laser emission frequency calculated in chapter 4 has an additional modulation of a frequency equal to the detuning between the external cavity longitudinal mode spacing and the external cavity phase modulation frequency. This additional modulation envelope is not seen in the experiments. The model must be investigated further to find the cause of this frequency and to eliminate it. It may be necessary to adapt the model to a multimode one to perform this work.

The sluggish phase conjugate feedback investigated in chapter 7 considered the time dependent reflectivity of the phase conjugate mirror by the use of a rise time, assuming an exponential response of the phase conjugate reflectivity. To accurately model the phase conjugate mirror the multi-wave mixing process forming the conjugate reflection must be considered in detail.

Appendix 1:

Single Mode Rate Equations.

A1.1 Explanation of Single Mode Rate Equations.

The behaviour of laser diodes is described by single mode rate equations [1-4]. The rate equation for the field E(t) within the laser can be found by considering the forward and backward travelling waves together with the optical gain [1], to give

$$\frac{dE(t)}{dt} = \left\{ j(\omega - \omega_{th}) + \frac{1}{2}\left\{ G_n(n(t) - n_o) - \frac{1}{\tau_{ph}} \right\} \right\} E(t), \qquad \text{(A1.1)}$$

where ω is the angular emission frequency, ω_{th} is the angular emission frequency at threshold, G_n is the gain slope, n(t) is the carrier density, and n_o is the transparency carrier density. The photon lifetime τ_{ph} is given by [1,2]

$$\tau_{ph} = \frac{\mu_g}{c\left(\alpha_i - \frac{\ln(R_2)}{\ell}\right)}, \qquad \text{(A1.2)}$$

where μ_g is the group refractive index, c is the speed of light, α_i is the internal losses per unit length, R_2 is the facet reflectivity, and ℓ is the cavity length.

The following method for manipulated (A1.1) into rate equations for photon density s(t) and phase ϕ(t) for ease of numerical solution is described in reference [1]. Two simple relationships between the photon density s(t), the electric field E(t), and the electric field phase ϕ(t) are

$$E(t) = \sqrt{s(t)}e^{j\phi(t)} \qquad \text{(A1.3)}$$

and

$$s(t) = E(t)E^*(t). \tag{A1.4}$$

The photon rate equation is calculated using the relationship

$$\frac{ds(t)}{dt} = \frac{d}{dt}\{E(t)E^*(t)\} = E(t)\frac{dE^*(t)}{dt} + E^*(t)\frac{dE(t)}{dt}. \tag{A1.5}$$

Substituting (A1.1) into (A1.5) gives

$$\frac{ds(t)}{dt} = E(t)E^*(t)\left\{G_n(n(t)-n_o) - \frac{1}{\tau_{ph}}\right\}. \tag{A1.6}$$

Placing (A1.4) into (A1.6) results in the standard rate equation for the photon density s(t)

$$\frac{ds(t)}{dt} = -\frac{s(t)}{\tau_{ph}} + s(t)G_n(n(t)-n_o). \tag{A1.7}$$

The phase rate equation is calculated using the following relationship by differentiation of (A1.3),

$$\frac{d\phi(t)}{dt} = \frac{1}{s(t)}\mathrm{Im}\left(E^*(t)\frac{dE(t)}{dt}\right). \tag{A1.8}$$

Inserting (A1.1) into (A1.8) gives

$$\frac{d\phi(t)}{dt} = \frac{1}{s(t)}\mathrm{Im}\left\{E^*(t)E(t)\left\{j(\omega-\omega_{th}) + \frac{1}{2}\left\{G_n(n(t)-n_o) - \frac{1}{\tau_{ph}}\right\}\right\}\right\}. \tag{A1.9}$$

Using (A1.4) results in

$$\frac{d\phi(t)}{dt} = \mathrm{Im}\left\{j(\omega-\omega_{th}) + \frac{1}{2}\left\{G_n(n(t)-n_o) - \frac{1}{\tau_{ph}}\right\}\right\}. \tag{A1.10}$$

Taking the imaginary part gives

$$\frac{d\phi(t)}{dt} = \omega - \omega_{th}. \tag{A1.11}$$

The emission frequency changes with carrier density because the refractive index is carrier dependent. The relationship between the emission frequency and the carrier density is given in [1] as

$$(\omega - \omega_{th}) = -\frac{\omega_{th}}{\mu_g}\frac{\partial \mu}{\partial n}(n - n_{th}), \tag{A1.12}$$

where ω_{th} is the emission frequency at threshold, μ is the refractive index, μ_g is the group refractive index, and n_{th} is the threshold carrier density. The refractive index can be split into its real and imaginary parts, thus

$$\mu = \mu' + j\mu''. \tag{A1.13}$$

Equation (A1.12) is real, therefore

$$\frac{\partial \mu}{\partial n} = \frac{\partial \mu'}{\partial n}. \tag{A1.14}$$

Substituting (A1.14), (A1.12) into (A1.11) and then splitting the partial derivative gives

$$\frac{d\phi}{dt} = -\frac{\omega_{th}}{\mu_g}\frac{\partial \mu'}{\partial \mu''}\frac{\partial \mu''}{\partial n}(n - n_{th}). \tag{A1.15}$$

Introducing the linewidth enhancement factor α,

$$\alpha = \frac{\partial \mu' / \partial n}{\partial \mu'' / \partial n}, \tag{A1.16}$$

and the group velocity v_g,

$$v_g = \frac{c}{\mu_g}, \tag{A1.17}$$

gives

$$\frac{d\phi(t)}{dt} = -\alpha\frac{\omega_{th} v_g}{c}\frac{\partial \mu''}{\partial n}(n - n_{th}). \tag{A1.18}$$

The imaginary part of the refractive index μ" is given in [1] as

$$\mu'' = \frac{-g\lambda}{4\pi} \tag{A1.19}$$

where g is the modal gain per unit length. Equation (A1.19) is differentiated to give

$$\frac{\partial \mu''}{\partial n} = \frac{-\lambda}{4\pi}\frac{\partial g}{\partial n}. \tag{A1.20}$$

Substituting (A1.20) into (A1.18) gives

$$\frac{d\phi(t)}{dt} = \frac{\alpha}{2} v_g \frac{\partial g}{\partial n}(n - n_{th}). \tag{A1.21}$$

Using the gain per unit time G

$$G = v_g g, \tag{A1.22}$$

gives

$$G_n = \frac{\partial G}{\partial n} = v_g \frac{\partial g}{\partial n}, \tag{A1.23}$$

which when substituted into (A1.21) results in the phase rate equation.

$$\frac{d\phi(t)}{dt} = \frac{\alpha}{2} G_n (n - n_{th}). \tag{A1.24}$$

The rate equation for the carrier density n(t) can be written as

$$\frac{dn(t)}{dt} = \frac{I(t)}{eV} - \frac{n(t)}{\tau_{sp}} - s(t) G_n \{n(t) - n_o\}, \tag{A1.25}$$

where the addition and loss of carriers is considered. The first term in (A1.25) is the injection of carriers by the current into the device. The second term in (A1.25) is the decay of carriers by spontaneous emission, with τ_{sp} is the carrier lifetime. The third term in (A1.25) is the usage of carriers by stimulated emission, and also appears in the photon density rate equation.

In summary the three rate equations describing the diode laser are

$$\frac{dn(t)}{dt} = \frac{I(t)}{eV} - \frac{n(t)}{\tau_{sp}} - s(t)G_n\{n(t)-n_o\}\left\{\frac{1}{1+\varepsilon s(t)}\right\} + F_n(t) \qquad \text{(A1.26)}$$

$$\frac{ds(t)}{dt} = \frac{\gamma n(t)\Gamma}{\tau_{sp}} - \frac{s(t)}{\tau_{ph}} + s(t)G_n\{n(t)-n_o\}\Gamma\left\{\frac{1}{1+\varepsilon s(t)}\right\} + F_s(t) \qquad \text{(A1.27)}$$

$$\frac{d\phi(t)}{dt} = \omega - \omega_{th} = \frac{\alpha}{2}G_n\{n(t)-n_{th}\}\Gamma + F_\phi(t) \qquad \text{(A1.28)}$$

To complete the model a confinement factor Γ, gain saturation ε and spontaneous emission are added. The confinement factor is the proportion of the optical field within the active region. The gain saturation is due to spectral hole burning. The spontaneous emission factor γ is the proportion of spontaneous emission falling into the lasing mode. The terms $F_n(t)$, $F_s(t)$, $F_\phi(t)$ are Langevin noise terms (see appendix 2) which model the random noise events caused by spontaneous emission of photons.

Appendix 1 References.

[1] K Petermann, "Laser Diode Modulation and Noise", Kluwer, 1988.

[2] G P Agrawal, "Long Wavelength Semiconductor Lasers", Van Nostrand Reinhold, 1986.

[3] B Clarke, "The Effect of Reflections on the System Performance of Intensity Modulated Laser Diodes", IEEE J. Lightwave Tech., Vol. 9, No. 6, pp. 741-749, 1991.

[4] D Marcuse, "Computer Simulation of Laser Photon Fluctuations: Theory of Single Cavity Laser", IEEE J. Quantum Electron., Vol. 20, No. 10, pp. 1139-1148, 1984

Appendix 2:

Langevin Noise Terms for Modelling Spontaneous Emission.

A2.1 Implementation of Langevin Noise.

The photon density s(t) can be written in terms of the electric field E(t) and its complex conjugate $E^*(t)$ using the following relation,

$$s(t) = E(t)E^*(t) \tag{A2.1}$$

which when differentiated gives

$$\frac{ds(t)}{dt} = E(t)\frac{dE^*(t)}{dt} + E^*(t)\frac{dE(t)}{dt} = 2\,\mathrm{Re}\left\{E^*(t)\frac{dE(t)}{dt}\right\}. \tag{A2.2}$$

The rate equation for the electric field within the laser is written as before in appendix 1 (A1.1) but with an additional term corresponding to the spontaneous emission noise $E_{sp}(t)$

$$\frac{dE(t)}{dt} = \left\{ j(\omega - \omega_{th}) + \frac{1}{2}\left\{ G_n(n(t) - n_o) - \frac{1}{\tau_{ph}} \right\} \right\} E(t) + E_{sp}(t). \tag{A2.3}$$

If (A2.3) is substituted into (A2.2) then the usual rate equation for photon density (A1.7) is found but with an additional term for the spontaneously emitted photons [1]. The extra term takes the form

$$2\,\mathrm{Re}\left\{E^*(t)E_{sp}(t)\right\}. \tag{A2.4}$$

In (A2.4) Re represents taking the real part of the expression in parenthesis. The spontaneous emission noise will be applied at time intervals of Δt, during which $E_{sp}(t)$

is held constant at a value E_{sp}. Within a time slot t_i to t_{i+1} with $\Delta t=t_{i+1}-t_i$ (A2.4) can be written as

$$2\mathrm{Re}\{E^*(t)E_{sp}(t)\}=2\mathrm{Re}\{E^*(t_i)E_{sp}+\Delta E^*(t)E_{sp}\}, \quad \text{(A2.5)}$$

where

$$\Delta E^*(t)=E^*(t)-E^*(t_i). \quad \text{(A2.6)}$$

The second term in (A2.5) is smaller than the first term and can be approximated by its mean value, giving

$$2\mathrm{Re}\{E^*(t)E_{sp}(t)\}=2\mathrm{Re}\{E^*(t_i)E_{sp}+\langle\Delta E^*(t)E_{sp}\rangle\}. \quad \text{(A2.7)}$$

The first term in (A2.7) has zero mean and will form the Langevin noise force $F_s(t)$ [1-4],

$$F_s(t)=2\mathrm{Re}\{E^*(t_i)E_{sp}\}. \quad \text{(A2.8)}$$

The second term will form the average spontaneous emission rate R_{sp} [1],

$$R_{sp}=2\mathrm{Re}\langle\Delta E^*(t)E_{sp}\rangle. \quad \text{(A2.9)}$$

The average spontaneous emission is also seen from appendix 1 to be

$$R_{sp}=\frac{\gamma n(t)\Gamma}{\tau_{sp}}, \quad \text{(A2.10)}$$

where n is the carrier density, τ_{sp} is the carrier lifetime, γ is the fraction of spontaneous emission into the lasing mode, and Γ is the overlap betwen the carrier distribution and the lasing mode.

The spontaneous emision field E_{sp} is a gaussian random process which can be described by [1]

$$E_{sp}=\sqrt{\frac{A}{\Delta t}}(x_1+jx_2), \quad \text{(A2.11)}$$

where x_1 and x_2 are gaussian random variables with zero mean and unity variance. For sufficiently short Δt, the correlated part of $\Delta E(t)$ is related to E_{sp} by [1]

$$\frac{d}{dt}\{\Delta E(t)\} \approx E_{sp}, \tag{A2.12}$$

which by substituting in (A2.11) and integrating yields

$$\Delta E(t) = t\sqrt{\frac{A}{\Delta t}}(x_1 + jx_2). \tag{A2.13}$$

So

$$\left\langle \Delta E^*(t) E_{sp} \right\rangle = \frac{1}{\Delta t}\int_0^{\Delta t} \Delta E^*(t) E_{sp} dt, \tag{A2.14}$$

which by using (A2.11) and (A2.13) can be evaluated to

$$\left\langle \Delta E^*(t) E_{sp} \right\rangle = A. \tag{A2.15}$$

Substituting (A2.15) into (A2.9) gives

$$A = \frac{R_{sp}}{2}. \tag{A2.16}$$

The Langevin noise source $F_s(t)$ [1-4] is given by placing (A2.16) and (A2.11) into (A2.8),

$$F_s(t) = 2\,\mathrm{Re}\left\{ E^*(t_i)\sqrt{\frac{R_{sp}}{2\Delta t}}(x_1 + jx_2) \right\}. \tag{A2.17}$$

$E(t_i)$ can be split into its amplitude and phase,

$$E(t) = \sqrt{s(t)}e^{j\phi(t)}, \tag{A2.18}$$

which when substituted into (A2.17) gives

$$F_s(t) = \sqrt{\frac{2s(t_i)R_{sp}}{\Delta t}}x_s, \tag{A2.19}$$

where

$$x_s = x_1 \cos\{\phi(t_i)\} + x_2 \sin\{\phi(t_i)\}. \tag{A2.20}$$

The Langevin noise source for the phase $F_\phi(t)$ [1-4] is found by differentiation of (A2.18),

$$F_\phi(t) = \frac{1}{S(t)} \mathrm{Im}\left\{ E^*(t) \frac{dE(t)}{dt} \right\}. \tag{A2.21}$$

By substituting (A2.3) into (A2.21) the usual rate equation for the phase (A1.24) is found but with an additional term for the spontaneous emission [1]. The extra term is the Langevin noise force for the phase $F_\phi(t)$ and takes the form below where Im represents taking the imaginary part of the expresion in parenthesis

$$F_\phi(t) = \frac{1}{s(t)} \mathrm{Im}\{ E^*(t) E_{sp}(t) \}. \tag{A2.22}$$

Equation (A2.22) can be expressed in a similar way to (A2.5) as

$$F_\phi(t) = \frac{1}{s(t)} \mathrm{Im}\{ E^*(t_i) E_{sp} + \langle \Delta E^*(t) E_{sp} \rangle \}, \tag{A2.23}$$

where $\Delta E^*(t)$ is given in (A2.6). Placing (A2.11), (A2.15) and (A2.16) into (A2.23) results in

$$F_\phi(t) = \frac{1}{s(t)} \mathrm{Im}\left\{ E^*(t_i) \sqrt{\frac{R_{sp}}{2\Delta t}} (x_1 + j x_2) + A \right\}. \tag{A2.24}$$

Again splitting the field into photon density and phase results in the Langevin noise force $F_\phi(t)$[1-4] for the phase being given as

$$F_\phi(t) = \frac{1}{s(t)} \sqrt{\frac{s(t_i) R_{sp}}{2\Delta t}} x_\phi, \tag{A2.25}$$

where

$$x_\phi = -x_1 \sin\{\phi(t_i)\} + x_2 \cos\{\phi(t_i)\}. \tag{A2.26}$$

It is noted that x_s and x_ϕ are also gaussian random variables with zero mean and unity variance, $\langle x_s^2 \rangle = \langle x_\phi^2 \rangle = 1$.

Finally the Langevin noise force for the carrier rate equation can be written as

$$F_n(t) = -F_s(t) + F_{shot}(t), \tag{A2.27}$$

where $F_{shot}(t)$ is the carrier shot noise, given by [3]

$$F_{shot}(t) = \sqrt{\frac{2n(t_i)}{\tau_{sp}\Delta t V}} x_n, \tag{A2.28}$$

with V representing the active region volume. Thus the carrier Langevin noise source is given by [2,3]

$$F_n(t) = -\sqrt{\frac{2s(t_i)R}{\Delta t}} x_s + \sqrt{\frac{2n(t_i)}{\tau_{sp}\Delta t V}} x_n. \tag{A2.29}$$

Equations (A2.19), (A2.25) and (A2.29) form the noise forces required in the rate equations of appendix 1 to simulate the noise processes within the laser diode [1-4].

Appendix 2 References.

[1] N Schunk, and K Petermann, "Noise Analysis of Injection-Locked Semiconductor Lasers", IEEE J. Quantum Electron., Vol. 22, No. 5, pp. 642-650, 1986.

[2] K Petermann, "Laser Diode Modulation and Noise", Kluwer, 1988.

[3] B Clarke, "The Effect of Reflections on the System Performance of Intensity Modulated Laser Diodes", IEEE J. Lightwave Tech., Vol. 9, No. 6, pp. 741-749, 1991.

[4] D Marcuse, "Computer Simulation of Laser Photon Fluctuations: Theory of Single Cavity Laser", IEEE J. Quantum Electron., Vol. 20, No. 10, pp. 1139-1148, 1984

Appendix 3:

Computer Simulation of Single Mode Rate Equations.

A3.1 Numerical Solution.

The single mode rate equations for a semiconductor laser with optical feedback are given in chapter 2 (2.19)-(2.22) for conventional mirror optical feedback, and in chapter 6 (6.17)-(6.20) for phase conjugate optical feedback. A flow diagram showing the method for solving the rate equations is shown in fig. A3.1. A routine written by NAG (Numerical Algorithms Group) for solving ordinary differential equations is used [1]. The solution routine uses a Runge-Kutta-Merson solution method [2]. The output time interval and solution accuracy are specified by the user, before calling the NAG routine. Langevin noise sources as in chapter 2 (2.23)-(2.25) are added and are applied at intervals Δt. The Langevin noise application interval Δt need not be the same as the data output interval. The program works by successively calculating the rate equation derivatives (dn/dt, ds/dt and $d\phi/dt$) and using them to calculate the carrier density n(t), photon density s(t), and electric field phase $\phi(t)$ at intervals of the output step. The optical feedback is modelled by storing the time series of the output power $P_o(t)$ in a large single dimension matrix. This matrix serves as a library of past output powers to use as reflection data. When the injection current I(t) rises the simulation time is recorded, and the computer awaits the simulation time at which the output power pulse occurs. The time difference between the two times is used to calculate the turn-on delay T_{on}. The turn-on delays are stored for later use to calculate the turn-on delay jitter, σ_T. The simulation then moves on to the next time output step.

Unfortunately, the single mode rate equations become a very stiff system when the Langevin noise terms for spontaneous emission are used. This can result in long solution times when long time series (more than 100 ns) of output data are required. Numerical integration methods other than the Runge-Kutta-Merson method, may

reduce the calculation time. The numerical solutions are calculated on a Hewlet Packard Series 700 workstation. The programming language used is Fortran 77.

Numerical accuracy of the simulations is checked by repeating the investigations using different iteration steps and various values of the accuracy tolerance parameter used in the Runge-Kutta-Merson ordinary differential equation solving routine.

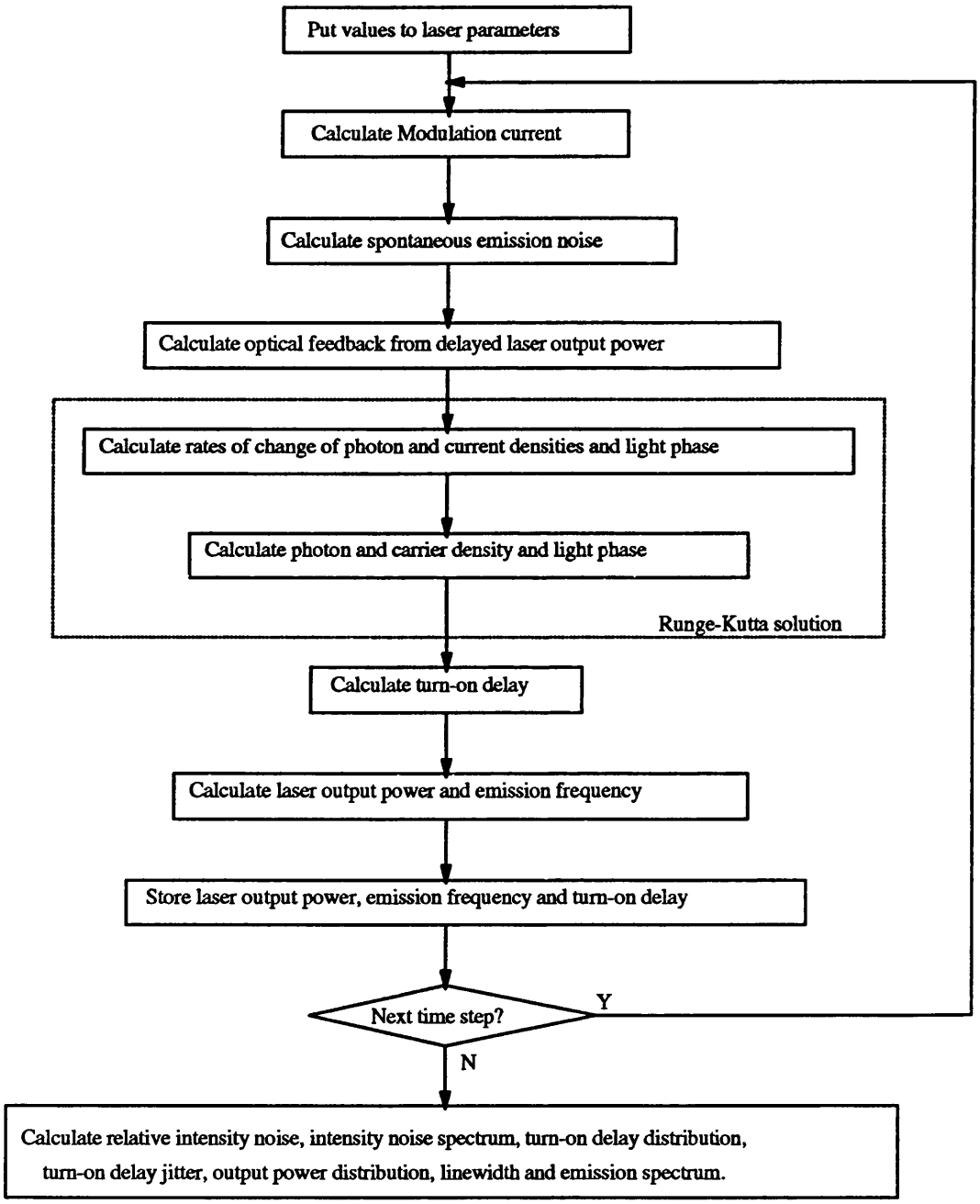

Fig. A3.1: Flow Chart of Numerical Solution of the Single Mode Rate Equations for a Laser Diode with Weak Optical Feedback.

A3.2 Postprocessing.

Once the simulation has been performed the output data consists of only the injection current I(t), carrier density n(t), photon density s(t), electric field phase $\phi(t)$ and output power $P_o(t)$ at fixed time intervals. Further information such as the Relative Intensity Noise (RIN), the output power fluctuations frequency spectrum RIN(f) (the frequency dependence of the RIN), the output power fluctuation probability density function (pdf), the spectral density of the frequency fluctuations $S_\phi(\omega)$, the emission spectrum $S_E(\omega)$, and turn-on delay jitter σ_T must be calculated. All the above information requires long time series of data (greater than 100 ns) so can only be found after the solution of the rate equations has finished.

The Relative Intensity Noise is calculated from a long time series of the output power $P_o(t)$ using (5.10)

$$RIN = \frac{\overline{P_o(t)^2 - \overline{P_o(t)}^2}}{\overline{P_o(t)}^2}. \qquad \text{(A3.1)}$$

The output power fluctuation spectrum (RIN spectrum) defined by

$$RIN(\omega) = \frac{\left\langle |\Delta P_o(\omega)|^2 \right\rangle}{P_o^2}, \qquad \text{(A3.2)}$$

is obtained by Fourier analysis of a long time series of the output power. A Fast Fourier Transform (FFT) is used for this purpose. The output power time series $P_o(t)$ is also used to calculate the output power probability distribution. The spectral density of the frequency fluctuations S_ϕ (6.29) defined by

$$S_\phi(\omega) = \left\langle \left| \frac{d\phi(\omega)}{dt} \right|^2 \right\rangle, \qquad \text{(A3.3)}$$

is calculated using an FFT of a long time series of the emission frequency $\omega(t)$. The laser emission spectrum defined by

$$S_E(\omega) = \left\langle |E(\omega)|^2 \right\rangle, \qquad \text{(A3.4)}$$

is obtained by taking an FFT of the complex electric field E(t). The turn-on delay jitter is calculated from the stored values of turn-on delay using the following from chapter 2 (2.27),

$$\sigma_T = \sqrt{\frac{\sum_{m=1}^{m=n}\left\{T_{on(m)} - \overline{T_{on}}\right\}^2}{n}}. \qquad \text{(A3.5)}$$

Appendix 3 References.

[1] Runge-Kutta-Merson Solution of Ordinary Differential Equations, D02BBF - NAG Fortran Library Document, Numerical Algorithms Group, Mk. 10, 1983.

[2] G Hall, and T M Watt, "Modern Numerical Methods for Ordinary Differential Equations", Clarendon Press, 1976.

Appendix 4:

Computer Simulation of Iterative Travelling Wave Model for Strong Optical Feedback.

A4.1 Numerical Solution.

The iterative travelling wave model for a semiconductor laser with strong optical feedback is given in chapter 3 (3.38)-(3.41). A flow diagram showing the method for solving the iterative equations is shown in fig. A4.1. The iteration time step is the same as the laser internal cavity round trip time τ_L. Langevin noise sources as described in chapter 3 (3.45)-(3.46) are added at each iteration step. At each iteration step the value of the electric field leaving the laser facet $A^+(t)$ is calculated from the multiple reflections from the external cavity. The carrier density n(t) is also modelled using an iterative equation. The photon density s(t) and output power $P_o(t)$ are calculated as in chapter 3 (3.42)-(3.44). The optical feedback is modelled by storing the time series of the electric field $A^+(t)$ in a large single dimension matrix. This matrix serves as a library of the past values of the electric field to use as reflection data.

The iterative equations are much more efficient in terms of computing time than the single mode rate equation calculations described in appendix 3. The enhancement can be up to ten times quicker, allowing the simulation of much longer time series of data (several 100 μs). The numerical solutions are calculated on a Hewlet Packard Series 700 workstation. The programming language used is Fortran 77. The calculation of additional data such as Relative Intensity Noise (RIN), output power fluctuations spectrum (RIN spectrum), spectral density of the frequency fluctuations $S_\phi(\omega)$, and the laser emission spectrum $S_E(\omega)$ are discussed in section A3.2 of appendix 3.

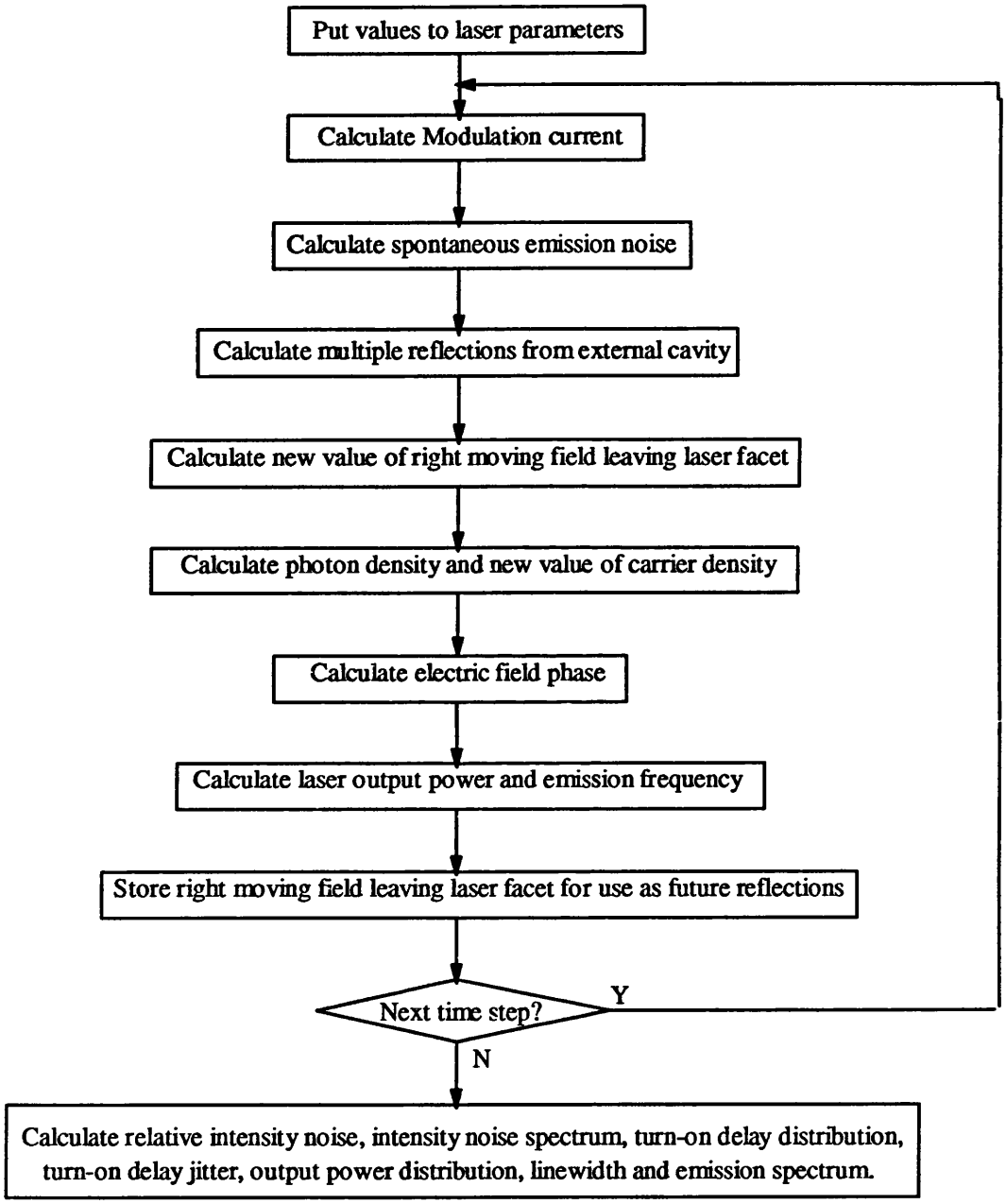

Fig. A4.1: Flow Chart of Numerical Solution of the Iterative Travelling Wave Model for a Laser Diode with Strong Optical Feedback.

Appendix 5:

Publications Arising from the Work in this Thesis

A5.1 Journal Papers.

The following journal papers are included after this thesis :-

L. N. Langley, and K. A. Shore, "The Effect of External Optical Feedback on the Turn-On Delay Statistics of Laser Diodes Under Pseudorandom Modulation", *IEEE Photonics Technology Letters*, Vol. 4, No. 11, pp. 1207-1209, 1992.

L. N. Langley, and K. A. Shore, "The Effect of External Optical Feedback on Timing Jitter in Modulated Laser Diodes", *IEEE Journal of Lightwave Technology*, Vol. 11, No. 3, pp. 434-441, 1993.

L. N. Langley, and K. A. Shore, "The Effect of Phase-Conjugate Optical Feedback on the Intensity Noise in Laser Diodes", *Optics Letters*, Vol. 18, No. 17, pp. 1432-1434, 1993.

L. N. Langley, and K. A. Shore, "Intensity Noise and Linewidth Characteristics of Laser Diodes with Phase Conjugate Optical Feedback", *IEE Proceedings: Optoelectronics*, Vol. 141, No. 2, pp. 103-108, 1994.

The following journal papers have been accepted for publication or have been submitted for publication :-

L. N. Langley, K. A. Shore, and J. Mørk, "Intensity Noise and Dynamics of Laser Diodes Subject to Strong Optical Feedback", *accepted for publication in Optics Letters*, 1994.

L. N. Langley, S. Turovets, and K. A. Shore, "Targetting Periodic Oscillations of External Cavity Laser Diodes", *accepted for publication in Optics Letters*, 1994.

L. N. Langley, S. Turovets, and K. A. Shore, "Targetting in Nonlinear Dynamics of Laser Diodes", *accepted to IEE Proceedings: Optoelectronics*, 1994

A5.2 Conference Papers.

The following conference papers have been presented from the work in this thesis :-

L. N. Langley, and K. A. Shore, "Turn-on Delay Statistics of Modulated External Cavity Semiconductor Lasers", *41st Scottish Universities/NATO ASI Summer School (Nonlinear Dynamics and Spatial Complexity in Optical Systems)*, Edinburgh, 1992.

L. N. Langley, and K. A. Shore, "The Effect of Phase Conjugate Optical Feedback on Intensity Noise in Laser Diodes", *Conference on Semiconductor and Integrated Optoelectronics (SIOE '93)*, Cardiff, 1993.

L. N. Langley, and K. A. Shore, "Influence of Optical Feedback on the Turn-on Delay Statistics of Modulated Laser Diodes", *Conference on Lasers and Electro-Optics (CLEO '93)*, OSA Technical Digest Series, Vol. 11, paper CWJ104, Baltimore, 1993.

L. N. Langley, and K. A. Shore, "Intensity Noise in Laser Diodes with Phase-Conjugate Optical Feedback", *Conference on Lasers and Electro-Optics (CLEO '93)*, OSA Technical Digest Series, Vol. 11, paper CThS36, Baltimore, 1993.

L. N. Langley, and K. A. Shore, "A Model for Strong Optical Feedback Effects in Laser Diodes", *Conference on Semiconductor and Integrated Optoelectronics (SIOE '94)*, Cardiff, 1994.

L. N. Langley, K. A. Shore, A. P. Willis, and D. M. Kane, "External Cavity FM Semiconductor Lasers: Theory and Experiment", *Conference on Semiconductor and Integrated Optoelectronics (SIOE '94)*, Cardiff, 1994.

L. N. Langley, K. A. Shore, and J. Mørk, "Dynamics of Laser Diodes Subject to Strong Optical Feedback", *European Quantum Electronics Conference (EQEC '94)*, paper QTuE3, Amsterdam, 1994.

L. N. Langley, K. A. Shore, and G. P. Agrawal, "Effect of Sluggish Phase Conjugate Feedback on Laser Diode Dynamics", *Conference on Lasers and Electro-Optics (CLEO/EUROPE '94)*, paper CMH4, Amsterdam, 1994.

A. P. Willis, D. M. Kane, L. N. Langley, and K. A. Shore, "Frequency Modulated External Cavity Diode Lasers: A Theoretical and Experimental Study", *Conference on Lasers and Electro-Optics (CLEO/EUROPE '94)*, paper CTuK15, Amsterdam, 1994.

K. A. Shore, L. N. Langley, and W. M. Yee, "Laser Diode Devices for Chaotic Optical Communications", *IEE Colloquium on Exploiting Chaos in Signal Processing*, London, 1994.

L. N. Langley, S. Turovets, and K. A. Shore, "Targetting Nonlinear Dynamics of Laser Diodes Using Optical Feedback", *OPTIK '94*, Berlin, 1994.

The Effect of External Optical Feedback on the Turn-On Delay Statistics of Laser Diodes Under Pseudorandom Modulation

L. N. Langley and K. A. Shore

Abstract—**The turn-on delay statistics of laser diodes with optical feedback are investigated by numerical modeling. Under pseudorandom modulation the optical feedback causes an increase in the average turn-on delay and multiplies the jitter considerably. The jitter increase due to optical feedback is largest at higher bias currents. Optical feedback from an external reflectivity of greater than 0.1% can destroy the pattern effects which occur for some operating conditions.**

I. Introduction

THE turn-on delay jitter plays a significant role in determining the system performance of semiconductor lasers and has been investigated both experimentally [1]–[3] and using numerical simulations [3]–[6]. The turn-on delay jitter is caused by spontaneous emission induced intensity noise in the laser optical output [1]–[6]. Random starting points for the rise in optical power at the onset of a pulse ensures that the turn-on delay is also random, giving rise to jitter. The turn-on delay jitter is greater when the laser is biased below threshold [2]–[6] and decreases for increasing bias current above threshold [2]–[5]. During pseudorandom modulation pattern effects become important and can cause the turn-on delay probability distribution function (pdf) to become double peaked, resulting in a very large jitter [5], [6].

The system performance of semiconductor lasers subject to directly intensity modulation can be significantly degraded due to external optical feedback of the levels typical in optical communications systems [7]–[10]. At large feedback levels the so-called "coherence collapse" regime may occur in which there is a very large amplitude intensity noise in th laser output power [8]–[10]. External optical feedback has been investigated both by numerical simulations [9], [10] and experimentally [8].

In the present letter external optical feedback and turn-on delay jitter are considered in conjunction for directly modulated semiconductor lasers under pseudorandom modulation. Recent work has shown that moderate optical feedback enhances the turn-on delay jitter in semiconductor laser diodes [11]. The spontaneous emission induced intensity noise in the laser output causes the turn-on delay fluctuations; therefore, it is expected that external optical feedback will also influence the turn-on delay and jitter as it also introduces intensity noise into the laser output.

Manuscript received July 7, 1992; revised August 12, 1992. This work was undertaken in a UK SERC CASE project supported by Northern Telecom, Paignton, Devon, UK.

The authors are with the School of Electronic and Electrical Engineering, Bath University, Bath BA2 7AY, UK.

IEEE Log Number 9204000.

II. Laser Model and Numerical Solution

The laser model used in this investigation is appropriate to a distributed feedback laser typically used in optical communications systems [10]. The rate equations are single-mode and include optical feedback and Langevin noise terms as follows:

$$\frac{dn}{dt} = \frac{I(t)}{eV} - \frac{n}{\tau_{sp}} - sG_n(n - n_t)(1 - \epsilon s) + F_n(t) \quad (1)$$

$$\frac{ds}{dt} = \frac{\gamma n \Gamma}{\tau_{sp}} - \frac{s}{\tau_{ph}} + sG_n(n - n_t)\Gamma(1 - \epsilon s) + 2k_c\sqrt{s}\sqrt{s(t - \tau_{ext})}\cos(\Delta(t)) + F_s(t) \quad (2)$$

$$\frac{d\phi}{dt} = \frac{\alpha}{2}G_n(n - n_0)\Gamma - k_c\frac{\sqrt{s(t - \tau_{ext})}}{\sqrt{s}}\sin(\Delta(t)) + F_\phi(t) \quad (3)$$

where

$$\Delta(t) = \omega_0\tau_{ext} + \theta_{ext} + \phi(t) - \phi(t - \tau_{ext}) \quad (4)$$

and

$$k_c = \frac{(1 - R_2)\sqrt{R_{ext}}\,\eta}{\sqrt{R_2}\,\tau_L}. \quad (5)$$

In the rate equation $n(t)$ is the carrier density, $s(t)$ is the photon density, $\varnothing(t)$ is the electric field phase, $I(t)$ is the injection current, and e is the electronic charge. Typical laser parameters for a DFB laser are used where V is the active region volume ($1.5 \times 10^{-16}\text{m}^3$), τ_{sp} is the carrier lifetime (2 ns), G_n is the gain slope ($2.125 \times 10^{-12}\text{m}^3\text{s}^{-1}$), n_t is the threshold carrier density ($4 \times 10^{-23}\text{m}^{-3}$), ϵ is the saturation parameter ($3 \times 10^{-23}\text{m}^3$), γ is the spontaneous emission factor (1×10^{-5}), τ_{ph} is the photon lifetime (2 ps), Γ is the confinement factor (0.4), α is the linewidth enhancement factor (5.5), n_o is the transparency carrier density ($9.9 \times 10^{23}\text{m}^{-3}$), ω is the

operating frequency ($\equiv 1.55$ μm), R_2 is the laser facet reflectivity (0.309), η is the laser to fiber coupling efficiency (0.4), and τ_L is the laser cavity round trip delay (9 ps). In the optical feedback terms, R_{ext} is the external reflector reflectivity, τ_{ext} is the external cavity round trip delay (1.7 ns) and $\varnothing_{ext}$ is the phase change in the external cavity (0 rad). The Langevin noise terms, $F_n(t)$, $F_s(t)$, and $F_{\varnothing}(t)$, are calculated as in Schunk and Petermann [9] or Clarke [10].

The rate equations with external optical feedback and Langevin noise terms are solved numerically using a variable-step, variable-order Runge–Kutta algorithm. Pseudorandom modulation in the GHz frequency range is modeled for the NRZ format. The threshold current, I_{th}, is 12.0 mA. An injection current of 3.5 I_{th} is used for the logic one state, corresponding to an output power of 2.0 mW. The laser and drive circuit parasitics are modeled by exponential current rises and falls.

The turn-on delay is defined as the time taken between the increase in injection current and the output power passing 50% of the logic one state output power when there is no optical feedback. The turn-on delay jitter is defined as the standard deviation of the turn-on delay probability distribution function (pdf). The number of data bits used to calculate the turn-on delay pdf's is 1000. The errors in the calculated values of average turn-on delay and jitter introduced by using this number of samples are smaller than the changes seen in these two quantities when optical feedback is introduced.

III. Pseudorandom Modulation

A data stream of random data bits is used to modulate the laser. Fig. 1 shows how the average turn-on delay, $\bar{T}_{on}$, and jitter, σ_T, change with increasing external optical feedback, for a bias current, I_b, 26% above threshold and modulated at 2 GHz. The average turn-on delay increases by a few percent as the level of the optical feedback increases. The jitter increases several fold as the level of the optical feedback increases.

The increases in the average turn-on delay and jitter seen in Fig. 1 are seen in the changing shape of the turn-on delay probability distribution function (pdf), shown in Fig. 2. Several turn-on delay pdf's are shown for increasing optical feedback. The modulation frequency investigated is sufficiently high to prevent the carrier density relaxing to its steady-state value during a single logic zero bit. Hence, different turn-on delays occur, depending on the number of preceding zero bits, and double peaks known as pattern effects are seen in the turn-on delay pdf with no external optical feedback present [6]. At lower frequencies the carrier density reaches its steady state value during a single logic zero bit, thus preventing pattern effects and giving a Gaussian turn-on delay pdf [2]. Such pattern effects also depend upon the device parameters and particularly the carrier lifetime. For shorter carrier lifetimes pattern effects will occur only at higher modulation frequencies. In addition, the pattern effect is dependent upon the modulation format with pattern effects in the *RZ* format occurring at lower frequencies compared to the NRZ format. This is because for the *RZ* format the current returns to its lower value for part of the bit period so that the carrier density has insufficient time to relax to the steady state value. Fig. 2 shows that at low levels of optical feedback the two peaks are broadened but remain distinguishable. At high levels of optical feedback the turn-on delay pdf is changed into a Gaussian shape. The two peaks have been broadened so much that they have been destroyed, but at the expense of increased jitter.

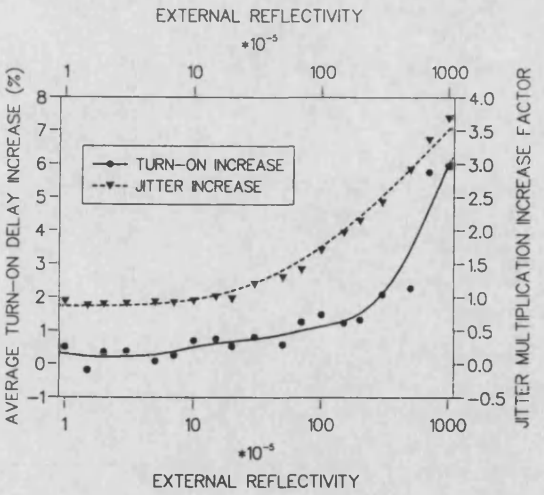

Fig. 1. Average turn-on delay and jitter for increasing external reflectivity ($I_{bias} = 1.26\ I_{th}$, $f_m = 2$ GHz).

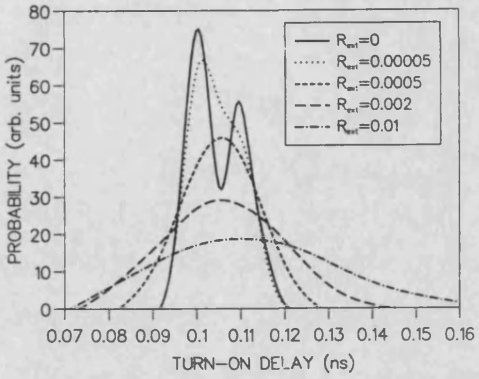

Fig. 2. Turn-on delay distribution for increasing external reflectivity ($I_{bias} = 1.26\ I_{th}$, $f_m = 2$ GHz).

At lower bias currents, the jitter is already large due to spontaneous emission noise, therefore the increase in jitter due to optical feedback is less at lower bias currents. The effect of changing the logic zero state bias current is shown in Fig. 3 for fixed optical feedback of external reflectivity, $R_{ext} = 0.005$. The modulation frequency is 2 GHz. It can be seen that the average turn-on delay with optical feedback is usually larger than when no optical

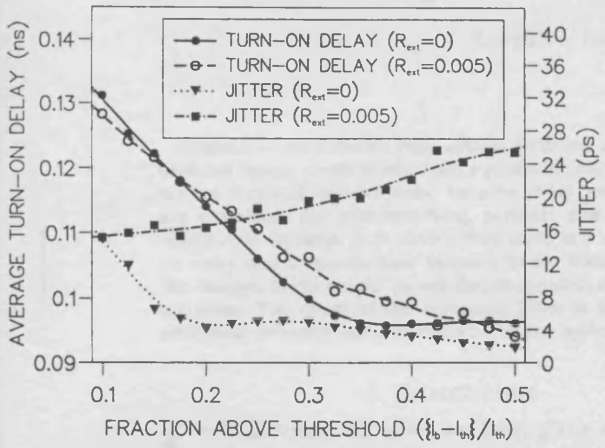

Fig. 3. Average turn-on delay and jitter with (R_{ext} = 0.005) and without optical feedback (R_{ext} = 0) for increasing bias current (f_m = 2 GHz).

feedback is present. The jitter without optical feedback decreases as the bias current increases. However, the jitter with optical feedback increases as the bias current increases. At low bias currents the jitter is already relatively large due to spontaneous emission. Therefore, the increase in jitter due to optical feedback is larger at high bias currents than at low bias currents. This leads to the increasing difference between the jitter with and without optical feedback seen in Fig. 3.

IV. Conclusion

Laser diodes operating under pseudorandom modulation conditions and subjected to optical feedback of the levels typical in communication systems have an increased average turn-on delay and a dramatically increased jitter. The increase in jitter due to optical feedback is greatest at higher bias currents. Even at relatively low optical feedback the increase in jitter can be large enough to destroy the pattern effects often seen in the turn-on delay probability distribution function during pseudorandom modulation.

Acknowledgment

The authors thank Dr. A. Janssen and Dr. B. Garrett of Northern Telecom for discussions.

References

[1] P. Spano, A. D'Ottavi, A. Mecozzi, and B. Daino, "Experimental observation of time jitter in semiconductor laser turn-on," *Appl. Phys. Lett.*, vol. 52, no. 26, pp. 2203–2204, June 27, 1988.

[2] T. Shen, "Timing jitter in semiconductor lasers under pseudorandom word modulation," *J. Lightwave Technol.*, vol. 7, pp. 1394–1399, Sept. 1989.

[3] A. Weber, W. Ronghan, E. Böttcher, M. Schell, and D. Bimberg, "Measurement and simulation of the turn-on delay time jitter in gain-switched semiconductor lasers," *IEEE J. Quantum Electron.*, vol. 28, pp. 441–445, Feb. 1992.

[4] S. Miller, "Turn-on jitter in nearly single-mode injection lasers," *IEEE J. Quantum Electron.*, vol. QE-22, pp. 16–19, Jan. 1986.

[5] C. Mirasso, P. Colet, M. San Miguel, "Pulse statistics in single-mode semiconductor lasers modulated at gigahertz rates," *Opt. Lett.*, vol. 16, no. 22, pp. 1753–1755, Nov. 15, 1991.

[6] ——, "Dependence of timing jitter on bias level for single mode semiconductor lasers under high speed modulation," *IEEE J. Quantum Electron.*, 1992.

[7] R. Lang and K. Kobayashi, "External optical feedback effects on semiconductor injection laser properties," *IEEE J. Quantum Electron.*, vol. QE-16, pp. 347–355, Mar. 1980.

[8] R. Tkach and a. Chraplyvy, "Regimes of feedback effects in 1.5μm distributed feedback lasers, *J. Lightwave Technol.*, vol. LT-4, pp. 1655–1661, Nov. 1986.

[9] N. Schunk and K. Petermann, "Numerical analysis of the feedback regimes for a single-mode semiconductor laser with external feedback," *IEEE J. Quantum Electron.*, vol. 24, pp. 1242–1247, July 1991.

[10] B. Clarke, "The effect of reflections on the system performance of intensity modulated laser diodes," *J. Lightwave. Technol.*, vol. 9, pp. 741–749, June 1991.

[11] H. Wu and H. Chang, "Turn-on jitter in semiconductor lasers with moderate reflecting feedback," *IEEE Photon. Technol. Lett.*, vol. 4, pp. 339–342, Apr. 1992.

The Effect of External Optical Feedback on Timing Jitter in Modulated Laser Diodes

Lloyd N. Langley and K. Alan Shore, *Member, IEEE*

Abstract—**Laser diodes with optical feedback are numerically modeled using single-mode rate equations. The effects of the optical feedback on the pulse turn-on delay and timing jitter are examined, for gain-switching, periodic and pseudorandom modulation formats. It is shown that there is a change in turn-on delay and a considerable increase in the timing jitter due to the changes in the output power distributions as optical feedback increases. The cause of the increased jitter is found to be the additional intensity noise introduced by the optical feedback.**

I. Introduction

CONSIDERABLE effort has been given to studying the effects of noise on the turn-on delay jitter which plays a significant role in determining the system performance of semiconductor lasers. Both experimental [1]–[6] and numerical simulations [5]–[10] have been used to investigate the turn-on delay jitter. The turn-on delay is the finite time between the application of an increase in injection current into the laser and the leading edge of the resultant optical pulse. The turn-on delay jitter is a measure of the variations in the turn-on delay and is defined as the standard deviation of the turn-on delay probability distribution function (pdf). The turn-on delay jitter is caused by spontaneous-emission-induced intensity noise in the laser optical output [1]–[10]. The carrier and photon fluctuations ensure that the rise in optical power at the onset of a pulse begins from a random starting value. Thus the time taken for the light pulse to be emitted is also random, resulting in different turn-on delays for each pulse. The turn-on delay jitter is significantly larger in distributed feedback lasers than in Fabry–Perot lasers [3], [6], [10]. It has been demonstrated that this is due to the rapidity of turn-on [10]. The rate of increase of the photon number during turn-on is lower in DFB than in Fabry–Perot lasers. Hence, a noise-induced change in the starting point for the photon number rise causes a larger change in the turn-on delay in a DFB laser, resulting in a larger value of jitter. The turn-on delay jitter degrades the laser performance by reducing the temporal resolution of the optical pulses. Analytical expressions for turn-on delay jitter have been found [4]–[6], [9] and lead to calculations of both the jitter-induced system bit-error rate and power penalty [5]. The turn-on delay jitter is greater when the laser is biased below threshold [1], [2], [5]–[9], [19] and decreases for increasing bias current above threshold [5]–[7], [8] but at the expense of reduced on/off ratio. Recent work has focused on the shape of the turn-on delay pdf and the dependence of the jitter on modulation frequency. For periodic modulation the turn-on delay pdf has been found to be approximately Gaussian in shape for bias currents both above and below threshold [5], [9]. For pseudorandom modulation, pattern effects become important and can cause the turn-on delay pdf to become double-peaked when the laser is operated above threshold, resulting in a very large jitter [8], [9]. There exists a value of bias current just below threshold at which pattern effects are negligible and the turn-on delay pdf is an approximately Gaussian shape for pseudorandom and periodic modulation [9].

The system performance of semiconductor lasers subject to direct intensity modulation can be significantly degraded due to external optical feedback. Much attention has been given to the dramatic changes in noise properties of the laser which can occur for feedback levels typical of optical communications systems [11]–[19]. Five regimes have been identified in which the semiconductor laser can operate when subjected to external optical feedback, depending on the strength of the feedback and the distance to the reflection [12]. At low feedback levels linewidth narrowing can occur but at larger feedback levels the so-called "coherence collapse" regime may occur. The "coherence collapse" regime is deterministic and chaotic, with the route to chaos being quasi-periodicity [13]. In the "coherence collapse" regime there is a very large amplitude intensity noise in the laser output power, and a large broadening of the optical field power spectral density [12], [14]–[16]. The intensity noise can significantly reduce the performance of optical communications systems due to the generation of false information bits, resulting in large power penalties. External optical feedback has been investigated both by numerical simulations [14], [15], [18], [19] and experimentally [11], [12], [16]. It has been found that very low external reflectivities such as occur from the connector on the fiber pigtail of a laser diode module can cause the laser to enter the very noisy "coherence collapse" regime.

In the present paper external optical feedback and turn-on delay jitter are considered in conjunction for directly modulated semiconductor lasers. Recent work has shown that moderate optical feedback enhances the turn-on delay jitter in semiconductor laser diodes [18]. It is the spontaneous emission-induced intensity noise in the laser output that causes the turn-on delay fluctuations, therefore it is expected that external optical feedback will also effect the turn-on delay and jitter as it also introduces intensity noise into the laser output.

Manuscript received June 17, 1992; revised October 12, 1992. This work was undertaken in a UK SERC CASE project supported by Northern Telecom, Paignton, Devon, UK.

The authors are with the School of Electronic and Electrical Engineering, Bath University, Bath, BA2 7AY, United Kingdom.

IEEE Log Number 9206409.

These two effects are investigated by numerical simulation of the single-mode rate equations for a typical distributed feedback laser. The model takes into account both external optical feedback and Langevin noise terms. It is shown that external optical feedback gives rise to markedly different changes in the turn-on delay jitter for pseudorandom and periodic modulation formats.

Section II of this paper describes the numerical model used to investigate the effect of external optical feedback on the turn-on delay jitter. Section III presents the results in three parts for gain-switching, periodic, and pseudorandom modulation regimes, respectively. Gain switching is considered as a form of digital modulation where each of the bits is independent of the previous one and allows the effects of external optical feedback to be considered alone. Thus pattern effects which may arise in pseudorandom modulation are avoided. Section IV states the conclusions and makes recommendations for practical systems.

II. Laser Model and Numerical Solution

The laser model used in this investigation is appropriate to a distributed feedback laser typically used in optical communications systems [15]. The system configuration is shown in Fig. 1. The rate equations are single-mode and include optical feedback and Langevin noise terms as follows:

$$\frac{dn}{dt} = \frac{I(t)}{eV} - \frac{n}{\tau_{sp}} - sG_n(n - n_t)(1 - \epsilon s) + F_n(t) \quad (1)$$

$$\frac{ds}{dt} = \frac{\gamma n\Gamma}{\tau_{sp}} - \frac{s}{\tau_{\text{ph}}} + sG_n(n - n_t)\Gamma(1 - \epsilon s) + 2k_c\sqrt{s}\sqrt{s(t - \tau_{\text{ext}})}\cos(\Delta(t)) + F_s(t) \quad (2)$$

$$\frac{d\phi}{dt} = \frac{\alpha}{2}G_n(n - n_0)\Gamma - k_c\frac{\sqrt{s(t - \tau_{\text{ext}})}}{\sqrt{s}}\sin(\Delta(t)) + F_\phi(t) \quad (3)$$

where

$$\Delta(t) = \omega_0\tau_{\text{ext}} + \theta_{\text{ext}} + \phi(t) - \phi(t - \tau_{\text{ext}}) \quad (4)$$

and

$$k_c = \frac{(1 - R_2)\sqrt{R_{\text{ext}}}\eta}{\sqrt{R_2}\tau_L}. \quad (5)$$

In the rate equations $n(t)$ is the carrier density, $s(t)$ is the photon density, $\phi(t)$ is the electric field phase, $I(t)$ is the injection current, and e is the electronic charge. The laser diode parameters are given in the Table I. In the optical feedback terms, R_{ext} is the external reflector reflectivity, τ_{ext} is the external cavity round trip delay, and θ_{ext} is the arbitrary phase change in the external cavity. An external cavity round trip delay of 1.7 ns is used which corresponds to reflections from a fiber pigtail of 17-cm length and the arbitrary phase change in the external cavity is assumed to be zero. The choice of $\tau_{\text{ext}} = 1.7$ ns introduces external cavity modes of spacing $1/\tau_{\text{ext}} \simeq 0.6$ GHz into the intensity spectrum. Resonance effects between the external cavity modes and the modulation frequency are avoided because the modulation frequencies of interest in this work are 2–4 GHz. The model represents the worse-case situation because the assumption in the rate equations is that the reflected light has the same polarization as the emitted light.

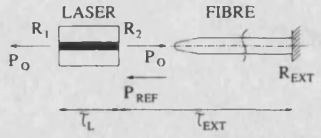

Fig. 1. Schematic diagram of the laser with optical feedback from the far end of a fiber pigtail.

TABLE I
Laser Parameters

Symbol	Description	Value
V	Active region volume	$1.5\text{x}10^{-16}$ m^3
τ_{sp}	Carrier lifetime	2 ns
G_n	Gain slope	$2.125\text{x}10^{-12}$ m^{3}s^{-1}
n_t	Threshold carrier density	$4\text{x}10^{23}$ m^{-3}
ϵ	Saturation parameter	$3\text{x}10^{-23}$ m^3
γ	Spontaneous emission factor	$1\text{x}10^{-5}$
Γ	Confinement factor	0.4
τ_{ph}	Photon lifetime	2 ps
α	Linewidth broadening factor	5.5
n_0	Transparency carrier density	$9.9\text{x}10^{23}$
ω_0	Operating wavelength	$\equiv$1.55 μm
R_2	Laser facet reflectivity	0.309
η	Laser to fibre coupling efficiency	0.4
τ_L	Laser cavity round trip time	9 ps
η_q	Quantum efficiency	0.4

The Langevin noise terms are calculated as follows:

$$F_n(t) = -\sqrt{\frac{2S(t_i)\gamma n\Gamma}{\tau_{sp}\Delta t}}x_s + \sqrt{\frac{2n(t_i)}{\tau_{sp}\Delta tV}}x_n \quad (6)$$

$$F_s(t) = \sqrt{\frac{2S(t_i)\gamma n\Gamma}{\tau_{sp}\Delta t}}x_s \quad (7)$$

$$F_\phi(t) = \frac{1}{S(t)}\sqrt{\frac{S(t_i)\gamma n\Gamma}{2\tau_{sp}\Delta t}}x_\phi. \quad (8)$$

Here, $s(t_i)$ is the photon density at the start of the interval Δt, $n(t_i)$ is the carrier density at the start of the interval Δt, and x_n, x_s, x_ϕ are Gaussian distributed random variables with zero mean and unity variance. The Langevin noise in the photon and electric field phase rate equations is due to the random nature of the spontaneous emission process. The Langevin noise in the carrier rate equation is due to the shot

noise nature of the injection current and spontaneous as well as stimulated recombination.

The rate equations with external optical feedback and Langevin noise terms are solved numerically using a variable-step, variable-order Runge–Kutta algorithm. To evaluate the reflection terms in the rate equations, values of photon density and electric field phase calculated at an earlier solution step are required. Thus at each solution step the values of photon density and electric field phase are recorded for use at a later solution step. The number of solution steps between the recording and the use of these values is equivalent to the external cavity round-trip delay. Langevin noise is modeled by applying random noise forces as calculated in (6)–(8). The Gaussian distributed random variables x_n, x_s, and x_ϕ are calculated at the start of, and are held constant throughout, each Langevin noise application interval Δt. The interval Δt is chosen to be 20 ps. This results in a power spectral density for the noise which has its first zero at a frequency $1/\Delta t = 50$ GHz. The noise forces should describe a white noise spectrum at least up to the relaxation oscillation frequency [17]. The influence of Δt on the power spectral density of the noise is discussed by Schunk and Petermann [17, appendix A]. The 3-dB frequency is found to be approximately 22 GHz, which is several times the maximum relaxation oscillation frequency encountered in the following investigations. Hence the condition that the noise spectrum is white up to a frequency greater than the relaxation oscillation frequency is satisfied.

Pseudorandom-modulation and periodic-modulation injection current formats in the gigahertz modulation frequency range are modeled; also gain switching is considered. The semiconductor laser and drive circuit parasitics are modeled by exponential current rises and falls. The threshold current is 12.0 mA. An injection current of $3.5I_{\text{th}}$ is used for the logic one state, corresponding to an output power of 2.0 mW.

The output power per facet passed into a fiber pigtail is calculated from the photon density using the following equation, with h being Planck's constant:

$$P_0(t) = \frac{\eta_q \omega_0 h \eta s(t) V}{4\pi \Gamma \tau_{\text{ph}}}. \tag{9}$$

The optical turn-on delay for each transition from the logic zero state up to the logic one state is recorded. The turn-on delay is defined as the time taken between the increase in injection current and the output power passing 50% of the logic one state output power when there is no optical feedback. This power level is termed the logic decision power. The number of data bits used in this paper to calculate the turn-on delay pdf's is 1000 for the periodic and pseudorandom modulation formats, and 100 for the gain-switching modulation format. Using these limited numbers of samples of the turn-on delay, the randomness of the noise processes investigated will introduce errors into the calculated values of the average turn-on delay and jitter. Repeated simulations for identical bias, modulation, and reflection conditions suggest that errors of up to ±0.5% in the average turn-on delay and ±2.5% in the jitter can be expected. These errors are much smaller than the changes seen in these parameters as optical feedback increases. The turn-on delay jitter is defined as the standard deviation of the turn-on delay pdf, and is calculated as below

$$\sigma_t = \sqrt{\frac{\sum_{m=1}^{m=n} (T_{\text{on}(m)} - \overline{T_{\text{on}}})^2}{n}} \tag{10}$$

where $\overline{T}_{\text{on}}$ is the average turn-on delay, $T_{\text{on}(m)}$ are the turn-on delays calculated from the numerical simulation, and n is the number of turn-on events used in the calculation.

III. Turn-On Jitter with External Feedback

A. Gain-Switched Lasers

In this modulation format single current pulses are used to modulate the laser, with sufficient time between them so that both carrier and photon densities have time to relax to their steady-state values before the onset of the next pulse. This ensures that each optical pulse is independent from the previous pulse. Fig. 2(a) and (b) shows how the average turn-on delay and jitter change with increasing external optical feedback, for a bias current of 26% and 10% above threshold, respectively. The average turn-on delay increases by a few percent when optical feedback is present for all bias currents above threshold. The shape of the graph of average turn-on delay shows a rise as external reflectivity increases. The turn-on delay increase is largely independent of the bias current. It is possible to decrease the average turn-on delay to a value below that of no optical feedback at some combinations of external reflectivities and operating conditions. This is achieved at an external reflectivity of below 10^{-4} for the 26% threshold bias current of Fig. 2(a). The turn-on delay jitter increases dramatically as the level of optical feedback increases. The jitter without optical feedback is lower at lower bias currents. The value of the jitter with no optical feedback is 3.1 ps at a bias current 10% above threshold. This value is close to an experimental value of approximately 4 ps obtained by Weber *et al.* for the same value of current pulse of $3.5I_{\text{th}}$ and similar modulation conditions [6]. The dramatic increase in jitter occurs at a higher external reflectivity when the laser is biased closer to threshold. Close to threshold there is already a large jitter due to spontaneous emission noise. Therefore, small amounts of optical feedback do not increase the jitter significantly. The values of jitter obtained in the simulation at large levels of optical feedback are similar to the value of 20.7 ps obtained in simulations by Wu and Chang for an external reflectivity of $R_{\text{ext}} = 0.005$ [18]. Both the turn-on delay changes and jitter increase are seen in the changing shape of the turn-on delay pdf as optical feedback increases, shown in Fig. 2(c), for a bias current 10% above threshold. The turn-on delay pdf is approximately Gaussian for all bias currents with no external optical feedback and remains so when external optical feedback is added. The turn-on delay pdf becomes considerably broadened when the external reflectivity exceeds 10^{-4}.

The mean intensity evolution together with the intensity standard deviation are shown in Fig. 2(d) for bias currents 10% and 26% above threshold. The graph shows the evolutions with and without optical feedback. As expected, the mean intensity

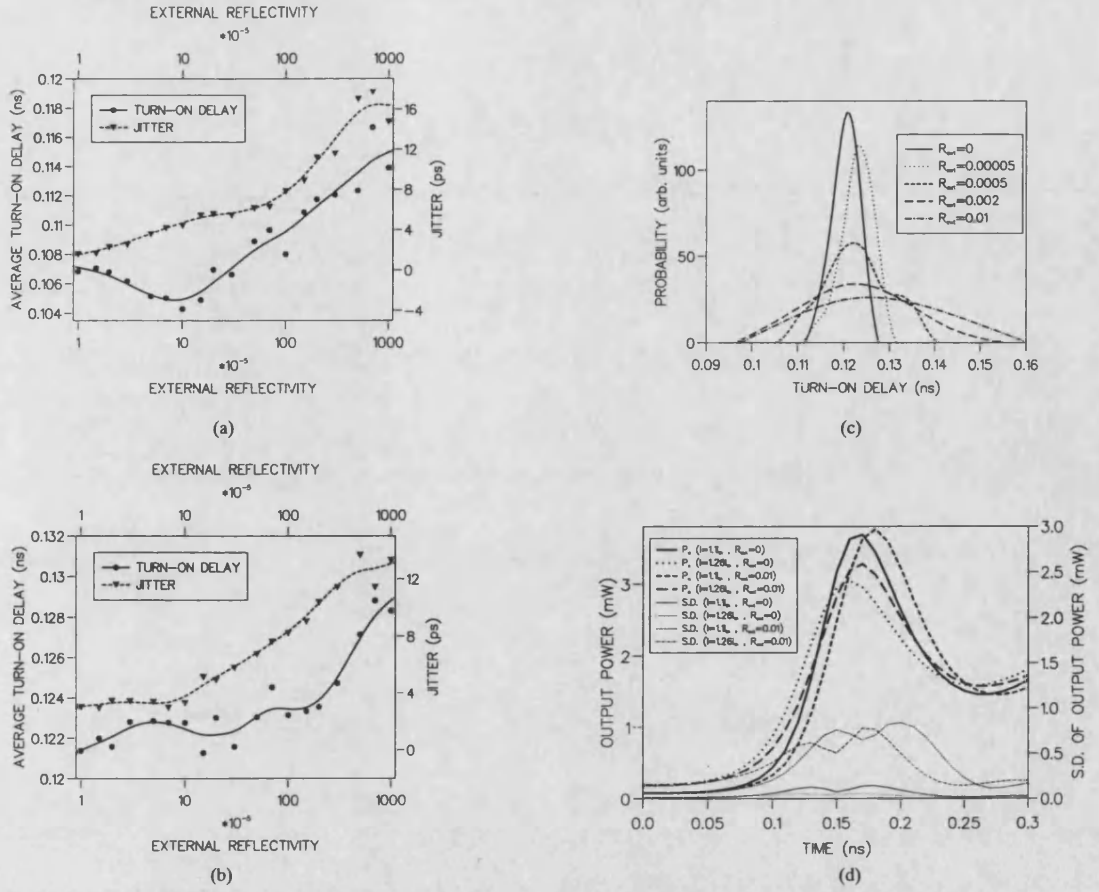

Fig. 2. (a) Average turn-on delay and jitter for increasing external reflectivity for the gain-switching modulation format ($I_{\text{bias}} = 1.26I_{\text{th}}$). (b) Average turn-on delay and jitter for increasing external reflectivity for the gain-switching modulation format ($I_{\text{bias}} = 1.1I_{\text{th}}$). (c) Turn-on delay distribution for the gain-switching modulation format for increasing external reflectivity ($I_{\text{bias}} = 1.1I_{\text{th}}$). (d) Mean intensity evolutions and the standard deviation of the intensity under gain-switching modulation for no optical feedback and with optical feedback from an external reflectivity of $R_{\text{ext}} = 0.01$ at bias currents of 10% and 26% above threshold.

evolution is slower at lower bias current. Optical feedback is seen to increase the intensity standard deviation, seen as jitter, and also slows down the mean intensity evolutions.

To explain these results it is recalled that optical feedback produces large amounts of intensity noise in the optical output power. The intensity noise is induced by the behavior of the laser when external optical feedback is introduced. This causes the output power pdf to be wider. Hence the spread of possible starting points for the carrier and photon density rises during the turn-on process is wider also, resulting in a broader turn-on delay pdf, seen as an increase in the jitter. It is well known that optical feedback increases the average output power by a small amount. Therefore, on first inspection, the average turn-on time would be expected to be decreased by external optical feedback, due to the smaller increase in carrier and photon densities required for the output power to exceed the logic decision power. Fig. 3(a) shows the output power pdf for a bias current 26% above threshold, which corresponds to an average output power of 0.2 mW. When no optical feedback is present the output power pdf is approximately Gaussian. The width of the output power pdf is approximately equal to the mean value which agrees with experiments performed at relatively low output power [20]. However, the output power pdf is no longer approximately Gaussian when reflections induce large output power fluctuations. This changed shape is because the time to recover to the average value is longer when the output light power is displaced below the average than when it is displaced above it. Hence the temporal power waveform appears to be spiked, as shown in Fig. 3(b), with longer periods of below-average power between the spikes, resulting in the non-Gaussian output power pdf's in Fig. 3(a) as external optical feedback increases. Therefore, since the average power has increased, the turn-on delay when starting from the average output power is decreased. However, since external optical feedback causes more time to be spent below the average output power than above it, the average turn-on delay is increased. The non-Gaussian output power pdf at high optical feedback does not prevent the turn-on delay pdf from being approximately Gaussian in shape. The sudden broadening of the turn-on delay pdf when the external reflectivity exceeds 10^{-4} is caused by the high levels of intensity noise than occurs as the laser enters the "coherence collapse" regime.

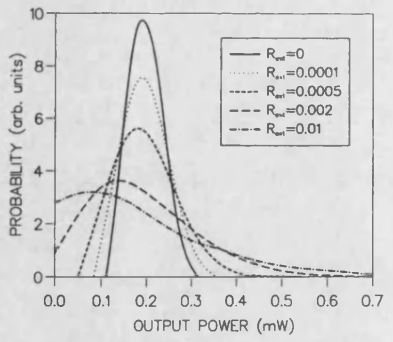

(a)

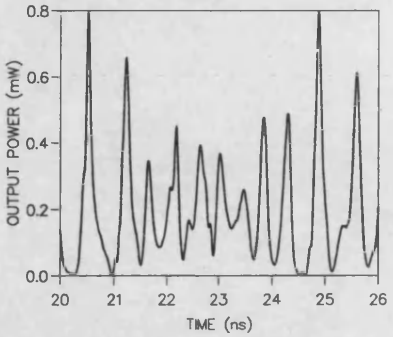

(b)

Fig. 3. (a) Output power distribution for increasing external reflectivity at constant current ($I_{bias} = 1.26I_{th}, \overline{P}_{OUT} = 0.2$ mW). (b) Output power waveform for constant current and high optical feedback ($I_{bias} = 1.26I_{th}, \overline{P}_{OUT} = 0.2$ mW, $R_{ext} = 0.01$).

B. Periodically Modulated Lasers

In this modulation format a data stream of alternating logic zero and logic one data bits is used to modulate the laser. The starting point for the power rise in each optical pulse is determined by the relaxation oscillations from the previous pulse. Fig. 4(a) shows how the average turn-on delay and jitter change with increasing external optical feedback, for a bias current 26% above threshold and a modulation frequency of 2 GHz. Fig. 4(c) shows the same parameters for 10% above threshold modulated at 2 GHz. Fig. 4(a) shows that the average turn-on delay is increased by a few percent by optical feedback for 26% above threshold and a modulation frequency of 2 GHz. At lower bias currents (Fig. 4(c)) and also at higher modulation frequencies the average turn-on delay decreases as optical feedback increases, but the change from that where no optical feedback is present is not as large as in the high bias current, low modulation frequency case of Fig. 4(a). Increasing the modulation frequency changes the initial starting point for the power increase in the next optical pulse by allowing less of the relaxation oscillation to occur between pulses. The turn-on delay jitter increases dramatically as the level of external optical feedback increases (Fig. 4(a)). The jitter increase is larger at higher bias currents (Fig. 4(c)). Further investigations show that the jitter increase is larger at higher modulation frequencies. The graphs of average turn-on delay and jitter do not show smooth changes as the level of optical feedback is increased. A possible reason for the peaks and troughs in the curves is that the optical-feedback-induced intensity noise does not always increase smoothly as the external reflectivity increases [15].

The above effects are seen in the changing shape of the turn-on delay pdf as optical feedback increases, shown in Fig. 4(b) and (d), for a bias current 26% and 10% above threshold, respectively. The modulation frequency is 2 GHz in both cases. The turn-on delay pdf remains approximately Gaussian for low feedback levels but changes to a very wide Gaussian pdf at high optical feedback levels. There appears to be a transition stage for moderate optical feedback levels where the turn-on delay pdf becomes highly non-Gaussian in shape and can even become double-peaked. The levels of optical feedback at which the turn-on pdf's are highly non-Gaussian are the same at which the average turn-on delay and jitter graphs do not show smooth changes. Hence the two observations are likely to be linked. A multiple-peaked pdf means that there is an effect taking place which causes two or more most likely starting points for the power rise in the pulses. The increase in jitter caused by optical feedback results again from the large amounts of intensity noise that optical feedback introduces.

The mean intensity evolution together with the intensity standard deviation are shown in Fig. 4(e) for bias currents 10% and 26% above threshold. The graph shows the evolutions with and without optical feedback and looks similar to that for the gain-switched modulation format, but the spread in the evolutions is wider. The intensity standard deviation during optical feedback has similar values to that under gain-switched modulation, even though the intensity standard deviation without optical feedback is larger in the periodic modulation regime.

C. Pseudorandomly Modulated Lasers

In this modulation format a data stream of random data bits is used to modulate the laser. Fig. 5(a) shows how the average turn-on delay and jitter change with increasing external optical feedback, for a bias current 26% above threshold and modulated at 2 GHz. Fig. 5(c) shows the same parameters for 10% above threshold modulated at 2 GHz. The average turn-on delay increases by a few percent for high bias current (Fig. 5(a)). At low bias currents the turn-on delay is virtually unchanged (Fig. 5(c)). At high bias currents the turn-on delay jitter increases dramatically as the level of optical feedback increases. The increase is greater at lower modulation frequency, and is less than in the gain-switching and periodic modulation regimes. At low bias currents the jitter remains virtually unchanged. The value of the jitter without any optical feedback at a bias current 10% above threshold is 19 ps. This can be compared to an experimental value obtained by Shen [5], whose value under pseudorandom modulation conditions at 1 GHz was 32 ps. The relatively lower value obtained in the simulation may be attributed to the presence of less spontaneous emission noise. This may occur by either using a lower value for the spontaneous emission factor, or by operating at a bias current further above threshold.

The above effects are seen in the changing shape of the turn-on delay pdf as optical feedback increases, shown in Fig. 5(b)

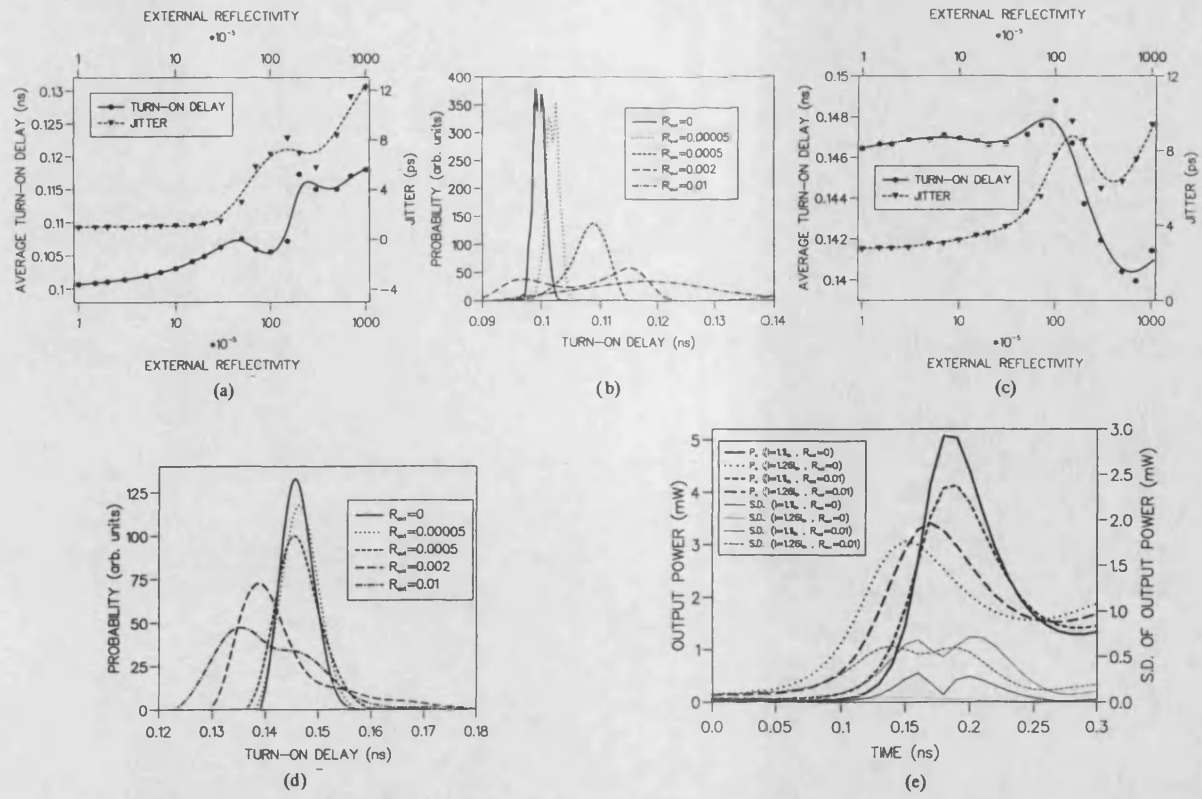

Fig. 4. (a) Average turn-on delay and jitter for increasing external reflectivity for the periodic modulation format ($I_{\text{bias}} = 1.26I_{\text{th}}, f_m = 2$ GHz). (b) Turn-on delay distribution for the periodic modulation format for increasing external reflectivity ($I_{\text{bias}} = 1.26I_{\text{th}}, f_m = 2$ GHz). (c) Average turn-on delay and jitter for increasing external reflectivity for the periodic modulation format ($I_{\text{bias}} = 1.1I_{\text{th}}, f_m = 2$ GHz). (d) Turn-on delay distribution for the periodic modulation format for increasing external reflectivity ($I_{\text{bias}} = 1.1I_{\text{th}}, f_m = 2$ GHz). (e) Mean intensity evolutions and the standard deviation of the intensity under periodic modulation for no optical feedback and with optical feedback from an external reflectivity of $R_{\text{ext}} = 0.01$ at bias current of 10% and 26% above threshold ($f_m = 2$ GHz).

and (d). At the modulation conditions investigated the turn-on delay pdf is double-peaked for no external feedback. The double-peaked distribution occurs because the modulation frequency is sufficiently high to prevent the carrier density relaxing to its steady-state value during a single logic bit. Hence different turn-on delays occur, depending on the number of preceding zero bits, and double peaks known as pattern effects are seen in the turn-on delay pdf with no external optical feedback present. At lower frequencies the carrier density reaches its steady-state value during a single logic zero bit, thus preventing pattern effects and giving a single-peaked turn-on delay pdf. Such pattern effects also depend upon the device parameters and particularly the carrier lifetime. For shorter carrier lifetimes pattern effects will occur only at higher modulation frequencies. The two peaks are broadened by external optical feedback but remain distinguishable for low external reflectivities. For high external reflectivities the turn-on delay pdf is changed into an approximately Gaussian-shaped pdf because the peaks are broadened so much that they are destroyed, but at the expense of increased jitter. At low bias currents the jitter is already very large and hence optical feedback does not increase it significantly. Whether the average turn-on delay increases or decreases with optical feedback is dependent on whether the single-peaked distribution that remains after the pattern effects have been destroyed lies nearer the faster or slower of the two original peaks. The increase in jitter caused by optical feedback is again resultant from the large amounts of intensity noise that optical feedback introduces. Therefore large amounts of optical feedback can be used to prevent the pattern effects which may occur at some combinations of modulation frequency and operating conditions.

It is useful to find out whether the turn-on delay pdf can be considered to be approximately Gaussian in shape. Errors in the transmitted data due to the turn-on delay jitter of the laser can occur when the turn-on delay is too long for the pulse to be detected by the receiver. Therefore, it is not strictly the shape of the turn-on delay pdf that is important. The jitter-induced error rate is dependent on the tails of the turn-on delay pdf. By approximating the turn-on delay pdf as a Gaussian shape with easily calculated tails, it is possible to calculate the system performance degradation due to jitter [5]. Calculation of the reflection-induced jitter performance degradation may be similarly performed and will be the subject of future work.

The mean intensity evolution together with the intensity standard deviation are shown in Fig. 5(e) for bias currents 10% and 26% above threshold. The graph shows the evolutions with and without optical feedback. The mean intensity

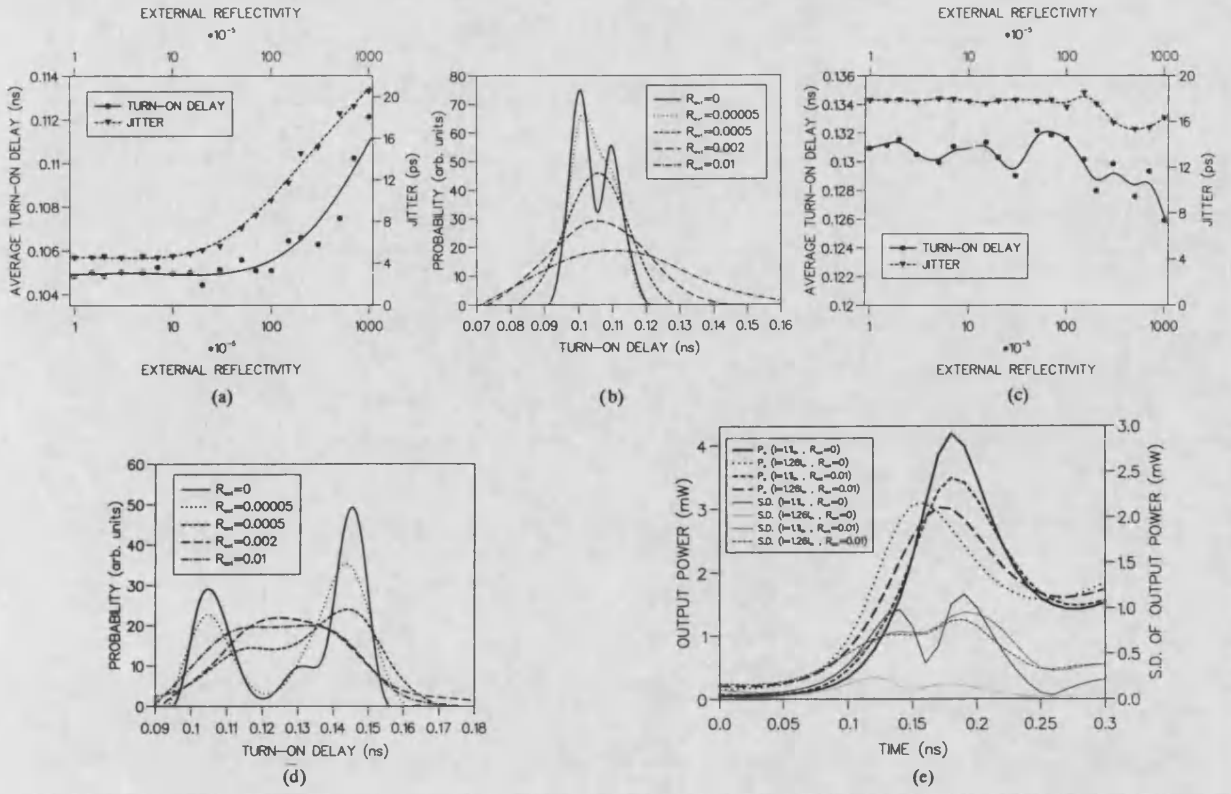

Fig. 5. (a) Average turn-on delay and jitter for increasing external reflectivity for the pseudorandom modulation format ($I_{\text{bias}} = 1.26I_{\text{th}}, f_m = 2$ GHz). (b) Turn-on delay distribution for the pseudorandom modulation format for increasing external reflectivity ($I_{\text{bias}} = 1.26I_{\text{th}}, f_m = 2$ GHz). (c) Average turn-on delay and jitter for increasing external reflectivity for the pseudorandom modulation format ($I_{\text{bias}} = 1.1I_{\text{th}}, f_m = 2$ GHz. (d) Turn-on delay distribution for the pseudorandom modulation format for increasing external reflectivity ($I_{\text{bias}} = 1.1I_{\text{th}}, f_m = 2$ GHz). (e) Mean intensity evolutions and the standard deviation of the intensity under pseudorandom modulation for no optical feedback and with optical feedback from an external reflectivity of $R_{\text{ext}} = 0.01$ at bias currents of 10% and 26% above threshold ($f_m = 2$ GHz).

evolutions show that optical feedback can increase or decrease the average turn-on delay. At the lower bias current of 10% above threshold the intensity standard deviation is already very large and is not altered very much by the addition of optical feedback. This agrees with the results of Fig. 5(c). For the higher bias current of 26% above threshold the intensity standard deviation is small without optical feedback but increases when optical feedback is present. This is seen as an increase of the jitter in Fig. 5(a).

IV. Conclusions

This paper has investigated the effect of external optical feedback on the turn-on delay characteristics of typical semiconductor lasers used in digital optical communications systems. Chaotic behavior introduced by the external optical feedback introduces additional intensity noise to that caused by spontaneous emission. The result is increased turn-on delay jitter in all of the gain-switching, periodic and pseudorandom modulation formats. The jitter is increased dramatically by high external reflectivity. The average turn-on delay is increased by optical feedback during the gain-switching modulation format. During periodic modulation and the more practical pseudorandom modulation regime the effect on the average turn-on delay is dependent on the modulation conditions, with the average turn-on delay either increasing or decreasing as the optical feedback increases. If under pseudorandom modulation the modulation conditions result in the turn-on delay pdf to be twin-peaked without feedback then large amounts of external optical feedback can change the pdf into a single-peaked pdf. Thus optical feedback can prevent the pattern effect from occurring, but at the expense of very large jitter. The increase in turn-on delay jitter caused by external optical feedback is less when the turn-on delay distribution is initially double-peaked since in this case a large jitter is already exhibited.

Acknowledgment

The authors wish to thank Dr. A. Janssen and Dr. B. Garrett of Northern Telecom for discussions.

References

[1] M. Choy, P. Liu, P. Shumate, T. Lee, and S. Tsuji, "Measurements of dynamic photon fluctuations in a directly modulated 1.5μm InGaAsP distributed feedback laser," *Appl. Phys. Lett.*, vol. 47, no. 5, pp. 448–450, Sept. 1985.

[2] E. Böttcher, K. Ketterer, and D. Bimberg, "Turn-on delay time fluctuations in gain-switched AlGaAs/GaAs multiple-quantum-well lasers," *J. Appl. Phys.*, vol. 63, no. 7, pp. 2469–2471, Apr. 1988.

[3] P. Spano, A. D'Ottavi, A. Mecozzi, and B. Daino, "Experimental observation of time jitter in semiconductor laser turn-on," *Appl. Phys. Lett.*, vol. 52, no. 26, pp. 2203–2204, June 1988.
[4] A. D'Ottavi, A. Mecozzi, P. Spano, and P. Piazolla, "Time jitter in multimode Fabry–Perot laser diodes," *Appl. Phys. Lett.*, vol. 53, no. 24, pp. 2362–2364, Dec. 1988.
[5] T. Shen, "Timing jitter in semiconductor lasers under pseudorandom word modulation," *J. Lightwave Technol.*, vol. 7, no. 9, pp. 1394–1399, Sept. 1989.
[6] A. Weber, W. Ronghan, E. Böttcher, M. Schell, and D. Bimberg, "Measurement and simulation of the turn-on delay time jitter in gain-switched semiconductor lasers," *IEEE J. Quant. Electron.*, vol. 28, no. 2, pp. 441–445, Feb. 1992.
[7] S. Miller, "Turn-on jitter in nearly single-mode injection lasers," *IEEE. J. Quantum. Electron.*, vol. QE-22, no. 1, pp. 16–19, Jan. 1986.
[8] C. Mirasso, P. Colet, and M. San Miguel, "Pulse statistics in single-mode semiconductor lasers modulated at gigahertz rates," *Opt. Lett.*, vol. 16, no. 22, pp. 1753–1755, Nov. 1991.
[9] ——, "Dependence of timing jitter on bias level for single mode semiconductor lasers under high speed modulation," *IEEE J. Quantum Electron.*, vol. 29, p. 23–32, Jan. 1992.
[10] E. Sano, M. Shinagawa, and R. Takahashi, "Theoretical analysis of timing jitter in gain-switched semiconductor lasers," *Appl. Phys. Lett.*, vol. 55, no. 6, pp. 522–524, Aug. 1989.
[11] R. Lang and K. Kobayashi, "External optical feedback effects on semiconductor injection laser properties," *IEEE. J. Quantum Electron.*, vol. QE-16, no. 3, pp. 347–355, Mar. 1980.
[12] R. Tkach and A. Chraplyvy, "Regimes of feedback effects in 1.5 μm distributed feedback lasers," *J. Lightwave Technol.*, vol. LT-4, no. 11, pp. 1655–1661, Nov. 1986.
[13] J. Mork, J. Mark, and B. Tromberg, "Route to chaos and competition between relaxation oscillations for a semiconductor laser with optical feedback," *Phys. Rev. Lett.*, vol. 65, no. 16, pp. 1999–2002, Oct. 1990.
[14] N. Schunk and K. Petermann, "Numerical analysis of the feedback regimes for a single-mode semiconductor laser with external feedback," *IEEE J. Quantum Electron.*, vol. 24, no. 7, pp. 1242–1247, July 1988.
[15] B. Clarke, "The effect of reflections on the system performance of intensity modulated laser diodes," *J. Lightwave Technol.*, vol. 9, no. 6, pp. 741–749, June 1991.
[16] D. Byrne, D. Maclean, and R. Plumb, "Optical feedback-induced noise in pigtailed laser diode modules," *IEEE Photonics Technol. Lett.*, vol. 3, no. 10, pp. 891–894, Oct. 1991.
[17] N. Schunk and K. Petermann, "Noise analysis of injection-locked semiconductor lasers," *IEEE J. Quantum Electron.*, vol. QE-22, no. 5, pp. 642–650, May 1986.
[18] H. Wu and H. Chang, "Turn-on jitter in semiconductor lasers with moderate reflecting feedback," *IEEE Photonics Technol. Lett.*, vol. 4, no. 4, pp. 339–342, Apr. 1992.
[19] K. Petermann, *Laser Diode Modulation and Noise.* Dordrecht, The Netherlands; Kluwer, 1988.
[20] P. Liu, L. Fencil, J. Ko, P. Kaminow, T. Lee, and C. Burrus, "Amplitude fluctuations and photon statistics of InGaAsP injection lasers," *IEEE J. Quantum Electron.*, vol. QE-19, no. 9, pp. 1348–1351, Sept. 1983.

Lloyd N. Langley was born in Newmarket, UK, on October 24, 1967. He received the B.Sc. degree in electrical and electronic engineering from the University of Bath, Bath, UK, in 1989.

From 1989 to 1991 he worked as an electronic engineer for DRA Aerospace, Farnborough, UK. Currently he is working towards the Ph.D. degree on the subject of optical feedback effects in laser diodes at the University of Bath.

K. Alan Shore (M'88) received the degree in mathematics from the University of Oxford, Oxford, UK, and the Ph.D. degree from the University of Wales, Cardiff, Wales, UK.

He was a Lecturer at the University of Liverpool (1979–1983) and then at the University of Bath where he became Senior Lecturer in 1986 and Reader in 1990. His work has been in the area of optoelectronic device simulation and modeling with particular emphasis on nonlinearities in laser diodes and semiconductor optical waveguides. He has authored or co-authored about 130 contributions to professional journals, books, and conferences. He cofounded and acts as Programme Committee Chair for the Conference on Semiconductor and Integrated Optoelectronics (SIOE) held annually in Cardiff, Wales, UK. He was a Visiting Researcher at the Center for High Technology Material, University of New Mexico, Albuquerque, in the summer of 1987. He received a Royal Society Travel Grant to visit universities and laboratories in Japan in July 1988. Between July and September 1989 he was a Visiting Researcher at the Huygens Laboratory, Leiden University, The Netherlands. During the Summers of 1990 and 1991 as well as Springs of 1991 and 1992 he worked at the Danish Telecom Research Laboratory (TFL) and the Technical University of Denmark, Laboratory of Applied Mathematical Physics (MIDIT). He was a guest researcher at the Electrotechnical Laboratory (ETL), Tsukuba, Japan in February/March 1991. He spent September 1992 as a visiting Professor at the Department of Physics, University de les Illes Balears, Palma-Mallorca, Spain.

Effect of phase-conjugate optical feedback on the intensity noise in laser diodes

L. N. Langley and K. A. Shore

School of Electronic and Electrical Engineering, University of Bath, Bath BA2 7AY, UK

Received March 19, 1993

The intensity noise and turn-on delay jitter of laser diodes with optical feedback from a phase-conjugate mirror are investigated numerically. Low levels of phase-conjugate optical feedback cause a small intensity noise reduction in semiconductor lasers. The behavior of the intensity noise for increased phase-conjugate feedback is shown to be different than that for increased conventional-mirror feedback.

The performance of a semiconductor laser is sensitive to optical feedback.[1,2] Low levels of optical feedback can be used to narrow the laser linewidth. Unwanted optical feedback of sufficient strength can cause the laser to enter the coherence collapse regime, which results in dramatically increased linewidth and intensity noise[2] and severely degrades the performance of communications systems. The effect of optical feedback on laser diodes is dependent on the strength of the optical feedback and on the distance between the laser diode and the external mirror. The external cavity length determines the external cavity round-trip time as well as the phase of the reflected light relative to the light emitted from the laser facet. Phase-conjugate optical feedback eliminates the laser's dependence on the external cavity phase change because any phase shift owing to the outward journey is canceled by the phase shift owing to the return path length. The feedback is, however, still delayed by the external cavity round-trip delay. Therefore there are significant differences between the behavior of laser diodes with optical feedback from conventional versus phase-conjugate mirrors.[3–5] Phase-conjugate feedback was used to narrow the linewidth of a semiconductor laser.[6,7] The intensity noise was also reduced in a gas laser by the use of external phase-conjugate optical feedback.[8]

The laser model used in this investigation is appropriate to a distributed-feedback laser with external phase-conjugate optical feedback.[3–5] The model is based on the single-mode rate equations, with additional terms for the phase-conjugate optical feedback,

$$\frac{\mathrm{d}}{\mathrm{d}t}N(t) = \frac{I(t)}{e(V)} - \frac{N(t)}{\tau_e} - G|E(t)|^2, \tag{1}$$

$$\frac{\mathrm{d}}{\mathrm{d}t}E(t) = i(\omega_0 - \Omega) + \frac{1}{2}\left(G - \frac{1}{\tau_p}\right)(1 - i\alpha)E(t) + \kappa E^*(t - \tau)\exp(i\Phi_{\mathrm{PCM}}). \tag{2}$$

In the rate equations, $N(t)$ is the carrier density, $E(t)$ is the optical field, $I(t)$ is the injection current, e is the electronic charge, V is the active region volume, τ_e is the carrier lifetime, $|E(t)|^2$ represents the photon density, ω_0 is the optical frequency with feedback, Ω is the optical frequency without feedback, τ_p is the photon lifetime, and α is the linewidth enhancement factor. The optical gain G is assumed to be of the form

$$G = G_N[N(t) - N_0][1 - \epsilon|E(t)|^2], \tag{3}$$

where G_N is the gain slope and ϵ is the saturation parameter.

In the optical feedback terms, $E^*(t - \tau)$ is the reflected phase-conjugate optical field, τ is the external cavity round-trip delay, Φ_{PCM} is an arbitrary constant phase change introduced by the phase-conjugate mirror, and κ is the feedback, given by

$$\kappa = \eta\frac{(1 - R)}{\tau_L}\left(\frac{R_{\mathrm{ext}}}{R}\right)^{1/2}. \tag{4}$$

In Eq. (4), η is the laser-to-external-cavity coupling efficiency, R is the laser facet reflectivity, τ_L is the laser internal round-trip delay, and R_{ext} is the phase-conjugate mirror reflectivity.

The difference between modeling optical feedback from conventional versus phase-conjugate mirrors lies in the optical feedback terms of Eq. (2). For phase-conjugate optical feedback, there is no external cavity phase shift $\omega_0\tau$ in the optical feedback term. The phase-conjugate mirror is assumed to introduce no frequency change during the reflection process. The phase-conjugate mirror is also assumed to have an instantaneous response time. If the response time of the phase-conjugate mirror is not instantaneous, then the feedback rate becomes time dependent. The rate equations are solved numerically, with Langevin noise terms included to model spontaneous emission noise.

Low-to-moderate levels of optical feedback are considered in this investigation (i.e., $R_{\mathrm{ext}} < 1\%$). This encompasses regimes I–IV of conventional-mirror feedback,[2] including the chaotic coherence collapse state.

First, constant-current simulations are considered for optical feedback from both conventional and phase-conjugate mirrors. The relative intensity noise is calculated for increasing external reflectivity for various bias currents, as shown in Fig. 1. The

0146-9592/93/171432-03$6.00/0

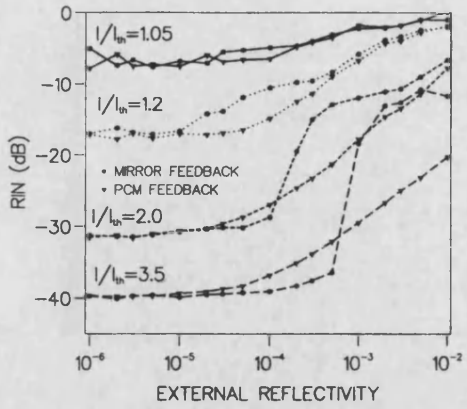

Fig. 1. Relative intensity noise (RIN) for both conventional-mirror and phase-conjugate-mirror (PCM) optical feedback versus increasing external reflectivity ($\tau = 2$ ns).

external cavity round-trip delay τ is 2 ns. It can be seen that optical feedback from a conventional mirror increases the intensity noise as the external reflectivity increases.[2] The sudden increase in the intensity noise corresponds to the laser entering the coherence collapse feedback regime. In contrast, in the case of optical feedback from a phase-conjugate mirror, the increase in intensity noise is much more gradual. Lower levels of phase-conjugate feedback are required to increase the intensity noise above that of the solitary laser than the levels required for conventional-mirror feedback. At low external reflectivity, the intensity noise with phase-conjugate optical feedback is larger than that caused by conventional-mirror feedback of the same strength. The situation is reversed at higher external reflectivity, in which case the intensity noise is greatest for conventional-mirror optical feedback. These results show that the laser becomes unstable and develops output power fluctuations at lower external reflectivity than occurs with conventional-mirror optical feedback.[9] At high levels of feedback, the laser output is chaotic, just as for conventional-mirror feedback, but the transition to chaos is at higher levels of phase-conjugate feedback than it is for conventional-mirror feedback. The difference in the laser intensity noise induced by the two types of optical feedback can be attributed to the round-trip phase-canceling property of the phase-conjugate mirror. The phase difference between the reflected and emitted light plays an important part in the determination of the intensity-noise properties of an external cavity laser. In the case of optical feedback from a conventional mirror, the round-trip phase change $\omega_0\tau$ that is due to the external cavity path length is unlikely to be a multiple of 2π rad. Therefore the reflected light is not in phase with the emitted light. A phase-conjugate mirror ensures that there is no phase change owing to the external cavity path length. Therefore the reflected light is in phase with the emitted light, and hence a different intensity-noise behavior results for the two types of optical feedback.

The output power probability distribution functions (PDF's), as shown in Fig. 2, give a clearer indication of the effect of lower levels of optical feedback from a phase-conjugate mirror on the intensity-noise properties of the laser. The laser is operated at twice the threshold current and with an external reflectivity of 2×10^{-6}. The output power PDF for the solitary laser corresponds to a relative intensity-noise value of -30.4 dB. The output power PDF with phase-conjugate optical feedback is narrower than that of the solitary laser, corresponding to a relative intensity-noise value of -31.7 dB, which is a small decrease in intensity noise. Hence phase-conjugate optical feedback has narrowed the output power PDF by reducing the intensity noise in the laser output. Further investigations show that the noise-reduction properties of the phase-conjugate optical feedback are independent of the external cavity round-trip delay. A lower level of intensity noise will result in a lower level of turn-on delay jitter, hence improving the error-rate performance of an optical communications system.

Figure 2 shows that it is possible for phase-conjugate feedback to cause a small decrease in the intensity noise in the laser output power.

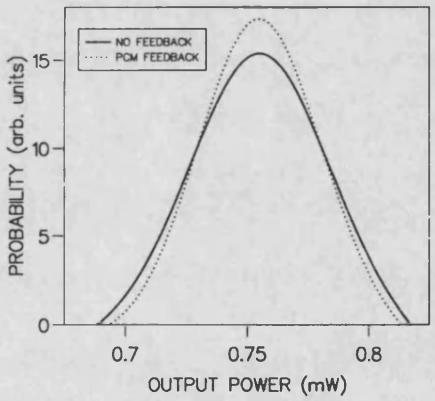

Fig. 2. Output power PDF's with and without phase-conjugate optical feedback ($I/I_{th} = 2.0$, $R_{ext} = 2 \times 10^{-6}$, $\tau = 2$ ns).

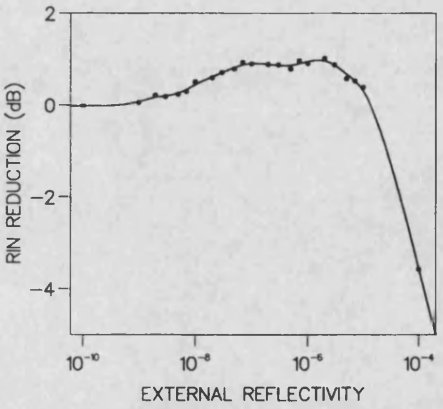

Fig. 3. Reduction of RIN owing to phase-conjugate optical feedback ($I/I_{th} = 2.0$, $\tau = 2$ ns).

Figure 3 shows the noise-reduction dependence on the level of phase-conjugate optical feedback. The intensity noise is reduced for a phase-conjugate reflectivity between 10^{-9} and 10^{-5}. For greater values of external reflectivity the intensity noise is increased. It was found that the phase-conjugate optical feedback can significantly reduce the low-frequency intensity noise[10] (as much as a few hundred megahertz). There is little reduction of the higher-frequency intensity noise. Since most intensity noise will be of frequencies around the relaxation oscillation frequency and above, the overall intensity-noise reduction will be small, as shown in this Letter.

In summary, the effect of optical feedback from a phase-conjugate mirror into a single-mode semiconductor laser has been studied with respect to the laser intensity-noise properties. The intensity-noise behavior of a laser diode with phase-conjugate optical feedback is quite different from that with conventional-mirror optical feedback. Phase-conjugate feedback of the appropriate level can be used to decrease the levels of intensity noise in the laser output power. The decrease in intensity noise owing to phase-conjugate optical feedback is attributed to the lack of an external round-trip phase change.

This study was undertaken in a UK Science and Engineering Research Council, Cooperative Awards in Science and Engineering project supported by Northern Telecom, Paignton, Devon, UK. The authors thank A. Janssen of Northern Telecom for discussions.

References

1. G. P. Agrawal and N. K. Dutta, *Long-Wavelength Semiconductor Lasers* (Van Nostrand Reinhold, New York, 1986), p. 271.
2. K. Petermann, *Laser Diode Modulation and Noise* (Kluwer Academic, Dordrecht, The Netherlands, 1988), p. 250.
3. G. P. Agrawal and J. T. Klaus, Opt. Lett. **16,** 1325 (1991).
4. G. H. M. van Tartwijk, H. J. C. van der Linden, and D. Lenstra, Opt. Lett. **17,** 1590 (1992).
5. G. P. Agrawal and G. R. Gray, Phys. Rev. A **46,** 5891 (1992).
6. K. Vahala, K. Kyuma, A. Yariv, S. K. Kwong, M. Cronin-Golomb, and K. Y. Lau, Appl. Phys. Lett. **49,** 1563 (1986).
7. M. Ohtsu, I. Koshiishi, and Y. Teramachi, Jpn. J. Appl. Phys. **29,** L2060 (1990).
8. N. McCarthy and D. Gay, Opt. Lett. **16,** 1004 (1991).
9. L. N. Langley and K. A. Shore, in *Conference on Lasers and Electro-Optics,* Vol. 11 of 1993 OSA Technical Digest Series (Optical Society of America, Washington, D.C., 1993), paper CThS36.
10. G. P. Agrawal, D. Huang, and G. R. Gray, in *Conference on Lasers and Electro-Optics,* Vol. 11 of 1993 OSA Technical Digest Series (Optical Society of America, Washington, D.C., 1993), paper CWJ43.

Intensity noise and linewidth characteristics of laser diodes with phase conjugate optical feedback

L.N. Langley
K.A. Shore

Indexing terms: Intensity noise, Laser diodes, Phase conjugate optical feedback

Abstract: The intensity noise and linewidth characteristics of semiconductor lasers with phase conjugate optical feedback are investigated numerically. The results are compared to those from conventional mirror optical feedback. The dynamics of semiconductor lasers with phase conjugate optical feedback are also considered. The relevance to phase conjugate optical feedback of the feedback regimes used to describe conventional mirror optical feedback is discussed.

1 Introduction

The use of phase conjugate feedback with semiconductor lasers has attracted attention recently [1–14]. Recent work has investigated the noise and dynamic properties of semiconductor lasers with phase conjugate feedback [1–4], showing that the laser properties are different to those with conventional mirror optical feedback. The intensity noise in a gas laser has been significantly reduced using phase conjugate feedback [5]. In semiconductor lasers phase conjugate feedback has been used to narrow the laser linewidth [6, 7]. Phase conjugate mirrors (PCM) have also attracted attention as a means of coupling together the individual laser elements in laser arrays [8].

Conventional mirror feedback even at very low levels can significantly affect the performance of semiconductor lasers [15–20]. Dramatic changes in the noise characteristics of semiconductor lasers occur under the influence of optical feedback. Unwanted optical feedback, such as may occur from components in optical communications systems, can increase the intensity noise [15, 16], resulting in higher error rates [15]. Five distinct regimes, denoted I–V, of the operating characteristics of semiconductor lasers with optical feedback have been identified and investigated [17, 18]. Factors influencing the laser with optical feedback are the external cavity round trip delay, the external reflectivity, and the external cavity round trip phase change. In feedback regime I, for very low feedback levels, the linewidth is increased or decreased depending on the phase of the light returned into the laser compared to that leaving the laser. In feedback regime II, multiple external cavity modes exist and the laser locks to the mode with the lowest linewidth. However, if several modes exist with similar linewidth mode hopping can cause the overall linewidth to be larger than that of the solitary laser. In regime III, the linewidth is significantly reduced with the reduction being independent of the phase of the reflected light. Regime IV is the so-called 'coherence collapse' state in which intensity noise and linewidth are significantly increased [17–19]. In this regime the laser output behaves chaotically. Regime V corresponds to stable operation at very high feedback levels but will not be considered in this work.

Phase conjugate mirrors used to provide optical feedback into semiconductor lasers have been implemented in two ways. The first of these is to use a nonlinear crystal [6, 9–12] to generate the reflected phase conjugate beam. The second is to perform four wave mixing (FWM) within another semiconductor optical amplifier [7]. Degenerate four wave mixing (DFWM) produces a reflection of the same frequency as the incident beam, whilst nondegenerate four wave mixing (NDFWM) produces a reflection of a slightly different frequency from the incident beam. Only DFWM phase conjugate feedback is considered in this work.

A phase conjugate mirror has the property of reversing the phase of the reflected light with respect to the incident light. This has the result that there is zero external cavity round trip phase change when a phase conjugate mirror is used to provide optical feedback into a laser [1]. Thus, it is to be expected that a semiconductor laser with phase conjugate feedback will behave differently to that with conventional mirror feedback. This paper investigates the effect of phase conjugate feedback on the semiconductor laser.

2 Numerical model of phase conjugate optical feedback

In this investigation, ideal phase conjugate feedback is considered in which the phase conjugate mirror has zero response time and introduces no frequency change in the reflected light. The system of a semiconductor laser with phase conjugate feedback is shown in Fig. 1. Using this idealised phase conjugate mirror, the carrier and electric field rate equations for a single mode semiconductor laser with phase conjugate optical feedback are [1, 2]

Paper 9917J (E3, E13), first received 30th June and in revised form 23rd September 1993

The authors are with the University of Bath, School of Electronic and Electrical Engineering, Bath, BA2 7AY, United Kingdom

This work was undertaken in a UK SERC CASE project supported by Northern Telecom, Paignton, Devon, UK. The authors thank Dr. A. Janssen of Northern Telecom for discussions.

$$\frac{d}{dt}n(t) = \frac{I}{eV} - \frac{n(t)}{\tau_e} - G|E(t)|^2 \quad (1)$$

$$\frac{d}{dt}E(t) = i(\omega_0 - \Omega) + \frac{1}{2}\left(G - \frac{1}{\tau_p}\right)(1 - i\alpha)E(t) + \kappa E^*(t - \tau)\exp\{i\Phi_{PCM}\} \quad (2)$$

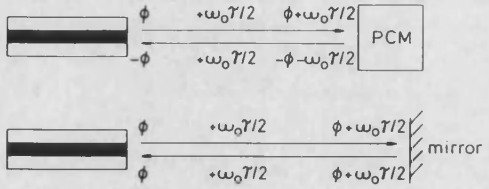

Fig. 1 *Comparison of external cavity phase changes for phase conjugate and conventional mirror feedback*

In the rate equations, $n(t)$ is the carrier density, I is the injection current and $E(t)$ is the electric field strength. The reflected phase conjugate electric field is $E^*(t - \tau)$, where τ is the external cavity round trip delay. The terms ω_0 and Ω are the laser frequency with and without optical feedback. An arbitrary phase change within the phase conjugate mirror, Φ_{PCM}, may be included, but is given the value zero in this work. The optical gain G is assumed to be of the form

$$G = G_n(n(t) - n_0)\frac{1}{(1 + \varepsilon|E(t)|^2)} \quad (3)$$

The feedback rate, κ, is given by

$$\kappa = \eta\frac{(1 - R)}{\tau_L}\sqrt{\left(\frac{R_{PCM}}{R}\right)} \quad (4)$$

where R_{PCM} is the phase conjugate mirror reflectivity. Other laser parameters used in the rate equations are listed with their values in Table 1.

Table 1: Laser parameters

Symbol	Description	Value
V	active region volume	1.5×10^{-16} m^3
e	electronic charge	1.6022×10^{-19} As
τ_e	carrier lifetime	2 ns
ω_0	operating frequency	$\equiv 1.55$ μm
τ_p	photon lifetime	2 ps
α	linewidth broadening factor	5.5
G_n	gain slope	2.125×10^{-12} m^3 s^{-1}
n_0	transparency carrier density	4×10^{23} m^{-3}
ε	saturation parameter	3×10^{-23} m^3
η	laser to fibre coupling efficiency	0.4
R	laser facet reflectivity	0.309
τ_L	laser cavity round trip time	9 ps
γ	spontaneous emission factor	10^{-5}
n_{th}	threshold carrier density	9.9×10^{23} m^{-3}
τ	external cavity round trip delay	2 ns

For ease of numerical solution, and to provide information on the photon density, the electric field rate equation is transformed into two rate equations for photon density and electric field phase [15, 16, 21]

$$\frac{ds}{dt} = \frac{\gamma n}{\tau_e} - \frac{s}{\tau_p} + Gs + 2\kappa\sqrt{(s)}\sqrt{[s(t - \tau)]}\cos[\theta(t)] \quad (5)$$

$$\frac{d\phi}{dt} = \frac{\alpha}{2}G_n(n - n_{th})\Gamma - \kappa\frac{\sqrt{[s(t - \tau)]}}{\sqrt{(s)}}\sin[\theta(t)] \quad (6)$$

For phase conjugate optical feedback generated using DFWM, $\theta(t)$ takes the form

$$\theta(t) = \phi(t) + \phi(t - \tau) + \Phi_{PCM} \quad (7)$$

If NDFWM is used to generate the phase conjugate reflection $\theta(t)$ has an additional term containing the detuning $\Delta\omega$, between the pump and signal beams [3]. Eqn. 7 should be contrasted with that for conventional mirror optical feedback,

$$\theta(t) = \omega_0\tau + \phi(t) - \phi(t - \tau) + \Phi_{ext} \quad (8)$$

where Φ_{ext} is an arbitrary phase change at the mirror. The arbitrary phase change is again chosen to be zero. The external mirror reflectivity R_{ext} should replace R_{PCM} when considering conventional mirror feedback.

The significant difference between the two types of feedback is the term $\omega_0\tau$ in eqn. 8. This is the external cavity round trip phase change. Fig. 1 shows why $\omega_0\tau$ does not appear in the model for phase conjugate feedback [1, 2]. The nature of the phase conjugate mirror is to reverse the phase of the incident light as it is reflected. Hence, any phase shift acquired by the light due to the outward path length is exactly cancelled by the phase shift acquired during the return path length. Therefore, the laser's dependence on the external cavity round trip phase change is eliminated. The phase conjugate feedback is, however, still retarded by the external cavity round trip delay.

Langevin noise sources are added to eqns. 1, 5 and 6 to model spontaneous emission noise [22]. They are calculated by

$$F_n(t) = -\sqrt{\left[\frac{2S(t_i)\gamma n}{\tau_e\,\Delta t}\right]}x_s + \sqrt{\left[\frac{2n(t_i)}{\tau_e\,\Delta t V}\right]}x_n \quad (9)$$

$$F_s(t) = \sqrt{\left[\frac{2S(t_i)\gamma n}{\tau_e\,\Delta t}\right]}x_s \quad (10)$$

$$F_\phi(t) = \frac{1}{S(t)}\sqrt{\left[\frac{S(t_i)\gamma n}{2\tau_e\,\Delta t}\right]}x_\phi \quad (11)$$

Here, $s(t_i)$ and $n(t_i)$ are the photon density and carrier density, respectively, within the interval t and $t + \Delta t$. γ is the spontaneous emission factor which determines the level of spontaneous emission. The symbols x_n, x_s, x_ϕ are Gaussian distributed random variables with zero mean and unity variance.

The rate equations with phase conjugate feedback and Langevin noise terms are solved numerically using a variable-step, variable-order Runge–Kutta algorithm. Interest is restricted to the static properties of the system where the injection current is held constant. To evaluate the reflection terms in the rate equations, values of photon density and electric field phase calculated at an earlier solution step are required. Thus, at each solution step, the values of photon density and electric field phase are recorded for use at a later solution step. The number of solution steps between the recording and the use of these values is equivalent to the external cavity round trip delay. Langevin noise is modelled by applying random noise forces as calculated in eqns. 9, 10 and 11. The Gaussian distributed random variables x_n, x_s and x_ϕ

are calculated at the start of, and are held constant throughout, each Langevin noise application interval, Δt. The interval Δt is chosen to be 10 ps. This results in a power spectral density for the noise which has its first zero at a frequency of 100 GHz ($1/\Delta t$). The noise forces should describe a white noise spectrum at least up to the relaxation oscillation frequency [22]. The influence of Δt on the power spectral density of the noise is discussed in Appendix A of Reference 20. The 3 dB frequency is found to be approximately 40 GHz, which is many times the maximum relaxation oscillation frequency encountered in the following investigations. Hence, the condition that the noise spectrum is white up to a frequency greater than the relaxation oscillation frequency is satisfied.

3 Intensity noise properties

First, noise properties of laser diodes in the case of constant injection current are considered for optical feedback from both conventional and phase conjugate mirrors. The noise properties are characterised by relative intensity noise (RIN), and is calculated from the expression

$$\mathrm{RIN} = \frac{\overline{P_0(t)^2} - \overline{P_0(t)^2}}{P_0(t)^2} \qquad (12)$$

where $p_0(t)$ are the output power samples. Fig. 2 shows the behaviour of the RIN for various injection currents as

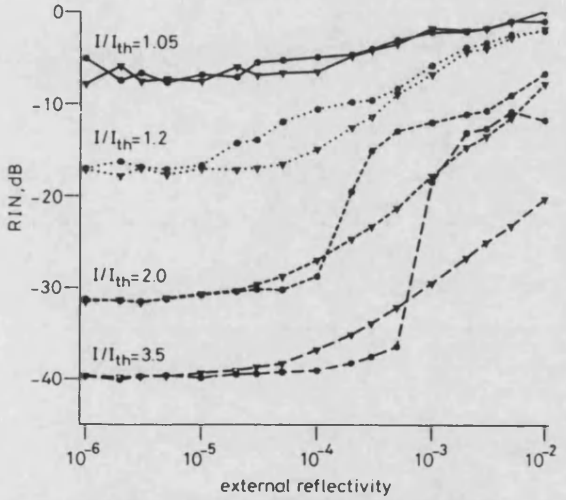

Fig. 2 *Relative intensity noise (RIN) for increasing levels of conventional mirror and phase conjugate feedback, at several injection currents*

● mirror feedback
▼ PCM feedback

the external reflectivity is increased. It can be seen that optical feedback from a conventional mirror increases the intensity noise as the external reflectivity increases [15–20]. The sudden increase in the intensity noise corresponds to the laser entering the coherence collapse feedback regime. In contrast, with optical feedback from a phase conjugate mirror the increase in intensity noise is much more gradual. Lower levels of phase conjugate feedback are required to increase the intensity noise above that of the solitary laser than is required for conventional mirror feedback. At low external reflectivity, the intensity noise with phase conjugate feedback is larger than that caused by conventional mirror feedback of the same strength. The situation is reversed at higher external reflectivity where the intensity noise is greatest for conventional mirror feedback. In the transition to coherence collapse, the increase in the RIN occurs at all frequencies to some extent, but particularly at the relaxation oscillation frequency of the solitary laser and at multiples of the inverse external cavity round trip delay. These results show that the laser becomes unstable and develops output power fluctuations (i.e. intensity noise) at lower external reflectivity for phase conjugate feedback than occurs with conventional mirror feedback [13].

The output power waveforms at four different levels of external reflectivity are shown in Fig. 3 for phase conjugate and conventional mirror feedback. The Langevin

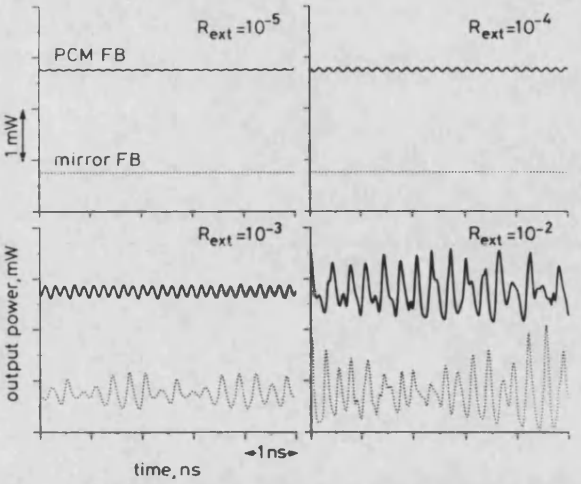

Fig. 3 *Comparison of optical output power fluctuations for several levels of phase conjugate and conventional mirror feedback*
$I = 2I_{th}$ power levels are displaced for clarity

noise sources have been disabled to obtain a clearer picture of the effects of optical feedback. The results agree with the observations from Fig. 2 that output power fluctuations occur at lower levels of external reflectivity with phase conjugate than for conventional mirror feedback. At low external reflectivity (10^{-5} and 10^{-4}) the phase conjugate feedback causes a single frequency oscillation in the output power. The frequency of the oscillation is twice the relaxation oscillation frequency of the solitary laser. At the same low levels of external reflectivity for conventional mirror feedback, the output power waveform is stable. At high external reflectivity (10^{-2}), the waveforms with both types of optical feedback appear to be chaotic. However, the output power waveform at moderate reflectivity (10^{-3}) for conventional mirror feedback appears to be almost chaotic, whilst that for phase conjugate feedback still has a regular period. Hence, the transition to a chaotic output occurs at higher levels of external reflectivity for phase conjugate feedback.

The output power fluctuation frequency spectra corresponding to Fig. 3 are shown in Figs. 4 and 5 for phase conjugate and conventional mirror feedback, respectively. These graphs are the intensity noise spectra due to optical feedback only, plotted on a linear vertical axis. At low feedback levels (10^{-5} and 10^{-4}) phase conjugate feedback results in a single frequency oscillation that is twice the relaxation oscillation frequency. No output power fluctuation frequency spectra are shown for conventional mirror feedback at low external reflectivities (10^{-5} and 10^{-4}) because the laser output is stable. At moderate external reflectivity (10^{-3}) it is seen that phase conjugate feedback causes only a few frequency components at integer multiples of the relaxation oscillation frequency. Conventional mirror feedback of the same strength causes many frequencies to be present

in the output power fluctuations, with spacing corresponding to the inverse of the external cavity round trip delay. Large numbers of frequency components indicate

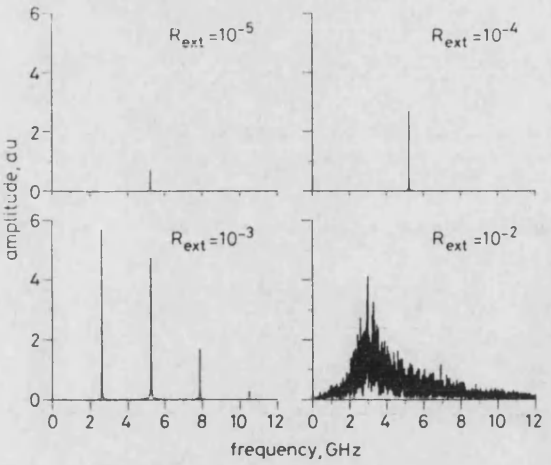

Fig. 4 *Optical output power fluctuation frequency components for several levels of phase conjugate feedback* $I = 2I_{th}$

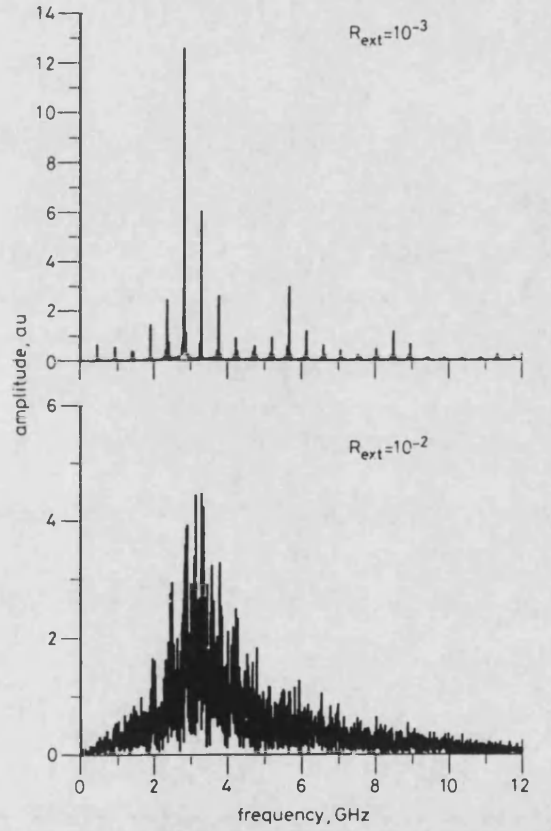

Fig. 5 *Optical output power fluctuation frequency components for several levels of conventional mirror feedback* $I = 2I_{th}$

that the laser is tending towards chaotic behaviour. For high levels of external reflectivity (10^{-2}), both types of feedback cause chaotic fluctuations, as seen from the very large number of frequency components present in the output power fluctuations. At this high reflectivity, both types of feedback cause the laser to operate in feedback regime IV (i.e. coherence collapse). The output power fluctuation frequency spectra confirm that phase conjugate optical feedback causes output power fluctuations at lower levels of external reflectivity than conventional mirror feedback; and that the transition to chaotic output power fluctuations is at a higher external reflectivity for phase conjugate than for conventional mirror feedback.

Fig. 6 shows the levels of RIN at different frequencies, for a phase conjugate reflectivity of 10^{-6}. This graph is

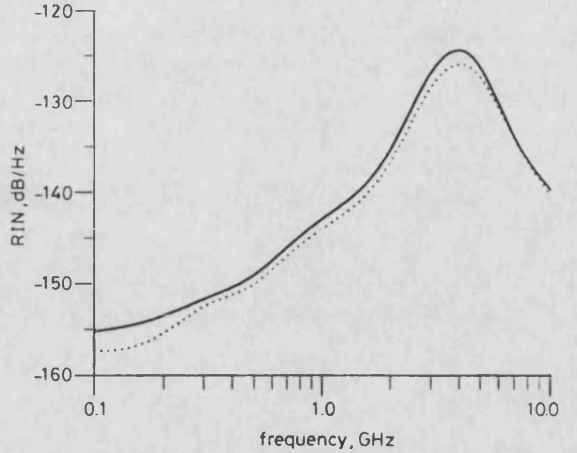

Fig. 6 *Variation of relative intensity noise (RIN) with frequency for solitary laser and for phase conjugate optical feedback* $I = 2I_{th}$, $R_{ext} = 10^{-6}$

——— $R_{ext} = 0$
····· $R_{ext} = 10^{-6}$

similar to that of Figs. 4 and 5, but with spontaneous emission noise included and plotted on a logarithmic vertical axis. At low levels of phase conjugate feedback, the intensity noise can be reduced [4, 14]. The reduction is a very small one, only becoming significant at very low frequencies of a few hundred MHz [13]. The intensity noise reduction is much less than that which has been achieved with phase conjugate feedback into a gas laser [5], and is not large enough to be of practical use.

The phase difference between the reflected and emitted light plays an important part in determining the intensity noise properties of an external cavity laser. With optical feedback from a conventional mirror the round trip phase change, $\omega_0 \tau$, due to the external cavity path length is very unlikely to be a multiple of 2π radians. Therefore, the reflected light is not in phase with the emitted light. A phase conjugate mirror ensures that there is zero phase change due to the external cavity path length. The reflected light is thus in phase with the emitted light, and hence a different intensity noise behaviour results for the two types of optical feedback. The difference in the intensity noise behaviour of a semiconductor laser induced by phase conjugate and conventional mirror feedback can be attributed to the round trip phase cancelling property of the phase conjugate mirror.

4 Linewidth behaviour and optical feedback regimes

The linewidth $\Delta\nu$ of a semiconductor laser can be determined from the two-sided spectral density of the frequency fluctuations S_ϕ

$$\Delta\nu = \frac{S_\phi}{2\pi} \tag{13}$$

This relation is defined for a white frequency noise spectrum. Optical feedback causes the frequency noise spectrum to be very unlike a white noise spectrum, as seen in

Fig. 7. However, eqn. 13 holds for a nonwhite frequency noise spectrum if S_ϕ is replaced by $S_\phi(f \to 0)$ [20].

The behaviour of the linewidth as the external reflectivity is increased is shown in Fig. 8. The graph shows

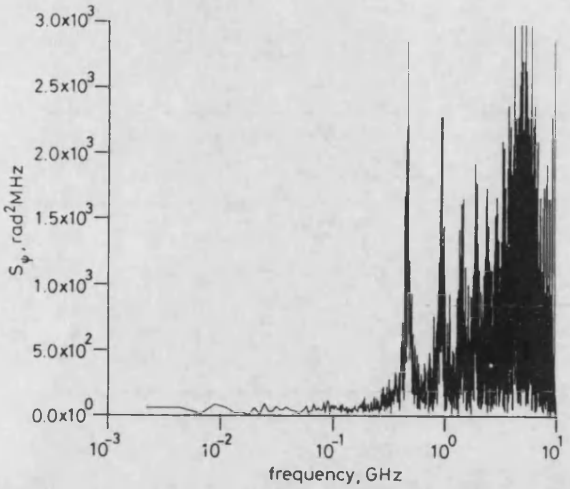

Fig. 7 *Two-sided spectral density of frequency fluctuations* ($I = 3.5I_{th}$, $R_{ext} = 10^{-3}$)

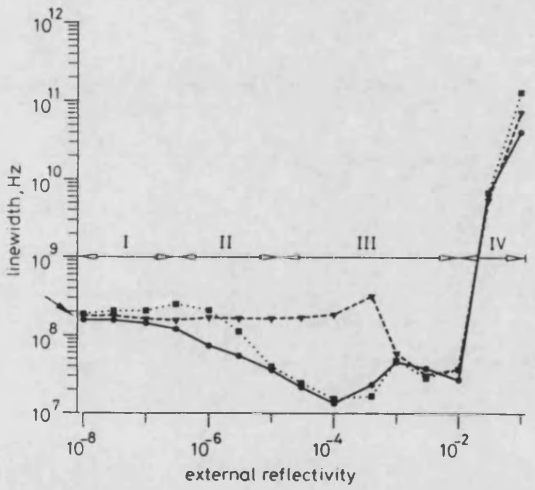

Fig. 8 *Linewidth for phase conjugate and conventional mirror optical feedback* $I = 3.5I_{th}$

Roman numerals indicate conventional mirror optical feedback regimes, solid arrow indicates solitary laser linewidth

—●— mirror FB ($\omega\tau = 0$)
- -■- - mirror FB ($\omega\tau = \pi/2$)
- -▼- - PCM FB

linewidth for increasing levels of phase conjugate feedback. The linewidth for increasing levels of conventional mirror feedback with two different external cavity round trip phase changes $\omega_0 \tau$ is also shown. It can be seen that there is a very different behaviour between the two types of optical feedback. The feedback regimes I–IV [17, 18] are shown for conventional mirror feedback. At low levels of mirror feedback, regimes I and II, the linewidth is increased or decreased depending on the phase of the reflected light. At higher levels of conventional mirror feedback, regime III, the linewidth is reduced and is independent of the phase of the reflected light. For very high levels of external reflectivity the laser enters regime IV, and the linewidth is dramatically increased. Since there is zero round trip phase change with phase conjugate feedback, it is anticipated that feedback regimes I and II do not exist. Fig. 8 confirms this. Quite large levels of phase conjugate feedback are required before the linewidth is altered from that of the solitary laser. The reduced linewidth regime III can be obtained with phase conjugate feedback but occurs at higher levels of external reflectivity than for conventional mirror feedback. A transition to regime IV, coherence collapse, is found for phase conjugate feedback as for conventional mirror feedback.

Phase conjugate feedback has a different effect on the linewidth behaviour of semiconductor lasers to that of conventional mirror feedback as the level of external reflectivity is increased. The feedback regimes I and II do not exist for phase conjugate optical feedback. Feedback regime III has a smaller range for phase conjugate than for conventional mirror feedback. Feedback regime IV is unchanged between the two types of optical feedback.

5 Conclusions

The intensity noise and linewidth characteristics of a semiconductor laser with phase conjugate feedback have been investigated. The results show that different intensity noise behaviour occurs with the two types of optical feedback as the external reflectivity is increased. Output power fluctuations occur at lower levels of phase conjugate external reflectivity than for conventional mirror feedback. However, the transition to the chaotic coherence collapse laser output state occurs at a higher level of external reflectivity for phase conjugate than for conventional mirror feedback. Low levels of phase conjugate feedback have the effect of reducing low frequency intensity noise, up to a few hundred Megahertz.

The behaviour of the linewidth with increasing external reflectivity is also qualitatively different for the two types of optical feedback. Higher levels of external reflectivity are required to decrease the linewidth with phase conjugate feedback than for conventional mirror feedback. The feedback regimes III and IV can be used to describe phase conjugate feedback effects in semiconductor lasers but regimes I and II cannot be used as they have a dependence on an external cavity phase change, which is eliminated by phase conjugate feedback. Phase conjugate mirrors fabricated from semiconductor optical amplifiers are quite capable of generating a very large external reflectivity. The behaviour of semiconductor lasers with high levels of phase conjugate feedback will be analogous to feedback regime V for conventional mirror feedback. Further work on the properties of semiconductor lasers with very high levels of phase conjugate feedback needs to be performed.

6 References

1 AGRAWAL, G.P., and KLAUS, J.T.: 'Effect of phase-conjugate feedback on semiconductor laser dynamics', *Optics Lett.*, 1991, **16**, pp. 1325–1327

2 AGRAWAL, G.P., and GRAY, G.R.: 'Effect of phase-conjugate feedback on the noise characteristics of semiconductor lasers', *Phys. Rev. A*, 1992, **46**, pp. 5890–5898

3 VAN TARTWIJK, G.H.M., VAN DER LINDEN, H.J.C., and LENSTRA, D.: 'Theory of a diode laser with phase conjugate feedback', *Optics Lett.*, 1992, **17**, pp. 1590–1592

4 LANGLEY, L.N., and SHORE, K.A.: 'The effect of phase conjugate optical feedback on the intensity noise in laser diodes', *Optics Lett.*, 1993, **18**, pp. 1432–1434

5 McCARTHY, N., and GAY, D.: 'Noise reduction in an argon laser with a phase-conjugating external cavity', *Optics Lett.*, 1991, **16**, pp. 1004–1006

6 VAHALA, K., KYUMA, K., YARIV, A., KWONG, S.K., CRONIN-GOLOMB, M., and LAU, K.Y.: 'Narrow linewidth single frequency semiconductor laser with a phase conjugate external cavity mirror', *Appl. Phys. Lett.*, 1986, **49**, pp. 1563–1565

7 OHTSU, M., KOSHIISHI, I., and TERAMACHI, Y.: 'A semiconductor laser as a stable phase conjugate mirror for linewidth reduction of another semiconductor laser', *Jap. J. Appl. Phys.*, 1990, **29**, pp. L2060–L2062
8 MACCORMAK, S., and EASON, R.W.: 'Near-diffraction-limited single-lobe emission from a high-power diode-laser array coupled to a photorefractive self-pumped phase-conjugate mirror', *Optics Lett.*, 1991, **16**, pp. 705–707
9 CHAMPAGNE, Y., McCARTHY, N., and TREMBLAY, R.: 'Optical phase-conjugate feedback effects in gain-guided diode laser characteristics', *IEEE J.*, 1989, **QE-25**, pp. 595–601
10 CRONIN-GOLOMB, M., and YARIV, A.: 'Self-induced frequency scanning and distributed Bragg reflection in semiconductor lasers with phase conjugate-feedback', *Optics Lett.*, 1986, **11**, pp. 455–457
11 BOCHOVE, E.J.: 'Transverse-mode instability and chaos in an optical cavity with phase-conjugate mirror', *Optics Lett.*, 1986, **11**, pp. 727–729
12 STEPHENS, R.R., LIND, R.C., and GIULIANO, C.R.: 'Phase conjugate master oscillator-power amplifier using $BaTiO_3$ and AlGaAs semiconductor diode lasers', *Appl. Phys. Lett.*, 1987, **50**, pp. 647–649
13 AGRAWAL, G.P., HUANG, D., and GRAY, G.R.: 'Effect of phase-conjugate feedback on the intensity and phase noise of semiconductor lasers'. Conference on lasers and electro-optics CLEO'93, Baltimore, Maryland, USA, 1993, CWJ43
14 LANGLEY, L.N., and SHORE, K.A.: 'Intensity noise in laser diodes with phase-conjugate optical feedback'. Conference on lasers and electro-optics CLEO'93, Baltimore, Maryland, USA, 1993, CThS36
15 PETERMANN, K.: 'Laser diode modulation and noise' (Kluwer Academic, Dordrecht, The Netherlands, 1988)
16 CLARKE, B.R.: 'The effect of reflections on the system performance of intensity modulated laser diodes', *IEEE J.*, 1991, **LT-9**, pp. 741–749
17 TKACH, R.W., and CHRAPLYVY, A.R.: 'Regimes of feedback effects in 1.5 μm distributed feedback lasers', *IEEE J.*, 1986, **LT-4**, pp. 1655–1661
18 SCHUNK, N., and PETERMANN, K.: 'Numerical analysis of the feedback regimes for a single-mode semiconductor laser with external feedback', *IEEE J.*, 1988, **QE-24**, pp. 1242–1247
19 LENSTRA, D., VERBEEK, B.H., and DEN BOEF, A.J.: 'Coherence collapse in single-mode semiconductor lasers due to optical feedback', *IEEE J.*, 1985, **QE-21**, pp. 674–679
20 SCHUNK, N., and PETERMANN, K.: 'Minimum bit rate of DPSK transmission for semiconductor laser with a long external cavity and strong linewidth reduction', *IEEE J.*, 1987, **LT-5**, pp. 1309–1314
21 AGRAWAL, G.P., and DUTTA, N.K.: 'Long-wavelength semiconductor lasers' (Van Nostrand Reinhold, New York, 1986)
22 SCHUNK, N., and PETERMANN, K.: 'Noise analysis of injection locked semiconductor injection lasers', *IEEE J.*, 1986, **QE-22**, pp. 642–650